MICROBIAL CARBON PUMP IN THE OCEAN

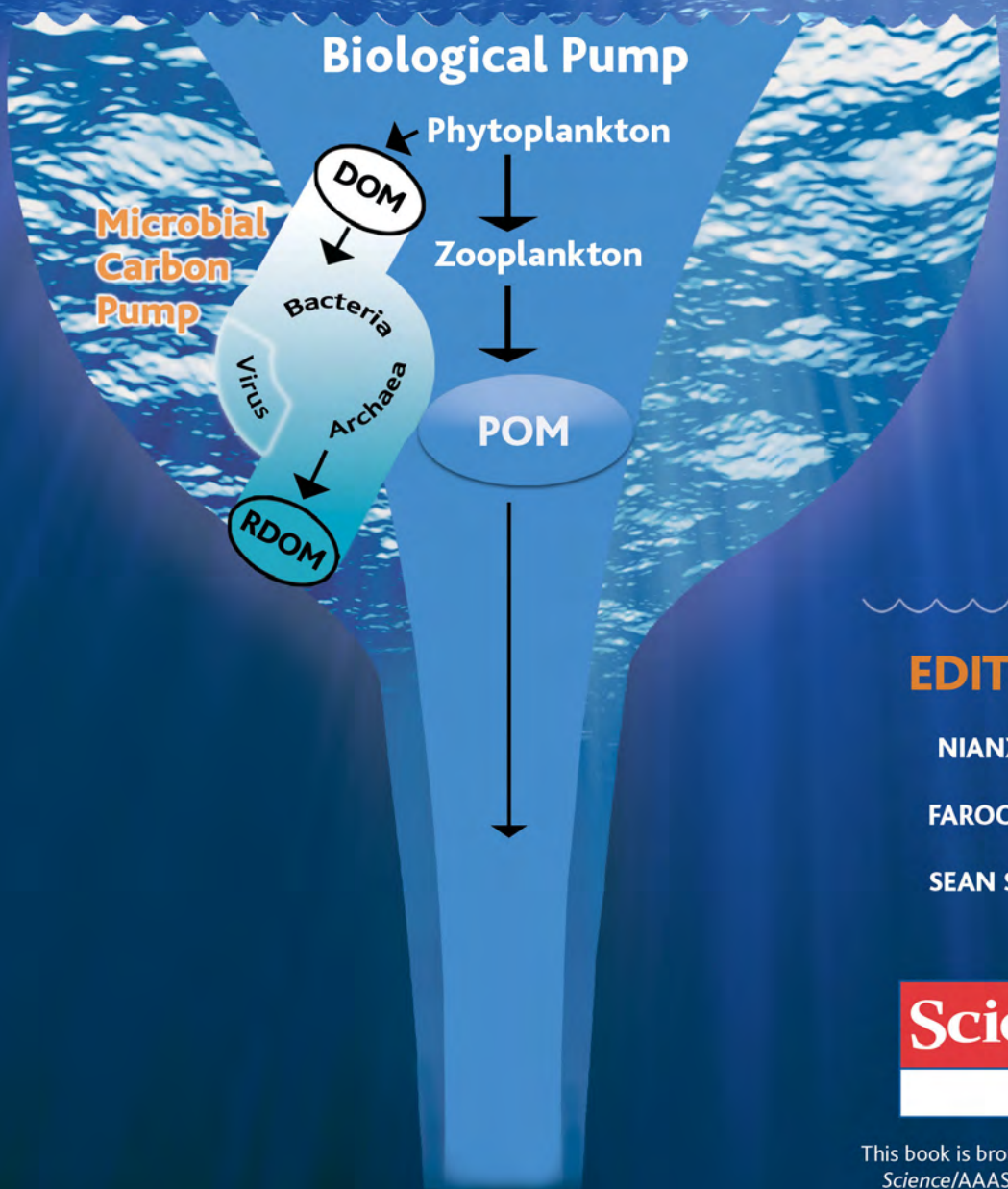

EDITED BY

NIANZHI JIAO

FAROOQ AZAM

SEAN SANDERS

Science

AAAS

This book is brought to you by the *Science*/AAAS Business Office

Supplement to *Science*

AAAS is here – connecting government to the scientific community.

As a part of its efforts to introduce fully open government, the White House is reaching out to the scientific community for a conversation around America's national scientific and technological priorities.

To enable the White House's dialogue with scientists, AAAS launched Expert Labs, under the direction of blogger and tech guru Anil Dash. Expert Labs is building online tools that allow government agencies to ask questions of the scientific community and then sort and rank the answers they receive.

On April 12, 2010, AAAS asked scientists everywhere to submit their ideas to the Obama administration and at the same time launched the first of Expert Labs tools, Think Tank, to help policy makers collect the subsequent responses. The result was thousands of responses to the White House's request, many of which are already under consideration by the Office of Science and Technology Policy.

As a AAAS member, your dues support our efforts to help government base policy on direct feedback from the scientific community. If you are not already a member, join us. Together we can make a difference.

To learn more, visit **aaas.org/plusyou/expertlabs**

AAAS + U = Δ

CONTENTS

Front and back cover images adapted from Jiao, N. *et al., Nature Reviews Microbiology,* 8, 593 (2010).
Front image (background) © istockphoto.com/BobHemphill

13 May 2011

Into the Depths

Microbes. Those unassuming and unseen inhabitants, occupying almost every niche on land and sea, have once more been found to have importance far beyond their physical stature. Microbes have been found living thousands of meters above sea level on Mount Everest, as well as in the deepest oceans, withstanding extraordinary hydrostatic pressure. Many scientists are familiar with *Thermus aquaticus*, a thermophilic microbe that can survive temperatures upwards of 70°C, discovered in a geyser in the Yellow Stone National Park and source of the first thermostable DNA polymerase, the eponymously named *Taq*. Microbes related to *T. aquaticus* even live at the deep-sea hydrothermal vents, often making use of sulfur from these vents as a source of energy. But in the water columns between the deep-sea vents and ocean surface lives an extraordinarily diverse range of interconnected microbial populations that are only now being characterized and understood. More importantly, scientists are uncovering new roles that these microbes play in the ocean carbon cycle and, consequently, in the global climate.

This volume seeks to bring together both the historical and the current research on this topic. In the first chapter are presented a selection of papers published in the last 20 years in *Science* that have helped us understand the chemical makeup of dissolved organic matter (DOM), how the carbon contained in them enters and exits the ocean carbon cycle, and how ocean-dwelling microbes interact with this cycle. Originally suspected to only assimilate or respire DOM, both Bacteria and Archaea have been demonstrated to play a much broader and more important role, in fact being integral cogs in the carbon cycle machine. The recently described microbial carbon pump (MCP), pictured on the cover of this booklet, provides a framework that describes how microbes are also DOM creators and, more importantly, contributors to the creation of refractory DOM (RDOM), a persistent form of DOM that can survive for thousands of years, constituting a previously undescribed mechanism of carbon sequestration.

The second chapter brings us right up to the present day with 10 review articles from some of the leading international scientists in a variety of fields—including marine biogeochemistry, microbiology, and genomics—who put the past three decades of work in perspective and give us a glimpse of where the research might take us in the near future. Covering ground from describing possible ways to model the MCP, to the contribution of virus activity to the creation of RDOM, to discussions of the underlying biochemical and molecular mechanisms at play in the MCP, these articles—vetted and reviewed by fellow scientists within the Scientific Committee for Oceanic Research working group—promise to be both enlightening and provocative.

Understanding and fully characterizing the MCP provides us with critical knowledge needed to refine current models of the ocean carbon cycle so that we may better predict its response to increases in atmospheric CO_2. Through this research, it should be possible to define the resilience of the ocean carbon cycle and its relationship to global climate. This will benefit climate change research as well as provide a robust scientific basis for crafting climate policy. Gaining a deeper understanding of these diverse and often unique microbial inhabitants in our oceans may also allow us to make them our allies as we face future uncertainties for our climate.

Sean Sanders, Ph.D.
Editor, *Science*/AAAS Custom Publishing

Dr. Sanders completed his undergraduate training at the University of Cape Town, South Africa, and his Ph.D. at the University of Cambridge, United Kingdom. Following postdoctoral training at the National Institutes of Health and Georgetown University, he worked for three years at a biotechnology startup before moving into editing. Dr. Sanders is currently the Editor, Custom Publishing for the journal *Science* and *Science* Careers, and Program Director for Outreach.

Revisiting the Ocean's Carbon Cycle

Whether the ocean could serve as a repository for anthropogenic CO_2, as it has for other human wastes, has prompted intense interest and inquiry into ocean carbon biogeochemistry. Fully one-half of global photosynthesis occurs in the ocean. It generates huge amounts of organic matter that is acted on by diverse biological and physical forces that modify, decompose, and redistribute its constituents in the ocean space in timeframes of hours to millennia. Most carbon is rapidly respired back to CO_2 by the diverse biota, while a minuscule fraction sinks, or is actively transported by biota, to the sea bottom (the "biological pump"). There, some of it is respired by the sediment microbes, while the remainder becomes part of the sediment. The biological pump has also been invoked in studies of the fate of anthropogenic pollutants entering the ocean, including radionuclides, to assess whether their association with sinking particles will rid us of them for long periods of time.

We now know that a large fraction of photosynthetically produced organic matter in fact becomes dissolved organic matter (DOM) by a variety of physiological and trophic mechanisms; hence, we need to know the biogeochemical behavior of DOM as well. While microbes readily respire most newly produced DOM, might a small fraction be (or become) refractory and join the enormous refractory DOM (RDOM) pool present in ocean water column, with turnover times of millennia? Even minor changes in RDOM concentration could significantly affect carbon sequestration in the ocean with consequences for the climate. The origin and fate of RDOM, and the underlying mechanisms for its formation and degradation are unknown. Why marine microbes are not able to degrade RDOM is still under investigation though their inability to do so is fortunate: if all RDOM were respired and the carbon released to the atmosphere, it would double the atmospheric CO_2 inventory. Looking at the other side of the equation we can ask: Do bacteria play a major role in the production of RDOM? Further, might the balance between microbial degradation of DOM and production of RDOM shift due to climate change and might the response of the RDOM pool exacerbate climate change impacts through a positive feedback loop? These are new challenges for climate change microbial ecology.

Progress in elucidating the role of microbes in carbon sequestration in the ocean had been limited not only by methodological limitations, but also by the lack of a unifying biogeochemical framework. In recent years, there has been a powerful convergence of marine genomics, ecophysiology, and new tools for DOM analysis. Therefore, the time is ripe for a fresh look at this "refractory" and important problem. The microbial carbon pump (MCP; Jiao *et al.* 2010. *Nat Rev Microbiol.* 8, 593–599) was proposed as a conceptual framework to formulate and test new hypotheses about DOM sources and sinks as well as the mechanistic bases for the regulation of microbial carbon storage in the refractory DOM pool. This research is necessarily highly interdisciplinary involving, at the minimum, microbial oceanographers, marine organic chemists, and geochemists.

A SCOR (Scientific Committee for Oceanic Research) working group (WG134) joined by 26 scientists from 12 countries has been formed to address the problem. In the past two years, the working group has convened several independent workshops, as well as MCP-focused sessions in conjunction with oceanography and microbial ecology conferences. These brainstorming sessions have provided the necessary, and rapidly broadening, interdisciplinary interactions, creating much excitement and momentum. It is our hope that the articles in this book convey this sense of excitement, and an optimism that we are making progress in solving this long-standing problem in science, one which is also of considerable societal import.

Farooq Azam, Ph.D.
Nianzhi Jiao, Ph.D.

Dr. Farooq Azam studies microbial oceanography and marine biogeochemistry. Dr. Azam and his students have made significant contributions to our understanding of the role of microbes in the functioning of marine ecosystems and carbon cycle. Dr. Azam is a Distinguished Professor at Scripps Institution of Oceanography, University of California, San Diego and co-chairs the Scientific Committee for Ocean Research (SCOR) Working Group 134 on "Microbial Carbon Pump in the Ocean."

Dr. Nianzhi Jiao is Cheung Kong Chair Professor at Xiamen University, China. After receiving his Ph.D. from Ocean University of Qingdao in 1991, he continued his studies at MIT in the United States, the University of Tokyo, and the National Institute for Environmental Studies, Japan. Dr. Jiao's research focuses on microbial ecology and carbon cycling. He is a co-chair of the Scientific Committee for Ocean Research (SCOR) Working Group 134 on "Microbial Carbon Pump in the Ocean."

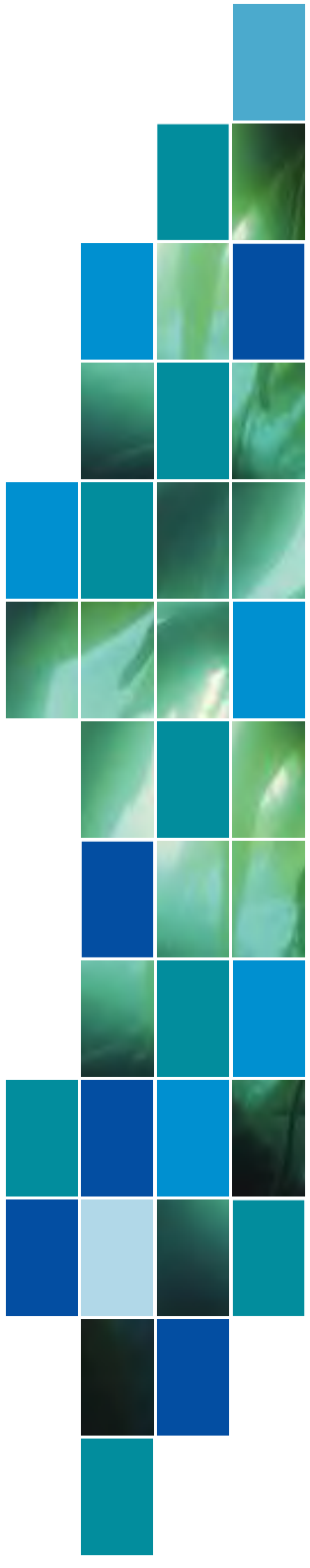

Chapter One

The Invisible Hand Behind A Vast Carbon Reservoir

A key element of the carbon cycle is the microbial conversion of dissolved organic carbon into inedible forms. Can it also serve to sequester CO_2?

XIAMEN, CHINA—For simple sea creatures, dissolved organic carbon (DOC) is the staff of life. Much of it, however, is as unpalatable as chaff and accumulates in the water column. Scientists are unraveling how organic matter in the marine food chain is converted into forms that less readily relinquish carbon in the form of carbon dioxide (CO_2). "The existence of this 'inedible' organic carbon in the ocean has been known for quite some time. But its role in the global carbon cycle has been recognized only recently," says Michal Koblížek, a microbiologist at the Institute of Microbiology in Trebon, Czech Republic.

New findings are unmasking the invisible processes that suspend immense amounts of carbon just below the ocean waves. "It's really huge. It's comparable to all the carbon dioxide in the air," says Jiao Nianzhi, a microbial ecologist here at Xiamen University. He and others are exploring the tantalizing prospect of sequestering CO_2 in this reservoir. It's too early to say whether the vast pool will respond to geoengineering, says Dennis Hansell, a marine biogeochemist at the University of Miami in Florida. However, he says, "I expect the light to come on over heads and we'll experience an 'ah ha!' moment."

Data from several research cruises have yielded a broad-brush view of what Jiao has dubbed the microbial carbon pump (MCP): the microbe-driven conversion of bioavailable organic carbon into difficult-to-digest forms known as refractory DOC. This summer, the European Project on Ocean Acidification is carrying out a slate of experiments in Arctic waters that includes probing the MCP. Then in October, Jiao's team heads to the opposite thermal extreme: They will explore the mechanisms of the MCP and CO_2 sequestration in the equatorial Indo-Pacific Warm Pool, the warmest marine waters in the world. The MCP will also be featured next month at a Gordon Research Conference on marine microbes, and it is outlined in a paper in press at *Nature Reviews Microbiology*. The concept "could revolutionize our view of carbon sequestration," says Markus Weinbauer, a microbial oceanographer at Laboratoire d'Océanographie de Villefranche in France.

The ocean surface is like a planet-sized set of lungs that inhale and exhale CO_2. As a global average, the oceans take up about 2% more of the gas than they release. Some CO_2 dissolves into the water column, forming carbonic acid. As atmospheric CO_2 levels rise, ocean pH decreases, a phenomenon called acidification that could endanger corals and other creatures by slowing the growth of carbonate skeletons (see *Science* 18 June 2010, p. 1500). Carbon also enters the seas through the foodweb: During photosynthesis, phytoplankton fixes CO_2 to organic carbon—as much as 60 gigatons of carbon per year, roughly the same amount fixed on land. "The carbon is not captured for long," says Koblížek. Most new marine biomass is consumed in days and returned to the air as CO_2. Some, however, ends up in the deep ocean sink, when remains of dead organisms fall to the sea floor. Each year, this biological pump deposits roughly 300 million tons of carbon in the seabed.

Even more massive amounts of carbon are suspended in the water column as DOC. The oceans hold an estimated 700 billion tons of carbon as DOC—more than all land biomass put together (600 billion tons of carbon) and nearly as much as all the CO_2 in the air (750 billion tons of carbon). About 95% of organic carbon is bound up as refractory DOC: "the largest pool of organic matter in the ocean," says Farooq Azam, a microbiologist at Scripps Institution of Oceanography in San Diego, California. In the December 2009 issue of *Oceanography*, a team led by Hansell and Craig Carlson of the University of California, Santa Barbara, compiled the first global map of DOC distribution. Carbon-14 studies suggest that refractory compounds swirl in this microbial eddy for more than 6000 years, several times the circulation time of the ocean.

DOC doc. Jiao Nianzhi formulated the MCP concept based on his studies of AAPB, an unusual kind of photosynthetic bacteria (*left*).

The realization that refractory DOC is a key element in the global carbon cycle has lit a fire under efforts to figure out what the stuff is and where it comes from. Researchers now know that refractory DOC consists of thousands of compounds, such as complex polysaccharides and humic acids. A team led by Xosé Antón Álvarez Salgado of the Instituto de Investigaciones Marinas in Vigo, Spain, has tracked the conversion of some forms of bioavailable carbon to refractory carbon by observing changes in their optical properties: Humic substances absorb UV light and re-emit it as blue fluorescence at specific wavelengths.

The origins of most refractory DOC are a black box. Some is produced when light degrades organic matter near the ocean surface. Oil seeps contribute to the pool. "The oil spill in the Gulf of Mexico is just one drastic example of how this material is released into the ocean," says Meinhard Simon, a microbial oceanographer at the University of Oldenburg in Germany. Other compounds are likely forged in underwater vents or in wildfires and swept into the sea. For the most part, however, says Azam, "we lack understanding of the mechanisms of its formation or variations in its magnitude and composition."

Azam and others credit Jiao with a key insight: the recognition that microbes play a dominant role in "pumping" bioavailable carbon into a pool of relatively inert compounds. Some refractory DOC hangs in the upper water column, while some gets shunted to the deep ocean interior via the biological pump. The MCP "may act as one of the conveyor belts that transport and store carbon in the deep oceans," says Chen-Tung "Arthur" Chen, an ocean carbonate chemist at National Sun Yat-sen University in Kaohsiung, Taiwan. The MCP also appears to function in deep waters, where bacteria adapted to the high-pressure environment may have "a special capacity" to degrade refractory DOC, says Christian Tamburini, a microbiologist at the Centre d'Océanologie de Marseille in France.

It took sharp sleuthing to uncover the microbial connection with refractory DOC. In a landmark paper in 2001, Hiroshi Ogawa of the University of Tokyo and colleagues showed that marine microbes are able to convert bioavailable DOC to refractory DOC (See page 9). Then a month later, Zbigniew Kolber, now at the Monterey Bay Aquarium Research Institute in Moss Landing, California, and colleagues reported that in the upper open ocean, an unusual class of photosynthetic bacteria called AAPB accounts for 11% of the total microbial community (*Science,* 29 June 2001, p. 2492). AAPBs seemed to be plentiful everywhere, according to measurements of infrared fluorescence from the microbe's light-absorbing pigments.

It turned out, though, that other organisms were throwing the AAPB estimates way off the mark. Using a new technique, Jiao's group determined that the fluorescent glow of phytoplankton was masking the glow of the target microbes. "Just like when the moon is bright, less stars are visible," Jiao says. He put the new approach through its paces in 2005, when China's *Ocean 1* research vessel conducted campaigns to mark the 600th anniversary of Admiral He Zheng's historic voyages. The observations "turned things upside down," Jiao says. His group found that AAPBs are more abundant in nutrient-rich waters than in the open ocean, indicating that AAPB population levels are linked with DOC, not light.

Next, Jiao found that AAPBs are prone to viral infection, and he isolated the first phage that's specific for these bacteria. Phages rip apart their hosts, spilling their guts, including organic carbon, into the water. This viral shunt acting on many marine bacteria "may be a significant player in the accumulation of refractory DOC compounds" in the water column, says Steven Wilhelm, a microbiologist at the University of Tennessee, Knoxville. Pulling together several strands—the ubiquity of AAPBs, their low abundance but high turnover rate, the tight link to DOC, and their susceptibility to infection—Jiao proposed that AAPBs and other microbes are a key mechanism for the conversion of bioavailable DOC to refractory DOC. That may seem counterintuitive, as microbes do not set out to produce refractory DOC; rather, the compounds are a byproduct of their demise. "This process is not beneficial to the cell," says Simon.

Because the buildup of refractory DOC in the water column is accidental, it will be a challenge to coax microbes to sequester more carbon. For decades, researchers have been tinkering with the biological pump to store more carbon in the deep ocean by seeding seas with iron fertilizer. The iron triggers phytoplankton blooms that suck more CO_2 from the air. That should also drive more carbon into the refractory pool, Koblížek says.

Even tweaking the MCP could have a profound effect. The water column holds on average 35 to 40 micromoles of carbon from refractory DOC per liter. An increase of a mere 2 to 3 micromoles per liter would sock away several billion tons of carbon, says Nagappa Ramaiah, a marine microbial ecologist at the National Institute of Oceanography in Goa, India. "We have to investigate any and all means to help sink the excess carbon," he says.

Two billion years ago, when bacteria ruled Earth, the oceans held 500 times as much DOC as today, most likely generated by the MCP, Jiao says. Ecosystem dynamics have changed immensely since then, but the microbial sequestration potential could still be huge, he argues. No chemical equilibrium would limit conversion of bioavailable DOC to refractory DOC, which in turn would not exacerbate ocean acidification, says Jiao, who is planning pilot experiments this summer. Ramaiah, meanwhile, says he is looking for enhanced sequestration potential in select marine bacteria strains.

There's no simple recipe—and some scientists are not convinced that it's feasible or even safe. "I do not think it is possible to enhance carbon sequestration by the MCP. We have no handle on any controls" of how refractory DOC is generated, says Simon. With the present knowledge, any sequestration effort, argues Weinbauer, "could come back like a boomerang and worsen the problem." At the same time, humans may already be "inadvertently stimulating the MCP," says Salgado. Global warming is increasing stratification, reducing deep convection, and stimulating microbial respiration—all of which favor the MCP, he says.

The MCP concept should help address critical issues, such as whether ocean acidification and warming will significantly alter carbon flux into refractory DOC, says Azam, who with Jiao chairs the Scientific Committee on Oceanic Research's new working group on the role of MCP in carbon biogeochemistry. The upcoming research cruises should fill in more details of how the MCP governs carbon cycling and how it may respond to climate change. As Wilhelm notes, "We are just at the dawn of developing this understanding."

–RICHARD STONE

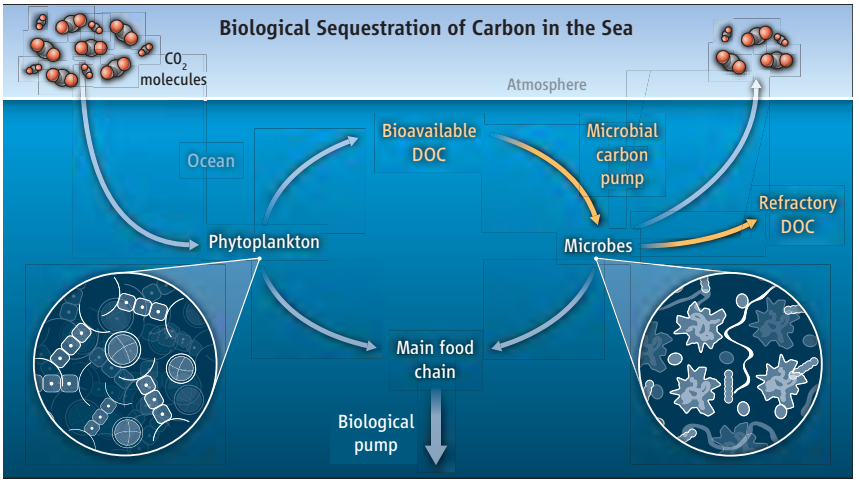

Double-barrel pump. Each year, the biological pump deposits some 300 million tons of carbon in the deep ocean sink. Even more massive amounts are suspended in the water column as dissolved organic carbon, much of which is converted into refractory forms by the microbial carbon pump.

CREDIT: C. BICKEL/*SCIENCE*

Microbial Control of Oceanic Carbon Flux: The Plot Thickens

Farooq Azam

Photosynthesis fixes carbon into organic matter in the ocean. Biological forces then paint intricate flux patterns for carbon in ocean space and in time, as it flows through the foodweb, becomes stored in the sediments and exchanged with the atmosphere. Predicting how these carbon flux patterns might respond to global change (or to human manipulation) is a primary reason for learning more about the workings of the ocean's carbon cycle. The flux patterns are a result of intricate interactions of a diverse biota with a physically and chemically complex pool of organic matter. It now seems that things will get even more complicated before they get simpler. New fundamental findings on the roles of microbes in the fate of organic matter and, recently, on the nature of the organic matter itself (*1*–*4*) must be properly assimilated before we can hope to construct ecosystem models to predict the patterns of carbon flux. This impetus could lead to a powerful new synthesis.

What biological forces act on photosynthetically produced organic matter in the ocean? Historically, the paradigm has been that essentially all primary production stays within the particle phase (*5*), it is eaten by herbivores, and the fate of carbon is determined by the "grazing food chain" (Fig. 1). Little dissolved organic matter is spilled for bacteria to use. It had, therefore, been implicitly assumed to be safe to ignore bacteria, protozoa, and viruses in studying the fate of organic matter—they were too sparse and not active enough (*5*). This is now changed (*5*–*8*): Major fluxes of organic matter, often eclipsing the grazing food chain in quantity, move via dissolved organic matter into bacteria and the "microbial loop" (*7*, *8*) (Fig. 1). Previous methods had missed >99% of microorganisms and had grossly underestimated their metabolism. Now we know from extensive field studies that in most of the ocean, organic matter flux into bacteria is a major pathway; one-half of oceanic primary production on average is channeled via bacteria into the microbial loop (*7*, *8*)—a major biological force in the ocean.

Ocean basin-scale biogeochemical studies now routinely quantify organic matter fluxes into bacteria in conjunction with other major flux pathways: grazing food chain, sinking flux, and dissolved organic matter "storage." The fraction of primary production used by bacteria (F_b) is highly variable over various time and space scales (*7*–*10*). The magnitudes and variability of the fluxes are large enough to cause variability in flux partitioning between competing pathways (Fig. 1)—the microbial loop, the grazing food chain, sinking fluxes, and storage of dissolved organic matter (*8*, *9*). Fish production in the eastern Mediterranean was diminished by a dominant microbial loop (F_b = 0.85) (*11*). In an earlier study (*12*), the richness of the fishery in coastal Newfoundland was ascribed to uncoupling of bacteria from primary production during the spring bloom. These are tantalizing but rare success stories where descriptive studies lead to interesting insights into the bacterial control of organic matter fluxes and ecosystem dynamics.

However, we lack a conceptual framework to predict variation in organic matter flux into bacteria and how it fits into the overall oceanic flux picture (for example, how the flux partitioning will respond to global change). This requires elucidating the causes and mechanisms of variability of organic matter flux into bacteria. How do bacteria interact with organic matter, and what regulates the flux of organic matter into them?

It is generally thought that pelagic bacteria passively receive dissolved organic matter leaking from the grazing food chain and diffused homogeneously. However, recent studies on the complex nature of the organic matter field (*1*–*4*, *13*) and behavioral strategies of bacteria (*14*) have suggested (*2*) that bacteria do not use only preformed dissolved organic matter; they also attack all organic matter, even live organisms, thus liberating dissolved organic matter. Hence, bacterial attack can profoundly modify the biogeochemical behavior of organic matter in ways not inferred from measuring cumulative organic matter fluxes into bacteria. Recognition of such "modification interactions" could add important new variables in biogeochemical models.

Our view of the organic matter in seawater has changed dramatically. The traditional dichotomy of particulate organic matter versus dissolved organic matter is being replaced by the concept of an organic matter continuum (*2*). Several new classes of abundant colloids, submicrometer particles, and transparent polymer particles have been discovered (*1*, *4*, *13*). This oceanic "dark matter" ranges in size from 20 nm to hundreds of micrometers. It has been proposed (*2*, *3*) that pelagic bacteria experience a gel-like polymeric matrix with colloids and particles embedded as suprapolymeric "hotspots" (*8*) (Fig. 2). The interaction of bacteria with the organic matter continuum, and their behavioral response to its heterogeneity, creates microscale features—activity hotspots—with distinctive natures and intensities of biogeochemical transformations. Patchiness may also support high bacterial diversity. An important recent study by Chin et al. (*1*) demonstrated that polymers in seawater indeed form a gel.

Do bacteria respond to the structure of the organic matter field? Large bacterial populations can develop on hotspots—for example, marine snow, dead and even living algae—and

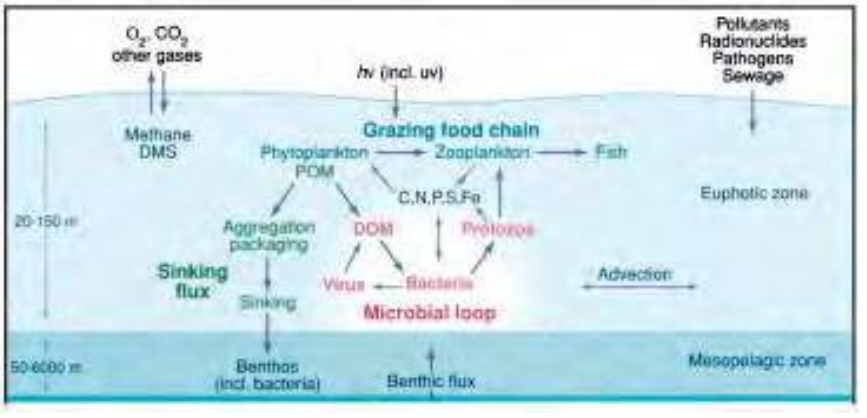

Fig. 1. The microbial loop: classical version. Modern view of the pelagic foodweb, emphasizing the microbial loop as a major path for organic matter flux. Competition between the three main flux paths—grazing food chain, microbial loop, and sinking—significantly affects oceanic carbon cycle and productivity. DOM, dissolved organic matter; DMS, dimethylsulfide.

The author is at the Scripps Institution of Oceanography, University of California, La Jolla, CA 92093, USA. E-mail: fazam@ucsd.edu

in association with the "dark matter." [In one study, 24 to 68% of bacteria were on transparent particles (*13*)]. Oceanic bacteria (*14*) exhibit sophisticated behavior—swimming speeds of hundreds of micrometers per second, unusual swimming (run reversals), and chemosensing. The organic matter field is dominantly polymeric and suprapolymeric, so most pelagic bacteria have a diverse repertoire of surface-bound enzymes (proteases, glucosidases, lipases, phosphatases, nucleases) to cause its hydrolysis (*15*). Small-scale variation of species composition can significantly change the distributions of enzyme activities (*16*). Pelagic bacteria also have multiphasic permeases for nutrient uptake (*17*), with nanomolar to millimolar half-saturation constants, suggesting their adaptations to life in a patchy environment. Considering the intimate contact of their "digestive system" with the organic matter gel, motile bacteria are the "ultimate swimming stomachs" (*18*). They cannot avoid interacting with and changing organic matter.

Bacterial action on components of the organic matter field can modify its character in varied ways without necessarily involving large organic matter fluxes into bacteria. Two examples illustrate this point. In a study of bacterial activity on marine snow (*19*), the colonizing bacteria grew slowly but expressed large amounts of ectohydrolases, which solubilized particulate organic matter; however, because of the low carbon demand of these bacteria, most hydrolysate diffused out ("uncoupled solubilization"), thus reducing the sinking flux. Also, enzyme action was thought to increase the efficiency of the oceanic carbon pump; protease and phosphatase activities were much higher than those of α- and β-glucosidases, and this would cause preferential nitrogen and phosphate retention compared with carbon in the photic layer where it supports more carbon fixation and export. Thus, bacteria influenced the fate of carbon without a significant carbon demand. Bacterial interaction with live diatoms was examined in a mesocosm (*20*). Bacteria colonized the diatoms, grew rapidly, and expressed large amounts of ectohydrolase. Experiments suggested that ectohydrolases of attached bacteria "prune" mucus from the surface of diatoms, thereby controlling diatom stickiness and inhibiting aggregation. Bacterial modification of algal surfaces, a microscale process, could increase the persistence and intensity of algal blooms, as well as influence the sinking flux, with profound ecological and biogeochemical implications. Attached bacteria could also expose the alga to high microscale concentrations of remineralized nutrients, thus enhancing carbon fixation. Partial hydrolysis of complex polysaccharides by bacterial attack could produce slow-to-degrade dissolved organic matter, resulting in carbon storage (high bacterial activity could actually produce more slow-to-degrade dissolved organic matter). This could be used by bacteria at a different place and time (for example, dissolved organic matter accumulating in Antarctic waters during summer could support the foodweb during winter). These and other examples show that the ecosystem-level consequences of bacteria-organic matter interactions may be pervasive in ways not currently being quantified, or even recognized, in ocean basin-scale biogeochemical studies.

Thus, behavioral and metabolic responses of bacteria to the complex and heterogeneous structure of the organic matter field at the microscale influence ocean basin-scale carbon fluxes in all major pathways: microbial loop, sinking, grazing food chain, carbon storage, and carbon fixation itself. However, studying such varied influences of bacteria on organic matter, and their spatial-temporal variations, in piecemeal fashion will only result in a conceptual patchwork without a unifying framework or predictive power. A unifying theme should derive from applying robust principles of biochemical adaptation in a realistic microenvironmental context. Biogeochemical variability could then be considered as a consequence of adaptive responses to (micro)environmental variations. This approach should also serve as a framework to understand the maintenance of microbial diversity and to make predictions on the survival of specific bacterial species, including human pathogens such as *Vibrio cholerae,* in response to ecosystem perturbations (*21*). This framework, which includes bacteria-algae interactions, should also be relevant to the prediction of algal blooms, including toxigenic species. Powerful new approaches are enabling us to study microbial ecology, including consortial activities, in an ecosystem context. New techniques allow multiple interrogations—phylogeny, metabolism, growth—at the individual cell level. These ideas and approaches should lead to a synthesis of bacterial adaptation, evolution, ecology, and biogeochemistry, and should form a basis for integrating the roles of bacteria in predictive biogeochemical models.

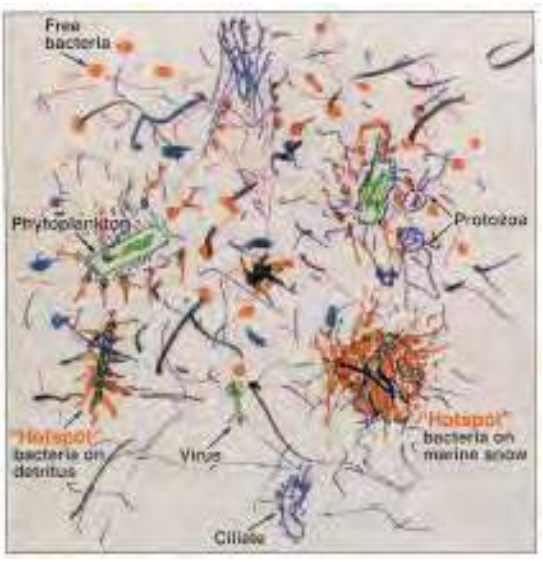

Fig. 2. The microbial loop: impressionist version. A bacteria-eye view of the ocean's euphotic layer. Seawater is an organic matter continuum, a gel of tangled polymers with embedded strings, sheets, and bundles of fibrils and particles, including living organisms, as "hotspots." Bacteria (red) acting on marine snow (black) or algae (green) can control sedimentation and primary productivity; diverse microniches (hotspots) can support high bacterial diversity.

References and Notes

1. W. C. Chin *et al*., *Nature* **391,** 568 (1998).
2. F. Azam *et al*., *Microbiol. Ecol.* **28,** 167 (1993).
3. F. Azam and D. C. Smith, in *Particle Analysis in Oceanography,* S. Demers, Ed. (Springer-Verlag, Berlin, 1991), pp. 213–236.
4. I. Koike *et al*., *Nature* **345,** 242 (1990) M. L. Wells and E. D. Goldberg, *ibid.* **353,** 342 (1991) R. A. Long and F. Azam, *Aquat. Microb. Ecol.* **10,** 213 (1996).
5. J. H. Steele, in *The Structure of Marine Ecosystems* (Harvard Univ. Press, Cambridge, MA, 1974)
6. L. R. Pomeroy, *Bioscience* **24,** 499 (1974) J. E. Hobbie *et al., Appl. Environ. Microbiol.* **33,** 1225 (1977).
7. F. Azam *et al*., *Mar. Ecol. Prog. Ser.* **10,** 257 (1983).
8. J. J. Cole *et al*., *ibid*. **43,** 1 (1988) J. A. Fuhrman and F. Azam, *Mar. Biol.* **66,** 109 (1982); A. Hagstrom *et al., Appl. Environ. Microbiol.* **37,** 805 (1979).
9. H. W. Ducklow and C. A. Carlson, *Adv. Microb. Ecol.* **12,** 113 (1993).
10. H. W. Ducklow, *Deep Sea Res.* **40,** 753 (1993).
11. N. Williams, *Science* **279,** 483 (1998).
12. L. R. Pomeroy and D. Deibel, *ibid.* **233,** 359 (1986).
13. A. L. Alldredge *et al*., *Deep Sea Res.* **40,** 1131 (1993).
14. J. G. Mitchell *et al*., *Appl. Environ. Microbiol.* **61,** 4436 (1995) H.-P. Grossart and F. Azam, paper presented at the Ocean Sciences Meeting, San Diego, CA, 9 to 13 February 1998.
15. H. G. Hoppe *et al*., *Mar. Ecol. Prog. Ser.* **93,** 277 (1993) J. T. Hollibaugh and F. Azam, *Limnol. Oceanogr.* **28,** 104 (1983).
16. E. F. DeLong *et al*., *Limnol. Oceanogr.* **38,** 924 (1993) A.-S. Rehnstam *et al., FEMS Microb. Ecol.* **102,** 161 (1993); J. Martinez *et al., Aquat. Microb. Ecol.* **10,** 223 (1996).
17. H. Nissen *et al*., *Mar. Ecol. Prog. Ser.* **16,** 155 (1984) G. G. Geesey and R. Y. Morita, *Appl. Environ. Microbiol*. **38,** 1092 (1979).
18. J. Stern, personal communication.
19. D. C. Smith *et al*., *Nature* **359,** 139 (1992) A. L. Alldredge and C. C. Gotschalk, *Cont. Shelf. Res.* **10,** 41 (1990).
20. D. C. Smith *et al*., *Deep Sea Res. II* **42,** 75 (1995) U. Passow and A. L. Alldredge, *ibid.*, p. 99.
21. P. R. Epstein, *Biosystems* **31,** 209 (1993) R. R. Colwell, *Science* **274,** 2025 (1996).

22. I thank H.-P. Grossart, R. A. Long, L. B. Fandino, K. D. Bidle, D. C. Smith, J. T. Hollibaugh, F. Rassoulzadegan for discussions and suggestions. Research supported by NSF grants NSF OPP96-17045 and OPP95-40851.

Production of Refractory Dissolved Organic Matter by Bacteria

Hiroshi Ogawa,[1*] Yukio Amagai,[1] Isao Koike,[1] Karl Kaiser,[2] Ronald Benner[2]

Most of the oceanic reservoir of dissolved organic matter (DOM) is of marine origin and is resistant to microbial oxidation, but little is known about the mechanisms of its formation. In a laboratory study, natural assemblages of marine bacteria rapidly (in <48 hours) utilized labile compounds (glucose, glutamate) and produced refractory DOM that persisted for more than a year. Only 10 to 15% of the bacterially derived DOM was identified as hydrolyzable amino acids and sugars, a feature consistent with marine DOM. These results suggest that microbial processes alter the molecular structure of DOM, making it resistant to further degradation and thereby preserving fixed carbon in the ocean.

DOM is the largest reservoir of fixed carbon in the ocean and is approximately equivalent to the reservoir of atmospheric CO_2. The major bioelements (C, N, and P) in DOM occur in functional groups common to biopolymers found in marine organisms (*1–3*). Specific cellular components of bacteria have been identified in marine DOM (*4*,*5*), indicating that bacteria are an important source of this material. These observations indicate the predominance of biomolecules in DOM, but <25% of marine DOM has been identified as specific biochemicals (*6*, *7*), suggesting that its molecular structure has been modified. It appears that these molecular modifications also reduce the bioavailability of the DOM. Physicochemical reactions were proposed as the dominant mechanism for the formation of molecularly uncharacterized and refractory DOM (*8*), but a few studies reported that microorganisms also produce DOM that is resistant to decomposition (*9–11*). In a series of experiments, we examined the bacterial utilization of simple biochemicals and traced the production of fresh DOM by the bacterial community.

We used seawater cultures with natural bacterial assemblages to examine DOM production by marine bacteria (*12*). Culture media were prepared with organic-free artificial seawater and either glucose or glutamate as the sole C source. Incubations with glucose received ammonium and phosphate as N and P sources and an inoculum from Gulf of Mexico surface water. Incubations with glutamate received phosphate as a P source and an inoculum from Sagami Bay, Japan. Concentrations of free glucose and glutamate were measured using high-performance liquid chromatography (HPLC) (*13*, *14*). Measurements of total organic carbon (TOC), dissolved organic carbon (DOC), and dissolved organic nitrogen (DON), were made using high-temperature combustion (*15*, *16*). Concentrations of total hydrolyzable neutral sugars (THNS), total hydrolyzable amino sugars (THAS), and total hydrolyzable amino acids (THAA) were measured by HPLC after acid hydrolysis (*17*). Both experiments were conducted at room temperature (22° to 28°C) with duplicate bottles under dark conditions.

Glucose (208 μM C) was rapidly consumed and undetectable after 2 days (Fig. 1). Within 2 days, TOC concentrations decreased by 78% due to respiration, and 7% of the initial glucose C was converted to particulate organic carbon (POC, i.e., bacterial biomass), whereas 15% was converted to DOC (Table 1). Similarly, glutamate was completely consumed within 2 days, and 66% of the added C was respired. Compared to the glucose incubations, glutamate incubations had a greater yield of bacterial biomass (22% of initial glutamate C), but a similar yield of DOC (13%). After 2 days, bacterial growth yields were 8% in the N-limited glucose incubations and 25% in the glutamate incubations, if bacterially derived DOC was excluded from yield calculations. Inclusion of bacterially derived DOC results in growth yield estimates of 22 and 35%, respectively, in the glucose and glutamate incubations.

Concentrations of bacterially derived DOC decreased gradually during the next week of decomposition (Stage II in Table 1). Assuming first-order kinetics, the average decay constant during Stage II was reduced by a factor of 8 compared with the utilization of glucose and glutamate (Stage I). It is generally recognized that bacteria in natural waters rapidly utilize labile compounds, such as free amino acids and monosaccharides, even at low (nM) concentrations (*18*, *19*). Therefore, it is unlikely that the concentrations of remaining bacterially derived DOC (20 to 30 μM C) would limit bacterial utilization. Neither ammonium nor phosphate was depleted after 1 week of incubation, suggesting nutrients were not limiting for decomposition. These results demonstrate that marine bacteria rapidly consumed labile DOM and produced DOM that was relatively resistant to decomposition.

The experiments were continued to examine the long-term persistence of bacterially derived DOM. Consequently, 10.5 and 9.0 μM DOC were measured after 1 and 1.5 years, respectively, of incubation in the glucose and glutamate experiments, corresponding to 5 and 7% of the initial DOC added in each experiment and to 37 and 50% of the bacterially derived DOC concentrations at the end of 2 days. Although the degradation of DOC continued throughout the incubation (Stage III in Table 1), the degradation rate was remarkably low, and the decay constants were up to 100 times lower than those in Stage II. These decay constants were similar to previous estimates from long-term degradation experiments with marine DOC from oligotrophic waters (*20*) and corresponded to residence times of 1.2 to 2.3 years. Thus, bacteria rapidly produced a major component of refractory DOM from labile substrates.

Chromatographic characterizations of major biogenic components of bacterially derived DOM indicated that THAA, THNS, and THAS accounted for 2.5 to 4.3%, 2.5 to 5.9%, and 0.7 to 1.5% of the DOC, respectively, during the first week in the glucose experiment (Table 2). Only 6 to 11% of the DOC was identified at the molecular level. Amino acids and amino sugars are also important nitrogenous components of DON. No DON was initially present in the glucose experiment, but concentrations of 0.6 to 1.0 μM DON were measured during the incubation. Marine bacteria produced DON from glucose and ammonium, and amino acids and amino sugars accounted for 22 to 29% and 3.4 to 6.6%, respectively, of the DON during the first week (Table 2). As with DOC, most (67 to 75%) of the DON was not characterized at the molecular level. The C:N ratio of the DOM was 28 to 32, indicating that bacterially derived DOM was C-rich relative to the initial substrates (glucose C:NH_4-N = 20:1). The C:N ratio for the molecularly characterized DOM (THAA+THNS+THAS) was 7.5 to 9.2. In contrast, the C:N ratio of the molecularly uncharacterized DOM was 37 to 41, indicating a N-poor composition.

In the glutamate experiment, only amino acids (THAA) were measured in bacterially derived DOM. The yields of THAA were 12

[1]Ocean Research Institute, The University of Tokyo, 1-15-1 Minamidai, Nakano, Tokyo 164-8639, Japan.
[2]Department of Biological Sciences and Marine Science Program, University of South Carolina, Columbia, SC 29208, USA.

*To whom correspondence should be addressed. E-mail: hogawa@ori.u-tokyo.ac.jp

Originally published 4 May 2001

to 18% of the DOC and 15 to 33% of the DON during the first week of the incubation. The uncharacterized fraction composed most of the DOM (82 to 88% of C and 67 to 85% of N). The C:N ratio of the total DOM was 5.1 to 9.3, whereas the C:N ratios of the THAA and uncharacterized fractions were 3.1 to 3.5 and 5.4 to 12, respectively, suggesting that most bacterially derived DOM was depleted in N relative to the initial substrate (glutamate C:N = 5). The yields of amino acids in DOM were higher and the C:N ratios were lower in the glutamate experiment compared with the glucose experiment, reflecting the different N content of initial substrates. By 1.5 years, the yields of amino acids decreased (3.1% of the DOC and 11% of the DON) in the glutamate experiment, and the C:N ratio of the

Table 1. Carbon balances and kinetic decay constants for DOM at different stages in seawater cultures with bacteria and glucose or glutamate as an initial substrate. The data are given as the mean ± |mean-replicate| of duplicate bottle incubations. Carbon balances were calculated at the end of each stage period, including remineralized % (i.e., the loss of TOC) and remaining % as DOC or POC relative to the initial TOC. The results of POC at Stage III were not available, because the difference between TOC and DOC were statistically insignificant or no measurement of TOC was made. The decay constants for DOC during each stage were calculated on the assumption of first-order decay kinetics.

Stage (days)	Remineralized %	Remaining %		Decay constant (day $^{-1}$)
		DOC	POC	
Glucose (208 ± 0 μM C)				
I (0–2)	78 ± 1	15 ± 0	7 ± 1	1.1 ± 0.0
II (2–7)	87 ± 1	8 ± 1	6 ± 1	0.13 ± 0.03
III (7–365)	95 ± 0	5 ± 0	–	0.0012 ± 0.0003
Glutamate (132 ± 2 μM C)				
I (0–2)	66 ± 5	13 ± 7	22 ± 2	1.1 ± 0.1
II (2–9)	77 ± 2	10 ± 1	13 ± 1	0.14 ± 0.08
III (9–560)	93 ± 1	7 ± 1	–	0.0023 ± 0.0003

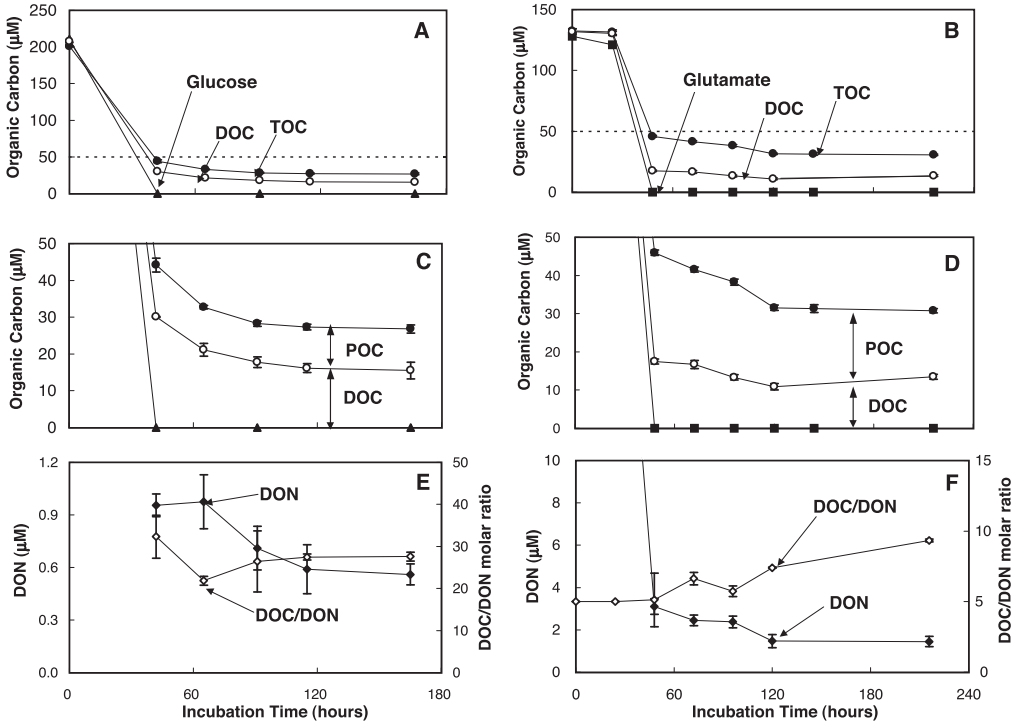

Fig. 1. Concentrations of free glucose (**A**), free glutamate (**B**), and TOC, DOC, POC, and DON in seawater cultures with natural bacterial assemblages and either glucose (**A, C,** and **E**) or glutamate (**B, D,** and **F**) as the sole carbon sources for bacterial growth. Panels (**C**) and (**D**) are re-illustrations of panels (**A**) and (**B**) with magnified scales of the y-axis. Each point and error bar represents the average and range of duplicate-bottle experiments. Water samples were gravity-filtered through a glass fiber filter (GF/F, Whatman) in the glucose experiments for separation of the particulate and dissolved phases. In the glutamate experiments, water samples were passed through a 0.1-μm polytetrafluoroethylene membrane filter (Omnipore, Millipore) under reduced pressure. The DON concentration at the beginning of the glucose experiment was omitted because it was not significantly different from zero. Initial concentrations of DOC in glucose and glutamate experiments were accounted for in the measured concentrations of these compounds, indicating that no other sources of DOC were in the initial culture medium.

Table 2. Chemical composition of bacterially derived DOM in the glucose and glutamate experiments. All are the mean of duplicate-bottle experiments, except for the data indicated by asterisks, which were obtained from single bottles. The mean deviation of replicates was 0.9 μM for DOC, 0.2 μM for DON, 2 for C/N ratio, and 1 to 2% of DOC, DON, THAS, and THAA compositions. The "uncharacterized" fraction in the glucose experiment is estimated as the difference between the total DOC and the DOC accounted for as THNS+THAS+THAA, and between the total DON and the DON accounted for as THAA+THAS, except for the data after 1 year, in which THNS was not included (data in parenthesis). The "uncharacterized" fraction in the glutamate experiment is based only on THAA, because THNS and THAS were not measured (indicated by "nm").

Chemical composition	Initial substrate							
	Glucose				Glutamate			
	Incubation time (days)				Incubation time (days)			
	2	4	7	365	2	4	9	560
	Concentration of the bulk DOM (μM)							
DOC	30	18	16	11	18	13	14	9.0
DON	1.0	0.7	0.6	1.2	3.1	2.4	1.5	0.7
	DOC composition (% as)							
THNS	2.5	4.9	5.9	nm	nm	nm	nm	nm
THAS	0.7	1.4	1.5	3.8	nm	nm	nm	nm
THAA	2.5	4.3	3.7	2.5	13	18*	12	3.1
Uncharacterized	94	89	89	(94)	87	82*	88	97
	DON composition (% as)							
THAS	3.4	5.5	6.6	5.6	nm	nm	nm	nm
THAA	22	29	27	6.4	15	31*	33	11
Uncharacterized	75	66	67	88	85	69*	67	89
	C:N molar ratio							
Bulk	32	26	28	8.9	5.1	5.7	9.3	13
Total characterized	7.5	7.9	9.2	(4.6)	3.5	3.1	3.3	3.6
Uncharacterized	41	37	37	(10)	5.4	6.3*	12	14
	THAS composition (mole %)							
GalN	20	26	31	33	nm	nm	nm	nm
GlcN	55	50	56	67	nm	nm	nm	nm
MA	26	24	12	0	nm	nm	nm	nm
	THAA composition (mole %)							
Acidic	26	27	21	30	26	12	17	28
Basic	12	10	11	11	8	6	7	8
Neutral	23	27	31	41	24	56	36	46
Hydrophobic	38	36	37	18	41	27	40	18

DOM increased to 13. In both experiments, bacterially derived DOM was largely uncharacterized at the molecular level and rich in C relative to N.

Most oceanic DOM is of marine origin (*21*, *22*), refractory (*20*, *21*, *23*), molecularly uncharacterized (*6*, *7*), rich in C relative to N (C:N = 10 to 25) (*16*, *24*), and exists as relatively small molecules (*1*, *15*, *24*). The simple experiments described here demonstrate that the bulk properties of bacterially derived DOM are similar to those of marine DOM. The size distribution of DOM in the glutamate experiment was investigated using ultrafiltration (*15*). After 6 months, 84 ± 3% of the DOC was <10 kD in size, consistent with the size distribution of marine DOM (>90% of DOC is <10 kD) (*15*).

The amino acid composition of marine DOM is relatively rich in neutral amino acids (30 to 40 mole %) and depleted in basic amino acids (5 to 10 mole %) (*25*, *26*) compared with marine organisms, including bacteria (neutral = 25 mole %; basic = 15 mole %) (*27*). During

the incubations, the amino acid compositions of bacterially derived DOM rapidly shifted from a composition similar to that of microorganisms to a composition similar to that of marine DOM (Table 2). A similar transition was observed in amino sugar compositions of bacterially derived DOM in the glucose incubations. The initial amino sugar composition of DOM in the incubations was similar to that in bacterial cells (*28*), whereas only glucosamine and galactosamine were detected at the end of the incubation (Table 2). The glucosamine:galactosamine ratio (2:1) in bacterially derived DOM at the end of the incubation was similar to the ratio of these amino sugars in seawater (*28*).

Recent studies have identified specific components of the cell envelopes of marine bacteria in DOM from the surface and deep ocean (*4*, *5*). In addition to this evidence for a bacterial source of marine DOM, laboratory studies with radiotracers and marine bacteria noted the production of refractory DOM from simple compounds (*9–11*). Results from our study support these observations, and indicate that diagenetic processing by microorganisms is rapid and critical for shaping the composition and refractory nature of marine DOM.

The amino sugar muramic acid is uniquely found in the repeating disaccharide backbone of the bacterial cell wall polymer commonly known as peptidoglycan, and it is therefore an excellent biomarker for peptidoglycan in DOM (*28*). In the glucose experiment, muramic acid C concentrations of 35 to 89 nM were measured during the first week of incubation, and based on a typical muramic acid content in peptidoglycan (*29*), we estimate that peptidoglycan accounted for ~1% of the C and ~7.5% of the N in DOM. Muramic acid concentrations were below detection after 1 year of incubation (Table *2*), indicating that peptidoglycan was absent in the refractory DOM derived from bacteria. This finding was unexpected given recent observations in marine DOM of high D/L enantiomer ratios in specific amino acids that are found in the peptide component of peptidoglycan (*5*). Overall, these results suggest that bacterial degradation sufficiently alters the structure of peptidoglycan so that its polysaccharide component is no longer recognizable at the molecular level.

Our results are inconsistent with several mechanisms that have been proposed for the formation of refractory organic matter in the ocean. It is unlikely that abiotic condensation reactions or humification processes (*8*) were important for producing refractory DOM in our study, because the incubations were conducted in the dark at low temperature, concentrations of reactants were low, and the compositional changes were rapid (hours to days). Thus, it appears that biological processes were critical for the formation of refractory DOM. Specific biochemical components of cells can be selectively preserved during diagenesis (*30*), but these are relatively minor constituents of cells that should only slowly accumulate. Amino acids, neutral sugars, and amino sugars typically compose >70% of bacterial biomass (*29*), but these biochemicals were relatively minor components of bacterially derived DOM. It appears that the selective preservation of unusual biochemical components of cells could not, by itself, account for the rapid formation and accumulation of bacterially derived DOM.

Components of bacterial cells are released into the surrounding water as DOM through a variety of biological processes, including direct release (*11*, *31*), viral lysis (*32*), and grazing (*33*). Exoenzyme activity is critical for the microbial utilization of this DOM, and it appears that enzymatic activity plays an important role in the formation of refractory DOM that is of small size (*34*). It is possible that nonspecific or promiscuous activities of enzymes, that occur with much lower efficiency than primary activities (*35*), occasionally produce fragments from macromolecules that escape recognition by bacterial enzymes and molecular-level chemical analyses. Given this scenario, the rate of formation of refractory DOM is dependent on the rate of microbial activity. This relatively simple mechanism could be responsible for much of the sequestration of fixed C in the ocean.

References and Notes

1. R. Benner, J. D. Pakulski, M. McCarthy, J. I. Hedges, P. G. Hatcher, *Science* **255**, 1561 (1992).
2. M. D. McCarthy, T. Pratum, J. Hedges, R. Benner, *Nature* **390**, 150 (1997).
3. L. L. Clark, E. D. Ingall, R. Benner, *Nature* **393**, 426 (1998).
4. E. Tanoue, S. Nishiyama, M. Kamo, A. Tsugita, *Geochim. Cosmochim. Acta* **59**, 2643 (1995).
5. M. D. McCarthy, J. I. Hedges, R. Benner, *Science* **281**, 231 (1998).
6. P. M. Williams, E. R. M. Druffel, *Oceanography* **1**, 14 (1988).
7. J. I. Hedges *et al.*, *Org. Geochem.* **31**, 945 (2000).
8. G. R. Harvey, D. A. Boran, L. A. Chesal, J. M. Tokar, *Mar. Chem.* **12**, 119 (1983).
9. J. E. Brophy, D. J. Carlson, *Deep-Sea Res.* **36**, 497 (1989).
10. L. J. Tranvik, *FEMS Microbiol. Ecol.* **12**, 177 (1994).
11. K. Stoderegger, G. J. Herndl, *Limnol. Oceanogr.* **43**, 877 (1998).
12. An artificial seawater medium (0 ± 1 μM C) was prepared using precombusted salts (NaCl, KCl, $MgSO_4$, $CaCl_2$) with $NaHCO_3$ and organic-free, deionized water (Milli-RO and Milli-Q UV Plus). The filtrate (<0.7 μm pore size GF/F) from seawater samples was used as a natural inoculum (2% v/v) of marine bacteria. Based on the DOC content in the Gulf of Mexico seawater inoculum, the final concentration of DOC in the inoculated medium prior to the addition of glucose was 1 ± 1 μM. Based on the DOC content in the Sagami Bay seawater inoculum, the final concentration of DOC in the inoculated medium prior to the addition of glutamate was 2 ± 1 μM.
13. A. Skoog, R. Benner, *Limnol. Oceanogr.* **42**, 1803 (1997).
14. P. Lindroth, K. Mopper, *Anal. Chem.* **51**, 1667 (1979).
15. H. Ogawa, N. Ogura, *Nature* **356**, 696 (1992).
16. H. Ogawa, R. Fukuda, I. Koike, *Deep-Sea Res. I* **46**, 1809 (1999).
17. THNS is the sum of seven neutral sugars (glucose, galactose, fucose, rhamnose, mannose, arabinose, and xylose), and THAS is the sum of three amino sugars [galactosamine (GalN), glucosamine (GlcN), and muramic acid (MA)], which were measured by HPLC after HCl hydrolysis (3 M, 5 hours, 100°C) (*13, 28*). No samples had measurable mannosamine. MA was not detected after 1 year. THAA is the sum of 17 amino acids determined by HPLC (*14*) after vapor-phase hydrolysis (*36*). THAA composition is presented in Table 2 as four families of amino acids: acidic (aspartic acid, glutamic acid), basic (arginine, histidine, lysine), neutral (serine, glycine, threonine, tyrosine), and hydrophobic (β-alanine, alanine, γ-aminobutyric acid, methionine, phenylalanine, valine, isoleucine, leucine). The concentrations of individual amino acids are available as supplementary Web tables at www.sciencemag.org/cgi/content/full/292/5518/917/DC1
18. J. A. Fuhrman, R. L. Ferguson, *Mar. Ecol. Prog. Ser.* **33**, 237 (1986).
19. J. Rich, H. W. Ducklow, D. L. Kirchman, *Limnol. Oceanogr.* **41**, 595 (1996)
20. N. Ogura, *Mar. Biol.* **13**, 89 (1972).
21. P. M. Williams, E. R. M. Druffel, *Nature* **330**, 246 (1987).
22. S. Opsahl, R. Benner, *Nature* **386**, 480 (1997).
23. R. T. Barber, *Nature* **220**, 274 (1968).
24. R. Benner, B. Biddanda, B. Black, M. D. McCarthy, *Mar. Chem.* **57**, 243 (1997).
25. M. McCarthy, J. Hedges, R. Benner, *Mar. Chem.* **55**, 281 (1996).
26. U. Hubberten, R. J. Lara, G. Kattner, *Mar. Chem.* **45**, 121 (1994).
27. G. L. Cowie, J. I. Hedges, *Limnol. Oceanogr.* **37**, 703 (1992).
28. K. Kaiser, R. Benner, *Anal. Chem.* **72**, 2566 (2000).
29. F. C. Neidhardt, J. L. Ingraham, M. Schaechter, *Physiology of the Bacterial Cell: A Molecular Approach* (Sinauer, Sunderland, MA, 1990), pp. 102–130.
30. P. G. Hatcher, E. C. Spiker, N. M. Szeverenyi, G. E. Maciel, *Nature* **305**, 498 (1983).
31. A. W. Decho, *Oceanogr. Mar. Biol. Annu. Rev.* **28**, 73 (1990).
32. L. M. Proctor, J. A. Fuhrman, *Nature* **343**, 60 (1990).
33. T. Nagata, D. L. Kirchman, *Mar. Ecol. Prog. Ser.* **83**, 233 (1992).
34. R. M. W. Amon, R. Benner, *Limnol. Oceanogr.* **41**, 41 (1996).
35. P. J. O'Brien, D. Herschlag, *Chem. Biol.* **6**, 91 (1999).
36. A. Tsugita, T. Uchida, H. W. Mewes, T. Atake, *J. Biochem.* **102**, 1593 (1987).

37. We thank Y. Fujimoto of the Ocean Research Institute for nutrient analyses. H.O. acknowledges for funding from the Ministry of Education, Science and Culture of Japan. R.B. acknowledges funding from NSF. We thank J. Hedges and the Marine Organic Geochemistry group of the University of Washington for comments that improved the manuscript.

21 November 2000; accepted 21 March 2001

Bulk Chemical Characteristics of Dissolved Organic Matter in the Ocean

Ronald Benner,* J. Dean Pakulski, Matthew McCarthy, John I. Hedges, Patrick G. Hatcher

Dissolved organic matter (DOM) is the largest reservoir of reduced carbon in the oceans. The nature of DOM is poorly understood, in part, because it has been difficult to isolate sufficient amounts of representative material for analysis. Tangential-flow ultrafiltration was shown to recover milligram amounts of >1000 daltons of DOM from seawater collected at three depths in the North Pacific Ocean. These isolates represented 22 to 33 percent of the total DOM and included essentially all colloidal material. The elemental, carbohydrate, and carbon-type (by ^{13}C nuclear magnetic resonance) compositions of the isolates indicated that the relative abundance of polysaccharides was high (~50 percent) in surface water and decreased to ~25 percent in deeper samples. Polysaccharides thus appear to be more abundant and reactive components of seawater DOM than has been recognized.

Dissolved organic matter (DOM) in the oceans is important in the global carbon cycle (*1*), supports heterotrophic activity (*2*), and affects the penetration of light and exchange of gases at the sea surface (*3*). Despite its importance, relatively little is known about the composition and reactivity of marine DOM because of the lack of suitable methods for its isolation from seawater. Direct biochemical analyses of DOM in seawater typically account for less than 15% of the total mixture (*4*, *5*), and many techniques that would provide more comprehensive structural information, such as nuclear magnetic resonance (NMR) and infrared spectroscopy, require the isolation of DOM from the much more abundant salts in seawater. The conventional method for isolation has been adsorption of acidified DOM onto nonionic XAD resins (*6*). However, this method typically recovers a small fraction (5 to 15%) of the total DOM in seawater, requires large manipulations of pH during isolation, and is selective for hydrophobic constituents.

In contrast, tangential-flow ultrafiltration concentrates organic molecules primarily on the basis of size rather than chemical properties (*7*) and requires no pH adjustments that may change chemical associations and structures. Ultrafiltration therefore appears to be a more appropriate method for isolating a representative fraction of DOM than adsorption on XAD resins. In this report we describe the bulk chemical properties of DOM isolated by tangential-flow ultrafiltration from three depths in the open North Pacific Ocean.

Samples were collected during April 1991 from Station ALOHA (22°45′N, 158°00′W) located about 100 km north of Oahu, Hawaii. Hydrographic and basic chemical and biological parameters have been monitored at this station since 1988 (*8*). We collected water samples in Niskin bottles fitted with Tefloncoated closure springs using a 24-bottle rosette. Samples for ultrafiltration (200 liters) were collected from three depths, 10, 765, and 4000 m, corresponding to the surface, oxygen-minimum, and deep waters (Table 1).

Immediately following collection, we pumped water samples through 0.2-μm pore size, prerinsed Nuclepore polycarbonate filters and subsequently through 1000-dalton cutoff (~1-nm pore size) spiralwound polysulfone filters using an Amicon DC1OL ultrafiltration system. Total processing time for each sample was ~12 hours. Dissolved organic carbon (DOC) is operationally defined here as all organic carbon passing a 0.2-μm pore size filter and therefore includes all colloids <0.2 μm. We measured concentrations of DOC by a high-temperature oxidation method (*9*) in which a Shimadzu TOC 5000 analyzer was used (*10*). Concentrations of DOC and volumes of water were recorded for the initial water, the ultrafiltered concentrate, and the ultrafiltrate so that a mass balance of DOC could be established (*11*). Most sea salts were removed from ultrafiltered concentrates by diafiltration, and the samples were stored frozen for transport to the laboratory. Samples were dried under vacuum in a Savant SpeedVac concentrator.

The concentration of DOC in surface water (82 μM) was approximately two times as large as concentrations in oxygen-minimum and deep waters (Table 1). DOC profiles of this magnitude and shape have been observed at many ocean sites and interpreted to reflect the presence of labile organic matter of planktonic origin in surface water that is absent from older water at depth. Mass balance calculations indicate that all of the DOC in initial water samples was accounted for in the ultrafiltered concentrates (> 1000 daltons) and ultrafiltrates (<1000 daltons) (Table 1); thus, contamination and processing losses were minimal. We recovered 33, 25, and 22% of the total DOC from surface, oxygen-minimum, and deep waters (Table 1). The observed trend of a decrease in the >1000-dalton fraction from surface water to deep water suggests that material in the colloidal size range comprised an important part of the reactive components of DOM.

Our results on the size distribution of DOM are similar to those of Carlson *et al.* (*11*), who found that ~34% of the persulfate-oxidizable DOC (~88 μM) in North Atlantic surface waters was > 1000 daltons. However, a recent investigation by Sugimura and Suzuki (*9*) in the Northwestern Pacific Ocean indicated that ~85% of the total DOC (~290 μM) in surface waters was >1800 daltons. Similarly, these investigators found that ~85% of the total DOC (~95 μM) in Northwestern Pacific deep water (4000 m) was >1800 daltons (*9*). Such large differences between studies are beyond the range expected for natural variability, especially for two samples from 4000-m depth in the North Pacific Ocean, and suggest that there are systematic biases in DOM measurement or characterization. Because of uncertainty about the accuracy of seawater DOC measurements (*5*, *9*), we also independently determined the organic carbon content of the ultrafiltered DOM (UDOM) by flash combustion (~1100°C) of the dried powder in a Carlo Erba 1106 CHN analyzer of the type used to quantitatively combust a wide variety of carbonaceous substances. The weight percentages of organic carbon measured were 10 to 25% lower than those calculated from the total DOC content (Shimadzu analyzer) and mass of the isolated samples (Table 1). Thus, we found no evidence for low DOC measurements that could be attributed to incomplete oxidation of the higher molecular weight or colloidal components of our DOM samples.

The atomic C/N values of the UDOM were lowest (15.3) in surface water and highest (22.5) in oxygen-minimum water (Table 2). These values lie in the middle of the range of 10 to 25 determined for bulk seawater DOM with the use of wet oxidation methods (*4*, *5*). Humic substances isolated from

R. Benner and J. D. Pakulski, Marine Science Institute, University of Texas at Austin, Port Aransas, TX 78373.
M. McCarthy and J. I. Hedges, School of Oceanography, University of Washington, Seattle, WA 98195.
P. G. Hatcher, Fuel Science Program, The Pennsylvania State University, University Park, PA 16802.

*To whom correspondence should be addressed.

Originally published 20 March 1992

Table 1. Hydrographic data for samples collected at Station ALOHA (22°45.0′N, 158°0.O′W) and the concentrations of dissolved organic carbon (DOC), percentages of DOC recovered using tangential-flow ultrafiltration, and weight percentages of organic carbon (Wt%OC) in the recovered isolates as determined by direct-injection, high-temperature catalytic oxidation (HTCO) and the dry weights of the recovered isolates and by flash combustion of dried powders in a CHN analyzer.

Depth (m)	Salinity (per mil)	Temperature (°C)	Dissolved O_2 (μM)	DOC (μM)	Volume (liters)	% DOC recovered	% initial* DOC	Wt%OC† HTCO	Wt%OC† CHN
10	34.960	23.28	222.2	82	200	33	110	7.37	5.95
765	34.309	4.72	31.8	38	200	25	118	2.17	1.70
4000	34.684	1.46	154.2	41	200	22	106	1.96	1.77

*% Initial DOC = 100 $(DOC_{concentrate} + DOC_{ultrafiltrate})(DOC_{initial\ water})^{-1}$. †Sea salts were not completely removed during diafiltration resulting in weight percentages of organic carbon that are lower than those expected (~45%) for pure organic matter.

Table 2. Atomic C/N ratios from elemental analysis and area percentages of the major ^{13}C NMR peaks for DOM isolated by ultrafiltration. Functional group assignments are: C-C, carbon singly bonded to carbon; C-O, carbon singly bonded to oxygen; O-C-O, carbon singly bonded to two oxygens; C=C, carbon doubly bonded to carbon; O-C=O, carboxyl and ester carbon; C=O, carbonyl carbon.

Depth (m)	C/N	C-C (%)	C-O (%)	O-C-O (%)	C=C (%)	O-C=O (%)	C=O (%)
10	15.3	26	43	11	7	13	3
765	22.5	32	24	5	21	14	4
4000	19.6	27	19	6	19	15	5

the Pacific Ocean are carbon-rich [C/N ratio ≈34 (*12*)] relative to our UDOM samples; this difference reflects the bias of XAD resins against more polar nitrogen-containing DOM. Concentrations of dissolved organic nitrogen (DON) in the >1000-dalton size fraction (0.4 to 1.8 μM; from Tables 1 and 2) agree with concentrations determined recently for total DON (2 to 6 FM) in the North Pacific Ocean with the use of both high-temperature combustion (1100°C) and ultraviolet oxidation methods (*13*) and agree as well with average concentrations of total DON (5 to 8 μM) reported for these same water samples (*14*). These measurements are at odds, however, with other recent estimates of DON concentrations and C/N values for marine DOM. Suzuki and colleagues (*9*, *15*) reported average C/N values near 7 for the total DOM in surface and deep waters of the Northwestern Pacific Ocean and concentrations of higher molecular weight (> 5000 daltons) DON that were 20 to 70 times as large as our estimates for DON >1000 daltons. As discussed above, these large differences are beyond those expected for natural variability.

Structural features of the isolated DOM were investigated by cross polarization magic angle spinning (CP/MAS) ^{13}C NMR (*16*). The ^{13}C NMR spectrum of the UDOM from surface water shows a dominant peak at 72 ppm and lesser peaks at 21, 40, 100, and 176 ppm (Fig. 1). Carbohydrates are the major family of biomolecules producing C–O resonances at 72 ppm and O–C–O resonances at 100 ppm. Unsubstituted alkyl carbons, such as methyl and methylene carbons, and amine carbons give rise to resonances between 0 and 50 ppm, and carboxyl, ester, and amide carbons produce resonances around 176 ppm.

Major compositional differences were apparent between UDOM from surface water and UDOM from oxygen-minimum and deep waters (Fig. 1). Integrated areas for C–O and O–C–O resonances indicate that there was a sharp decrease in the relative abundance of carbohydrate carbon from 54% in the UDOM from surface water to 29 and 25% in UDOM from oxygen-minimum and deep waters (Table 2). Surface-water UDOM had a threefold lower relative abundance of aromatic or olefinic carbons (in 110 to 160 ppm) than UDOM from deeper waters (Table 2). On the basis of these data and the vertical distribution of radiocarbon in DOM in the North Pacific Ocean (*17*), which indicates that labile and refractory components of DOM coexist in surface water, whereas refractory components dominate in deeper waters, it appears that high molecular weight polysaccharides (> 1000 daltons) made up an important part of the labile DOM in surface water. Estimates of carbohydrate concentrations in the colloidal size fraction (1 to 200 nm) of DOM ranged from ~14 μM C in surface waters to ~2 μM C in deeper waters (Fig. 2).

The main structural features of the surface-water UDOM were very different from those of humic substances isolated by hydrophobic adsorption from seawater. The UDOM from surface water was rich in carbohydrates, whereas XAD-isolated humic substances are rich in unsubstituted alkyl and carboxyl carbons (*18*). Moreover, structural features of XAD-isolated DOM revealed by ^{1}H- and ^{13}C-NMR depict a material that is compositionally invariant with oceanic environment (*18*) and depth (*19*); these characteristics suggest that the XAD-isolated DOM is composed primarily of the older, more refractory components of DOM. There are, however, some similarities between the structural features of UDOM and humic substances from deep water. Both of the isolated fractions contained a significant aromatic or olefinic component and similar carboxyl contents, but the deepwater UDOM sample was enriched in carbohydrate and depleted in unsubstituted alkyl carbon relative to deep-water humic substances (*19*).

We also determined the carbohydrate content of the UDOM samples using a modified MBTH assay (*20*) to confirm the ^{13}C-NMR carbohydrate estimates. In the modified MBTH assay hydrochloric acid was replaced with sulfuiric acid to more completely hydrolyze resistant polysaccharides, such as cellulose and chitin (*21*). The modified MBTH assay indicated that carbohydrates accounted for 49, 18, and 19% of the total C in surface, oxygen-minimum, and deep-water UDOM samples. The similarity between these data and those determined by ^{13}C-NMR confirms our estimate of carbohydrates in the UDOM samples and indicates that the modified

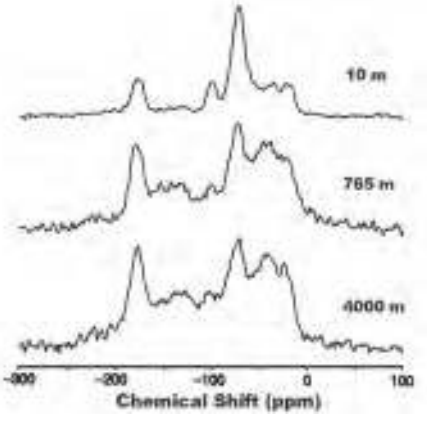

Fig. 1. Conventional CP/MAS ^{13}C NMR spectra of DOM isolated by ultrafiltration (>1000 daltons) from surface water (10 m), oxygen-minimum water (765 m), and deep water (4000 m) at 22°45′N, 158°00′W in the Pacific Ocean.

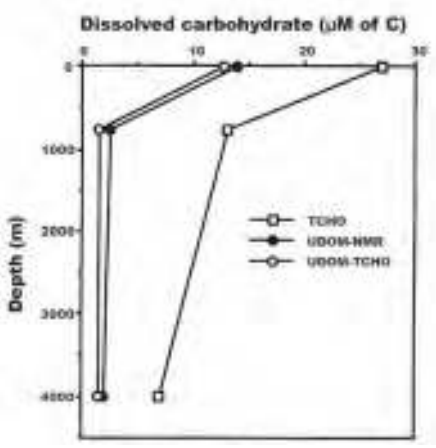

Fig. 2. Concentrations of dissolved carbohydrates in ultrafiltered DOM as determined by ^{13}C NMR (UDOM-NMR) and a modified MBTH assay (UDOM-TCHO) and the concentrations of total dissolved carbohydrates as determined by using the same modified MBTH assay (TCHO).

MBTH assay yielded reasonably accurate estimates of total carbohydrate content.

Because ~70% of marine DOM was <1000 daltons (<1 nm), we do not know if the composition of the UDOM was representative of the total DOM. We used the modified MBTH assay to determine the total dissolved carbohydrate concentrations in the seawater samples collected for ultrafiltration. The modified MBTH assay yielded total dissolved carbohydrate concentrations of 27, 13, and 7 μM C in surface, oxygen-minimum, and deep-water samples (Fig. 2). These dissolved carbohydrate concentrations corresponded to 33, 34, and 17% of the total DOC, and were similar to those in the UDOM samples. Thus, ultrafiltration recovered a representative fraction of the MBTH-reactive carbohydrates from seawater.

Our measurements of total dissolved carbohydrate concentrations are higher than most earlier estimates, which indicated that carbohydrates accounted for 10 to 15% of the total DOC measured by wet oxidation methods (*5*, *22*) although values as high as ~35% were reported for the Caribbean Sea (*23*). We believe that the higher concentrations of carbohydrates measured with the modified MBTH assay result from the more complete hydrolysis of structural polysaccharides (*21*), which, as we have shown, appear to be abundant in the upper ocean.

The application of tangential-flow ultrafiltration to seawater samples has allowed a broad chemical characterization of a relatively large fraction of marine DOM, including all colloidal material. Compared to conventional hydrophobic adsorption techniques, ultrafiltration is less chemically selective and capable of recovering a greater portion of DOM. Our initial characterizations indicated that the concentration of the >1000- dalton size fraction of seawater DOM is one-tenth of that indicated by Suzuki and colleagues (*9*, *15*) and that the C/N values are two to three times as large. Despite these differences, we concur that high molecular weight components of DOM are reactive and suggest that polysaccharides are dominant components of this reactive material, perhaps supporting much of the heterotrophic activity in the surface ocean. Use of ultrafiltration to recover DOM from seawater for experimental manipulations and detailed molecular-level characterizations will help resolve the above differences and provide a new understanding of the sources and reactions of the organic molecules composing this major carbon reservoir.

References and Notes

1. W. F. Pitt *et al.*, *Am. Sci.* **78**, 310 (1990); J. I. Hedges, *Mar. Chem.*, in press.
2. L. R. Pomeroy, *BioScience* **24**, 499 (1974); F. Azam *et al.*, *Mar. Ecol. Progr. Ser.* **10**, 257 (1983).
3. E. Goldberg and A. Bard, *Appl. Geochem.* **3**, 3 (1988).
4. P. J. Williams, in *Chemical Oceanography*, J. P. Riley and G. Skirrow, Eds. (Academic Press, London, 1975), pp. 301–363.
5. P. M. Williams and E. R. M. Druffel, *Oceanography* **1**, 14 (1988).
6. E. M. Thurman, *Organic Geochemistry of Natural Waters* (Nijhoff/Junk, Dordrecht, the Netherlands, 1985), chap. 10.
7. M. Cheryan, *Ultrafiltration Handbook* (Technomic, Lancaster, 1986), chap. 1.
8. S. Chiswell, E. Firing, D. Karl, R. Lukas, C. Winn, *School of Ocean and Earth Science and Technology Technical Report 1* (University of Hawaii, Honolulu, 1990).
9. Y. Sugimura and Y. Suzuki, *Mar. Chem.* **24**, 105 (1988).
10. Analyses of DOC were made using a Pt catalyst (0.5% Pt on Al_2O_3 support) at 680°C. Samples were filtered (0.2-μm pore size), acidified (10% H_3PO_4) to a pH of −2, and purged for 5 min immediately before analysis with the same ultrahigh instrument blank (22 ± 3 μM C) were measured at the time of sample analysis [R. Benner and M. Strom, *Mar. Chem.*, in press].
11. D. J. Carlson, M. L. Brann, T. H. Magur, L. M. Mayer, *Mar. Chem.* **16**, 155 (1985).
12. K. J. Meyers-Schulte and J. I. Hedges, *Nature* **321**, 61 (1986).
13. T. W. Walsh, *Mar. Chem.* **26**, 295 (1989).
14. J. I. Hedges, B. A. Bergamaschi, R. Benner, *ibid.*, in press.
15. Y. Suzuki, Y. Sugimura, T. Itoh, *ibid.* **16**, 83 (1985).
16. Solid-state NMR spectra were obtained using a Chemagnetics Inc. M-100 spectrometer. Conditions were chosen to insure that the NMR signal intensities quantitatively represented the carbon types observed in the samples [M. A. Wilson, *NMR Techniques and Applications in Geochemistry and Soil Chemistry* (Pergamon, Oxford, 1987)]. Approximately 50,000 transients, having pulse delays of 1 s, sweep widths of 14 kHz, contact times of 1 ms, and 90° ^1H pulses of 5.8 s were acquired at a field strength of 2.35 Tesla.
17. P. M. Williams and E. R. M. Druffel, *Nature* **330**, 246 (1987).
18. D. H. Stuermer and J. R. Payne, *Geochim. Cosmochim. Acta* **40**, 1109 (1976); R. B. Gagosian and D. *ibid.* **12**, 119 (1983); M. A. Wilson, A. H. Gillam, P. J. Collin, *Chem. Geol.* **40**, 187 (1983); R. Malcolm, *Anal. Chim. Acta* **232**, 19 (1990).
19. J. I. Hedges, P. G. Hatcher, J. R. Ertel, K. J. Meyers-Schulte, *Geochim. Cosmochim. Acta*, in press.
20. C. M. Burney and J. McN. Sieburth, *Mar. Chem.* **5**, 15 (1977).
21. J. D. Pakulski and R. Benner, in preparation.
22. C. M. Burney, K. M. Johnson, D. M. Lavoie, J. McN. Sieburth, *Deep-Sea Res.* **26A**, 1267 (1979).
23. C. M. Burney, P. G. Davis, K. M. Johnson, J. McN. Sieburth, *Mar. Biol.* **67**, 311 (1982).

24. We thank the scientists, captain, and crew on the R.V. *Alpha Helix* for assistance collecting water samples and D. Karl and R. Lukas for providing logistical support. We are grateful to M. Strom for assistance with DOC measurements and ultrafiltration experiments. We also acknowledge J. Schmover for help with integration of the NMR spectra. This research was supported by grants from the National Science Foundation (BSR 8910766 and OCE 9102407 to R.B. and BSR 8718423 and OCE 9102150 to J.H.). Contribution 830 of the University of Texas Marine Science Institute and contribution 1918 of the University of Washington School of Oceanography.

12 November 1991; accepted 31 January 1992

Microbes, Molecules, and Marine Ecosystems

Farooq Azam and Alexandra Z. Worden

Antonie van Leeuwenhoek (1632–1723), the first observer of bacteria, would be surprised that over 99% of microbes in the sea remained unseen until *after* Viking Lander (1976) set out to seek microbial life on Mars. Through much of the 19th and 20th centuries, microbiologists focused on life-threatening pathogenic microbes or microbes as models of how life "works" at the molecular level. But heightened concerns for ocean health and biodiversity, highlighted in the 2003 Pew Oceans Commissions report (*1*), prompted microbial explorations of the sea with state-of-the-art tools such as satellite and laser-based imaging, as well as massive genomic surveys rivaling the human genome project. This has led to a gold rush of discoveries underscoring critical influences of microbes on marine ecosystems and carrying significant implications for sustainability, global climate, and human health. The challenge is integrating these discoveries at the systems level to elucidate microbial roles in overall system resilience. Understanding the role of microbes in structuring healthy and stressed marine ecosystems will provide the mechanistic basis for prognostic models. Accomplishing this may require a new and unifying framework for conceptualizing these ecosystems.

Excitement over the "microbial ocean" was roused by the 1977 seminal discovery by Hobbie (*2*) and later studies that pelagic bacteria are hugely abundant (10^6 ml^{-1}), accounting for most oceanic biomass and metabolism (*3*). They had eluded detection because most are extremely small—only a few percent of *Escherichia coli* in volume—and uncultivable. Thus, in order to measure bacterial biodiversity and in situ metabolism, microbial oceanographers had to devise cultivation-independent methods. Results show that bacteria are a major biological force in the oceanic carbon cycle and ecosystem structure.

Photosynthetic bacteria *Prochlorococcus* and *Synechococcus* are the most abundant oceanic primary producers, and their sequenced genomes provide new ecological insights (*4*–*6*). Other discoveries confront oceanographers and conservation biologists with the probability that many functional capabilities and mechanisms remain unknown. For instance, a bacterial gene for proteorhodopsin was discovered 3 years ago (*7*). This pigment, thought to exist only in Archaea, converts light energy directly into an electrical gradient across the cell membrane. The gene occurs in divergent marine bacterial taxa and diverse environments (*8*); hence, inclusion of proteorhodopsin activity may change oceanic energy budgets. Another important example is the discovery of oceanwide distribution of anoxygenic phototrophic bacteria that contribute to oceanic energy and carbon budgets (*9*). Nitrogen budgets, a regulating force of carbon processing and sequestration, must also be reconsidered given new evidence for microbial N_2 fixation as a common feature of oceanic systems (*10*, *11*). Despite tremendous diversity, a single bacterial clade can dominate numerically. The α-proteobacterial clade SAR11 constitutes ~30% of Sargasso Sea surface cells (*12*), and a newly discovered cluster within the *Roseobacter* clade, found throughout temperate and polar regions, makes up ~20% of Southern Ocean bacteria (*13*). Finally, massive marine prokaryotic metagenome sequencing is providing a tremendous database for discovering metabolic capabilities and new ways to conceptualize and study prokaryotic biodiversity (*14*).

Environmental genomics is also revealing bacterial interactions with marine animals, and their influences on animal populations and ecosystem function. Corals offer an excellent example. A recent study discovered 430 novel bacterial ribotypes associated with three coral species (*15*), and shifts in bacterial species composition appear to underlie coral health and disease (*16*, *17*). Appreciating this diversity in conservation efforts is important because functional redundancy cannot be assumed.

Marine bacteria are but one microbial realm in the ocean for which discoveries with ecosystem consequences abound. Viruses were not studied until 1989 yet are the most abundant biological entities in the sea (10^7 ml^{-1}). Bacteriophages induce bacterial mortality, creating a futile carbon cycle in which dissolved organic matter assimilated by bacteria is released via bacterial lysis and metabolized by other bacteria, enhancing upper-ocean respiration (*18*). Species specificity and host density-dependence lead phage to "kill the winner," maintaining bacterial diversity, with implications for organic matter decomposition (*19*, *20*). Phage diversity studies were initially restricted by the requirement for cultivated hosts. Now, cultivation-independent genomics reveal enormous diversity, including a picorna-like superfamily implicated in phytoplankton mortality, even of toxic bloom-forming algae (*21*, *22*). Furthermore, specific cyanophage distributions vary from coastal to open ocean, likely influencing *Prochlorococcus* or *Synechococcus* host distributions differentially (*23*).

In view of microbial abundance, diversity, dynamics, and influence on ocean chemistry, ecosystem-based conservation models must explicitly include microbes, to develop a functional view that integrates microbes, macrobes, and abiotic ecosystem components. This requires going beyond biodiversity assessment, because functional diversity depends on the environmental context of microbial expression. The task concerns an age-old theme in ecology: scale, both spatial and temporal, and the integration of scales (see the figure). Microbes are no different from larger organisms in this sense—one must study them at habitat scales relevant to their adaptive strategies to determine how their metabolism influences larger-scale ecosystem dynamics. For microbes this spatial scale is miniscule, from micrometers to millimeters. Because microbes influence ecosystems through molecular interactions, for example, involving cell surface receptors, permeases, or enzymes, the scale reduces to macromolecular, or nanometers. Thus, microbes' ecosystem activities, whether they involve carbon cycling or pathogenesis toward marine animals, should be modeled as molecular events.

Studies of biochemical interactions and fluxes have yielded valuable insights. The oceanic silicon cycle is being revised following the discovery that colonizing bacteria cause postmortem dissolution of silica from diatom cell walls (frustules). These bacteria secrete proteases that denude the silica shell of its protective protein layer and enhance silica dissolution rates (*24*, *25*). Silicon cycling, in turn, regulates diatom productivity, which is important, for example, in carbon cycling and fisheries.

Genomics opens another dimension for integrating cell biochemistry and ecosystem dynamics. Genomic exploration of two *Prochlorococcus* ecotypes has not only identified features with "…obvious roles in the relative fitness of the ecotypes in response to key environmental variables…" but has also

F. Azam is in the Marine Biology Research Division, Scripps Institution of Oceanography, University of California, San Diego, La Jolla, CA 92093, USA. E-mail: fazam@ucsd.edu
A. Z. Worden is at the Marine Biology and Fisheries Division, Rosenstiel School of Marine and Atmospheric Science, University of Miami, Miami, FL 33149, USA. E-mail: aworden@rsmas.miami.edu

Originally published 12 March 2004

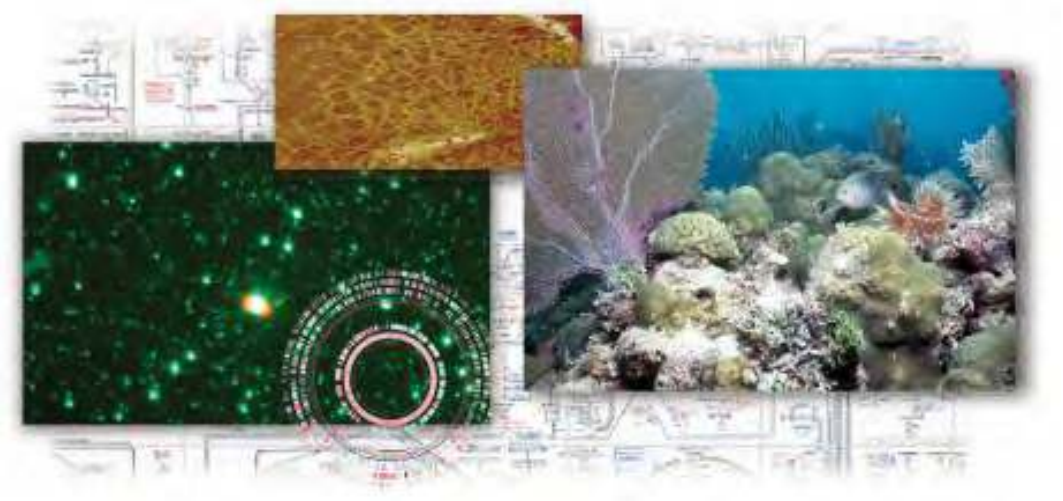

Microbes in marine ecosystems. Highly abundant and diverse bacteria and viruses (green dots) interact with biotic and abiotic ecosystem components at the molecular, or nanometer, scale yet critically influence the functioning of complex, large-scale marine ecosystems [e.g. endangered coral reefs (**right**)]. An atomic force microscope image of marine polysaccharides (**top**), a biochemical pathways chart (**background**) and genome map of *Prochlorococcus* provide examples of the context for analysis of complex marine ecosystems as dynamic molecular architectures.

inferred biochemical bases for ecotype-specific environmental impacts (*5*). The *Silicibacter pomeroyi* genome is yielding ecophysiological insights into bacteria producing dimethyl sulfide (DMS), a volatile compound that influences cloud formation (*26*, *27*). *S. pomeroyi* degrades dimethylsulfoniopropionate (DMSP) via several pathways, but only one leads to DMS; thus, the relative expression of particular DMSP-degrading enzymes regulates climate. Overarching the microbial activities is the physical organization of organic matter in seawater, allowing the visualization of ecosystems as molecular architectures. Seawater is structured with cross-linked polymers, colloids, and nano- and microgels, creating an organic matter continuum and a wealth of surfaces displaying activity and biodiversity hot-spots (*3*). This structure provides a spatial context for microbial interactions and adaptations, and permits ecosystem analysis in terms of molecular architecture and biochemical fluxes.

These discoveries illustrate that nanoscale biochemical bases of ecosystem function are tractable, informative, and indeed essential, if we are to develop mechanistic models of ocean-basin biogeochemical dynamics. Microbial oceanography has made remarkable strides toward system inventory, exposing tremendous diversity of microbial capabilities, and spatial and temporal dynamics. Although they reveal the incredible capacity of microbes to interact with ocean systems, these studies do not address system structure or organizational processes. Biosystems exhibit variability at all organizational scales, from gene expression to groups of diverse individuals, but all display molecular interconnectedness. Analysis of marine ecosystems as biochemical matrices is complex, but not unlike, for example, that of neurobiology and systems biology. Modeling efforts must incorporate interaction mechanisms and variability at all ecosystem scales, including the nanometer-to-millimeter realm of microbes and molecules. Such an analysis can now begin, but it will require a convergence of genomics and the nascent field of microscale biogeochemistry, addressing spatially explicit biochemical interactions and their ecosystem consequences. This approach will lead to new testable hypotheses and prognostic models.

We propose consideration of concepts that are driving systems biology with its goal of elucidating all significant molecular interactions underlying the structure and functioning of a cell or an organism. The approach can be extended to marine ecosystem analysis ("ecosystems biology"), in essence treating the ecosystem as dynamic molecular architecture and appreciating real-time expression as the mechanistic basis of ecosystem dynamics. Although the goal of treating organisms and the environment as a molecular continuum is huge, the rate of progress in genomics and proteomics and its integration into oceanography—a field rich in computational talent—promises success. Ecosystems biology offers a framework for integrating genomic, biochemical, and environmental data. This framework will also unify efforts for biodiversity conservation and conservation of desirable biogeochemical states of the ocean.

PHOTO CREDITS: (CORAL REEF) DAVID I. KLINE; (EPIFLUORESCENCE MICROGRAPH) J. FUHRMAN; (ATOMIC FORCE MICROGRAPH) V. SVETLI I & E. BALNOIS. PUBLISHED IN V. SVETLI I *ET AL.. CROAT CHEM. ACTA* 79, 107 (2006); (BIOCHEMICAL PATHWAYS) © ROCHE DIAGNOSTICS GmbH

References and Notes

1. Pew Foundation Ocean Commissions report, www.pewoceans.org/oceans/oceans_report.asp (2003).
2. J. E. Hobbie *et al., Appl. Environ. Microbiol.* **33**, 1225 (1977).
3. F. Azam, *Science* **280**, 694 (1998).
4. A. Dufresne *et al., Proc. Natl. Acad. Sci. U.S.A.* **100**, 10020 (2003).
5. G. Rocap *et al., Nature* **424**, 1042 (2003).
6. B. Palenik *et al., Nature* **424**, 1037 (2003).
7. O. Beja *et al., Science* **289**, 1902 (2000).
8. J. R. de la Torre *et al., Proc. Natl. Acad. Sci. U.S.A.* **100**, 12830 (2003).
9. Z. S. Kolber *et al., Science* **292**, 2492 (2001).
10. D. G. Capone, J. P. Zehr, H. W. Paerl, B. Bergman, E. J. Carpenter, *Science* **276**, 1221 (1997).
11. J. P. Zehr *et al., Nature.* **412**, 635 (2001).
12. R. M. Morris *et al., Nature* **420**, 806 (2002).
13. N. Seije, M. Simon, T. Brinkhoff, *Nature*, **427**, 445 (2004).
14. J. C. Venter *et al., Science*, published online 4 March 2004 (10.1126/science.1093857).
15. F. Rohwer, V. Seguritan, F. Azam, N. Knowlton, *Mar. Ecol. Prog. Ser.* **243**, 1 (2002).
16. K. Patterson *et al., Proc. Natl. Acad. Sci. U.S.A.* **99**, 8725 (2002).
17. J. Frias-Lopez, A. L. Zerkle, G. T. Bonheyo, B. W. Fouke, *Appl. Environ. Microbiol.* **68**, 2214 (2002).
18. J. A. Fuhrman, *Nature* **399**, 541 (1999).
19. T. F. Thingstad, R. Lignell, *Aquat. Microbiol. Ecol.* **13**, 19 (1997).
20. J. A. Fuhrman, M. Schwalbach, *Biol. Bull.* **204**, 192 (2003).
21. M. Breitbart *et al., Proc. Natl. Acad. Sci. U.S.A.* **99**, 14250 (2002).
22. A. I. Culley, A. S. Lang, C. A. Suttle, *Nature* **424**, 1054 (2003).
23. M. B. Sullivan, J. Waterbury, S. W. Chisholm, *Nature* **424**, 1047 (2003).
24. K. Bidle, F. Azam, *Nature* **387**, 508 (1999).
25. K. Bidle, M. Manganelli, F. Azam, *Science* **298**, 1980 (2002).
26. J. M. Gonzalez *et al., Int. J. Syst. Evol. Microbiol.* **53**, 1261 (2003).
27. M. A. Moran, J. M. Gonzalez, R. P. Kiene, *Geomicrobiol. J.* **20**, 375 (2003).
28. We thank T. Hollibaugh, J. Fuhrman, and C. Beardsley for critical reading of the manuscript; V. Svetlicic, E. Balnois, and D. Kline for sharing unpublished images. Work supported by NSF (OCE132677) and NIH (RO1 A146600).

Major Bacterial Contribution to Marine Dissolved Organic Nitrogen

Matthew D. McCarthy,* John I. Hedges, Ronald Benner

Next to N_2 gas, the largest pool of reduced nitrogen in the ocean resides in the enormous reservoir of dissolved organic nitrogen (DON). The chemical identity of most of this material, and the mechanisms by which it is cycled, remain fundamental questions in contemporary oceanography. Amino acid enantiomeric ratios in the high molecular weight fraction of DON from surface and deep water in three ocean basins show substantial enrichment in D enantiomers of four amino acids. The magnitude and pattern of these D/L enrichments indicate that peptidoglycan remnants derived from bacterial cell walls constitute a major source of DON throughout the sea. These observations suggest that structural properties of specific bacterial biopolymers, and the mechanisms for their accumulation, are among the central controls on long-term cycling of dissolved organic nitrogen in the sea.

Most of the surface ocean is characterized by low to undetectable mineral nutrient concentrations. Such oligotrophic regions are central to global geochemical cycles, accounting for almost 40% of global primary production (*1*). Recently, the accumulation and advected export of dissolved organic matter (DOM) from such environments has been recognized as a major pathway for C flux in the upper ocean (*2*), a process likely regulated in part by the low levels of biologically available N (*3*). Yet these same waters contain substantial concentrations of fixed N in dissolved organic compounds (*4*). The apparent lower biological accessibility of this large organic N reservoir thus represents both a major control on upper ocean carbon cycles, and a corresponding "N pump" fundamental to closing oceanic N budgets (*3*, *4*).

The chemical identity of DON is key to understanding the mechanisms by which it is formed and escapes remineralization. Although amino acids account for most N in organisms, only a small fraction of seawater DON can be identified as amino acid by common hydrolytic methods (*5*). The vast majority of this dissolved nitrogenous material appears to be contained in amide functional groups (*6*), suggesting that most long-lived DON is hydrolysis-resistant or composed of recalcitrant nonprotein amide-containing biochemicals.

Amino acid enantiomeric ratios can provide a powerful tool for characterizing nitrogenous materials (*7*). Early work identified elevated levels of D-aspartic acid and D-alanine in the open sea, indicating that D-amino acids may serve as indicators for both DOM sources (*8*) and for abiotic transformation reactions (*9*). Limitations of earlier filtration methods, however, prevented living bacteria from being excluded as a principle source of these observations (*8*), and interpretation was further complicated by substantial variability in the observed magnitude and distribution of D/L ratios with methods then available (*10*). Recent application of large-scale tangential-flow ultrafiltration to ocean waters has allowed reproducible isolation of DOM from seawater with essentially no contamination by living organisms or particulate matter (*11*, *12*), in quantities sufficient to determine a full range of amino acid enantiomeric ratios. We have used this method to examine amino acid D/L ratios in the high molecular weight fraction of oceanic DOM from the central Pacific Ocean, the Gulf of Mexico, and the North Sea (*13*). These samples include surface and abyssal depths in two oligotrophic open ocean basins, as well as a biologically dynamic coastal region.

Recovery efficiencies of ultrafiltered DOM

M. D. McCarthy and J. I. Hedges, University of Washington, School of Oceanography, Box 357940, Seattle, WA 98195, USA. R. Benner, University of Texas, Marine Science Institute, Port Aransas, TX 78373, USA.

*To whom correspondence should be addressed.

Table 1. Bulk properties and D/L–amino acid ratios from a marine cyanobacterium and for UDOM from the Central Pacific, Gulf of Mexico, and North Sea (*13*). Bulk properties include ultrafiltered dissolved organic carbon (UDOC) and nitrogen (UDON) concentrations, and atomic carbon/nitrogen ratios (C/N)a. UDOC and UDON concentrations are derived from C/N data, the dry weight recovered, and the volume filtered. D–amino acids for UDOM-hydrolyzable amino acids (*14*) are expressed as simple enantiomeric ratios, not corrected for the racemization blanks, which are shown for comparison. Sample collection depth is indicated in meters. Asterisks indicate samples in which the D/L ratio could not be quantified reliably due to chromatographic mixtures (as indicated by GC-MS); ND (not detected), samples in which the value was less than 1.5 × racemization blank. *S. bacillaris*, *Synechococcus bacillaris* (*25*).

Bulk properties and D/L–amino acid ratios	Blank	*S. bacillaris*	Central Pacific				Gulf of Mexico			N. Sea
			2	100	375	4000 m	10	2	400 m	2 m
DOC (μM)	–	–	82	85	53	45	95	97	58	76
UDOC (μM)	–	–	22.2	22.2	10.6	8.08	21.1	9.73	1.26	10.1
UDON (μM)	–	–	1.33	1.42	0.63	0.45	1.19	0.63	0.09	0.71
(C/N)a	–	–	16.8	15.6	16.9	18.4	17.8	15.4	14.2	14.2
Asp	0.09	0.14	0.39	0.39	0.36	0.33	0.28	0.18	0.22	0.17
Glu	0.06	0.09	0.23	0.17	0.20	0.19	0.16	0.13	0.14	0.12
Ser	0.03	ND	0.19	0.19	0.28	0.18	0.21	0.18	0.28	0.15
Thr	0.00	ND	ND	ND	ND	0.15	**	ND	0.05	ND
Ala	0.03	0.38	0.52	0.54	0.47	0.49	0.53	0.47	0.61	0.37
Tyr	0.04	ND	ND	0.10	**	**	ND	ND	0.10	ND
Met	0.08	ND	ND	ND	**	ND	ND	ND	ND	ND
Val	0.02	ND	ND	0.07	ND	0.06	ND	ND	0.13	ND
Phe	0.02	0.04	0.04	0.05	0.04	0.04	**	0.11	0.04	**
Leu	0.07	ND	0.12	0.13	0.12	**	ND	0.14	**	ND
Lys	0.04	0.07	ND	0.09	0.12	0.09	ND	0.08	ND	ND

Originally published 10 July 1998

(UDOM) are typically ~20% in deep waters and ~30% in surface waters (Table 1) (*12*), although very large sample sizes decrease relative recoveries (*13*). Average C/N ratios for this sample set were 17.0 for surface and 16.5 for deep water UDOM, respectively (Table 1). Hydrolyzable amino acids in these, as well as similar samples, constitute 10 to 20% of total UDOM N (*5*, *6*). Surface and deep UDOM samples show substantial and highly characteristic D/L–amino acid ratios for all the sampled ocean basins (Table 1 and Fig. 1). Alanine (Ala), aspartic acid (Asp), glutamic acid (Glu), and serine (Ser) consistently have D/L ratios far above blank levels (Table 1 and Fig. 2) (*14*). Ala shows the most pronounced enrichment, with D/L ratios near 0.5, whereas Asp, Glu, and Ser ratios generally fall between 0.2 and 0.4. No other D–amino acids could be repeatably detected above blank levels (Fig. 1). The D/L ratios of these four were remarkably consistent between widely separate locations, sampling times, and ocean depths (Fig. 1) and appear to represent a fundamental signature of UDOM throughout the ocean.

D–Amino acids are gradually produced in ancient organic matrices by abiotic racemization and may also be formed by degradation reactions of specific protein L–amino acids (*9*). However, the amino acid D/L and molar signatures in UDOM are not consistent with either of these origins. Bada and Hoopes (*9*) suggested abiotic dehydration of Ser as the most likely explanation for the near racemic D/L-Ala ratios they observed in the deep Pacific. This mechanism should produce linked decreases in Ser and threonine (Thr) as well as a concomitant buildup of α-amino butyric acid (Aba) (*9*). UDOM isolates, however, exhibit no increased D-Ala at depth and minimal variation in mole percent Ser or Thr (*5*). Similarly, no Aba was detected by gas chromatographic–mass spectral (GC-MS) analysis of any sample.

Although abiotic equilibration of enantiomeric forms is a well-known D–amino acid source, stereochemical inversion rates at ocean temperatures should be far too slow (*8*, *15*) to account for appreciable racemization over average DOM residence times of 4000 to 6000 years (*16*, *17*). Even if D–amino acid signatures represent a far older component of UDOM, the observed highly selective pattern of D enrichment remains inconsistent with abiotic generation. Although multiple factors affect geochemical racemization rates (*18*), relative rates among different amino acids generally follow a regular succession (*19*). Ala in particular is among the slower amino acids to racemize (*20*). At the observed Ala D/L ratio of ~0.5, abiotically derived D/L ratios of both phenylalanine (Phe) and in particular Asp (*21*) should be approaching their equilibrium D/L value of 1.0 (Fig. 2). However, in UDOM values of Asp are among the lowest observed D/L ratios, and D-Phe was near blank levels (Fig. 2). Moreover, the absence of any depth trend in the D/L ratios of any amino acid (Fig. 1) argues strongly that the stereoisomeric compositions of UDOM amino acids are not generated by aging or

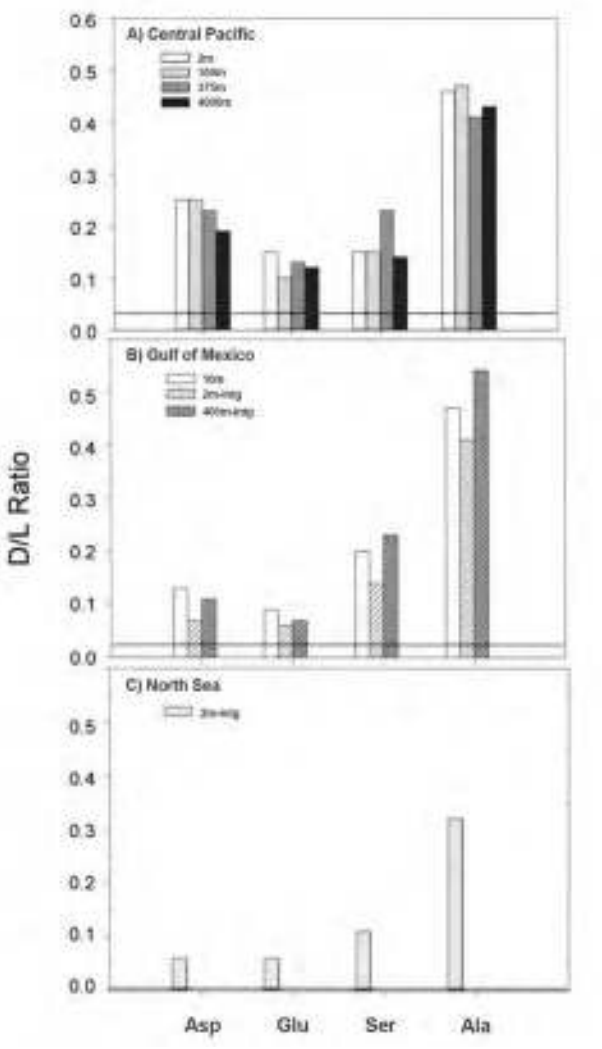

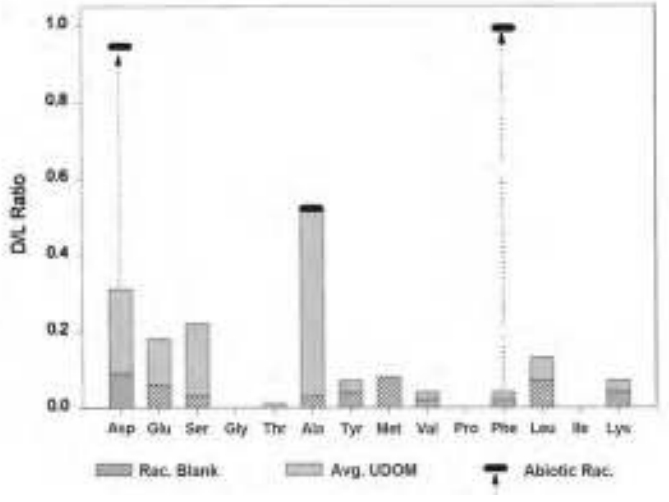

Fig. 1. (left). UDOM D/L ratios for (**A**) Central Pacific, (**B**) Gulf of Mexico, and (**C**) North Sea at various depths for the four principle amino acids. Open bar for Gulf of Mexico represents the surface sample (10 m) independently processed with 0.2-μm cartridge filters (*13*). Dashed lines reflect average values for all the other amino acids measured. D/L values in this figure have been adjusted for racemization blanks by subtracting molar quantities expected from hydrolytic racemization from total molar quantities of d-acid measured. These estimates do not account for reverse racemization of original dforms, and thus represent minimum ratios.

Fig. 2. (above). Alternative d–amino acid sources: Comparison of the magnitudes and distributions of D–amino acid ratios encountered in UDOM with those from other potential sources. Hydrolysis: Average hydrolysis blank D/L ratios (hatched bars) are superimposed on overall average UDOM D/L ratios (solid bars). Average racemization blanks were D/L ratios produced from pure L mixtures during hydrolysis. Abiotic racemization: Relative abiotic D/L ratios (dark bars), based on relative racemization rates for natural waters (*20*), were estimated to correspond with a hypothetical average "abiotic" UDOM D/L-Ala ratio of 0.5.

selective utilization of L–amino acids over time, but instead represent an intrinsic biochemical signature of seawater DON.

The principal biochemical sources of D–amino acids are peptidoglycans, the main structural component of bacterial cell walls. Peptidoglycans are heterogeneous polymers composed of an amino-sugar backbone cross-linked with peptide bridges. The bridging peptides are characterized by a number of unusual nonprotein amino acids and D–amino acids. In particular, the D-enantiomeric forms of Ala, Glu, and Asp are prevalent (*22*). D-Ala is the most abundant D–amino acid in most peptidoglycans and the only one that is universally incorporated (*23*). The enantiomeric patterns that characterize UDOM thus closely match those characteristic of bacterial peptidoglycans.

Because free-living bacteria are abundant in ocean water, direct contamination of DON isolates must be carefully excluded (*8*). Our UDOM isolation protocol was designed to remove essentially all natural microorganisms, and its efficacy has been verified both by filter intercomparison and direct bacterial counts. On average, >99% of oceanic bacteria are removed by the 0.1-μm pore size filters with which most samples were processed before UDOM isolation. In addition, the central Pacific samples were directly examined by epifluorescence microscopy after passage through the 0.1-μm pore size prefilter, and bacterial numbers were below detection (*12*). Typical estimates for N per cell of oceanic bacteria (*24*) indicate that even a maximal limit of 10% of original microbes passing the 0.1-μm pore size filter would contribute less than 1% to total UDOM amino acids. The previously mentioned lack of any depth trend in UDOM D–amino acid abundance, despite a corresponding 10-fold decrease in bacterial abundance (*12*), confirms that the observed D–amino acids derive not from concentrated bacteria, but from the vastly larger pool of nonliving DOM.

The observed high D/L ratios strongly suggest that peptidoglycans constitute a major component of UDOM N. Most characterized oceanic water column bacteria are Gram-negative, typified by relatively thin peptidoglycan layers (*22*). Although the specific bacterial sources of peptidoglycan in the open sea are unknown, the cell wall–enriched fraction of a cosmopolitan oceanic cyanobacterium, *Synechococcus bacillaris*, gives Ala D/L ratios of 0.38, in the same general range as UDOM values (Table 1) (*25*). This supports prior evidence that cell wall material of marine bacteria is compositionally similar to that of terrestrial bacteria (*26*). The contrasting relative amounts of other D–amino acids from *Synechococcus* suggests, as would be expected, that this bacterial species alone does not dominate UDOM sources.

Because of the inherent variability among known peptidoglycan structures (*27*) and the poorly defined species compositions of marine bacterial communities, finite percentages of peptidoglycan in UDOM isolates cannot be quantified with certainty. However, the following rough estimate of relative N contributions can be made using broad structural information. Ala represents the most useful source tracer, because it is a main component of proteins and has the most consistent D/L ratios within studied peptidoglycans (*22*, *23*). The D enantiomer makes up about 30% of total hydrolyzable Ala in UDOM [percent D = D/(D+L), thus 30% D is equivalent to a D/L ratio of ~0.5], whereas pure peptidoglycans contain ~40 to 50% D-Ala. On the basis of these D–amino acid contents and average structural features of common peptidoglycans and proteinacous materials, a calculation of the relative total N contributions from these two biochemical types can be made. Such a calculation (*28*) indicates that peptidoglycan accounts for a similar amount of the total N (45 to 80%) as is derived from hydrolyzable protein. Thus, in terms of N, this one structural biopolymer may be at least as abundant in UDOM as conventional proteinaceous material. In fact, this could be a minimal estimate, because conventional hydrolytic methods are optimized at near 100% for proteins (*29*) and might be substantially less efficient for peptidoglycan residues in an environmental matrix. Methods that define "protein" on the basis of total hydrolyzable amino acid yields from seawater DOM would also actually include a component of peptidoglycan-derived amino acid.

Such a large peptidoglycan component carries major implications regarding the chemical composition of the high molecular weight fraction of marine DOM. For example, UDOM also should be enriched in amino sugar, a major component of peptidoglycan. Such an enrichment is consistent with aldose-poor UDOM sugar composition (*5*), as well as the specific identification of an amino sugar component by thermal desorbtion–mass spectrometry (*30*) and pyrolysis (*31*). In addition, comparison of average amino acid compositions of UDOM (*5*) with those of planktonic sources (*32*) indicates that UDOM is measurably enriched in Ala, Glu, and Ser, consistent with an additional nonproteinaceous source for these specific amino acids. Finally, evidence for an important peptidoglycan component is supported by previously mentioned observations (*6*) of a predominant amide component not quantifiable by conventional amino acid analysis.

Although UDOM alone accounts for a substantial fraction of total oceanic DOM, the extent to which these results apply to all dissolved nitrogenous material will be determined by overall size-related compositional trends. The extent of such size-related differences within the oceanic DOM pool are not fully known. However, comparisons of many properties of UDOM and total DOM (for example, C/N ratios, stable isotopic ratios, radiocarbon content, amino acid yields, and molecular-level signatures) indicate a high degree of overall compositional similarity (*5*, *11*, *12*). Recent studies of filtered whole seawater from the surface Arctic Ocean has yielded almost identical D–amino acid distributions and ratios as those in our UDOM isolates, yet from a distinctly separate ocean region (*33*). Earlier identification of high D–amino acid concentrations in unfractionated seawaters (*8*, *9*), though more variable, is also consistent with the presence of peptidoglycan structural remnants in smaller size classes of dissolved material.

Given that N from algae, as well as most of that from bacteria, is in the form of proteins containing no D–amino acids, the elevated D/L ratios in UDOM indicate that the high molecular weight nitrogenous material dissolved in seawater is enriched in bacterial cell wall material. Bacteria are widely recognized as major consumers of organic matter and in some oligotrophic ocean regions may also be the major primary producers (*34*). Thus, abundant potential sources for bacterial cell-wall material likely exist throughout the water column. The accumulation and environmental persistence of these materials may also be related in part to intrinsic structural properties. Structural polymers can display long-term geochemical stability (*35*). The interwoven polysaccharide matrix of peptidoglycan, coupled with the unusual peptide substituents and structural variability, creates a heteropolymer resistant to many common hydrolytic enzymes (*36*). In addition, laboratory experiments and the identification of specific bacterial membrane proteins in seawater (*37*, *38*) suggest that more labile biochemicals may also be shielded by close association in a cell-wall matrix.

The high D/L-amino acid ratios found in UDOM indicate that a substantial fraction of dissolved organic N in the sea is of bacterial origin. This result challenges the common paradigm that the enormous reservoir of oceanic dissolved material is predominantly derived from algal sources. Central oceanic ecosystems are characterized by intensive bacterial recycling of DOM, coupled with similarly dynamic bacterial removal by protozoans and viruses (*39*). These processes represent direct pathways for introduction of bacterial cell wall structures into dissolved and colloidal seawater pools (*38*, *40*), where minor differences in bioreactivity may result in substantial accumulation. Bacterial predation, coupled with the intrinsic structural properties of bacterial cell wall material, may thus be among the major controls on the long-term cycling of organic N in the sea.

References and Notes

1. S. D. Killops and V. J. Killops, *An Introduction to Organic Geochemistry*, R. C. O. Gill, Ed. (Longman Geochemistry Series, Longman, New York, ed. 1, 1993).
2. C. A. Carlson, H. W. Ducklow, A. F. Michaels, *Nature*

371, 405 (1994); A. F. Michaels, N. R. Bates, K. O. Buesseler, C. A. Carlson, A. H. Knap, *ibid.* **372**, 537 (1994).
3. P. J. L. B. Williams, *Mar. Chem.* **51**, 17 (1995).
4. G. A. Jackson and P. M. Williams, *Deep Sea Res.* **32**, 223 (1985).
5. M. D. McCarthy, J. I. Hedges, R. Benner, *Mar. Chem.* **55**, 281 (1996).
6. M. D. McCarthy, J. I. Hedges, T. Pratum, R. Benner, *Nature* **390**, 150 (1997).
7. K. Kvenvolden, *Annu. Rev. Earth Planet. Sci.* **3**, 183 (1975).
8. C. Lee and J. Bada, *Limnol. Oceanogr.* **22**, 502 (1977).
9. J. L. Bada and E. A. Hoopes, *Nature* 282, 822 (1979).
10. In whole seawater hydrolysates from the central Pacific, Lee and Bada (*8*) found D/L ratios of Ala and Asp to be similar in both surface and deep waters, ranging from 0.05 to 0.16. They also reported, however, substantial differences in Asp D/L ratio between the Atlantic and Pacific. In contrast, Bada and Hoopes (*9*), using similar isolation methods, reported D/L-Ala ratios between 0.4 and 0.7 in surface Pacific waters, increasing to near racemic values of 0.8 to 1.0 in the deep.
11. R. Benner, J. D. Pakulski, M. D. McCarthy, J. I. Hedges, P. G. Hatcher, *Science* **255**, 1561 (1992).
12. R. Benner, B. Biddanda, B. Black, M. D. McCarthy, *Mar. Chem.* **57**, 243 (1997).
13. Most samples were prefiltered with an Amicon DC10 ultrafiltration system with a 0.1-μm pore size polysulfone hollow-fiber filter, before isolation of UDOM [1 nm < UDOM < 0.1 μm]. The first set of Gulf of Mexico isolates (27°N, 95°W) was prefiltered with Nucleopore 0.2-μm cartridges as an alternate and independent method. Central Pacific samples were collected in April 1992 at 12°S, 135°W from 2 to 4000 m. Gulf of Mexico samples were collected on two separate cruises. In August 1991, the 10-m sample (1000 liters) was collected at 27°N, 95°W. In July of 1995, two very large integrated samples (4000+ liters) were collected from 2 and 400 m at regular intervals on a transect between Corpus Christi, Texas, and Key West, Florida. The North Sea surface sample was also integrated on a transect across the central North Sea in April 1995. Such very large sample sizes are compositionally representative, but result in substantial decreases in relative recovery (Table 1) due to high concentration factors (*11*).
14. UDOM amino acid hydrolysis was conducted at 150°C for 70 min, generally with the method of Cowie and Hedges (*29*). Individual D– and L–amino acids were quantified as pentafluoropropyl isopropyl esters by gas chromatography with flame ionization detection (*41*), and peak identities were verified by GC-MS. Analytical variability in D/L ratios of UDOM samples was less than 15%. Racemization blanks were determined by multiple hydrolyses of pure L–amino acid mixtures, as well as protein standards. Enantiomeric ratios in commercially available D–amino acid–containing peptides could be repeatably determined to within 5%.
15. J. L. Bada and E. H. Mann, *Earth Sci. Rev.* **16**, 21 (1980).
16. P. M. Williams and E. R. M. Druffel, *Nature* **330**, 246 (1987).
17. P. H. Santschi *et al.*, *Geochim. Cosmochim. Acta* **59**, 625 (1995).
18. R. Mitterer and N. Kriausakul, *Org. Geochem.* **7**, 91 (1984); R. W. L. Kimber and P. E. Hare, *Geochim. Cosmochim. Acta*. **56**, 739 (1992).
19. J. L. Bada, in *Chemistry and Biochemistry of the Amino Acids*, G. C. Barrett, Ed. (Chapman & Hall, New York, 1985), p. 684.
20. _____, in *Kinetics of the Non-Biological Decomposition and Racemization of Aminos Acids in Natural Waters,* J. D. Hem, Ed. (American Chemical Society, Washington, DC, 1971), pp. 308–331.
21. G. A. Goodfriend, *Nature* **357**, 399 (1992).
22. H. J. Rogers, in *Aspects of Microbiology* [Van Nostrand Reinhold, Wokingham, UK, 1983), vol. 7, pp. 6–25.
23. J.-M. Ghuysen and G. D. Shockman, in *Bacterial Membranes and Walls*, L. Leive, Ed. (Dekker, New York, 1973), vol. 1.
24. J. Fuhrman, in *Primary Productivity and Biogeochemical Cycles in the Sea* (Plenum, New York, 1992), pp. 361–383.
25. Insoluble structural and cell-wall material was concentrated from lysed cells of the cosmopolitan cyanobacterium *S. bacillaris*, as described (A. Biersmith and R. Benner, *Mar. Chem.*, in press).
26. D. J. W. Moriarty, *Oecologia* **26**, 317 (1977).
27. K. H. Schleifer and O. Kandler, *Bacteriol. Rev.* **36**, 407 (1972).
28. Relative contributions of total UDOM N from proteinaceous material and peptidoglycan were estimated using the proportions of D- and L-Ala necessary to produce observed UDOM D/L ratios. All D-Ala was assumed to derive from peptidoglycans, and L-Ala was assumed to come from a mixture of peptidoglycan and proteinaceous material. Relative amino acid compositions in marine proteinaceous sources are largely invariant (*32*), and accordingly the total proteinaceous N can be approximated as 12 × (Ala-N). Similarly, an estimate of total peptidoglycan N can be derived from common peptidoglycan architecture as roughly 5.7 × (D-Ala N), which includes N contribution from both amino sugar backbone and peptide interbridges (*22*). For UDOM D/L ratios of 0.5 to 0.6 (equivalent to ~30% D) and peptidoglycan D/L ratios of 0.7 to 1.0 (equivalent to near 50% D), this calculation indicates that the peptidoglycan N is 45 to 80% as large as the proteinaceous N contribution.
29. G. L. Cowie and J. I. Hedges, *Mar. Chem.* **37**, 223 (1992).
30. J. J. Boon, V. Klap, T. Eglinton, *Org. Geochem.*, in press.
31. J. D. H. van Heemst, M. Baas, J. W. de Leeuw, R. Benner, in *Organic Geochemistry*, K. Oygard, Ed. (Falch Hurtigtrykk, Oslo, Norway, 1993), pp. 694–698.
32. G. L. Cowie and J. I. Hedges, *Limnol. Oceanogr.* **37**, 703 (1992).
33. H. P. Fitznar, J. M. Lobbes, G. Kattner, personal communication.
34. L. Campbell, H. A. Nolla, D. Vaulot, *Limnol. Oceanogr.* **39**, 954 (1994).
35. J. W. de Leuuw and C. Largeau, in *Organic Geochemistry*, M. Engle and S. A. Macko, Eds. (Plenum, New York, 1993), pp. 23–72.
36. H. J. Rogers, *Ann. N.Y. Acad. Sci.* **235**, 29 (1974).
37. E. Tanoue, *Mar. Chem.* **51**, 239 (1995).
38. T. Nagata and D. L. Kirchman, *Adv. Microb. Ecol.* **15**, 81 (1997).
39. J. A. Fuhrman and R. T. Noble, *Limnol. Oceanogr.* **40**, 1236 (1995).
40. J. A. Fuhrman and C. A. Suttle, *Oceanography* **6**, 51 (1993).
41. M. H. Engel and P. E. Hare, in *Chemistry and Biochemistry of the Amino Acids*, G. C. Barrett, Ed. (Chapman & Hall, New York, 1985), pp. 461–479.
42. We thank G. Cowie for inspiration and help with amino acid analysis, B. Black for help with sample processing, H. P. Fitznar for sharing work in progress, C. Lee for valuable discussions and insight, and D. Bear for guidance and support.

31 March 1998; accepted 11 June 1998

Dissolved Organic Carbon Support of Respiration in the Dark Ocean

Javier Arísteguí,[1*] Carlos M. Duarte,[2] Susana Agustí,[2]
Marylo Doval,[3] Xosé A. Álvarez-Salgado,[4] Dennis A. Hansell[5]

Recent evidence that dissolved organic carbon (DOC) is a significant component of the organic carbon flux below the photic layer of the ocean (*1*), together with verification of high respiration rates in the dark ocean (*2*), suggests that the downward flux of DOC may play a major role in supporting respiration there. Here we show, on the basis of examination of the relation between DOC and apparent oxygen utilization (AOU), that the DOC flux supports ~10% of the respiration in the dark ocean.

concurrent DOC and AOU observations collected in cruises conducted throughout the world's oceans (fig. S1, table S1) to examine the relative contribution of DOC to AOU and, therefore, respiration in the dark ocean. AOU increased from an average (±SE) 96.3 ± 2.0 μM at the base of the surface mixed layer (100 m) to 165.5 ± 4.3 μM at the bottom of the main thermocline (1000 m), with a parallel decline in the average DOC from 53.5 ± 0.2 to 43.4 ± 0.3 μM C (Fig. 1). In contrast, there is no significant decline in

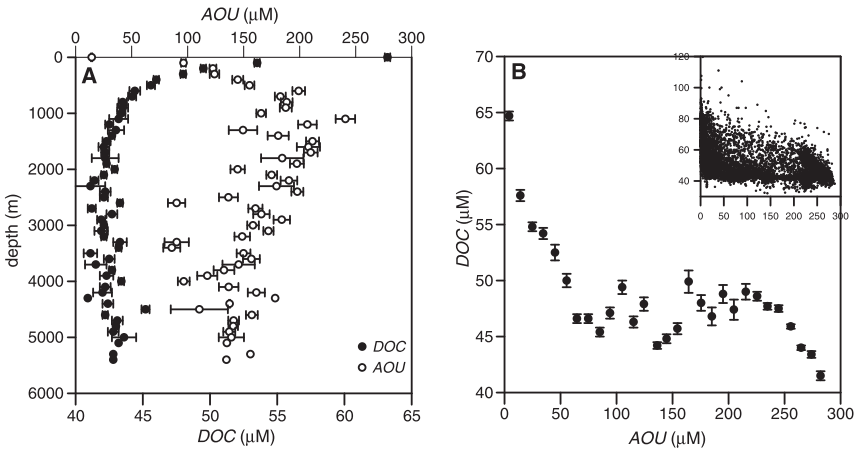

Fig. 1. The depth distribution of the average (mean ± SE of data grouped by 100-m bins, N = 9578) DOC (full circles) concentration and AOU (empty circles) in the ocean (**A**) and the relation between DOC and AOU in the ocean (**B**). The symbols represent mean ± SE DOC concentrations of data grouped by 10 μM AOU bins (N = 9824). The inset in (B) shows the relation for the raw data (N = 9824), which is described, in the interval 0 < AOU < 150, by the fitted regression equation DOC = 60.3 (±0.2) − 0.136 (±0.003) AOU (R^2 = 0.28, P < 0.0001, N = 5541). Multiple regression analysis, also using water temperature (°C) as an independent variable, improves the fit, yielding the equation DOC = 48.0 (±0.2) + 0.81 (±0.01) T − 0.058 (±0.002) AOU (R^2 = 0.69, P < 0.0001, N = 5371). The monotonic decrease of DOC for AOU > 225 corresponds to the oxygen minimum zones of the Arabian Sea, Indian Ocean, and equatorial Pacific Ocean.

The contribution of DOC to pelagic respiration below the surface mixed layer can be inferred from the relation between DOC and apparent oxygen utilization (AOU, μM O_2), a variable quantifying the cumulative oxygen consumption since a water parcel was last in contact with the atmosphere. However, assessments of DOC/AOU relations have been limited to specific regions of the ocean (*3*, *4*) and have not considered the global ocean. We assembled a large data set (N = 9824) of

DOC with increasing depth beyond 1000 m depth (Fig. 1), indicating that DOC exported with overturning circulation plays a minor role in supporting respiration in the ocean interior (*5*). Assuming a molar respiratory quotient of 0.69, the decline in DOC accounts for 19.6 ± 0.4% of the AOU within the top 1000 m (Fig. 1). This estimate represents, however, an upper limit, because the correlation between DOC and AOU is partly due to mixing of DOC-rich warm surface waters with DOC-poor cold thermocline waters (*6*). Removal of this effect by regressing DOC against AOU and water temperature indicates that DOC supports only 8.4 ± 0.3% of the respiration in the mesopelagic waters.

These results confirm that DOC makes a small but significant contribution toward the maintenance of respiratory processes in the dark ocean. DOC use accounts for only <10% of the AOU in mesopelagic waters, indicating that the bulk of the respiration within the mesopelagic zone is supported by the flux of sinking POC. This estimate for the contribution of DOC oxidation to global AOU is supported by the independent findings that net DOC production accounts for <20% of net community production in the surface ocean (*7*), that DOC export contributes to 10 % of the export below 500 m (*8*), and that the total AOU in the deep ocean is in agreement with that expected from the flux of sinking POC (*9*). It is the DOC accumulating as a function of primary production in the surface ocean, which is exported with overturning circulation, that dominates the DOC fraction of AOU development. Our findings indicate that the POC flux, which appears to be severely underestimated by sediment traps in the mesopelagic zone (*10*), is much greater than the DOC flux and supports the bulk (~90%) of the respiratory carbon demand in the dark ocean.

References

1. C. A. Carlson, H. W. Ducklow, A. F. Michaels, *Nature* **371**, 405 (1994).
2. P. A. del Giorgio, C. M. Duarte, *Nature* **420**, 379 (2002).
3. M. D. Doval, D. A. Hansell, *Mar. Chem.* **68**, 249 (2000).
4. E. T. Peltzer, N. A. Hayward, *Deep Sea Res. Part II* **43**, 155 (1996).
5. D. A. Hansell, C. A. Carlson, *Nature* **395**, 263 (1998).
6. X. A. Álvarez-Salgado, F. F. Pérez, A. F. Ríos, M. D. Doval, *Sci. Mar.* **65**, 1 (2001).
7. D. A. Hansell, C. A. Carlson, *Global Biogeochem. Cycles* **12**, 443 (1998).
8. D. A. Hansell, in *Biogeochemistry of Marine Dissolved Organic Matter*, D. A. Hansell, C. A. Carlson, Eds. (Academic, San Diego, CA, 2002), pp. 685–715.
9. R. A. Jahnke, *Global Biogeochem. Cycles* **10**, 71 (1996).
10. J. C. Scholten *et al.*, *Deep Sea Res. Part II* **48**, 243 (2001).

Supporting Online Material
www.sciencemag.org/cgi/content/full/298/5600/1967/DC1
Fig. S1
Table S1

[1]Facultad de Ciencias del Mar, Campus Universitario de Tafira, Universidad de las Palmas de Gran Canaria, 35017 Las Palmas de Gran Canaria, Spain. [2]IMEDEA (CSIC-UIB), Instituto Mediterráneo de Estudios Avanzados, Miquel Marqués 21, 07190 Esporles (Islas Baleares), Spain. [3]CCCMM (XUGA), Centro de Control de Calidade do Medio Mariño, Peirao de Vilaxoán s/n, Vilagarcía de Arousa, Spain. [4]IIM (CSIC), Instituto de Investigacións Mariñas, Eduardo Cabello 6, 36208 Vigo, Spain. [5]RSMAS, University of Miami, Miami, FL 33149, USA.

*To whom correspondence should be addressed. E-mail: jaristegui@dbio.ulpgc.es

Originally published 6 December 2002

Community Genomics Among Stratified Microbial Assemblages in the Ocean's Interior

Edward F. DeLong,[1]* Christina M. Preston,[2] Tracy Mincer,[1] Virginia Rich,[1] Steven J. Hallam,[1] Niels-Ulrik Frigaard,[1] Asuncion Martinez,[1] Matthew B. Sullivan,[1] Robert Edwards,[3] Beltran Rodriguez Brito,[3] Sallie W. Chisholm,[1] David M. Karl[4]

Microbial life predominates in the ocean, yet little is known about its genomic variability, especially along the depth continuum. We report here genomic analyses of planktonic microbial communities in the North Pacific Subtropical Gyre, from the ocean's surface to near–sea floor depths. Sequence variation in microbial community genes reflected vertical zonation of taxonomic groups, functional gene repertoires, and metabolic potential. The distributional patterns of microbial genes suggested depth-variable community trends in carbon and energy metabolism, attachment and motility, gene mobility, and host-viral interactions. Comparative genomic analyses of stratified microbial communities have the potential to provide significant insight into higher-order community organization and dynamics.

Microbial plankton are centrally involved in fluxes of energy and matter in the sea, yet their vertical distribution and functional variability in the ocean's interior is still only poorly known. In contrast, the vertical zonation of eukaryotic phytoplankton and zooplankton in the ocean's water column has been well documented for over a century (*1*). In the photic zone, steep gradients of light quality and intensity, temperature, and macronutrient and trace-metal concentrations all influence species distributions in the water column (*2*). At greater depths, low temperature, increasing hydrostatic pressure, the disappearance of light, and dwindling energy supplies largely determine vertical stratification of oceanic biota.

For a few prokaryotic groups, vertical distributions and depth-variable physiological properties are becoming known. Genotypic and phenotypic properties of stratified *Prochlorococcus* "ecotypes" for example, are suggestive of depth-variable adaptation to light intensity and nutrient availability (*3*–*5*). In the abyss, the vertical zonation of deep-sea piezophilic bacteria can be explained in part by their obligate growth requirement for elevated hydrostatic pressures (*6*). In addition, recent cultivation-independent (*7*–*15*) surveys have shown vertical zonation patterns among specific groups of planktonic *Bacteria, Archaea,* and *Eukarya.* Despite recent progress however, a comprehensive description of the biological properties and vertical distributions of planktonic microbial species is far from complete.

Cultivation-independent genomic surveys represent a potentially useful approach for characterizing natural microbial assemblages (*16*, *17*). "Shotgun" sequencing and whole genome assembly from mixed microbial assemblages has been attempted in several environments, with varying success (*18*, *19*). In addition, Tringe *et al.* (*20*) compared shotgun sequences of several disparate microbial assemblages to identify community-specific patterns in gene distributions. Metabolic reconstruction has also been attempted with environmental genomic approaches (*21*). Nevertheless, integrated genomic surveys of microbial communities along well-defined environmental gradients (such as the ocean's water column) have not been reported.

To provide genomic perspective on microbial biology in the ocean's vertical dimension, we cloned large [~36 kilobase pairs (kbp)] DNA fragments from microbial communities at different depths in the North Pacific Subtropical Gyre (NPSG) at the open-ocean time-series station ALOHA (*22*). The vertical distribution of microbial genes from the ocean's surface to abyssal depths was determined by shotgun sequencing of fosmid clone termini. Applying identical collection, cloning, and sequencing strategies at seven depths (ranging from 10 m to 4000 m), we archived large-insert genomic libraries from each depth-stratified microbial community. Bidirectional DNA sequencing of fosmid clones (~10,000 sequences per depth) and comparative sequence analyses were used to identify taxa, genes, and metabolic pathways that characterized vertically stratified microbial assemblages in the water column.

Study Site and Sampling Strategy

Our sampling site, Hawaii Ocean Time-series (HOT) station ALOHA (22°45′ N, 158°W), represents one of the most comprehensively characterized sites in the global ocean and has been a focal point for time series–oriented oceanographic studies since 1988 (*22*). HOT investigators have produced high-quality spatial and time-series measurements of the defining physical, chemical, and biological oceanographic parameters from surface waters to the seafloor. These detailed spatial and temporal datasets present unique opportunities for placing microbial genomic depth profiles into appropriate oceanographic context (*22*–*24*) and leverage these data to formulate meaningful ecological hypotheses. Sample depths were selected, on the basis of well-defined physical, chemical, and biotic characteristics, to represent discrete zones in the water column (Tables 1 and 2, Fig. 1; figs. S1 and S2). Specifically, seawater samples from the upper euphotic zone (10 m and 70 m), the base of the chlorophyll maximum (130 m), below the base of the euphotic zone (200 m), well below the upper mesopelagic (500 m), in the core of the dissolved oxygen minimum layer (770 m), and in the deep abyss, 750 m above the seafloor (4000 m), were collected for preparing microbial community DNA libraries (Tables 1 and 2, Fig. 1; figs. S1 and S2).

The depth variability of gene distributions was examined by random, bidirectional end-sequencing of ~5000 fosmids from each depth, yielding ~64 Mbp of DNA sequence total from the 4.5 Gbp archive (Table 1). This represents raw sequence coverage of about 5 (1.8 Mbp sized) genome equivalents per depth. Because we surveyed ~180 Mbp of cloned DNA (5000 clones by ~36 kbp/clone per depth), however, we directly sampled ~100 genome equivalents at each depth. We did not sequence as deeply in each sample as a recent Sargasso Sea survey (*19*), where from 90,000 to 600,000 sequences were obtained from small DNA insert clones, from each of seven different surface-water samples. We hypothesized, however, that our comparison of microbial communities collected along well-defined environmental gradients (using large-insert DNA clones), would facilitate detection of ecologically meaningful taxonomic, functional, and community trends.

Vertical Profiles of Microbial Taxa

Vertical distributions of bacterial groups were assessed by amplifying and sequencing small subunit (SSU) ribosomal RNA (rRNA) genes from complete fosmid library pools at each

[1]Massachusetts Institute of Technology, Cambridge, MA 02139, USA. [2]Monterey Bay Aquarium Research Institute, Moss Landing, CA 95064, USA. [3]San Diego State University, San Diego, CA 92182, USA. [4]University of Hawaii Honolulu, HI 96822, USA.

* To whom correspondence should be addressed. E-mail: delong@mit.edu

Originally published 27 January 2006

Table 1. HOT samples and fosmid libraries. Sample site, 22°45′ N, 158°W. All seawater samples were pre-filtered through a 1.6-μm glass fiber filter, and collected on a 0.22-μm filter. See (*35*) for methods.

Depth (m)	Sample date	Volume filtered (liters)	Total fosmid clones	Total DNA (Mbp)	
				Archived	Sequenced
10	10/7/02	40	12,288	442	7.54
70	10/7/02	40	12,672	456	11.03
130	10/6/02	40	13,536	487	6.28
200	10/6/02	40	19,008	684	7.96
500	10/6/02	80	15,264	550	8.86
770	12/21/03	240	11,520	415	11.18
4,000	12/21/03	670	41,472	1,493	11.10

depth (Fig. 2; fig. S3). Bacterial phylogenetic distributions were generally consistent with previous polymerase chain reaction–based cultivation-independent rRNA surveys of marine picoplankton (*8*, *15*, *25*). In surface-water samples, rRNA-containing fosmids included those from *Prochlorococcus; Verrucomicrobiales; Flexibacteraceae;* Gammaproteobacteria (SAR92, OM60, SAR86 clades); Alphaproteobacteria (SAR116, OM75 clades); and Deltaproteobacteria (OM27 clade) (Fig. 2). Bacterial groups from deeper waters included members of *Deferribacteres; Planctomycetaceae; Acidobacteriales; Gemmatamonadaceae; Nitrospina; Alteromonadaeceae;* and SAR202, SAR11, and Agg47 planktonic bacterial clades (Fig. 2; fig. S2). Large-insert DNA clones previously recovered from the marine environment (*9*, *10*) also provide a good metric for taxonomic assessment of indigenous microbes. Accordingly, a relatively large proportion of our shotgun fosmid sequences most closely matched rRNA-containing bacterioplankton artificial clones previously recovered from the marine environment (fig. S3).

Taxonomic bins of bacterial protein homologs found in randomly sequenced fosmid ends (Fig. 2; fig. S4) also reflected distributional patterns generally consistent with previous surveys in the water column (*8*, *15*). Unexpectedly large amounts of phage DNA were recovered in clones, particularly in the photic zone. Also unexpected was a relatively high proportion of Betaproteobacteria-like sequences recovered at 130 m, most sharing highest similarity to protein homologs from *Rhodoferax ferrireducens.* As expected, representation of *Prochlorococcus*-like and *Pelagibacter*-like genomic sequences was high in the photic zone. At greater depths, higher proportions of *Chloroflexi*-like sequences, perhaps corresponding to the cooccurring SAR202 clade, were observed (Fig. 2). *Planctomycetales*-like genomic DNA sequences were also highly represented at greater depths.

All archaeal SSU rRNA–containing fosmids were identified at each depth, quantified by macroarray hybridization, and their rRNAs sequenced (figs. S5 and S6). The general patterns of archaeal distribution we observed were consistent with previous field surveys (*15*, *25*, *26*). Recovery of "group II" planktonic *Euryarchaeota* genomic DNA was greatest in the upper water column and declined below the photic zone. This distribution corroborates recent observations of ion-translocating photoproteins (called proteorhodopsins), now known to occur in group II *Euryarchaeota* inhabiting the photic zone (*27*). "Group III" *Euryarchaeota* DNA was recovered at all depths,

Table 2. HOT sample oceanographic data. Samples described in Table 1. Oceanographic parameters were measured as specified at (*49*); values shown are those from the same CTD casts as the samples, where available. Values in parentheses are the mean ± 1 SD of each core parameter during the period October 1988 to December 2004, with the total number of measurements collected for each parameter shown in brackets. The parameter abbreviations are Temp., Temperature; Chl a, chlorophyll a; DOC, dissolved organic carbon; N+N, nitrate plus nitrite; DIP, dissolved inorganic phosphate; and DIC, dissolved inorganic carbon. The estimated photon fluxes for upper water column samples (assuming a surface irradiance of 32 mol quanta m^{-2} d^{-1} and a light extinction coefficient of 0.0425 m^{-1}) were: 10 m = 20.92 (65% of surface), 70 m = 1.63 (5% of surface), 130 m = 0.128 (0.4% of surface), 200 m = 0.07 (0.02% of surface). The mean surface mixed-layer during the October 2002 sampling was 61 m. Data are available at (*50*). *Biomass derived from particulate adenosine triphosphate (ATP) measurements assuming a carbon:ATP ratio of 250. ND, Not determined.

Depth (m)	Temp. (°C)	Salinity	Chl a (μg/kg)	Biomass* (μg/kg)	DOC (μmol/kg)	N + N (nmol/kg)	DIP (nmol/kg)	Oxygen (μmol/kg)	DIC (μmol/kg)
10	26.40	35.08	0.08	7.21 ± 2.68	78	1.0	41.0	204.6	1,967.6
	(24.83 ± 1.27)	(35.05 ± 0.21)	(0.08 ± 0.03)	[78]	(90.6 ± 14.3)	(2.6 ± 3.7)	(56.0 ± 33.7)	(209.3 ± 4.5)	(1,972.1 ± 16.4)
	[2,104]	[1,611]	[320]		[140]	[126]	[146]	[348]	[107]
70	24.93	35.21	0.18	8.51 ± 3.22	79	1.3	16.0	217.4	1,981.8
	(23.58 ± 1.00)	(35.17 ± 0.16)	(0.15 ± 0.05)	[86]	(81.4 ± 11.3)	(14.7 ± 60.3)	(43.1 ± 25.1)	(215.8 ± 5.4)	(1,986.9 ± 15.4)
	[1,202]	[1,084]	[363]		[79]	[78]	[104]	[144]	[84]
130	22.19	35.31	0.10	5.03 ± 2.30	69	284.8	66.2	204.9	2,026.5
	(21.37 ± 0.96)	(35.20 ± 0.10)	(0.15 ± 0.06)	[90]	(75.2 ± 9.1)	(282.9 ± 270.2)	(106.0 ± 49.7)	(206.6 ± 6.2)	(2,013.4 ± 13.4)
	[1,139]	[980]	[350]		[86]	[78]	[68]	[173]	[69]
200	18.53	35.04	0.02	1.66 ± 0.24	63	1,161.9 ± 762.5	274.2 ± 109.1	198.8	2,047.7
	(18.39 ± 1.29)	(34.96 ± 0.18)	(0.02 ± 0.02)	[2]	(64.0 ± 9.8)	[7]	[84]	(197.6 ± 7.1)	(2,042.8 ± 10.5)
	[662]	[576]	[97]		[113]			[190]	[125]
500	7.25	34.07	ND	0.48 ± 0.23	47	28,850	2,153	118.0	2197.3
	(7.22 ± 0.44)	(34.06 ± 0.03)		[107]	(47.8 ± 6.3)	(28,460 ± 2210)	(2,051 ± 175.7)	(120.5 ± 18.3)	(2,200.2 ± 17.8)
	[1,969]	[1,769]			[112]	[326]	[322]	[505]	[134]
770	4.78	34.32	ND	0.29 ± 0.16	39.9	41,890	3,070	32.3	2323.8
	(4.86 ± 0.21)	(34.32 ± 0.04)		[107]	(41.5 ± 4.4)	(40,940 ± 500)	(3,000 ± 47.1)	(27.9 ± 4.1)	(2,324.3 ± 6.1)
	[888]	[773]			[34]	[137]	[135]	[275]	[34]
4,000	1.46	34.69	ND	ND	37.5	36,560	2,558	147.8	2325.5
	(1.46 ± 0.01)	(34.69 ± 0.00)			(42.3 ± 4.9)	(35,970 ± 290)	(2,507 ± 19)	(147.8 ± 1.3)	(2,329.1 ± 4.8)
	[262]	[245]			[83]	[108]	[104]	[210]	[28]

but at a much lower frequency (figs. S5 and S6). A novel crenarchaeal group, closely related to a putatively thermophilic *Crenarchaeota* (*28*), was observed at the greatest depths (fig. S6).

Vertically Distributed Genes and Metabolic Pathways

The depths sampled were specifically chosen to capture microbial sequences at discrete biogeochemical zones in the water column encompassing key physicochemical features (Tables 1 and 2, Fig. 1; figs. S1 and S2). To evaluate sequences from each depth, fosmid end sequences were compared against different databases including the Kyoto Encyclopedia of Genes and Genomes (KEGG) (*29*), National Center for Biotechnology Information (NCBI)'s Clusters of Orthologous Groups (COG) (*30*), and SEED subsystems (*31*). After categorizing sequences from each depth in BLAST searches (*32*) against each database, we identified protein categories that were more or less well represented in one sample versus another, using cluster analysis (*33*, *34*) and bootstrap resampling methodologies (*35*).

Cluster analyses of predicted protein sequence representation identified specific genes and metabolic traits that were differentially distributed in the water column (fig. S7). In the photic zone (10, 70, and 130 m), these included a greater representation in sequences associated with photosynthesis; porphyrin and chlorophyll metabolism; type III secretion systems; and aminosugars, purine, proponoate, and vitamin B6 metabolism, relative to deep-water samples (fig. S7). Independent comparisons with well-annotated subsystems in the SEED database (*31*) also showed similar and overlapping trends (table S1), including greater representation in photic zone sequences associated with alanine and aspartate; metabolism of aminosugars; chlorophyll and carotenoid biosynthesis; maltose transport; lactose degradation; and heavy metal ion sensors and exporters. In contrast, samples from depths of 200 m and below (where there is no photosynthesis) were enriched in different sequences, including those associated with protein folding; processing and export; methionine metabolism; glyoxylate, dicarboxylate, and methane metabolism; thiamine metabolism; and type II secretion systems, relative to surface-water samples (fig. S7).

COG categories also provided insight into differentially distributed protein functions and categories. COGs more highly represented in photic zone included iron-transport membrane receptors, deoxyribopyrimidine photolyase, diaminopimelate decarboxylase, membrane guanosine triphosphatase (GTPase) with the lysyl endopeptidase gene product LepA, and branched-chain amino acid–transport system components (fig. S8). In contrast, COGs with greater representation in deep-water samples included transposases, several dehydrogenase categories, and integrases (fig. S8). Sequences more highly represented in the deep-water samples in SEED subsystem (*31*) comparisons included those associated with respiratory dehydrogenases, polyamine adenosine triphosphate (ATP)–binding cassette (ABC) transporters, polyamine metabolism, and alkylphosphonate transporters (table S1).

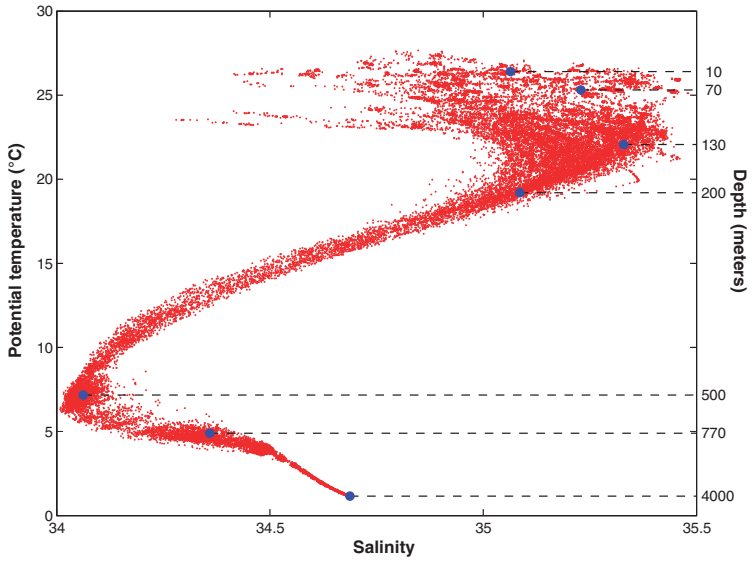

Fig. 1. Temperature versus salinity (T-S) relations for the North Pacific Subtropical Gyre at station ALOHA (22°45′N, 158°W). The blue circles indicate the positions, in T-S "hydrospace" of the seven water samples analyzed in this study. The data envelope shows the temperature and salinity conditions observed during the period October 1988 to December 2004 emphasizing both the temporal variability of near-surface waters and the relative constancy of deep waters.

Habitat-enriched sequences. We estimated average protein sequence similarities between all depth bins from cumulative TBLASTX high-scoring sequence pair (HSP) bitscores, derived from BLAST searches of each depth against every other (Fig. 3). Neighbor-joining analyses of a normalized, distance matrix derived from these cumulative bitscores joined photic zone and deeper samples together in separate clusters (Fig. 3). When we compared our HOT sequence datasets to previously reported Sargasso Sea microbial sequences (*19*), these datasets also clustered according to their depth and size fraction of origin (fig. S9). The clustering pattern in Fig. 3 is consistent with the expectation that randomly sampled photic zone microbial sequences will tend on average to be more similar to one another, than to those from the deep-sea, and vice-versa.

We also identified those sequences (some of which have no homologs in annotated databases) that track major depth-variable environmental features. Specifically, sequence homologs found only in the photic zone unique sequences (from 10, 70, and 130 m), or deepwater unique sequences (from 500, 770, and 4000 m) were identified (Fig. 3). To categorize potential functions encoded in these photic zone unique (PZ) or deep-water unique (DW) sequence bins, each was compared with KEGG, COG, and NCBI protein databases in separate analyses (*29*, *30*, *36*).

Some KEGG metabolic pathways appeared more highly represented in the PZ than in DW sequence bins, including those associated with photosynthesis; porphyrin and chlorophyll metabolism; propanoate, purine, and glycerphospholipid metabolism; bacterial chemotaxis; flagellar assembly; and type III secretion systems (Fig. 4A). All proteorhodopsin sequences (except one) were captured in the PZ bin. Well-represented photic zone KEGG pathway categories appeared to reflect potential pathway interdependencies. For example the PZ photosynthesis bin [3% of the total (Fig. 4A)] contained *Prochlorococcus*-like and *Synechococcus*-like photosystem I, photosystem II, and cytochrome genes. In tandem, PZ porphyrin and chlorophyll biosynthesis sequence bins [~3.9% of the total (Fig. 4A)] contained high representation of cyanobacteria-like cobalamin and chlorophyll biosynthesis genes, as well as photoheterotroph-like bacteriochlorophyll biosynthetic genes. Other probable functional interdependencies appear reflected in the corecovery of sequences associated with chemotaxis (mostly methyl-accepting chemotaxis proteins), flagellar biosynthesis (predominantly flagellar motor and

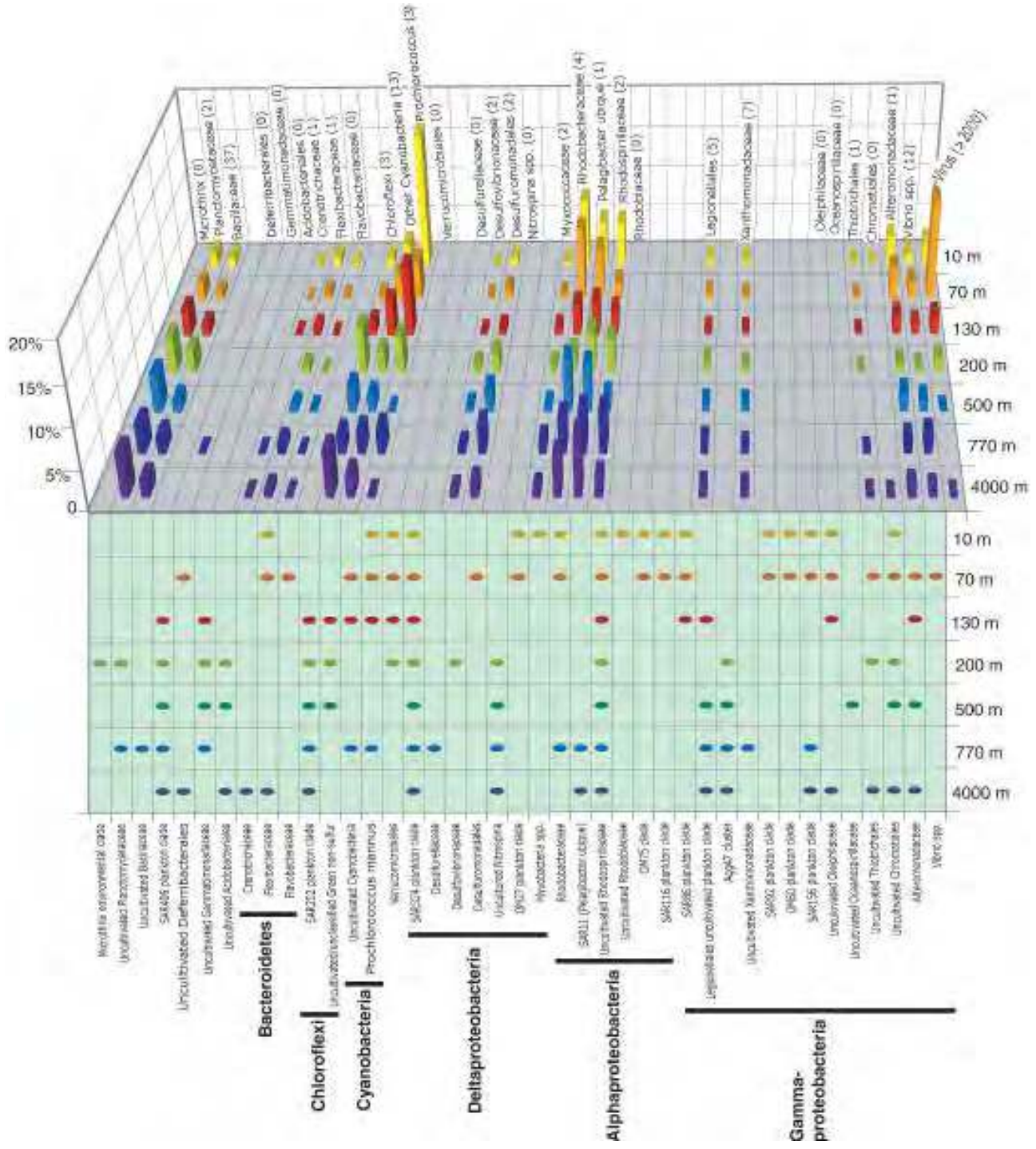

Fig. 2. Taxon distributions of top HSPs. The percent top HSPs that match the taxon categories shown at expectation values of $\leq 1 \times 10^{-60}$. Values in parentheses indicate number of genomes in each category, complete or draft, that were in the database at the time of analysis. The dots in the lower panel tabulate the SSU rRNAs detected in fosmid libraries from each taxonomic group at each depth (*35*) (figs. S3 and S6).

hook protein-encoding genes), and type III secretory pathways (all associated with flagellar biosynthesis) in PZ (Fig. 4A).

DW sequences were enriched in several KEGG categories, including glyoxylate and dicarboxylate metabolism (with high representation of isocitrate lyase– and formate dehydrogenase–like genes); protein folding and processing (predominantly chaperone and protease like genes); type II secretory genes (~40% were most similar to pilin biosynthesis genes); aminophosphonate, methionine, and

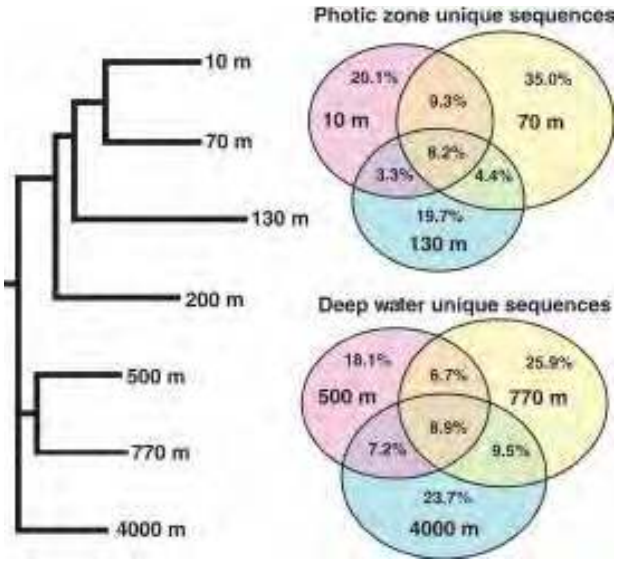

Fig. 3. Habitat-specific sequences in photic zone versus deep-water communities. The dendrogram shows a cluster analysis based on cumulative bitscores derived from reciprocal TBLASTX comparisons between all depths. Only the branching pattern resulting from neighbor-joining analyses (not branch-lengths) are shown in the dendrogram. The Venn diagrams depict the percentage of sequences that were present only in PZ sequences (n = 12,713) or DW sequences (n = 14,132), as determined in reciprocal BLAST searches of all sequences in each depth versus every other. The percentage out of the total PZ or DW sequence bins represented in each subset is shown. See SOM for methods (*35*).

sulfur metabolism; butanoate metabolism; ion-coupled transporters; and other ABC transporter variants (Fig. 4B). The high representation in DW sequences of type II secretion system and pilin biosynthesis genes, polysaccharide, and antibiotic synthesis suggest a potentially greater role for surface-associated microbial processes in the deeper-water communities. Conversely, enrichment of bacterial motility and chemotaxis sequences in the photic zone indicates a potentially greater importance for mobility and response in these assemblages.

Similar differential patterns of sequence distribution were seen in COG categories (Fig. 4B). COGs enriched in the PZ sequence bin included photolyases, iron-transport outer membrane proteins, Na+-driven efflux pumps, ABC-type sugar-transport systems, hydrolases and acyl transferases, and transaldolases. In deeper waters, transposases were the most enriched COG category (~4.5% of the COG-categorized DW), increasing steadily in representation with depth from 500 m to their observed maximum at 4000 m (Fig. 4B; fig. S9). Transposases represented one of the single-most overrepresented COG categories in deep waters, accounting for 1.2% of all fosmids sequenced from 4000 m (fig. S8). Preliminary analyses of the transposase variants and mate-pair sequences indicate that they represent a wide variety of different transposase families and originate from diverse microbial taxa. In contrast, other highly represented COG categories appeared to reflect specific taxon distribution and abundances. For example, the enrichment of transaldolases at 70 m (Fig. 4B; fig. S9) were mostly derived from abundant cyanophage DNA that was recovered at that depth (see discussion below).

Sargasso Sea surface-water microbial sequences (*19*) shared, as expected, many more homologous sequences with our photic zone sequences than those from the deep sea (fig. S10). There were 10 times as many PZ than DW sequences shared in common with Sargasso Sea samples 5 through 7 (*19*) (fig. S10). In contrast, PZ-like sequences were only three times higher in DW when compared with sequences from Sargasso Sea sample 3 (fig. S10). The fact that Sargasso sample 3 was collected during a period of winter deep-water mixing likely contributes to this higher representation of DW-like homologs. Sargasso Sea homologs of our PZ sequence bin included, as expected, sequences associated with photosynthesis; amino acid transport; purine, pyrimidine and nitrogen metabolism; porphyrin and chlorophyll metabolism; oxidative phosphorylation; glycolysis; and starch and sucrose metabolism (fig. S10).

Tentative taxonomic assignments of PZ or DW sequences (top HSPs from NCBI's non-redundant protein database) were also tabulated (fig. S11). As expected, a high percentage of *Prochlorococcus*-like sequences was found in PZ (~5% of the total), and a greater representation of Deltaproteobacteria-like, *Actinobacteria*-like and *Planctomycete*-like sequences were recovered in DW. Unexpectedly, the single most highly represented taxon category in PZ (~21% of all identified sequences in PZ) was derived from viral sequences that were captured in fosmid clones (fig. S11).

Community Genomics and Host-Virus Interactions

Viruses are ubiquitous and abundant components of marine plankton, and influence lateral gene transfer, genetic diversity, and bacterial mortality in the water column (*37–40*). The large number of viral DNA sequences in our dataset was unexpected (Fig. 5; fig. S12), because we expected planktonic viruses to pass through our collection filters. Previous studies using a similar approach found only minimal contributions from viral sources (*19*, *40*). The majority of viral DNA we captured in fosmid clone libraries apparently originates from replicating viruses within infected host cells (*35*). Viral DNA recovery was highest in the photic zone, with cyanophage-like sequences representing 1 to 10% of all fosmid sequences (Fig. 5), and 60 to 80% of total virus sequences there. Below 200 m, viral DNA made up no more than 0.3% of all sequences at each depth. Most photic zone viral sequences shared highest similarity to T7-like and T4-like cyanophage of the Podoviridae and Myoviridae. This is consistent with previous studies (*40–42*), suggesting a widespread distribution of these phage in the ocean.

Analyses of 1107 fosmid mate pairs provided further insight into the origins of the viral sequences. About 67% of the viruslike clones were most similar to cyanophage on at least one end, and half of these were highly similar to cyanophage at both termini. Many of the cyanophage clones showed apparent synteny with previously sequenced cyanophage genomes (fig. S12). About 11% of the cyanophage paired-ends contained a host-derived cyanophage "signature" gene (*43*) on one terminus. The frequency and genetic-linkage of phage-encoded (but host-derived) genes we observed, including virus-derived genes involved in photosynthesis (*psbA*, *psbD*, *hli*), phosphate-scavenging genes (*phoH*, *pstS*), a cobalamin biosynthesis gene (*cobS*), and carbon metabolism (*transaldolase*) supports their widespread distribution in natural viral populations and their probable functional importance to cyanophage replication (*43*, *44*).

If we assume that the cyanophages' DNA was derived from infected host cells in which phage were replicating, the percentage of cyanophage-infected cells was estimated to range between 1 and 12% (*35*). An apparent cyanophage infection maxima was observed at 70 m, coinciding with the peak virus:host ratio (Fig. 5). Although these estimates are tentative, they are consistent with previously reported ranges of phage-infected picoplankton cells in situ (*38, 45*).

About 0.5% of all sequences were likely prophage, as inferred from high sequence similarity to phage-related integrases and known

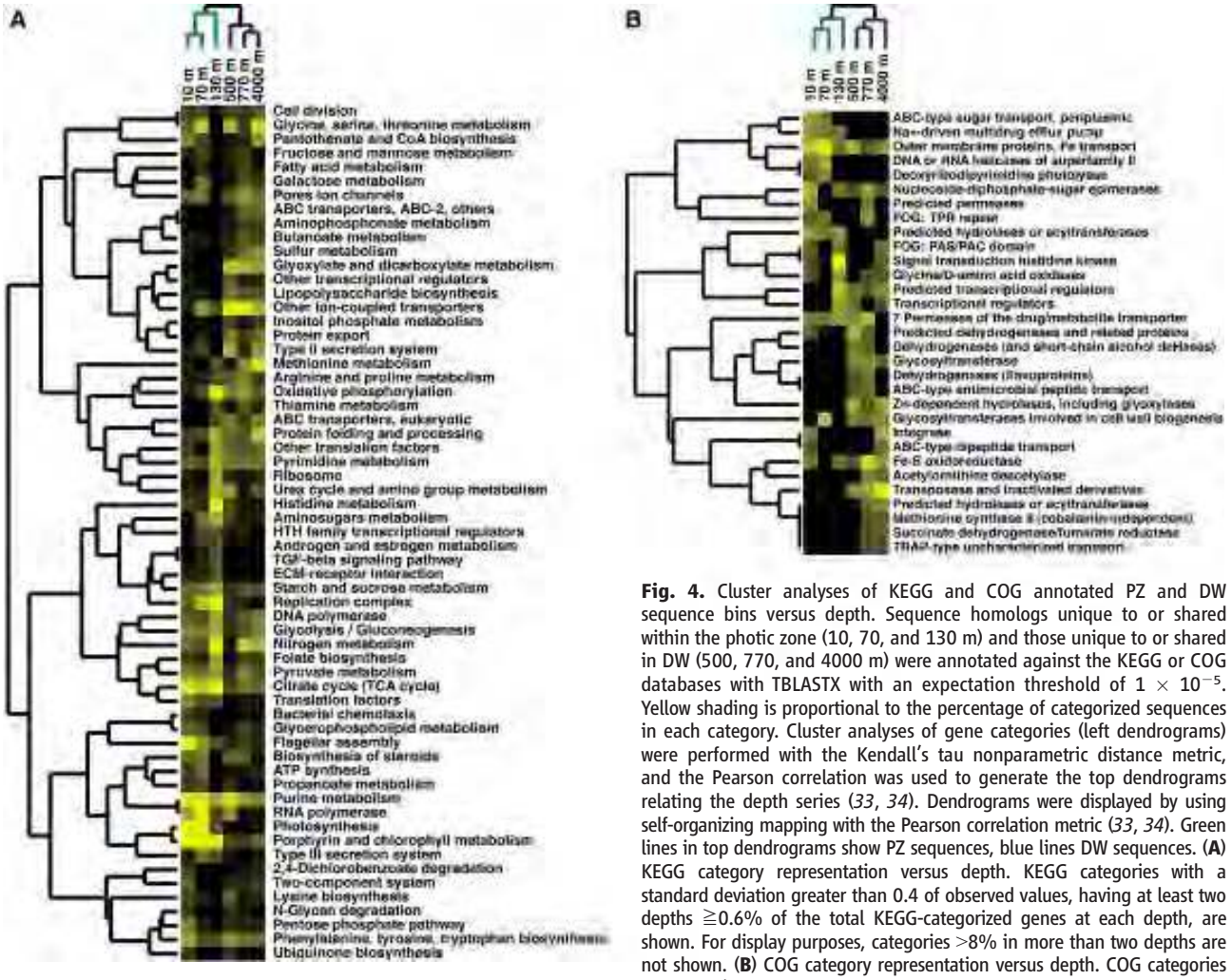

Fig. 4. Cluster analyses of KEGG and COG annotated PZ and DW sequence bins versus depth. Sequence homologs unique to or shared within the photic zone (10, 70, and 130 m) and those unique to or shared in DW (500, 770, and 4000 m) were annotated against the KEGG or COG databases with TBLASTX with an expectation threshold of 1×10^{-5}. Yellow shading is proportional to the percentage of categorized sequences in each category. Cluster analyses of gene categories (left dendrograms) were performed with the Kendall's tau nonparametric distance metric, and the Pearson correlation was used to generate the top dendrograms relating the depth series (*33*, *34*). Dendrograms were displayed by using self-organizing mapping with the Pearson correlation metric (*33*, *34*). Green lines in top dendrograms show PZ sequences, blue lines DW sequences. (**A**) KEGG category representation versus depth. KEGG categories with a standard deviation greater than 0.4 of observed values, having at least two depths ≧0.6% of the total KEGG-categorized genes at each depth, are shown. For display purposes, categories >8% in more than two depths are not shown. (**B**) COG category representation versus depth. COG categories with standard deviations greater than 0.2 of observed values, having at least two depths ≧0.3% of the total COG-categorized genes at each depth, are shown.

prophage genes (*35*). Paired-end analyses of viral fosmids indicated that ~2.5% may be derived from prophage integrated into a variety of host taxa. A few clones also appear to be derived from temperate siphoviruses, and a number of putative eukaryotic paired-end viral sequences shared highest sequence identity with homologs from herpes viruses, mimiviruses, and algal viruses.

Ecological Implications and Future Prospects

Microbial community sampling along well-characterized depth strata allowed us to identify significant depth-variable trends in gene content and metabolic pathway components of oceanic microbial communities. The gene repertoire of surface waters reflected some of the mechanisms and modes of light-driven processes and primary productivity. Environmentally diagnostic sequences in surface waters included predicted proteins associated with cyanophage, motility, chemotaxis, photosynthesis, proteorhodopsins, photolyases, carotenoid biosynthesis, iron-transport systems, and host restriction-modification systems. The importance of light energy to these communities as reflected in their gene content was obvious. More subtle ecophysiological trends can be seen in iron transport, vitamin synthesis, flagella synthesis and secretion, and chemotaxis gene distributions. These data support hypotheses about potential adaptive strategies of heterotrophic bacteria in the photic zone that may actively compete for nutrients by swimming toward nutrient-rich particles and algae (*46*). In contrast to surface-water assemblages, deep-water microbial communities appeared more enriched in transposases, pilus synthesis, protein export, polysaccharide and antibiotic synthesis, the glyoxylate cycle, and urea metabolism gene sequences. The observed enrichment in pilus, polysaccharide, and antibiotic synthesis genes in deeper-water samples suggests a potentially greater role for a surface-attached life style in deeper-water microbial communities. Finally, the apparent enrichment of phage genes and restriction-modification systems observed in the photic zone may indicate a greater role for phage parasites in the more productive upper water column, relative to deeper waters.

At finer scales, sequence distributions we observed also reflected genomic "microvariability" along environmental gradients, as evidenced by the partitioning of high- and low-light *Prochlorococcus* ecotype genes observed in different regions of the photic zone (Fig. 5). Higher-order biological interactions were also evident, for example in the negative correlation of cyanophage versus *Prochlorococcus* host gene sequence recovery (Fig. 5).

This relation between the abundance of host and cyanophage DNA probably reflects specific mechanisms of cyanophage replication in situ. These host-parasite sequence correlations we saw demonstrate the potential for observing community-level interspecies interactions through environmental genomic datasets.

Obviously, the abundance of specific taxa will greatly influence the gene distributions observed, as we saw, for example, in *Prochlorococcus* gene distribution in the photic zone. Gene sequence distributions can reflect more than just relative abundance of specific taxa, however. Some depth-specific gene distributions we observed [e.g., transposases found predominantly at greater depths (Fig. 4B; fig. S8)], appear to originate from a wide variety of gene families and genomic sources. These gene distributional patterns seem more indicative of habitat-specific genetic or physiological trends that have spread through different members of the community. Community gene distributions and stoichiometries are differentially propagated by vertical and horizontal genetic mechanisms, dynamic physiological responses, or interspecies interactions like competition. The overrepresentation of certain sequence types may sometimes reflect their horizontal transmission and propagation within a given community. In our datasets, the relative abundance of cyanobacteria-like *psbA*, *psbD*, and transaldolase genes were largely a consequence of their horizontal transfer and subsequent amplification in the viruses that were captured in our samples. In contrast, the increase of transposases from 500 to 4000 m, regardless of community composition, reflected a different mode of gene propagation, likely related to the slower growth, lower productivity, and lower effective population sizes of deep-sea microbial communities. In future comparative studies, similar deviations in environmental gene stoichiometries might be expected to provide even further insight into habitat-specific modes and mechanisms of gene propagation, distribution, and mobility (*27*, *47*). These "gene ecologies" could readily be mapped directly on organismal distributions and interactions, environmental variability, and taxonomic distributions.

The study of environmental adaptation and variability is not new, but our technical capabilities for identifying and tracking sequences, genes, and metabolic pathways in microbial communities is. The study of gene ecology and its relation to community metabolism, interspecies interactions, and habitat-specific signatures is nascent. More extensive sequencing efforts are certainly required to more thoroughly describe natural microbial communities. Additionally, more concerted efforts to integrate these new data into studies of oceanographic, biogeochemical, and environmental processes are necessary (*48*). As the scope and scale of genome-enabled ecological studies matures, it should become possible to model microbial community genomic, temporal, and spatial variability with other environmental features. Significant future attention will no doubt focus on interpreting the complex interplay between genes, organisms, communities and the environment, as well as the properties revealed that regulate global biogeochemical cycles. Future efforts in this area will advance our general perspective on microbial ecology and evolution and elucidate the biological dynamics that mediate the flux of matter and energy in the world's oceans.

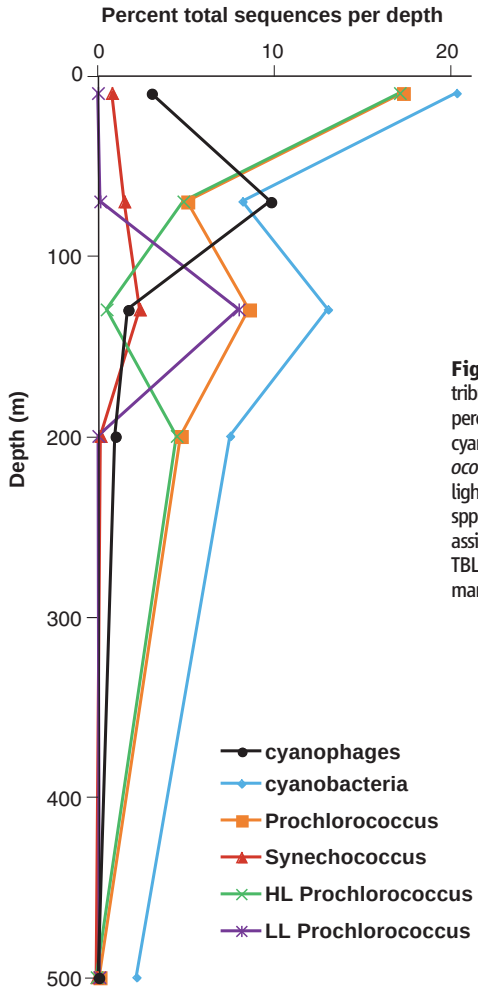

Fig. 5. Cyanophage and cyanobacteria distributions in microbial community DNA. The percentage of total sequences derived from cyanophage, total cyanobacteria, total *Prochlorococcus* spp., high-light *Prochlorococcus*, low-light *Prochlorococcus* spp., or *Synechococcus* spp., from each depth. Taxa were tentatively assigned according to the origin of top HSPs in TBLASTX searches, followed by subsequent manual inspection and curation.

References and Notes

1. E. Forbes, in *Physical Atlas of Natural Phenomena*, A. K. Johnston, Ed. (William Blackwood & Sons, London and Edinburgh, 1856).
2. P. W. Hochachka, G. N. Somero, *Biochemical Adaptation* (Princeton Univ. Press, Princeton, NJ, 1984), pp. 450–495.
3. G. Rocap *et al.*, *Nature* **424**, 1042 (2003).
4. Z. I. Johnson *et al.*, manuscript submitted.
5. N. J. West *et al.*, *Microbiology* **147**, 1731 (2001).
6. A. A. Yayanos, *Annu. Rev. Microbiol.* **49**, 777 (1995).
7. N. R. Pace, *Science* **276**, 734 (1997).
8. M. S. Rappé, S. J. Giovannoni, *Annu. Rev. Microbiol.* **57**, 369 (2003).
9. M. T. Suzuki *et al.*, *Microb Ecol* (2005).
10. O. Béjà *et al.*, *Environ. Microbiol.* **2**, 516 (2000).
11. R. M. Morris, M. S. Rappé, E. Urbach, S. A. Connon, S. J. Giovannoni, *Appl. Environ. Microbiol.* **70**, 2836 (2004).
12. S. Y. Moon-van der Staay *et al.*, *Nature* **409**, 607 (2001).
13. J. A. Fuhrman, K. McCallum, A. A. Davis, *Nature* **356**, 148 (1992).
14. E. F. DeLong, *Proc. Natl. Acad. Sci. U.S.A.* **89**, 5685 (1992).
15. M. B. Karner *et al.*, *Nature* **409**, 507 (2001).
16. J. Handelsman, *Microbiol. Mol. Biol. Rev.* **68**, 669 (2004).
17. E. F. Delong, *Nat Rev Microbiol* (2005).
18. G. W. Tyson *et al.*, *Nature* **428**, 37 (2004).

19. J. C. Venter *et al.*, *Science* **304**, 66 (2004).
20. S. G. Tringe *et al.*, *Science* **308**, 554 (2005).
21. S. J. Hallam *et al.*, *Science* **305**, 1457 (2004).
22. D. M. Karl, R. Lukas, *Deep-Sea Res. II* **43**, 129 (1996).
23. D. M. Karl *et al.*, *Deep-Sea Res. II* **48**, 1449 (2001).
24. R. M. Letelier *et al.*, *Limnol. Oceanogr.* **49**, 508 (2004).
25. E. F. DeLong *et al.*, *Appl. Environ. Microbiol.* **65**, 5554 (1999).
26. A. Pernthaler *et al.*, *Appl. Environ. Microbiol.* **68**, 661 (2002).
27. N. U. Frigaard *et al.*, *Nature* **439**, 847 (2006).
28. S. M. Barns, C. F. Delwiche, J. D. Palmer, N. R. Pace, *Proc. Natl. Acad. Sci. U.S.A.* **93**, 9188 (1996).
29. M. Kanehisa *et al.*, *Nucleic Acids Res.* **32**, D277 (2004).
30. R. L. Tatusov *et al.*, *BMC Bioinformatics* **4**, 41 (2003).
31. R. Overbeek *et al.*, *Nucleic Acids Res.* **33**, 5691 (2005).
32. S. F. Altschul *et al.*, *J. Mol. Biol.* **215**, 403 (1990).
33. M. J. L. de Hoon *et al.*, *Bioinformatics* **12**, 1453 (2004).
34. M. B. Eisen, P. T. Spellman, P. O. Brown, *Proc. Natl. Acad. Sci. U.S.A.* **94**, 14863 (1998).
35. Materials and methods are available as supporting material on *Science* Online.
36. K. D. Pruitt, T. Tatusova, D. R. Maglott, *Nucleic Acids Res.* **33**, D501 (2005).
37. M. G. Weinbauer, *FEMS Microbiol. Rev.* **28**, 127 (2004).
38. J. Waterbury, F. Valois, *Appl. Environ. Microbiol.* **59**, 3393 (1993).
39. M. B. Sullivan *et al.*, *Nature* **424**, 1047 (2003).
40. R. A. Edwards, F. Rohwer, *Nat. Rev. Microbiol.* **3**, 504 (2005).
41. J. Filee, F. Tetart, C. A. Suttle, H. M. Krisch, *Proc. Natl. Acad. Sci. U.S.A.* **102**, 12471 (2005).
42. M. Breitbart, J. H. Miyake, F. Rohwer, *FEMS Microbiol. Lett.* **236**, 249 (2004).
43. M. B. Sullivan *et al.*, *PLoS Biol.* **3**, e144 (2005).
44. D. Lindell *et al.*, *Proc. Natl. Acad. Sci. U.S.A.* **101**, 11013 (2004).
45. M. G. Weinbauer, I. Brettar, M. G. Hofle, *Limnol. Oceanogr.* **48**, 1457 (2003).
46. F. Azam, *Science* **280**, 694 (1998).
47. C. R. Woese, *Microbiol. Mol. Biol. Rev.* **68**, 173 (2004).
48. E. F. DeLong, D. M. Karl, *Nature* **437**, 336 (2005).
49. (http://hahana.soest.hawaii.edu/hot/parameters.html).
50. (http://hahana.soest.hawaii.edu/hot/hot-dogs).
51. This work was supported by a grant from the Gordon and Betty Moore Foundation, NSF grants MCB-0084211, MCB-0348001, and MCB-0509923 to E.F.D., and OCE-0326616 to D.M.K., and sequencing support from the U.S. Department of Energy Microbial Genomics Program. We thank Dennis Ryan for help with scripting and sequence analyses, the officers and crew of the R/V Ka'imikai-O-Kanaloa and the HOT team for assistance at sea, and L. Fujieki for help with oceanographic data display. J. Chapman, A. Salamov, and P. Richardson of the DOE Joint Genome Institute provided advice and assistance in DNA sequencing and analyses. Sequences have been deposited in GenBank with accession numbers DU731018-DU796676 and DU800850-DU800864 corresponding to fosmid end sequences, and accession numbers DQ300508-DQ300926 corresponding to SSU rRNA gene sequences.

Supporting Online Material

www.sciencemag.org/cgi/content/full/311/5760/496/DC1
Materials and Methods
Figs. S1 to S12
Table S1
References and Notes

16 September 2005; accepted 21 December 2005
10.1126/science.1120250

Variability in Radiocarbon Ages of Individual Organic Compounds from Marine Sediments

Timothy I. Eglinton,* Bryan C. Benitez-Nelson, Ann Pearson, Ann P. McNichol, James E. Bauer, Ellen R. M. Druffel

Organic carbon (OC) from multiple sources can be delivered contemporaneously to aquatic sediments. The influence of different OC inputs on carbon-14–based sediment chronologies is illustrated in the carbon-14 ages of purified, source-specific (biomarker) organic compounds from near-surface sediments underlying two contrasting marine systems, the Black Sea and the Arabian Sea. In the Black Sea, isotopic heterogeneity of *n*-alkanes indicated that OC was contributed from both fossil and contemporary sources. Compounds reflecting different source inputs to the Arabian Sea exhibit a 10,000-year range in conventional carbon-14 ages. Radiocarbon measurements of biomarkers of marine photoautotrophy enable sediment chronologies to be constructed independent of detrital OC influences.

Molecular-level studies of organic compounds in marine sediments can provide a wealth of information on the carbon cycle in past and present-day oceans as well as information on the depositional setting and origin of organic matter. Of greatest utility are lipid biomarkers that are specific to individual or a restricted range of organisms and that are sufficiently refractory to be preserved in sediments. Three characteristic features of individual organic compounds are currently exploited by biogeochemists: precise molecular structure, absolute or relative abundance, and stable carbon isotopic composition. A fourth feature, the radiocarbon content, has been added to the list (*1*). The ^{14}C content provides a means to evaluate the source and fate of natural and anthropogenic organic compounds in the biogeosphere.

Organic materials from various sources and with different ages are deposited concurrently in marine sediments. This is particularly the case near continents where fresh vascular plant debris, soil organic matter, and OC eroded from sedimentary rocks may be deposited together with autochthonous biomass synthesized in the water column. The construction of carbon budgets and sediment chronologies based on ^{14}C measurements of total organic carbon (TOC) depends on being able to accurately quantify these inputs. The ages of specific OC inputs and their influence on TOC ^{14}C ages have remained elusive. Measurements of different compound classes in sediments have indicated that ^{14}C contents are heterogeneous (*2*), but it is only at the biomarker level that these variations are fully expressed and can be attributed to specific inputs.

Here we present an assessment of radiocarbon ages measured in individual biomarkers from two contrasting marine sedimentary systems. The Black Sea is a stratified anoxic marine basin, and the Arabian Sea is a highly productive system supported by intense seasonal upwelling. Organic carbon–rich sediments accumulating in both seas are strongly influenced by terrigenous inputs. Numerous large rivers drain into the western Black Sea and affect the hydrography and geochemistry of this system (*3*), whereas eolian dust associated with seasonal monsoons is the primary mode of supply of continental OC to the Arabian Sea (*4*).

In the Black Sea, we studied laminated OC-rich (TOC, 5.5%) sediments at a depth of 4 to 7 cm recovered by a Mk-III box corer (BC4, station 2; 42°51′N, 31°57′E, at a water depth of 2129 m) during leg 134-9 of the 1988 R/V *Knorr* expedition. In the Arabian Sea, we studied a sediment sample (box core 6BC, depth of 2 to 4 cm; TOC, 6.7%) obtained from the Oman upwelling region in the Arabian Sea (17°48.7′N, 57°30.3′E, at a water depth of 747 m) during leg TN041 of the R/V T.G. *Thompson* expedition in 1994. We measured the natural ^{14}C content of specific biomarker compounds chosen to reflect both autochthonous and allochthonous inputs (*5*) in order to evaluate the magnitude and source of age variation in these components of sedimentary organic matter.

We selected a series of long chain (C_{37-39}) alkenes (compounds i in Table 1), the dominant unsaturated hydrocarbons in the Black Sea lipid extract, for radiocarbon dating as biomarkers of marine photoautotrophy. These compounds are derived from prymnesiophyte algae, such as the coccolithophorid *Emiliania huxleyi*, a major phytoplankter and important contributor to sinking particulate matter in the contemporary Black Sea (*6*). An autochthonous origin for these compounds is supported by their $\delta^{13}C$ values (Table 1), which are consistent with values for lipids from marine phytoplankton (*7*). The similarity in both ^{13}C values and the conventional ^{14}C ages (*8*) (Table 1) between the alkenes [average $\delta^{13}C = -25.5$ per mil; 950 years before the present (B.P.), respectively] and TOC ($\delta^{13}C = -24.2$ per mil; 880 years B.P.) suggests that modern photoautotrophic biomass is a major component of the bulk OC in these sediments. The similarity in ^{14}C ages between prymnesiophyte alkenes and TOC also suggests that, contrary to previous assumptions (*9*), older detrital OC inputs have a minimal influence on the $^{14}C_{TOC}$ age of late Holocene Black Sea sediments. Conversion of conventional radiocarbon ages to reservoir-corrected ages for marine carbon requires that the reservoir age be accounted for before calibration against tree-ring records of atmospheric ^{14}C abundance (*10*). The reservoir age describes the difference in ^{14}C activity between atmospheric CO_2 and surface-dissolved inorganic carbon (DIC) in marine systems resulting from the mixing of older waters from depth into the surface layer of the ocean. For a reservoir correction of 400 years (*9*), the alkenes yield a revised ^{14}C age for the depth interval of 4 to 7 cm of 550 years B.P. and a calibrated (calendar) age of ~1425 A.D., consistent with published ^{210}Pb and ^{14}C profiles from abyssal Black Sea sediment cores. This age implies that sedimentation rates were 10 to 20 cm per thousand years during the late Holocene (*9*,*11*).

We assessed directly the allochthonous OC inputs from ^{14}C measurements of individual C_{29} and C_{31} *n*-alkanes (compounds v and vi, respectively) (Fig. 1A). The chain length distribution, odd over even carbon number predominance (OEP), and $\delta^{13}C$ compositions (Table 1) of these hydrocarbons are highly characteristic of leaf wax inputs from C_3 vascular (land) plants (plants in which the first product of photosynthesis is a three-carbon acid) (*12*). The young conventional ^{14}C ages for the C_{29} and C_{31} homologs relative to bulk OC (Fig. 2A) demonstrate that corrections for detrital contributions to Black Sea sediments should not necessarily invoke older OC inputs. In-

T. I. Eglinton, B. C. Benitez-Nelson, A. Pearson, Department of Marine Chemistry and Geochemistry, Woods Hole Oceanographic Institution, Woods Hole, MA 02543, USA.
A. P. McNichol, National Ocean Sciences Accelerator Mass Spectrometry Facility, Woods Hole Oceanographic Institution, Woods Hole, MA 02543, USA.
J. E. Bauer, School of Marine Science, College of William and Mary, Gloucester Point, VA 23062, USA.
E. R. M. Druffel, Department of Earth System Science, University of California, Irvine, CA 92697, USA.

*To whom correspondence should be addressed.

Originally published 8 August 1997

deed, accounting for the reservoir age correction for the prymnesiophyte alkenes (vascular plants fix atmospheric CO_2 directly, so their ^{14}C compositions are not subject to any reservoir correction), we find that the *n*-C_{29} and *n*-C_{31} alkanes are similar in calendar age to the marine phytoplanktonic biomarkers. Taken together, these data indicate that relatively fresh terrestrial (land plant) debris is deposited with autochthonous OC of similar age in Black Sea sediments.

In contrast, a suite of shorter chain (C_{23} to C_{27}) *n*-alkanes (compounds ii through iv) as well as the total saturated hydrocarbon (HC) fraction exhibit significantly older ^{14}C ages than either the vascular plant *n*-alkanes or TOC (Fig. 2A and Table 1). Given the similarity in $\delta^{13}C$ values to those of the longer chain alkanes, an independent source for the shorter chain *n*-alkanes seems unlikely. Instead, we infer that fossil hydrocarbons partly contribute to the lower molecular weight homologs. Assuming that there was simple mixing of two end members, we can substitute $\Delta^{14}C$ values (*8*) (Table 1) into an isotopic mass balance (*1*) to estimate the proportion of fossil hydrocarbon required to produce the observed radiocarbon values. For a ^{14}C-free signature ($\Delta^{14}C$ = –1000 per mil) for the fossil component and –66 per mil for a fresh higher plant component (*n*-C_{31} alkane, Table 1), the measured $\Delta^{14}C$ value for the C_{23} *n*-alkane (–153 per mil) would correspond to 9% fossil *n*-alkane. Similarly, given the $\Delta^{14}C$ value of the saturated HC fraction (–155 per mil), fossil hydrocarbons likely represent a small but significant component of this fraction. This minor contribution would have little influence on the carbon number distribution or $\delta^{13}C$ values but is clearly revealed by ^{14}C analysis. Thermogenic hydrocarbons have been detected (*13*) in suspended particles from the Black Sea on the basis of a low OEP *n*-alkane distribution dominated by lower carbon number homologs (C_{23} to C_{27}). If a similar input was responsible for the fossil hydrocarbons we observed, the C_{23} and C_{25} *n*-alkanes would be most strongly influenced by the fossil sources. Because abyssal Black Sea sediments are finely laminated (nonbioturbated) and the depth interval we studied is believed to predate significant human use of fossil fuels (pre-1880), we conclude that these hydrocarbons entered sediments by natural processes such as erosion of petroleum-bearing sediments (*14*) or seepage from depth (*15*).

We selected two sterenes (compounds e and f) as generic markers of marine primary productivity from the Arabian Sea sediment sample because sterols, their precursor natural products (*16*), are biosynthesized by a wide range of phytoplankton and some zooplankton. Conventional ^{14}C ages of these compounds (mean = 680 years B.P.) are significantly younger than the TOC age (890 years B.P.). Consequently, in contrast to the Black Sea, the offset between sterene and TOC conventional ^{14}C ages likely reflects contributions of older OC to the sediment. This age discrepancy is amplified further when a series of highly branched isoprenoid (HBI) alkenes (compounds a through d), characteristic diatom biomarkers (*17*), are examined (Fig. 2B). The C_{25} HBI alkenes exhibit substantially younger ^{14}C ages (mean = 280 years B.P.) than both the sterenes and TOC. Their ^{14}C compositions would yield present-day ^{14}C ages after a 400-year reservoir correction is applied and are likely the result of downward mixing of surficial material containing bomb radiocarbon (from nuclear weapons testing). This mixing could result from sediment winnowing, a process that has been suggested to be a dominant control on the composition of Arabian Sea sediments (*18*). An alternative explanation giving rise to ^{14}C variations in different photoautotrophic biomarkers is heterogeneity in the reservoir age of the DIC pool. The strong seasonal variations in phytoplankton productivity, community structure, and vertical distribution in the Arabian Sea are related to wind-driven (monsoonal) upwelling and mixing of the water column (*19*). The balance between the upwelling of deep waters (low ^{14}C activity) and the physical invasion or biologically driven draw-down of atmospheric CO_2 (high ^{14}C activity) into the surface ocean may give rise to spatial and temporal variability in $^{14}C_{DIC}$ (and, consequently, planktonic ^{14}C). Consequently, differences in ^{14}C and ^{13}C composition, such as those between the C_{25} and C_{30} HBI alkenes, may be a function of the ecological characteristics (such as depth of growth) of their photoautotrophic source—the former having been identified in *Haslea* sp. and the latter in *Rhizosolenia* sp. (*20*). Such discrepancies between ^{14}C ages of phytoplanktonic markers raise the possibility that information on past variations in water column structure may be carried by the isotopic signatures of

Table 1. Isotopic composition of bulk fractions and isolated compounds. The $\delta^{13}C$ values were determined by irm-GC-MS (*5*), except when noted, and were calculated relative to PDB. The ^{14}C age is the conventional radiocarbon age (*8*, *10*). Prym., prymnesiophytes; Vas., vascular (higher) plant; Fos., fossil carbon; Diat., diatoms; Phyt., phytoplankton; Bac., bacteria; ID, compound identification; n.d., not determined ($\delta^{13}C$ assumed as –25 per mil in these instances).

Compound or fraction	Inferred source	ID	$\delta^{13}C$ (per mil)	$\Delta^{14}C$ (per mil)	^{14}C age (years B.P.)
Black Sea core BC4, 4 to 7 cm					
TOC	–	–	−24.2*	−108 ± 3	880 ± 25
TLE†	–	–	n.d.	−113 ± 7	925 ± 65
Saturated HC	–	–	n.d.	−155 ± 15	1,310 ± 150
Autochthonous biomarkers					
C_{37-39} alkenes‡	Prym.	i	−25.5	−116 ± 10	950 ± 100
Allochthonous biomarkers					
n-C_{23} alkane	Vas./Fos.	ii	−30.7	−153 ± 13	1,290 ± 130
n-C_{25} alkane	Vas./Fos.	iii	−29.5	−158 ± 17	1,340 ± 170
n-C_{27} alkane§	Vas./Fos.	iv	−31.1	−136 ± 9	1,130 ± 90
n-C_{29} alkane	Vas.	v	−32.2	−78 ± 9	610 ± 90
n-C_{31} alkane	Vas.	vi	−30.2	−66 ± 11	500 ± 100
Arabian Sea core 6BC, 2 to 4 cm					
TOC	–	–	−21.7*	−109 ± 3	890 ± 30
TLE	–	–	n.d.	−100 ± 6	800 ± 60
Autochthonous biomarkers					
$C_{25:4}$ HBI alkene	Diat.	a	−23.2	−40 ± 15	270 ± 130
$C_{25:3}$ HBI alkene	Diat.	b	−20.2	−47 ± 6	350 ± 50
$C_{25:2}$ HBI alkene	Diat.	c	−19.9	−33 ± 8	225 ± 70
$C_{30:4}$ HBI alkene	Diat.	d	−37.1	−73 ± 8	570 ± 70
C_{30} sterene	Phyt.	e	−18.5	−81 ± 7	630 ± 70
Cholest-2-ene	Phyt.	f	−25.0	−92 ± 6	735 ± 55
22,29,30-trisnorhop-17(21)-ene	Bac.	g	−22.3	−139 ± 11	1,170 ± 100
Hop-21-ene	Bac.	h	−20.5	−125 ± 13	1,030 ± 110
30-norhop-17(21)-ene	Bac.	i	−22.3	−131 ± 9	1,080 ± 90
C_{30} hopene	Bac.	j	−24.1	−147 ± 9	1,240 ± 90
Hop-22(29)-ene	Bac.	k	−23.9	−120 ± 9	985 ± 85
22,29,30-trisnorhop-13(18)-ene¶	Bac.	l	−23.2	−597 ± 4	7,250 ± 70
Allochthonous biomarkers					
17α,21β-homohopane#	Bac./Fos.	m	−21.9	−608 ± 4	7,480 ± 80
n-C_{23} alkane	Vas./Fos.	n	−26.7	−724 ± 10	10,300 ± 300
n-C_{27} alkane	Vas./Fos.	o	−26.7	−677 ± 6	9,050 ± 160
n-C_{29} alkane	Vas./Fos.	p	−28.0	−594 ± 5	7,200 ± 90

*Determined by irMS. †Average of two values. ‡C_{37-39} alkenes were analyzed as a composite sample to maximize yield and because they were insufficiently resolved to be isolated as pure compounds. §Contains an additional C_{27} hydrocarbon. ¶Contains a small portion (~10%) of unresolved material. #Also contains fernene.

different photoautotrophic biomarkers and preserved in the sedimentary record.

The hopanoid alkenes (compounds g through l), which were chosen as bacterial biomarkers (*21*), yielded with one exception (*22*) conventional ^{14}C ages that are 300 to 400 years older than the sterenes. The structures of the individual compounds measured do not permit categoric assignment of precursor organisms; however, their relatively uniform $\delta^{13}C$ compositions (Table 1) clearly point to a marine origin. Deep-dwelling cyanobacteria could yield older ^{14}C ages as a result of uptake of respired DIC emanating from the O_2-depleted waters underlying the Oman upwelling zone (*7*), whereas benthic heterotrophic or chemoautotrophic bacteria may consume older carbon associated with bottom waters or sediments (*23*).

We determined the ^{14}C compositions of selected saturated hopanoid (compound m) and normal (compounds n through p) hydrocarbons to investigate isotopic characteristics of allochthonous sources of OC. In marked contrast to the sterenes and HBI alkenes, these hydrocarbons display much older conventional ^{14}C ages ranging from 7200 to 10,000 years B.P. (Fig. 2B). As for the Black Sea sample, a pronounced OEP for the C_{25} to C_{31} *n*-alkanes indicates that OC from higher plants was supplied to the sediments (Fig. 1B). Plant detritus is likely delivered to this region by eolian processes, primarily the Somali Jet, which entrains dust from the Arabian Peninsula and the Horn of Africa (*4*). Older ages for the *n*-alkanes could be expected because the OC

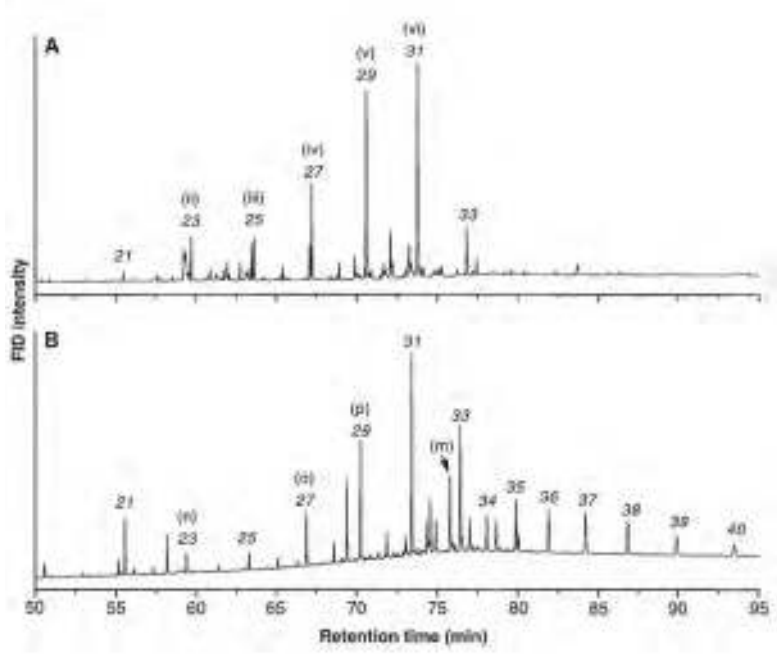

Fig. 1. Partial high-resolution gas chromatograms [with flame ionization detection (FID)] of total saturated hydrocarbon fractions from (**A**) Black Sea core BC4 (4 to 7 cm), and (**B**) Arabian Sea core AS-2 (2 to 4 cm). Numbers in italics indicate carbon chain lengths of *n*-alkanes. Numbers and letters in parentheses denote compounds isolated for ^{14}C analysis from these fractions (see Table 1).

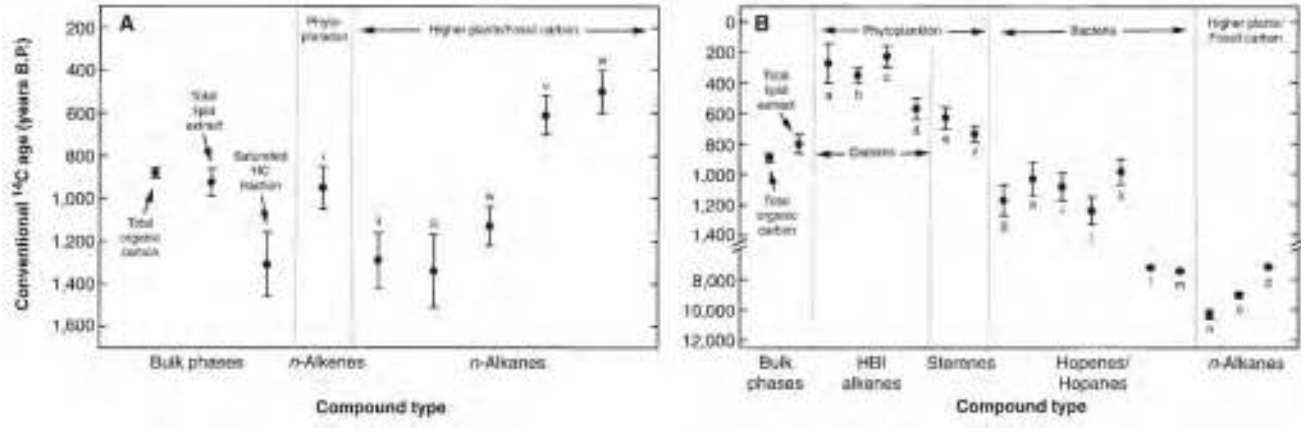

Fig. 2. Plot of conventional ^{14}C ages (determined by AMS) for individual hydrocarbons and bulk fractions: (**A**) Black Sea core BC4, 4 to 7 cm, and (**B**) Arabian Sea core 6BC, 2 to 4 cm. See Table 1 for individual compound identifications. Note break in y-axis in (B). Error bars represent uncertainty associated with statistics of the AMS measurement. Overall error is believed to be better than 5% (in $\Delta^{14}C$) (*1*).

in dust plumes from this region are believed to arise from desiccated lacustrine sediments and paleosols formed at times when the climate in eastern Africa was less arid (before ~6000 years B.P.) (*24*). The hopanoid alkane (compound m) may derive from similar sources (soil or lacustrine bacteria); however, the similarity of its $\delta^{13}C$ value to the photoautotrophic biomarkers suggests that is has a marine origin. We suspect that the old ^{14}C ages of the *n*-alkanes and hopane are a result in part of the presence of fossil OC. Support for this interpretation is provided by the lack of OEP in a series of *n*-alkanes extending to C_{40} (Fig. 1B), indicating the presence of thermogenic hydrocarbons. The lack of an associated unresolved envelope suggests that these fossil hydrocarbons are protected from microbial degradation, possibly through association with mineral matrices (*25*). The overlap in then-alkane envelopes from the higher plant and fossil inputs (Fig. 1B) provides an opportunity to estimate the ^{14}C age for the plant wax contribution. For infinite ^{14}C age petrogenic contributions of 30, 40, and 50% (*26*) to the C_{23}, C_{27}, and C_{29} *n*-alkane, respectively, application of a similar mass balance approach to that described above for the Black Sea *n*-alkanes yields a ^{14}C age of between 4000 and 5000 years B.P. for the land plant component, quite consistent with the timing for the onset of deterioration of climatic conditions in East Africa (*24*).

In both sediments, the maximal variation in radiocarbon ages observed between compounds exceeds the estimated <300-year age span (based on published sedimentation rates) for either of the intervals sampled. Our results reveal that compounds of the same class and belonging to the same homologous series (Black Sea *n*-alkanes) can exhibit distinctly different radiocarbon ages. Compounds having similar $\delta^{13}C$ values may display significantly different ^{14}C ages (Black Sea *n*-alkanes) or, conversely, compounds of similar ^{14}C age may have various $\delta^{13}C$ values (Arabian Sea HBI alkenes). These molecular isotopic measurements thus illustrate how different sources can affect sedimentary $^{14}C_{TOC}$ composition.

Differences in ^{14}C age can now be explained in the context of isotopic characteristics of specific source inputs and hence can be used to interpret the biogeochemical processes that govern their provenance in sediments. Two examples of long-standing issues in biogeochemistry that benefit from molecular ^{14}C measurements are the origin of non-zero $^{14}C_{TOC}$ ages commonly observed for marine surface sediments (*27*), and the development of refined chronostratigraphies free of interferences due to detrital OC inputs and selective degradation of different organic components. The latter also holds promise for other disciplines where accurate ^{14}C measurements are important (such as archeology) but may be compromised by the presence of extraneous carbon-containing material.

References and Notes

1. T. I. Eglinton, L. I. Aluwihare, J. E. Bauer, E. R. M. Druffel, A. P. McNichol, *Anal. Chem.* **68,** 904 (1996).
2. X.-C. Wang, E. R. M. Druffel, C. Lee W. Giger *et al., Nucl. Instr. Meth. Phys. Res.* B5, **394** (1984); X.-C. Wang, E. R. M. Druffel, C. Lee, *Geophys. Res. Lett.* **23,** 3583 (1996).
3. E. Izdar and J. W. Murray, Eds., *Black Sea Oceanography* (Kluwer, Dordrecht, Netherlands, 1991).
4. F. Sirocko and M. Sarnthein, in *Paleoclimatology and Paleometeorology: Modern and Past Patterns of Global Atmospheric Transport,* M. Leinen and M. Sarnthein, Eds. (Kluwer, Dordrecht, Netherlands, 1989), pp. 401–433.
5. The sediment samples, stored frozen (–20°C) from the time of collection until analysis, were thawed, and a portion was dried and acidified (2N HCl) for determination of bulk elemental and isotopic composition [$\delta^{13}C_{TOC}$ by isotope ratio mass spectrometry (irMS), and $^{14}C_{TOC}$ by accelerator mass spectrometry (AMS)]; ~30 g (equivalent dry weight, Black Sea sample) or ~200 g (Arabian Sea sample) was extracted with a Soxhlet apparatus with CH_3OH and CH_2Cl_2. An aliphatic hydrocarbon fraction was isolated from the resulting total lipid extract (TLE) by silica gel chromatography with *n*-C_6H_{14} as the eluent. After removal of elemental sulfur (with an activated Cu column), saturated hydrocarbons (*n*-C_6H_{14} eluent) were separated from unsaturated counterparts ($C_2H_5OC_2H_5$ eluent) by $AgNO_3$-SiO_2 column chromatography. Compound identifications were made by gas chromatography–mass spectrometry (GC-MS), and $\delta^{13}C$ compositions were determined by isotope ratio monitoring GC-MS (irm-GC-MS). Individual compounds were isolated from the purified hydrocarbon fractions by preparative capillary gas chromatography (PCGC). Compounds were trapped during PCGC in cryogenically cooled glass u-tubes, and on completion of the sequence (typically about 100 repeated PCGC runs of each fraction yielded sufficient quantities of compound for AMS ^{14}C analysis), the products were recovered by dissolution in CH_2Cl_2 and transferred to quartz combustion tubes. After some of the sample was removed (for determination of yield and purity by GC), solvent was eliminated from the combustion tubes under a stream of nitrogen, CuO was added, and tubes were evacuated and flame-sealed. The samples were combusted (900°C, 5 hours), and the resulting CO_2 was purified, measured, and subsequently converted to graphite by reduction over Co catalyst in the presence of H_2 for radiocarbon analysis by AMS. AMS was performed at either Woods Hole Oceanographic Institution or Lawrence Livermore National Laboratory.
6. J. K. Volkman, G. Eglinton, E. D. S. Corner, T. E. V. Forsberg, *Phytochemistry* **19,** 2619 (1980); H. A. Benli, in P*article Flux in the Ocean,* E. T. Degens, E. Izdar, S. Honjo, Eds. (SCOPE/UNEP Sonderbrand, West Germany, Heft 62, 1987), pp. 77–87; B. J. Hay, M. A. Arthur, W. E. Dean, E. D. Neff, S. Honjo, *Deep Sea Res.* **38,** 1211 (1991).
7. K. H. Freeman, S. G. Wakeham, J. M. Hayes, *Org. Geochem.* **21,** 629 (1994).
8. Conventional ^{14}C ages (in years B.P.) are calculated with a Libby half-life of 5568 years and take into account ^{13}C fractionation (corrected to a $\delta^{13}C$ value of –25 per mil) but not differences in specific ^{14}C activity of reservoirs or calibration to calendar years. In oceanography, $\Delta^{14}C$ is the per mil deviation of the $^{14}C/12C$ ratio (^{13}C normalized and corrected to A.D. 1950) for the sample relative to the $^{14}C/12C$ ratio of the absolute international standard (95% of the A.D. 1950 activity of NBS HOxI, normalized to $\delta^{13}C = -19$ per mil).
9. G. A. Jones, A. R. Gagnon, *Deep Sea Res.* **41,** 531 (1994).
10. M. Stuiver and H. A. Polach, *Radiocarbon* **19,** 355 (1977); M. Stuiver, G. W. Pearson, T. Braziunas, *ibid.* 28, 980 (1986).
11. S. E. Calvert, *et al., Nature* **350,** 692 (1991); J. Crusius, R. F. Anderson, *Paleoceanography* **7,** 215 (1992).
12. G. Eglinton, R. J. Hamilton, *Science* **156,** 1322 (1967); B. N. Smith, S. Epstein, *Plant Physiol.* **47,** 380 (1971); G. Rieley, *et al., Nature* **352,** 425 (1991); J. W. Collister, G. Rieley, B. Stern, G. Eglinton, B. Fry, *Org. Geochem.* **21,** 619 (1994); S. G. Wakeham, *Mar. Chem.* **53,** 187 (1996); B. R. T. Simoneit, *Deep Sea Res.* **24,** 813 (1977).
13. S. G. Wakeham, J. A. Beier, C. H. Clifford, in (3), pp. 319–341.
14. S. J. Rowland, J. R. Maxwell, *Geochim. Cosmochim. Acta* **48,** 617 (1984).
15. J. E. Bauer, R. B. Spies, J. S. Vogel, D. E. Nelson, J. R. Southon, *Nature* **348,** 230 (1990).
16. R. B. Gagosian, S. O. Smith, C. Lee, J. W. Farrington, N. M. Frew, in *Advances in Organic Geochemistry,* 1979, A. G. Douglas and J. R. Maxwell, Eds. (Pergamon, Oxford, UK, 1980), pp. 407–419.
17. P. D. Nichols, J. K. Volkman, A. C. Palmisano, G. A. Smith, D. C. White, *J. Phycol.* **24,** 90 (1988); R. E. Summons, R. A. Barrow, R. J. Capon, J. M. Hope, C. Stranger, Aust. *J. Chem.* **46,** 907 (1993).
18. T. F. Pederson, G. B. Shimmield, N. B. Price, *Geochim. Cosmochim. Acta* **56,** 545 (1992).
19. B. Haake *et al., Deep Sea Res.* **40,** 1323 (1993); F. Pollehne, B. Klein, B. Zeitzschel, *ibid.*, p. 737.
20. J. K. Volkman, S. M. Barrett, G. A. Dunstan, *Org. Geochem.* **21,** 407 (1994).
21 G. Ourisson, M. Rohmer, K. Poralla, *Annu. Rev. Microbiol.* **41,** 301 (1987).
22. The reason for the old hopene ^{14}C age is unclear, but it may be related to a small proportion of unresolved material that was trapped with this compound during PCGC isolation.
23. J. E. Bauer, C. E. Reimers, E. R. M. Druffel, P. M. Williams, *Nature* **373,** 686 (1995).
24. H. A. McClure, *ibid* **263,** 755 (1976).
25. The GC profiles for the higher plant waxes and petrogenic hydrocarbons as well as the OEP (Fig. 1 B) were used to estimate contributions from each source to individual *n*-alkanes.
26. R. C. Barrick, J. I. Hedges, M. L. Peterson, *Geochim. Cosmochim. Acta* **44,** 1349 (1980).
27. K. O. Emery and E. E. Bray, Bull. *Am. Assoc. Petrol. Geol.* **46,** 1832 (1962); G. J. Benoit, K. K. Turekian, L. K. Benninger, Estuarine Coastal Mar. Sci. 9, 171 (1979); S. Emerson *et al., Nature* **329,** 51 (1987).

28. We thank M. Kashgarian, J. Southon, I. Proctor, and L. Osborne for assistance with AMS analyses, J. Primack and J. Hayes for irm-GC-MS analyses, and D. Repeta and J. Sachs for the sediment samples. This work was supported in part by NSF grants (OCE-94155680; OCE-801015) and a Woods Hole Oceanographic Institution (WHOI) Independent Study Award. This is WHOI contribution n. 9476.

23 April 1997; accepted 13 June 1997

Lipid-Like Material as the Source of the Uncharacterized Organic Carbon in the Ocean?

Jeomshik Hwang and Ellen R. M. Druffel

The composition and formation mechanisms of the uncharacterized fraction of oceanic particulate organic carbon (POC) are not well understood. We isolated biologically important compound classes and the acid-insoluble fraction, a proxy of the uncharacterized fraction, from sinking POC in the deep Northeast Pacific and measured carbon isotope ratios to constrain the source(s) of the uncharacterized fraction. Stable carbon and radiocarbon isotope signatures of the acid-insoluble fraction were similar to those of the lipid fraction, implying that the acid-insoluble fraction might be composed of selectively accumulated lipid-like macromolecules.

Less than 40% of sinking POC collected below the euphotic zone can be molecularly characterized (*1*, *2*). The uncharacterized fraction constitutes an increasing proportion of POC with the depth at which it is collected, with the highest fraction in sedimentary organic carbon (*1*). What is the composition of the uncharacterized fraction and how is it formed?

One hypothesis for the formation of the uncharacterized fraction is abiological recombination of small molecules such as amino acids and carbohydrates produced by degradation of labile organic matter (*3*, *4*). This hypothesis has been challenged by results of ^{13}C and ^{15}N nuclear magnetic resonance (NMR) spectroscopy (*5*, *6*). A second hypothesis is that biologically produced refractory compounds are selectively accumulated whereas labile compounds are remineralized (*7*, *8*). Hydrolysis-resistant cell wall–derived material has been observed in recent and ancient sediments (*9*–*11*). A third hypothesis involves physical protection of organic carbon by refractory organic or inorganic matrices (*12*, *13*). A recent study explored solid-state ^{13}C NMR spectra of plankton and sinking POC collected at shallow and deep waters (*14*). The similarity of the spectra led Hedges *et al.* to suggest that the uncharacterized fraction was the same organic material produced biologically but was protected by mineral matrices or refractory biomacromolecules.

Biologically produced lipids, amino acids, and carbohydrates have distinct stable carbon isotope [$\delta^{13}C$ (*15*)] signatures because of the different physiological fractionation of carbon during their syntheses (*16*, *17*). Therefore, comparison of the $\delta^{13}C$ signature of the uncharacterized fraction with those of other organic fractions will provide insights as to its source(s). The radiocarbon isotope [$\Delta^{14}C$ (*18*)] signatures of all organic fractions are the same when measured in plankton from the surface water because they are fractionation-corrected. The overall signature changes when carbon with a different $\Delta^{14}C$ signature is incorporated and when the carbon is aged (*19*). Therefore, organic fractions that have similar sources, sinks, and residence times in the ocean will have similar $\Delta^{14}C$ signatures.

We measured $\delta^{13}C$ and $\Delta^{14}C$ values in sinking POC collected from a depth of 3450 m, at a site (Station M, 4100 m deep at the bottom, 34°50′N, 123°00′W) 220 km west of the California coast. We isolated biologically important compound classes: lipids, total hydrolyzable amino acids (THAA), total hydrolyzable neutral carbohydrates (TCHO), and a proxy of the uncharacterized fraction, the acid-insoluble fraction (*20*). The acid-insoluble fraction that remains after organic solvent extraction and acid hydrolysis accounts for ~70% of the uncharacterized fraction (*21*).

Sinking POC originates mainly from dissolved inorganic carbon (DIC) in surface waters, and it reaches the deep water on a time scale of months. Therefore, bulk sinking POC is expected to have similar $\Delta^{14}C$ values to those of DIC in surface waters [40 to 80 per mil (‰) (*22*)]. The observed $\Delta^{14}C$ values of bulk sinking POC collected at a depth of 3450 m are lower than the expected values, which means that sinking POC acquired old carbon from other carbon reservoirs during the transit from the surface to the sampling depth. Thus, $\Delta^{14}C$ can be an indicator of diagenetic status of POC (i.e., how much old, degraded carbon is incorporated into sinking POC), assuming constant $\Delta^{14}C$ values of the source organic carbon.

The weight percentages of the characterizable fractions such as lipids, THAA, and TCHO are positively correlated with the $\Delta^{14}C$ values of bulk POC, whereas that of the acid-insoluble fraction is negatively correlated (Fig. 1). Thus, the higher the fraction of acid-insoluble organic carbon, the lower the bulk POC $\Delta^{14}C$ value.

The $\Delta^{14}C$ values of each organic fraction are plotted with respect to the bulk POC $\Delta^{14}C$ to show the relative amounts of old and new carbon (Fig. 2). The $\Delta^{14}C$ values of THAA and TCHO are similar to each other and close to those of surface water DIC. The $\Delta^{14}C$ values of lipids and the acid-insoluble fractions are similar to each other but are lower than those of THAA and TCHO. The $\Delta^{14}C$ values of lipids and the acid-insoluble fraction decrease at slightly higher rates than THAA and TCHO, making the difference between the two groups bigger as the bulk POC $\Delta^{14}C$ values decrease. The slopes of the lines imply that $\Delta^{14}C$ values will converge at or around the range of DIC $\Delta^{14}C$ in surface waters. The $\Delta^{14}C$ values of the four fractions from plankton collected at the same station were equal to the range of DIC $\Delta^{14}C$ (*23*). This indicates that all organic frac-

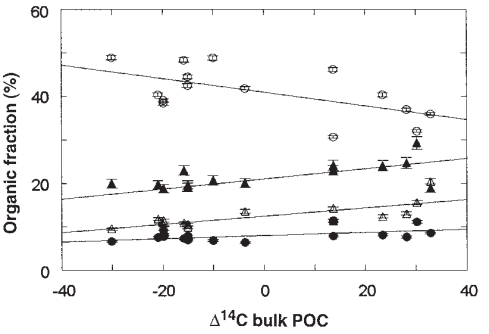

Fig. 1. Percent of each organic compound class (lipids, solid circles; THAA, solid triangles; TCHO, open triangles; acid-insoluble fraction, open circles) separated from several 10-day samples of sinking POC collected at a depth of 3450 m at Station M in the Northeast Pacific. The amounts of CO_2 of each compound class were measured manometrically after combustion and were compared to the organic carbon content measured with an element analyzer. The uncertainty is the larger value of 1σ of either the yield of standard material (replicate number >5) or a duplicate run of samples (3% for lipids, 5% for THAA, 3% for TCHO, and 1% for acid-insoluble fraction).

Department of Earth System Science, University of California Irvine, Irvine, CA 92697–3100, USA. E-mail: jeomshik@uci.edu (J.H.); edruffel@uci.edu (E.R.M.D.)

Originally published 7 February 2003

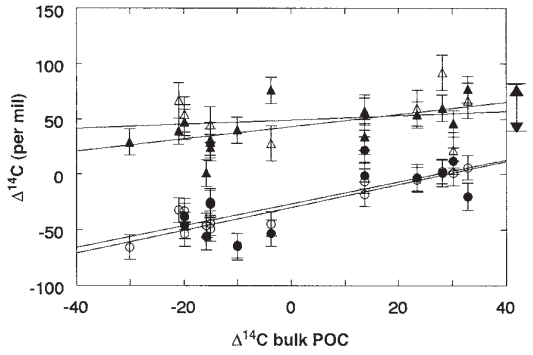

Fig. 2. The $\Delta^{14}C$ values of each organic compound class (symbols are as defined in Fig. 1). The black arrow by the right *y*-axis indicates the range of DIC $\Delta^{14}C$ values in surface waters at Station M. The $\Delta^{14}C$ values are blank-corrected. We measured $\Delta^{14}C$ of an amino acid standard solution (mixture of 17 amino acids), D-glucose powder, and cod liver oil by the same methods as the samples. We compared these values with those of unprocessed standards to calculate the $\Delta^{14}C$ values of the blanks. The amounts of the blank were measured manometrically by combining five or six blanks together. Blanks were higher for THAA and TCHO, because there were more steps involved in their separation. The acid-insoluble fraction was not blank-corrected because the blank was smaller than 0.01 mg (<0.7% of the sample). The uncertainty is the larger value of 1σ of either standard material (replicate number >5) or duplicates of samples.

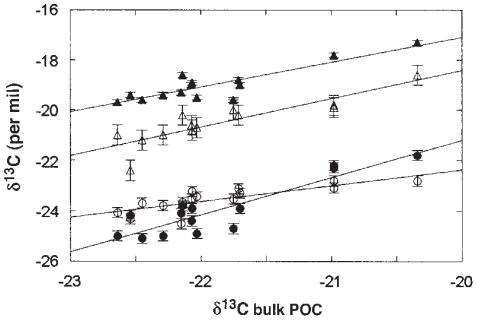

Fig. 3. The $\delta^{13}C$ values of each compound class (symbols are as defined in Fig. 1). The $\delta^{13}C$ values are blank-corrected by the same method as $\Delta^{14}C$. The uncertainty is the larger value of 1σ of either standard material or duplicates of samples.

tions of sinking POC originated from modern source(s) of carbon, but lipids and the acid-insoluble fraction acquired more old carbon than did THAA and TCHO.

The $\delta^{13}C$ values of lipids are 3 to 4‰ lower than those of THAA and TCHO (Fig. 3), as expected from physiological fractionation (*16*, *17*), but approximately equal to those of the acid-insoluble fraction. The differences in $\delta^{13}C$ between the organic fractions for each sample are constant even though $\delta^{13}C$ values in bulk POC samples vary by 2.5‰.

The constant differences in $\delta^{13}C$ between the acid-insoluble fraction and the other organic fractions provide constraints on its source(s). One possible scenario is that the acid-insoluble fraction is synthesized by the reaction between THAA and TCHO that are tightly bound with particles. However, the differences in $\delta^{13}C$ between the acid-insoluble fraction and THAA and TCHO (~4‰) argue against the degradation-recombination hypothesis of amino acids and carbohydrates for the formation of the acid-insoluble fraction. Two ^{13}C-enriched fractions cannot combine to form a ^{13}C-depleted fraction unless kinetic fractionation occurs during the chemical reactions. If kinetic fractionation occurs, one would expect ^{13}C to be enriched in remaining THAA and TCHO (*24*). However, the $\delta^{13}C$ values of the compound fractions were reported to remain constant for organic carbon of detrital aggregates, sediment floc, and sediment (0 to 20 cm) at the same location, and Wang *et al.* concluded that $\delta^{13}C$ signatures of each organic fraction were not affected by decomposition processes of organic matter (*23*).

The differences in $\delta^{13}C$ between the acid-insoluble fraction and THAA and TCHO argue against nonselective mineral protection as well. If the acid-insoluble fraction is simply the same material produced biologically as lipids, THAA, and TCHO, with the only difference that they are protected by mineral matrices, its isotopic signature should be similar to those of THAA and TCHO. Furthermore, treatment of the acid-insoluble fraction of POC with an HCl-HF solution to dissolve the mineral phases did not increase the extractable fraction of THAA and TCHO significantly [<5% of total organic carbon (OC)] (*25*, *26*). However, our data do not argue against the hypothesis of selective mineral protection.

Another possibility is that the acid- insoluble fraction is protected lipids, THAA, and TCHO and contains a small fraction of old carbon [for example, old terrestrial carbon considering the location of the sampling site (220-km offshore)]. About 10% of the acid-insoluble fraction needs to be old carbon to explain observed low $\Delta^{14}C$ values (*27*). However, in order to explain the low $\delta^{13}C$ values of the acid-insoluble fraction, a much larger fraction (up to 50%) needs to be terrestrial carbon (*27*). Therefore, this mechanism cannot satisfy the $\delta^{13}C$ and $\Delta^{14}C$ results at the same time.

It is most likely that the major part of the acid-insoluble fraction is a selectively preserved part of organisms that is chemically different from amino acids and carbohydrates. Low $\Delta^{14}C$ values can be explained if the major portion of the acid-insoluble fraction is surface-originated fresh carbon and only a small fraction is older carbon that has aged and was incorporated into the particles. The source of the old carbon can be either dissolved organic carbon (DOC) or suspended POC. Resuspended sedimentary organic carbon will be old, but $\delta^{13}C$ values will be very similar to those of POC (*28*). Old carbon from eroded marine-origin bedrock is another possible source of old suspended POC (*29*).

The incorporation of old carbon into particles occurs more actively for lipids and the acid-insoluble fraction. Because lipids are hydrophobic and water-insoluble, they are more likely to be adsorbed to particles than are THAA and TCHO, most of which are water-soluble (*30*). The fact that the acid-insoluble fraction has similar $\Delta^{14}C$ values to those of lipids suggests that the two fractions have similar physicochemical properties. The similarity of $\delta^{13}C$ in lipids and the acid-insoluble fractions may suggest that both fractions are synthesized by similar biochemical pathways that are different from those for THAA and TCHO.

Our results suggest that the major portion of the acid-insoluble fraction is composed of lipid-like material that is biosynthesized by similar pathways to the extractable lipids, but somehow is resistant to organic solvents and acids. In fact, lipids are enriched in resistant parts of organisms such as membranes, spores, and cuticles (*4*). Selective preservation of these resistant lipids has been considered as one method of kerogen formation (*4*). The refractory cell wall–derived material of microalgae and bacteria, known as algaenans and bacterans, respectively, were found to make up a large part of kerogen and refractory organic carbon in sediments (*8*, *11*, *31–33*). They are, essentially, highly aliphatic lipids (i.e., a large number of carbon-to-carbon bonds) evidenced by release of *n*-alkane and *n*-alka-1-ene upon pyrolysis and by a high alkyl signal in ^{13}C NMR spectra. A network structure built up by cross-linking of long hydrocarbon chains was suggested as a protection mechanism against chemical

attack (*9*). Considering that the mechanisms of lipid synthesis are similar in all organisms (*17*), these refractory macromolecules might be expected to have similar $\delta^{13}C$ signatures as those for the extractable lipids. The similarity of the nonhydrolyzable fraction and nonprotein alkyl carbon in chemical composition and abundance was observed in sediment from the continental margin of northwestern Mexico, and it was suggested that those components were compositionally similar to cell wall–derived algaenans (*33*). Even though these refractory lipid-like macromolecules have been studied only in sediments, selective accumulation of the lipids is likely to occur in the water column as the POC sinks. Selective accumulation of the refractory lipid-like material in the water column was evidenced by the observation that alkanes accounted for increasing fractions of the pyrolyzates of sinking POC as depth increased in the Equatorial Pacific (*34*) and the Mediterranean Sea (*35*).

Even though results of the ^{13}C NMR spectroscopy and direct temperature-resolved mass spectrometry on the samples from the Equatorial Pacific do not support the predominance of lipid-like material in sinking POC (*14*, *34*), the composition of sinking POC might vary depending on the local environment (*36*). The percentage of lipid in sinking POC in the Arabian Sea was twice as high as that in the Equatorial Pacific (*14*). Also, our sampling site can be influenced by laterally transported old carbon from the continental shelf or slope and from rivers in the California coast (*37*). Further study will be necessary to confirm if our observation is universal in the oceans. These results should provide important information to understand how organic carbon is preserved and removed from the carbon cycle in the ocean.

References and Notes

1. S. G. Wakeham, C. Lee, J. I. Hedges, P. J. Hernes, M. L. Peterson, *Geochim. Cosmochim. Acta* **61**, 5363 (1997).
2. J. I. Hedges *et al.*, *Org. Geochem.* **31**, 945 (2000).
3. J. I. Hedges, *Geochim. Cosmochim. Acta* **42**, 69 (1978).
4. B. P. Tissot, D. H. Welte, *Petroleum Formation and Occurrence* (Springer, Heidelberg, Germany, ed. 2, 1984), part II, chap. 2.
5. H. Knicker, A. W. Scaroni, P. G. Hatcher, *Org. Geochem.* **24**, 661 (1996).
6. M. McCarthy, T. Pratum, J. Hedges, R. Benner, *Nature* **390**, 150 (1997).
7. P. G. Hatcher, E. C. Spiker, N. M. Szeverenyi, G. E. Maciel, *Nature* **305**, 498 (1983).
8. E. W. Tegelaar, J. W. de Leeuw, S. Derenne, C. Largeau, *Geochim. Cosmochim. Acta* **53**, 3103 (1989).
9. J. W. de Leeuw, C. Largeau, in *Organic Geochemistry: Principles and Applications*, M. H. Engel, S. A. Macko, Eds. (Plenum, New York, 1993), pp. 23–72.
10. C. Flaviano, F. Le Berre, S. Derenne, C. Largeau, J. Connan, *Org. Geochem.* **22**, 759 (1994).
11. C. Largeau, J. W. de Leeuw, in *Advances in Microbial Ecology*, J. G. Jones, Ed. (Plenum, New York, 1995), vol. 14, pp. 77–117.
12. R. G. Keil, D. B. Montluçon, F. G. Prahl, J. I. Hedges, *Nature* **370**, 549 (1994).
13. R. A. Armstrong, C. Lee, J. I. Hedges, S. Honjo, S. G. Wakeham, *Deep-Sea Res. II* **49**, 219 (2002).
14. J. I. Hedges *et al.*, *Nature* **409**, 801 (2001).
15. The stable carbon isotope ratio is expressed as a relative ratio to the Pee Dee Belemnite standard, given by $\delta^{13}C = [(^{13}C/^{12}C)\text{sample}/(^{13}C/^{12}C)\text{standard} - 1] \times 1000$.
16. E. T. Degens, M. Behrendt, B. Gotthardt, E. Reppmann, *Deep-Sea Res.* **15**, 11 (1968).
17. M. J. DeNiro, S. Epstein, *Science* **197**, 261 (1977).
18. The $\Delta^{14}C$ value is the per mil deviation of the $^{14}C/^{12}C$ ratio relative to a standard. It is normalized to a $\delta^{13}C$ of –25‰ to remove isotopic fractionation effect. The half-life of ^{14}C is 5730 years. See (*38*).
19. E. R. M. Druffel, P. M. Williams, J. E. Bauer, J. R. Ertel, *J. Geophys. Res.* **97**, 15639 (1992).
20. Sinking POC was collected in a sediment trap equipped with an automatic sequencer set to collect samples at 10-day periods. The filtered POC (1 μm pore size) was dried at 50°C, ground, and stored in a freezer until analysis. The sample was cavitated with an ultrasonicator in a 2:1 volume/volume mixture of methylene chloride:methanol, and then was centrifuged. The extraction was repeated four times, and the combined supernatant was used as the lipid extract. Roughly half (weighed) of the residue was hydrolyzed for total hydrolyzable amino acids (THAA) (6 M HCl under N_2 gas for 19 hours) and the other half for total hydrolyzable neutral carbohydrates (TCHO) (2 hours in 72% H_2SO_4, then 3 hours in 0.6 M H_2SO_4). The hydrolyzates were eluted through ion exchange columns for the separation of THAA and TCHO. The organic carbon left after THAA extraction was used for the acid-insoluble fraction. Each organic carbon extract was acidified with 1 ml of 3% H_3PO_4, dried under vacuum, and combusted at 850°C for 2 hours with CuO and silver foil in a sealed tube. The resultant CO_2 was graphitized at 600°C on a Co catalyst. The $\Delta^{14}C$ measurements were performed at either the National Ocean Sciences Accelerator Mass Spectrometry Facility (NOSAMS), Woods Hole Oceanographic Institution (WHOI), or the Center for Accelerator Mass Spectrometry (CAMS), Lawrence Livermore Laboratory (LLNL). For a detailed description of the method, see (*23*).
21. The percentage was calculated from the ratio of the acid-insoluble fraction to the uncharacterized fraction that is the difference between the total organic carbon and the characterized fractions (lipids, THAA, and TCHO).
22. C. A. Masiello, E. R. M. Druffel, J. E. Bauer, *Deep-Sea Res. II* **45**, 617 (1998).
23. X.-C. Wang, E. R. M. Druffel, S. Griffin, C. Lee, M. Kashgarian, *Geochim. Cosmochim. Acta* **62**, 1365 (1998).
24. Y. Qian, M. H. Engel, S. A. Macko, *Chem. Geol.* **101**, 201 (1992).
25. J. Hwang, unpublished data.
26. After the extraction of lipid and acid-soluble fractions, the acid-insoluble fraction was treated with HCl-HF solution (5 ml of 1.5 M HCl and 5 ml of 50% HF) for 24 hours at room temperature, then was dried completely to remove HF. The extraction of lipids and acid-soluble fractions was performed on the demineralized fraction.
27. The fraction of old carbon was calculated by a mass-balance equation assuming that the acid-insoluble fraction is composed of lipids, THAA, and TCHO. Weighted averages of the lipids, THAA, and TCHO are 40‰ and –20.3‰ for $\Delta^{14}C$ and $\delta^{13}C$, respectively. The observed values of the acid-insoluble fraction are –23‰ and –23.5‰ for $\Delta^{14}C$ and $\delta^{13}C$, respectively. Assuming –500‰ and –27‰ for $\Delta^{14}C$ and $\delta^{13}C$ of terrestrial carbon, respectively, the percentage of terrestrial carbon (f) can be calculated by $40 \times (1 - f) + (-500) \times f = -23$ ($f = 0.12$ for $\Delta^{14}C$); $-20.3 \times (1 - f) + (-27) \times f = -23.5$ ($f = 0.48$ for $\delta^{13}C$).
28. R. M. Sherrell, M. P. Field, Y. Gao, *Deep Sea Res. II* **45**, 733 (1998).
29. C. A. Masiello, E. R. M. Druffel, *Global Biogeochem. Cycles* **15**, 407 (2001).
30. S. M. Henrichs, *Mar. Chem.* **49**, 127 (1995).
31. T. Eglinton, *Org. Geochem.* **21**, 721 (1994).
32. A. Garcette-Lepecq, S. Derenne, C. Largeau, I. Bouloubassi, A. Saliot, *Org. Geochem.* **31**, 1663 (2000).
33. Y. Gélinas, J. A. Baldock, J. I. Hedges, *Science* **294**, 145 (2001).
34. E. C. Minor, S. G. Wakeham, C. Lee, *Geochim. Cosmochim. Acta*, in preparation.
35. S. Peulvé, J. W. de Leeuw, M.-A. Sicre, M. Baas, A. Saliot, *Geochim. Cosmochim. Acta* **60**, 1239 (1996).
36. X.-C. Wang, E. R. M. Druffel, *Mar. Chem.* **73**, 65 (2001).
37. K. L. Smith, R. S. Kaufmann, R. J. Baldwin, A. F. Carlucci, *Limnol. Oceanogr.* **46**, 543 (2001).
38. M. Stuiver, H. A. Polach, *Radiocarbon* **19**, 355 (1977).

39. We thank S. Griffin for guidance in laboratory work and C. Masiello, X.-C. Wang, C. Lee, and A. Ingalls for discussion on the experiments; K. Smith, J. Bauer, D. Wolgast, R. Baldwin, R. Glatts, F. Uhlman, R. Wilson, and the crews of the R/V *New Horizon* for help with sample collection; S. Trumbore and S. Zheng for shared equipment; A. McNichol, R. Schneider, J. Hayes, and colleagues at NOSAMS, WHOI, and J. Southon and colleagues at CAMS, LLNL, for the $\Delta^{14}C$ measurement; A. Gagnon for the $\delta^{13}C$ measurement; M. McCarthy for discussion and review of the manuscript; and C. Lee, T. Komada, S. Beaupré, and an anonymous reviewer for helpful comments on the manuscript. Supported by the Chemical Oceanography Program of NSF and the University of California Office of the President (fellowship to J.H.).

17 September 2002; accepted 7 January 2003

Two Chemically Distinct Pools of Organic Nitrogen Accumulate in the Ocean

Lihini I. Aluwihare,[1]* Daniel J. Repeta,[2] Silvio Pantoja,[3] Carl G. Johnson[2]

The chemical dynamics of marine dissolved organic nitrogen (DON), a reservoir featuring surface accumulations even in areas where nitrogen limits productivity, have yet to be resolved. We exploited differences in the acid lability of amide bonds within high-molecular-weight (HMW) DON to show that vertical DON profiles result in part from the presence of two chemically distinct pools of amide. Half of HMWDON in surface waters is present as N-acetyl amino polysaccharides. In contrast, nearly all deep-sea HMWDON, and therefore, most HMWDON, is present in amides that resist both chemical hydrolysis and biological degradation.

Low concentrations of inorganic nitrogen (such as nitrates and ammonia) are assumed to limit primary production over wide expanses of the surface ocean. However, in many of these areas, dissolved organic nitrogen (DON) accumulates to measurable quantities (*1*–*3*) despite a demonstrated role in fueling both primary and secondary production (*4*). Given the importance of nitrogen for limiting ocean productivity, mechanisms that regulate DON production and removal could help control both the ocean's N balance and, consequently, the sequestration of atmospheric carbon dioxide.

Processes that lead to DON accumulation in seawater are unclear, but vertical profiles show that upper ocean DON concentrations are enhanced by 30 to 50% over deep water values (*5*). This observation suggests a major source for DON in the upper ocean and is consistent with findings that a large fraction of inorganic N assimilated by marine phytoplankton can be returned to seawater as DON (*6*). However, an important step for explaining DON profiles in the ocean is to identify compositional features that differentiate DON fractions with diverse biological reactivity. Here we report evidence for major structural differences between the DON pools of the surface and the deep ocean.

About 30% of DON occurs as a high-molecular-weight fraction (HMWDON) that can be sampled by ultrafiltration (*6*, *7*). The depth profile of HMWDON is similar to that of total DON, with high near-surface concentrations. Despite a decline in HMWDON concentrations below the mixed layer, nuclear magnetic resonance (NMR) spectra and amino acid analyses imply a homogenous chemical composition throughout the water column (*8*, *9*). Nitrogen-15 NMR (^{15}N-NMR) spectroscopy shows that nearly all HMWDON in the ocean is chemically bound as amide functional groups (*8*). Amides are commonly found in living marine organisms within proteins and biopolymers of *N*-acetyl amino polysaccharides (*N*-AAPs, e.g., chitin and peptidoglycan). However, acid hydrolysis of HMWDON yields only small amounts of amino acids and amino sugars, suggesting that HMWDON is deficient in these polymers (*9*, *10*). However, previous studies have also demonstrated that it is difficult to draw quantitative conclusions from analyses that require depolymerization of HMWDON compounds (*10*).

Rather than relying on a hydrolysis method that efficiently depolymerizes polysaccharides and proteins, we exploited differences in the amide bonds of proteins and *N*-AAPs to quantify the contribution of these biochemicals to marine DON. Amide bonds in proteins are an integral part of the peptide linkage, and amide hydrolysis depolymerizes proteins to yield amino acids (Fig. 1). Amide bonds in *N*-AAPs are not an integral part of the glycosidic linkage, and amide hydrolysis of *N*-AAPs is not directly coupled to depolymerization. Instead, amide hydrolysis de-acetylates the polysaccharide, releasing 1 mole of acetic acid for each mole of amide-N that is hydrolyzed (Fig. 1). Therefore, proteins can be quantified and distinguished from *N*-AAPs by the products of acid hydrolysis (amino acids and acetic acid, respectively). In both cases (proteins and *N*-AAPs), the hydrolysis of the amide bond produces amine-N. We used solid-state (cross-polarization magic-angle spinning) ^{15}N-NMR spectroscopy to follow the hydrolysis of HMWDON amide and quantify the conversion of amide-N to amine-N. Concurrent measurements of acetic and amino acid generation were used to partition HMWDON into proteins and *N*-AAPs. These experiments allowed us to construct a budget of nitrogen-containing biopolymers in marine HMWDON.

High molecular weight dissolved organic matter (HMWDOM) in surface seawater is rich in carbohydrate (60 to 80% of total C) and acetate (5 to 7% of total C), as seen in the ^{1}H-NMR spectrum for Woods Hole surface seawater (Fig. 2A) [carbohydrates, 5.2, 4.5-3.2, and 1.3 parts per million (ppm); acetate, 2 ppm]. Previous studies have shown that the chemical composition of Woods Hole HMWDOM is representative of marine HMWDOM in general (*10*, *11*). The ^{15}N-NMR for this sample (Fig. 2B) shows one major resonance at 124 ppm for amide-N (92% of total N) and a minor resonance at 35 ppm for amine-N (8% of total N). We hydrolyzed

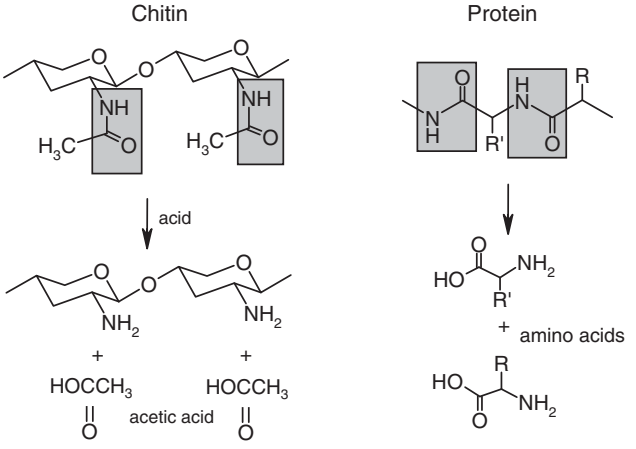

Fig. 1. Schematic showing the effect of mild acid hydrolysis on the amide linkage of proteins and *N*-AAPs (chitin). Mild acid hydrolysis (*13*) completely destroys the amide linkage (gray shaded area) in an *N*-AAP and quantitatively releases acetic acid. However, the glycosidic linkage remains unaffected, and the macromolecule is not depolymerized. Mild acid hydrolysis could likewise destroy the amide linkage in proteins (gray shaded area), thereby depolymerizing the macromolecule to release amino acids. If proteins and *N*-AAPs are the major biochemical components of HMWDON, then the sum of acetic and amino acids recovered after mild acid hydrolysis should equal the amount of amide destroyed during the reaction.

[1]Geosciences Research Division, Scripps Institution of Oceanography, La Jolla, CA 92093, USA. [2]Department of Marine Chemistry and Geochemistry, Woods Hole Oceanographic Institution, Woods Hole, MA 02543, USA. [3]Department of Oceanography and Fondap Copas Center, University of Concepción, Casilla 160-D, Concepción, Chile.

*To whom correspondence should be addressed. E-mail: laluwihare@ucsd.edu

Originally published 13 May 2005

Woods Hole HMWDON using conditions that were considerably milder than those typically employed for peptide bond hydrolysis (*12*) but that quantitatively release acetic acid from *N*-acetyl glucosamine and chitotriose (*13*). As expected in the case of *N*-AAPs, the acid hydrolysis (*13*) removed acetic acid from our samples (Fig. 2C) in quantifiable yield (Table 1) (*14*). Concurrent with the loss of acetic acid, there was a decrease in amide-N from 92% of the total N (7.1 μmol of N) to 35%, and an increase in the amount of amine-N from 8% of the total (0.6 μmol of N) to 65% (5 μmol of N) N (Fig. 2D and Table 1). Amino acid analysis showed that some proteins were hydrolyzed to amino acids that were recovered at 13% (Table 1) of the total N (*15*). The amount of amide-N converted to amine-N during acid hydrolysis, as quantified by ^{15}N-NMR spectroscopy, nearly equaled the molar sum of acetic and amino acids recovered by molecular level techniques (4.4 versus 4.3 μmol) (Table 1). The agreement between NMR spectroscopy and these molecular level analyses confirms that the hydrolyzed amide was originally present in HMWDON as proteins and *N*-AAPs. Under stronger hydrolysis conditions (*12*), we were able to recover 21% (1.6 μmol of N) of the total N in the sample as amino acids.

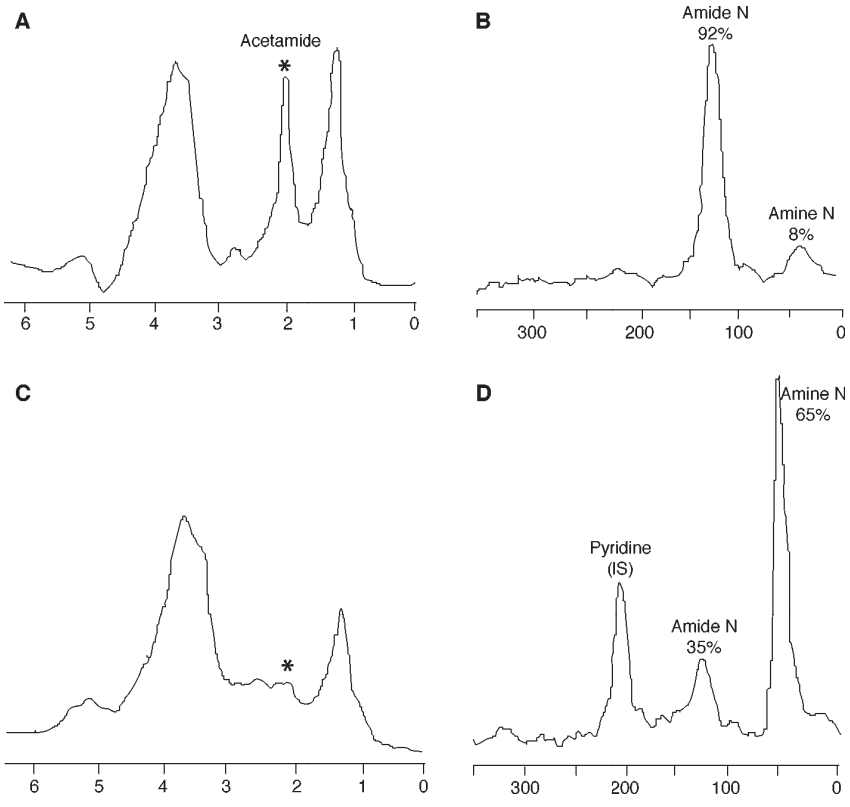

Fig. 2. The effect of mild acid hydrolysis (*13*) on the amide linkages of HMWDON isolated from Woods Hole surface seawater. (**A**) The ^{1}H-NMR spectrum [300 MHz, D_2O, δ (chemical shift in ppm downfield from tetramethylsilane)] shows bound acetic acid (*, 2.0 ppm). (**B**) The ^{15}N-NMR spectrum [400 MHz, solid-state, δ (chemical shift in ppm downfield from liquid NH_3)] before acid hydrolysis shows most nitrogen (92%) bound as amide. (**C**) Mild acid hydrolysis and organic extraction removes acetic acid, demonstrating complete de-acetylation. (**D**) This hydrolysis converts 57% of the amide-N into amine, commensurate with the amount of acetic and amino acids recovered by molecular level analyses (56%) (Table 1) and increases the total amine-N to 65%. Pyridine added to quantify losses during sample processing showed 98% recovery of HMWDON. IS, internal standard.

Using acetic acid as a proxy for *N*-AAPs, our results indicate that HMWDON in surface seawater is 43% *N*-AAPs (Table 1), 21% hydrolyzable protein, and 29% (2.2 μmol of N) nonhydrolyzable amide (*16*). The remaining HMWDON in our Woods Hole sample (8%, 0.6 μmol of N) initially present as amine was not characterized by our analyses but may be present as basic or N-terminal amino acids of proteins or as amino sugars. We obtained a similar agreement between the quantity of N converted from amide to amine and the molar sum of amino acids plus acetic acid recovered by molecular level analyses for HMWDON sampled from the North Pacific Ocean (Table 1); the agreement confirms the ubiquity of *N*-AAPs. Our analyses demonstrate that soluble *N*-AAP biopolymers contribute ~26% of the carbon and 40 to 50% of the nitrogen to surface ocean HMWDOM (*16*).

Peptidoglycan, currently assumed to dominate the oceanic reservoir of HMWDON, is rich in *N*-acetyl glucosamine and *N*-acetyl muramic acid (present in a 1:1 ratio) (*9*). Both sugars contain amide-N and are potential sources for the *N*-AAPs we quantified by our NMR experiment. The presence of acetylated amino sugars in HMWDON has been inferred previously from mass spectrometric data (*17*, *18*), but recoveries of *N*-acetyl glucosamine and *N*-acetyl muramic acid, which make up the amide-rich glycan of peptidoglycan, are low (*10*, *11*, *19*). Even under conditions specific for peptidoglycan hydrolysis (*20*, *21*), we were unable to detect muramic acid in our samples. Glucosamine, though present, contributed <1% of the total carbon, far lower than the ~10% HMWDOM-carbon ex-

Table 1. Change in amide content and yields of acetic and amino acids, upon mild acid hydrolysis of HMWDON. All percentages are expressed relative to total μmol of N.

Sample	Total (μmol N)*	Amide (μmol N)	Δ Amide (μmol N)†	Acetic acid (μmol)	Amino acids (μmol)	∑Acetic + amino acids (μmol)	Unhydrolyzed amide (μmol N)‡
Woods Hole (5 m)	7.7	7.1 (92%)	–4.4	3.3 (43%)	1.0 (13%)	4.3	2.7 (35%)
MAB (1000 m)	7.7	7.7 (100%)	–1.8	1.3 (17%)	0.8 (10%)	2.1	5.8 (76%)
Hawaii (23 m)	6.2	6.2 (100%)	–3.7	3.3 (53%)	0.5 (8%)	3.8	2.4 (39%)
Hawaii (600 m)	6.2	6.2 (100%)	–3.7	3.4 (55%)	0.4 (6%)	3.8	2.4 (39%)

*Values are expressed per 100 μmol of HMW dissolved organic carbon and calculated based on the C/N ratio of each sample. †Δ Amide is the change in the amount of amide-N after hydrolysis, as quantified by integration of the ^{15}N-NMR spectra. In all cases, hydrolysis resulted in the loss of amide-N. ‡The quantity (μmol of N) of amide remaining in the sample after mild (*13*) hydrolysis, quantified directly by ^{15}N-NMR spectroscopy. Higher concentrations of HCl (*12*) hydrolyzed a greater percentage of the amide-N, leaving slightly less (2.2 and 5.5 μmol) amide-N unhydrolyzed in the Woods Hole and MAB samples, respectively. In order to quantify the amount of amide-N remaining after strong acid hydrolysis the Σacetic acid (mild) + amino acids (strong) was first determined and then subtracted from the initial amide content of the HMWDON sample (before hydrolysis) (*16*). Here, acetic acid is being used as a proxy for *N*-AAPs.

pected if all of the acetic acid in our samples was from peptidoglycan. Possible explanations for the general discrepancy between NMR-derived estimates of *N*-AAPs and molecular-level carbohydrate analyses are incomplete depolymerization of *N*-AAPs and rapid Maillard condensation reactions of hydrolysis products (*22*).

Muramic acid also contains lactic acid, which can be quantitatively released from peptidoglycan without depolymerizing the glycan (*23*). For peptidoglycan, 1 mol of lactic acid will be released for every 2 mol of acetic acid. Concentrations of lactic acid (*14*) in our samples were <0.4% of HMWDOM-carbon, an order of magnitude less than expected if all of the acetic acid we recovered was from peptidoglycan. The low concentration of lactic acid measured in this study and the low concentration of D-amino acids previously reported for HMWDON (*9*) together suggest that peptidoglycan is at best only a minor component of HMWDON. In addition, the D-amino acids in HMWDON so far identified to be present in peptidoglycan (*9*) could be present in a number of compounds synthesized by prokaryotes and eukaryotes (*24*, *25*).

Because *N*-AAPs represent ~40 to 50% of the HMWDON in surface waters, and given that 40 to 50% of HWMDON is removed below the mixed layer (*6*, *8*), we hypothesize that the global decrease in HMWDON with depth in the oceans results from the selective removal of *N*-AAPs. To test this hypothesis, we analyzed HMWDOM collected from a depth of 1000 m in the Middle Atlantic Bight (MAB), which has radiocarbon, ^{1}H-NMR, and molecular-level properties characteristic of deep-sea HMWDOM (*10*). In agreement with previous ^{15}N-NMR spectra of deep sea HMWDON (*8*), the ^{15}N-NMR spectrum of our sample shows one major resonance characteristic of amide-N (100% of total N) (Fig. 3A). Mild acid hydrolysis (*13*) decreased amide-N from 100% to 76% of total N and increased amine-N from undetectable levels to 24% of total N (Fig. 3B and Table 1). After acid hydrolysis, acetic acid was released from HMWDOM, as were amino acids, which increased from undetectable levels to 10% of total N. The sum of acetic plus amino acids (2.1 μmol) in the hydrolysis products was similar to the increase in amine-N (1.8 μmol of N) observed with ^{15}N-NMR spectroscopy. Molecular-level analyses after strong acid hydrolysis showed deep-sea HMWDON was 17% *N*-AAPs (Table 1), 12% hydrolyzable protein, and 71% nonhydrolyzable amide (5.5 μmol of N) (*16*). Despite the surface water abundance, a large fraction of *N*-AAPs are lost during mixing into the deep ocean. Proton NMR spectra of numerous deep-sea samples showed a sharp decrease in acetate below the mixed layer, confirming the loss of *N*-AAPs with depth (Fig. 4). The loss in *N*-AAPs and the relative increase in nonhydrolyzable amides will not result in any change to the ^{15}N-NMR spectrum (*8*).

The lack of amines in marine HMWDON implies that amine-N is more labile than amide-N. Many marine microorganisms have cell surface–bound deaminases that are capable of extracting amine-N from a variety of organic compounds (*26*). These enzymes could render HMW amine-N more biologically available by allowing organisms to bypass polymer hydrolysis or uptake. The eventual depth-dependent loss of *N*-AAPs from HMWDON suggests either that *N*-AAP compounds are labile or that organisms have developed a mechanism to access the nitrogen in *N*-AAPs without complete hydrolysis of the polymer (perhaps through cell surface–bound acetamidases). Although we were unable to depolymerize *N*-AAPs using acid hydrolysis, the capacity to enzymatically degrade *N*-AAPs may be widespread among marine microbes. In particular, the ability to hydrolyze chitin [β (1→ 4)-(*poly*) *N*-acetyl D-glucosamine] is notable in members of the marine α-proteobacteria and the *Cytophaga-Flavobacter* cluster (*27*, *28*). The widespread occurrence of chitinase activity and the ubiquity of chitinase genes in marine bacteria (*29*) imply that chitin-like biopolymers are important substrates in the marine environment, consistent with the abundance of *N*-AAPs in HMWDON. The presence of specialized bacteria could explain the ultimate removal of *N*-AAPs from the marine environment.

More than 90% of DON is sequestered in the deep sea, and most deep-sea HMWDON

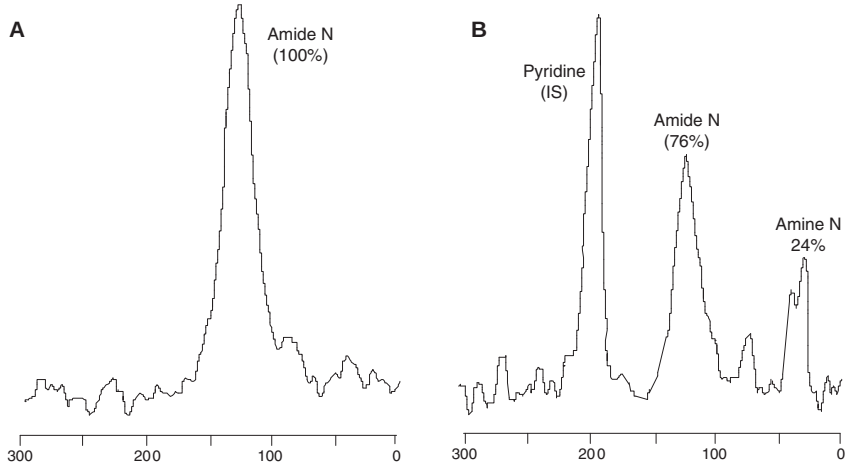

Fig. 3. The effect of mild acid (*13*) hydrolysis on the amide linkage of deep-sea HMWDON. (**A**) The ^{15}N-NMR spectrum of HMWDON shows only one resonance for amide-N [400 MHz, solid state δ (chemical shift in ppm downfield from liquid NH_3)]. (**B**) Treatment of the sample with mild acid converts 24% of the nitrogen to amine but does not affect most (76%) of the nitrogen. Pyridine (IS), added as an internal recovery standard, showed >98% N recovery through the hydrolysis procedure. Deep-sea HMWDON may also include some (<13% total N) contribution from pyrrole- and indole-N, which resonate between 130 and 215 ppm and overlap with the amide region in our ^{15}N-NMR spectrum.

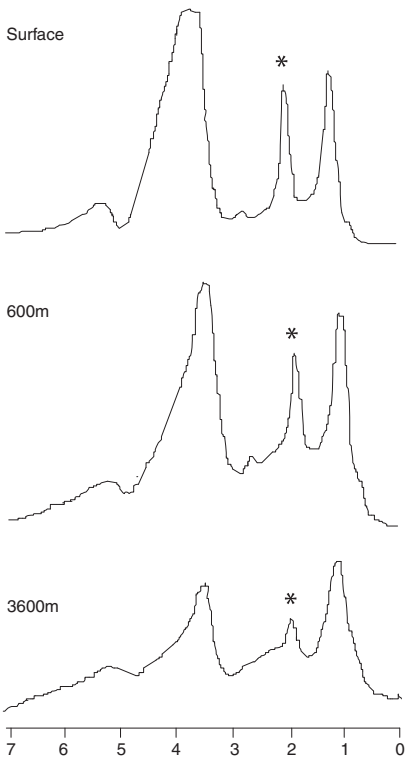

Fig. 4. The ^{1}H-NMR spectra [400 MHz, D_2O, δ(ppm)] of HMWDOM isolated from several depths (surface, 600 m, and 3600 m) in the Pacific Ocean (31°N, 159°W; the total water column depth was 5770 m). The peak at 2.0 ppm (*) arises from acetate, which is presumed to be present in *N*-AAPs. The clear decrease in the relative amount of acetate with depth is interpreted as a depth-dependent loss of *N*-AAPs.

is not hydrolyzed by treatment with strong acids (Table 1). Hydrolysis-resistant amides have been observed in marine particulate matter and sediments, where the resistance to chemical hydrolysis has been attributed to physical sorption and encapsulation (*30*). Amide-N in DON is not physically protected, but previous experiments have shown that the biodegradation rate of labile compounds such as proteins is substantially reduced by abiotic complexation within marine DOM (*31*). Long-term protein-DOM interactions may lead to structural modifications that render proteins resistant to chemical hydrolysis and unavailable to bacteria. This mechanism could lead to the sequestration of nitrogen in the dissolved phase (*32*) and give rise to the hydrolysis-resistant amide-N observed by ^{15}N-NMR.

Our data show that two chemically distinct pools of organic nitrogen accumulate in the ocean. The higher concentration of HMWDON in the mixed layer (relative to deep ocean values) largely reflects the presence of *N*-AAPs, which degrade on time scales of upper ocean mixing. These newly added biopolymers are chemically distinct from the refractory HMWDON pool that exists throughout the water column. If we assume the proportion of *N*-AAPs, protein, and nonhydrolyzable amide measured in our samples is representative of global HMWDON, then as much as 80% of the decrease in HMWDON with depth involves the removal of *N*-AAPs. The abundance of amide-N throughout the water column suggests amides are more biologically recalcitrant than other forms of organic-N. The ubiquity of amide linkages in HMWDON is not surprising, given that most organic nitrogen in phytoplankton is protein. However, the important contribution of *N*-AAPs to upper ocean HMWDOM, and the resistance of amides in deep sea HMWDOM to chemical and biological degradation, are unexpected results that help elucidate the currency of DON in the marine nitrogen cycle.

References and Notes

1. J. Abell, S. Emerson, P. Renaud, *J. Mar. Res.* **58**, 203 (2000).
2. M. J. Church, H. W. Ducklow, D. M. Karl, *Limnol. Oceanogr.* **47**, 1 (2002).
3. P. Libby, P. Wheeler, *Deep-Sea Res.* **44**, 345 (1997).
4. N. J. Antia, P. J. Harrison, L. Oliveira, *Phycologia* **30**, 1 (1991).
5. T. Berman, D. A. Bronk, *Aquat. Microb. Ecol.* **31**, 279 (2003).
6. D. A. Bronk, in *Biogeochemistry of Marine Dissolved Organic Matter*, D. A. Hansell, C. A. Carlson, Eds. (Academic Press, San Diego, CA, 2002), pp. 163–247.
7. HMWDON is defined here as the fraction of DON retained by an ultrafiltration membrane with a pore size of 1 nm. This fraction is expected to have a nominal molecular weight of >1 kD.
8. M. D. McCarthy, T. Pratum, J. I. Hedges, R. A. Benner, *Nature* **390**, 150 (1997).
9. M. D. McCarthy, J. I. Hedges, R. A. Benner, *Science* **281**, 231 (1998).
10. L. I. Aluwihare, D. J. Repeta, R. F. Chen, *Deep-Sea Res. II* **49**, 4421 (2002).
11. L. I. Aluwihare, D. J. Repeta, R. F. Chen, *Nature* **387**, 166 (1997).
12. S. Henrichs, P. M. Williams, *Mar. Chem.* **17**, 141 (1985).
13. De-acetylation of HMWDON samples was performed in 1 N HCl. Samples were heated overnight at 90°C under an atmosphere of N_2. The acetic acid produced during the hydrolysis was extracted from a weighed aliquot of the hydrolysate into either ethyl ether or dichloromethane. After extraction, the presence of acetic acid in the organic fraction was confirmed by solution-state ^{1}H-NMR before low molecular weight acids (e.g., acetic acid) were quantified. The aqueous fraction of the hydrolysate was lyophilized and, as shown in the ^{1}H-NMR (Fig. 2C), no longer contained acetamide. Changes in C and N were assessed with solid-state ^{13}C- and ^{15}N-NMR spectroscopy. Under these hydrolysis conditions, no muramic acid (de-acetylated) or amino sugar monomers were detected.
14. D. B. Albert, C. S. Martens, *Mar. Chem.* **56**, 27 (1997).
15. M. Zhao, J. L. Bada, *J. Chromatogr. A.* **690**, 55 (1995).
16. The percentage of N in each sample represented by *N*-AAPs, hydrolyzable protein, and nonhydrolyzable amide was calculated as follows: Because 1 mol of *N*-AAP sugar is de-acetylated for every mole of acetic acid released, we assumed that μmoles of acetic acid were equal to μmoles of N in *N*-AAPs; hydrolyzable protein N was calculated on the basis of the recoveries of amino acid N after strong acid hydrolysis (*12*); nonhydrolyzable amide was determined after strong acid hydrolysis (Table 1). Higher amino acid yields were obtained when HMWDON was hydrolyzed with strong acid. As a result, after strong acid hydrolysis, only 2.2 (29% of total N) and 5.5 μmol (71% of total N) of amide-N remained unhydrolyzed in the Woods Hole and MAB samples, respectively. In order to quantify the amount of amide-N remaining after strong acid hydrolysis, the sum Σacetic acid (mild) + amino acids (strong) was first determined and then subtracted from the initial amide content of the HMWDON sample (before hydrolysis). In all cases, percentages are expressed relative to total N in each sample. We calculated the amount of *N*-AAP carbon with the C/N ratio in HMWDOM (Table 1) and assumed 8 μmol of C per μmol of *N*-AAP (e.g., *N*-acetyl glucosamine).
17. J. J. Boon, V. A. Klap, T. I. Eglinton, *Org. Geochem.* **29**, 1051 (1998).
18. J. A. Leenheer, T. I. Noyes, C. E. Rostad, M. L. Davisson, *Biogeochemistry* **69**, 125 (2004).
19. K. Kaiser, R. Benner, *Anal. Chem.* **72**, 2566 (2000).
20. D. L. Popham, J. Helin, C. E. Costello, P. Setlow, *J. Bacteriol.* **178**, 6451 (1996).
21. We modified the method provided in (*20*) and hydrolyzed samples (in 4 N HCl) overnight at 90°C. We recovered no muramic acid and only small amounts of glucosamine and galactosamine from surface samples. This modified hydrolysis method was tested on chitin oligomers, peptidoglycan (from *Bacillus subtilus*), and bacterial cells (mixed laboratory culture) to ensure the quantitative (>90%) recovery of glucosamine and de-acetylated muramic acid. We assessed amino sugar recoveries by high-performance liquid chromatography and fluorescence detection of *o*-phthaldialdehyde-derivatized samples (*15*) or gas chromatography after derivatizing to alditol acetates (*10*).
22. J. I. Hedges *et al.*, *Org. Geochem.* **31**, 945 (2000).
23. O. Hadja, *Anal. Biochem.* **60**, 512 (1974).
24. Y. Nagata, T. Fujiwara, K. Kawaguchinagata, Y. Fukumori, T. Yamanaka, *Biochim. Biophys. Acta* **1379**, 76 (1998).
25. J. S. Martinez *et al.*, *Science* **287**, 1245 (2000).
26. B. Palenik, S. E. Henson, *Limnol. Oceanogr.* **42**, 1544 (1997).
27. M. T. Cottrell, D. L. Kirchman, *Appl. Environ. Microbiol.* **66**, 1692 (2000).
28. A. L. Svitil, D. L. Kirchman, *Microbiol.* **144**, 1299 (1998).
29. M. T. Cottrell, D. N. Wood, L. Yu, D. L. Kirchman, *Appl. Environ. Microbiol.* **66**, 1195 (2000).
30. H. Knicker, P. G. Hatcher, *Naturwissenschaften* **84**, 231 (1997).
31. R. G. Keil, D. L. Kirchman, *Mar. Chem.* **45**, 187 (1994).
32. E. Tanoue, S. Nishiyana, M. Kamo, A. Tsugita, *Geochim. Cosmochim. Acta* **59**, 2643 (1995).

33. We thank A. Beilecki, then at Brüker Instruments, for assistance with ^{15}N-NMR spectroscopy; M. Pullin and D. Albert for assistance in the determination of acetic acid; and the staff at the Natural Energy Laboratory in Kona, Hawaii, and E. Smith for assistance in sample collection. Supported by the Chemical and Biological Oceanography Programs at the National Science Foundation; the Carbon Sequestration Program at the U.S. Department of Energy; the Rhinehart Coastal Research Center of the Woods Hole Oceanographic Institution; and the Fundación Andes, Chile.

20 December 2004; accepted 9 March 2005
10.1126/science.1108925

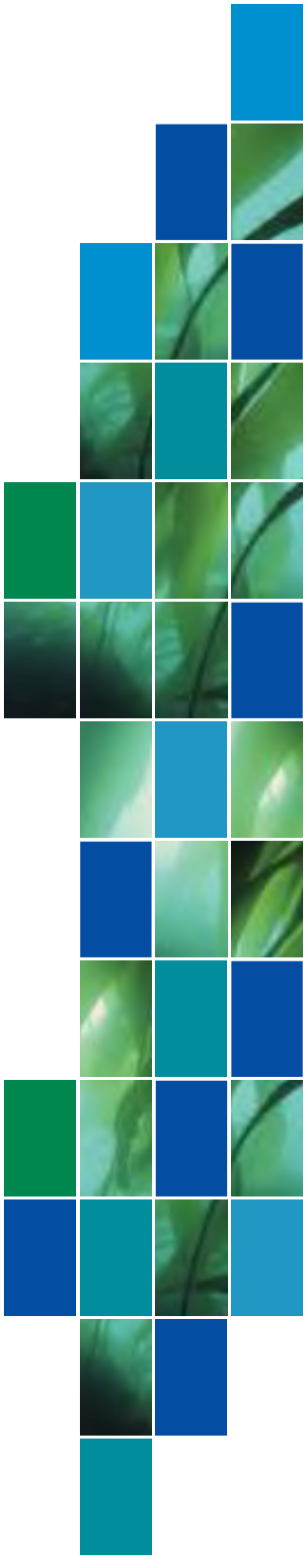

Chapter Two

To cite articles from Chapter Two of this booklet, please use the following format: [Author name(s)] in *Microbial Carbon Pump in the Ocean,* N. Jiao, F. Azam, S. Sanders, Eds. (*Science*/AAAS, Washington, DC, 2011), pp. xx-xx.

Microbial Carbon Pump and its Significance for Carbon Sequestration in the Ocean

Nianzhi Jiao[1] and Farooq Azam[2]

The generally accepted biogeochemical mechanism of long-term carbon sequestration in the ocean is the biological pump, which is based on the process of downward flux of particulate organic matter and its burial in the ocean bottom. The recently proposed microbial carbon pump (MCP) conceptualizes a dissolved phase sequestration mechanism based on the microbial generation of refractory dissolved organic matter (RDOM), which is resistant to biological decomposition and assimilation and thus persists in the water column. The central questions of the MCP concern the structure-specific molecular consequences of microbe and organic matter interactions. Understanding the molecular nature and global scope of the MCP calls for a multidisciplinary approach and the development of new tools to, for instance, chemically characterize RDOM in concert with microbial functional gene analysis. The MCP and the biological pump are mechanistically interconnected in the ocean carbon cycle, requiring the integration of quantitative, mechanistic, and predictive studies in order to understand ocean carbon biogeochemistry and how it interacts with climate change.

Concerns over climate change due to anthropogenic CO_2 have stimulated intensive research on the capacity of the ocean for long-term carbon sequestration. Historically, it has been recognized since the 1970s that solving this problem would necessitate a fundamental understanding of the functioning of the global ocean carbon cycle (*1*, 2). In order to address this, large multidisciplinary studies were conducted on ocean carbon biogeochemistry over the past three decades [see (*1*) for a historical account]. The goals of these studies have been to quantify, model, and predict the spatial-temporal patterns of downward flux of organic matter and its relationship to primary productivity and foodweb dynamics in the water column. This research led to the formulation and development of the paradigm of the biological pump: A variable fraction of the biogenic debris from the upper ocean escapes decomposition and respiration, sinking down to the deep sea and to the seafloor and becoming buried in the sediments.

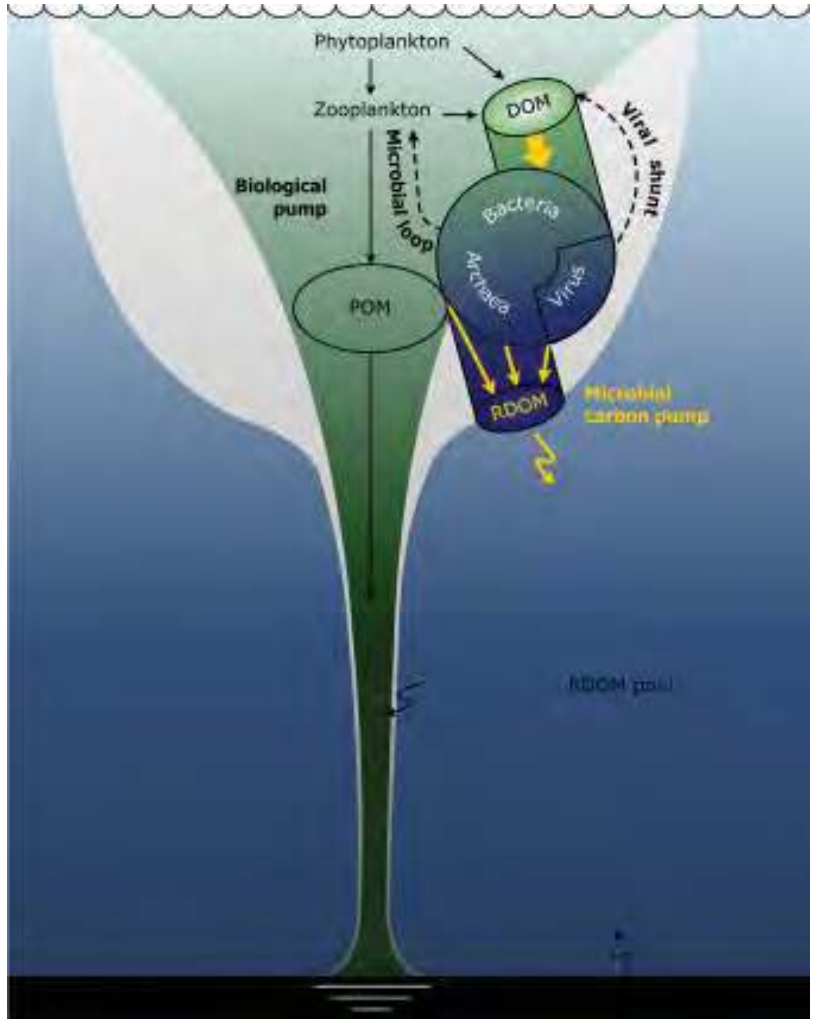

Fig. 1. Diagram showing the MCP and its relationship with the biological pump. The MCP and the biological pump are intertwined in the ocean carbon cycle. While the majority of the primary production is in the form of POM, a portion of the fixed carbon is released as DOM into the water. This DOM together with DOM from other sources along the food chain can be partially transformed by the MCP into RDOM. During the sinking process, a great deal of POM is hydrolyzed by attached microbes and becomes DOM contributing to the MCP, while some RDOM molecules are scavenged by POM, joining the biological pump. In contrast to the exponential attenuation of the POM flux along water depth, the RDOM persists throughout the water column. The relative importance of MCP vs. the biological pump varies with environmental scenarios. [after Jiao *et al.*, 2010 (*4*)]

The advent of the microbial loop in the 1980s revealed that approxi-

[1]State Key Laboratory of Marine Environmental Sciences, Xiamen University, Xiamen 361005, P. R. China (jiao@xmu.edu.cn)
[2]Scripps Institution of Oceanography, UCSD, La Jolla CA, 92093, USA (fazam@ucsd.edu)

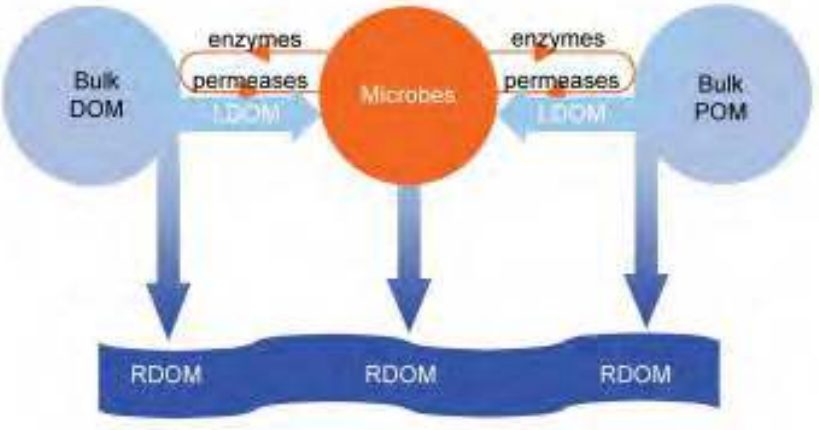

Fig. 2. Three pathways of RDOM generation are summarized in the MCP: direct production of RDOM from microbial cells (center), RDOM derived from POM degradation (right), and residual DOM after microbial modification of the bulk DOM (left). In the direct pathway, the main mechanisms are exudation from active microbial cells and release form viral lysis or grazing. Viral lysis can offset as much as half of the microbial production and one-quarter of primary production in the ocean; a portion of the DOM produced by viral lysis could be RDOM (*19*, *20*). About 25% of the ocean RDOM is estimated to be of bacterial origin (*6*). For the POM pathway, ectoenzymes expressed by microorganisms convert POM to DOM at rates that often exceed microbial uptake of the DOM (*21*, *22*) and some byproducts of this hydrolytic activity could be resistant to further utilization by microbes (either free-living or attached to POM), thus becoming RDOM. In the residual DOM pathway, a part of bulk DOM can remain/become RDOM after microbial processing, such as acylheteropolysaccharide originated from products of phytoplankton and bacteria (*23*).

mately one-half of the fixed carbon in fact flows through the dissolved organic matter (DOM) pathways, with most presumed to be rapidly respired or assimilated (labile DOM) by heterotrophic bacteria (now known to include Archaea) (*3*). However, these rapid fluxes of labile DOM occur in the presence of an enormous pool of refractory dissolved organic matter (RDOM), which accounts for >90% of the organic matter in seawater and may persist for thousands of years. Thus far, the biogeochemical behavior of RDOM, its origin, and its place in the ocean carbon cycle has been technically difficult to determine.

The Microbial Carbon Pump

Synthesizing the knowledge on microbial carbon cycling in the ocean, Jiao *et al.* (*4*) proposed that microbial metabolism of labile DOM and trophic interactions within the microbial loop generate RDOM. This process would result in long-term carbon sequestration in the dissolved phase throughout the water column. It could be a modulating factor in the redistribution of carbon among the Earth's surface reservoirs and thus influence climate change (*5*). The proposed pathway (the microbial carbon pump, MCP) had not previously been explicitly included in ocean carbon cycle. It is argued that the MCP is a quantitatively significant biogeochemical pathway for RDOM generation and carbon sequestration that should be specified in ocean carbon models (*4, 6*). The MCP framework also enables researchers to explore the hypothesis that shifts in metabolic accessibility of RDOM to bacteria and Archaea, resulting in its respiration, could influence the global carbon cycle and climate. Microbial generation and cycling of RDOM could thus be significant variables in the ocean carbon cycle (Fig. 1).

RDOM Biogeochemistry, a Molecular Problem

Measurements of particle flux, elemental analysis, and primary productivity can reasonably well constrain the biological pump models of carbon sequestration and its relationship to surface productivity. In contrast, the kinetics and mechanisms of carbon sequestration by the MCP is more complex, determined by intricate interactions of molecules and microbes (Fig. 1). This is also true of metabolic interactions of bacteria with organic particles since bacteria must first hydrolyze the particles to diffusible molecules within their microenvironments. Studies to understand MCP-mediated carbon sequestration must therefore contend with great molecular and microbial diversity and system complexity—as well as minuscule, nanometer to micrometer, ecosystem scales relevant to the realms of microbes and molecules. Further, the need is to measure the production of molecules of currently unknown structures (*7*). Thus, MCP research will require new approaches and tools that enable studies at a molecular resolution and distinct from those used in studying particle phase sequestration by the biological pump. This also argues in favor of a dedicated focus on the MCP component of the ocean carbon cycle, while also integrating these findings with data on the biological pump.

New Tools of the Trade

Taken together, these considerations underscore the usefulness of the MCP as a framework for studying carbon sequestration in the dissolved phase throughout the ocean's water column on both a molecular and global level. Molecular characterization of RDOM has been largely intractable thus far, but recent analytical advances [for example, ultrahigh resolution mass spectrometry] (*7*) are beginning to resolve this fundamental problem. While the technique has already yielded thousands of molecular formulas for DOM components, the challenge to determine the corresponding chemical structures still remains. On the microbial side of the interactions, advances in genomics, transcriptomics, and proteomics can be applied to determine the metabolic capabilities of the microbes involved and how they might modify the labile organic matter to produce RDOM. Simultaneous expression profiles of thousands of relevant genes can be determined by Q-CHIP technology (*8*). This technique could, in principle, be configured to detect the expression of genes relevant to the presence of specific DOM components, once their chemical structures have been determined. Developing tools to accurately measure respiration in minimally perturbed samples is an important goal, as it may elucidate how microbial metabolism partitions DOM between respiration and sequestration in changing biogeochemical scenarios in the ocean. Respiration methods that do not require physical separation of bacteria and Archaea from other plankton are being developed (*9*) and should provide better quantitative constraints on bacterial processing of DOM and generation of RDOM.

RDOM Sources, Mechanisms, and Constraints on Decomposition

Jiao *et al*. (*4*) have argued that microbes generate RDOM as they act on diverse dissolved and particulate sources of organic matter (Fig. 2) as well as participate in foodweb trophic dynamics (Fig. 1). These interactions have the potential to generate molecular diversity that may include RDOM. Highly abundant and diverse lytic viruses may generate unique RDOM as they probably lyse most marine organisms and release (rather than digest) the cellular material (*10*). In addition, some RDOM may be produced de novo by the metabolic activities of phyto-

plankton or bacteria (mechanistically distinct from the bacteria acting on organic matter). New approaches are already emerging to quantify the overall contribution of microbes to RDOM generation (*6*) and future analyses need to identify the dominant pathways within the MCP and the necessary ecosystem conditions for RDOM formation. While MCP studies are mainly focused on the contribution of microbes to carbon sequestration, other biotic and abiotic RDOM sources should also be taken into consideration when carbon budget and age are concerned. For example, the old DOM from seafloor seeps (*11, 12*) may not necessarily be all RDOM (*13*).

Understanding the MCP also challenges scientists to elucidate the mechanistic underpinnings of RDOM generation, which will be essential for developing refined models of carbon sequestration. There is good reason to believe that the mechanisms of RDOM generation will eventually be revealed at the biochemical level. For example, it was recently demonstrated that incomplete hydrolysis of organic matter by bacterial ectohydrolases could lead to RDOM formation (*14*). Further, bacterial ectohydrolases have already been shown to be central to connecting the biological pump with the MCP, particularly through particle hydrolysis (*15*).

A question of great interest is why bacteria and Archaea do not metabolize RDOM. This question is critical for predicting long-term net carbon sequestration in the dissolved phase. Highlighting this longstanding question in the context of the MCP is stimulating research on whether the persistence of RDOM could be due to the extreme dilution of individual molecular species, making their utilization energetically unfavorable for bacteria and Archaea (*7*). Another unanswered question is whether there are structural constraints on RDOM decomposition. This should benefit from the development of model systems of known RDOM components (currently none is known) and bacteria.

Integration of MCP and Biological Pump

The MCP and the biological pump are mechanistically intertwined in the ocean carbon cycle, a fact that necessitates integrated research strategies. For example, bacteria act on sinking particles to cause quantitatively major particulate organic matter (POM) to DOM flux, some of which may become RDOM. Conversely, sinking particles can scavenge RDOM from seawater and carry it into the carbon sequestration process of the biological pump. The interconnection between the MCP and the biological pump is also apparent from the concept that organic matter cannot be neatly divided into DOM and POM, but instead exists as a continuum of small molecules to large sinking particles (*16–18*). Therefore, the realms of the MCP and the biological pump can overlap as microbes and other organisms interact with the organic matter continuum and among themselves to create overlapping yet distinctive patterns of carbon cycling and sequestration. This view of the organic matter continuum underscores a need for an integrated approach to further our understanding of the mechanistic and predictive nature of the carbon cycle. Further, a "cultural integration" of the biological pump community and the emergent MCP community could move us towards this goal.

Future

The unfolding climate change scenarios will demand a quantitative, mechanistic, and predictive understanding of ocean carbon biogeochemistry to guide policy and advise the global society on adaptive measures. Explicit incorporation of the MCP into the concept and models of the ocean carbon cycle will be essential and will require new emphasis on methods development and global ocean field programs. It is important that the MCP community collaborates closely with other geochemists and biogeochemists to develop an integrated view of the ocean carbon cycle and its response to climate change.

References and Notes

1. E. A. Laws, P. G. Falkowski, W. O. Smith Jr, H. Ducklow, J. J. McCarthy, *Global Biogeochem. Cy.* **14**, 1231 (2000).
2. K. L. Denman, M. A. Pena, in *The changing ocean carbon cycle: a midterm synthesis of the Joint Global Ocean Flux Study,* R. B. Hanson, H. W. Ducklow, J. G. Field, Eds. (Cambridge Univ. Press, New York, 2000), pp. 469–490.
3. F. Azam *et al., Mar. Ecol. Prog. Ser.* **10**, 257 (1983).
4. N. Jiao *et al., Nat. Rev. Microbiol.* **8**, 593 (2010).
5. P. F. Sexton *et al., Nature* **471**, 349 (2011).
6. R. Benner, G. Herndl, in *Microbial Carbon Pump in the Ocean,* N. Jiao, F. Azam, S. Sanders, Eds. (*Science*/AAAS, Washington, DC, 2011), pp. 46–48.
7. G. Kattner, M. Simon, B.P. Koch, in *Microbial Carbon Pump in the Ocean,* N. Jiao, F. Azam, S. Sanders, Eds. (*Science*/AAAS, Washington, DC, 2011), pp. 60–61.
8. J. D. Van Nostrand, J. Zhou, in *Microbial Carbon Pump in the Ocean,* N. Jiao, F. Azam, S. Sanders, Eds. (*Science*/AAAS, Washington, DC, 2011), pp. 64–65.
9. C. Robinson, N. Ramaiah, in *Microbial Carbon Pump in the Ocean,* N. Jiao, F. Azam, S. Sanders, Eds. (*Science*/AAAS, Washington, DC, 2011), pp. 52–53.
10. M. G. Weinbauer, F. Chen, S. W. Wilhelm, in *Microbial Carbon Pump in the Ocean,* N. Jiao, F. Azam, S. Sanders, Eds. (*Science*/AAAS, Washington, DC, 2011), pp. 54–56.
11. J. W. Pohlman, J. E. Bauer, W. F. Waite, C. L. Osburn, N. R. Chapman, *Nat. Geosci.* **4**, 37 (2011).
12. M. D. McCarthy *et al., Nat. Geosci.* **4**, 32 (2011).
13. Not all fossil components of the DOM entering the water column through seabed seeps are refractory; some are readily available for microbial respiration and thus do not contribute to carbon sequestration. However, being much older than the biogenic DOM, they would increase the radiocarbon age of the DOM pool. Only that DOM which is resistent to microbial respiration/decompostion, whether biogenic or fossil in origin, can persist in the water column for a long time, constituting carbon sequestration.
14. H. Ogawa, Y. Amagai, I. Koike, K. Kaiser, R. Benner, *Science* **292**, 917 (2001).
15. D. C. Smith, M. Simon, A. L. Alldredge, F. Azam, *Nature* **359**, 139 (1992).
16. F. Azam, *Science* **280**, 694 (1998).
17. F. Azam, A. Z. Worden, *Science* **303**, 1622 (2004).
18. P. Verdugo *et al., Mar. Chem.* **92**, 67 (2004).
19. T. Nagata, D. L. Kirchman, in *Mortality of Microbes in Aquatic Environments, Microbial Biosystems: New Frontiers, Proceedings of the 8th International Symposium on Microbial Ecology* C. R. Bell, M. Brylinsky, P. Johnson-Green, Eds. (Halifax, Canada, 1999), pp. 153–158.
20. K. E. Stoderegger, G. J. Herndl, *Limnol. Oceanogr.* **43**, 877 (1998).
21. M. Karner, G. J. Herndl, *Mar. Biol.* **113**, 341 (1992).
22. T. Nagata, H. Fukuda, R. Fukuda, I. Koike, *Limnol. Oceanogr.* **45**, 426 (2000).
23. D. J. Repeta, T. M. Quan, L. Aluwihare, A. Accardi, *Geochim. Cosmochim. Acta* **66**, 955 (2002).

24. We thank the SCOR WG134 members, and all the authors and those acknowledged in the Jiao *et al., Nature Reviews Microbiology* (2010) for discussions and comments. This work was supported by NSFC 91028001, SOA201105021 to N. Jiao, and grants from Gordon and Betty Moore foundation Marine Microbiology Initiative and the US NSF 0962721 to F. Azam. This document is based on work partially supported by the US NFS on Oceanic Research under grant number OCE-0938349.

Bacterially Derived Dissolved Organic Matter in the Microbial Carbon Pump

Ronald Benner[1*] and Gerhard J. Herndl[2]

Most of the carbon fixed through photosynthesis is rapidly respired to CO_2 by biota in the surface ocean, but a small fraction of this carbon is transformed into dissolved organic carbon (DOC) that persists for extended periods of time. Seawater bioassay experiments demonstrate that bacteria rapidly transform labile DOC to semilabile and refractory forms, suggesting enzymatic activity plays an important role in the transformation process. A fundamental understanding of this process has yet to be obtained, but the molecular signatures of the transformed DOC are observed throughout the ocean water column. Bacterial transformations in the microbial carbon pump (MCP) have sequestered about 10 Pg of semilabile DOC and about 155 Pg of refractory DOC in the global ocean. The annual production of semilabile and refractory DOC in the upper ocean MCP is estimated to be 0.74 to 2.23 Pg and 0.008 to 0.023 Pg, respectively. This sequestration of reduced carbon as semilabile and refractory DOC contributes to the regulation of greenhouse gases on decadal to millennial time scales and influences trace metal and nutrient availability.

About 660 petagrams (Pg; 10^{15} g) of dissolved organic carbon (DOC) resides in the global ocean, but the origin, formation, structure, and reactivity of this large reservoir of reduced carbon are largely unknown (*1, 2*). The vast majority of this dissolved organic matter (DOM), which includes DOC as well as other dissolved organic elements, is resistant to biodegradation and comprises carbon sequestered from the atmosphere over timescales of decades to millennia. The recognition that relatively small changes in the ocean reservoir of DOC can have significant impact on the atmospheric reservoir of CO_2 (*1, 2*) has stimulated research on the mechanisms of production of semilabile and refractory DOM in the ocean. Heterotrophic bacteria process about half of net primary production and thereby play a dominant role in the microbial carbon pump (MCP) by altering and transforming labile forms of organic matter into refractory forms that persist in the ocean (*3*). This article provides a short review of bioassay experiments describing the transformation of labile to refractory DOM, the use of biomarkers to trace DOC of bacterial origin in the ocean, and the size of the ocean reservoirs of semilabile and refractory DOC produced by the MCP.

Microbial Transformations of Labile to Semilabile and Refractory DOM

Early bioassay experiments demonstrating the microbial production of refractory DOM from labile substrates were conducted in natural seawater samples amended with simple ^{14}C-labeled compounds, such as glucose and leucine (*4*). Rapid (between two to five days) transformations of labile substrates to semilabile and refractory forms of DOM were observed in surface and deep waters incubated in the dark for several months (*4, 5*). Dissolved humic substances were formed (*6*), and the molecular weight distribution of labeled DOM at the end of the incubations was similar to that of natural marine DOM suggesting the processes occurring in these laboratory experiments were similar to those in the ocean. It was demonstrated that bacterial capsular material is an important component of the DOM produced during these experiments (*7*). The yields of biorefractory DOM production from simple substrates ranged from 1 to 5% (*4*). These studies linked refractory DOM formation with microbial transformations, but they were not able to identify the specific microbial origins, chemical forms, or mechanisms of production of refractory DOM.

More recent bioassay experiments have added labile substrates, such as glucose and glutamate, as the sole carbon sources to artificial seawater inoculated with natural microbial assemblages. Bacteria rapidly used the added labile substrates and produced semilabile and refractory DOM that was chemically complex and included combined forms of neutral sugars, amino acids, and amino sugars (*8*). Bacteria shaped the composition of the DOM, and its refractory nature was demonstrated during long-term (1 to 1.5 yr) incubations. The DOM produced in these experiments was of similar composition and molecular weight distribution as natural marine DOM (*9–11*). Bacteria also release refractory forms of chromophoric DOM (CDOM) of varying molecular weight during the utilization of glucose (*12, 13*). Fluorescent components of the CDOM were resistant to photodegradation, and photochemical transformations of the DOM did not enhance its subsequent bioavailability. These experiments suggest that bacteria are a likely source of the fluorescent DOM maximum observed in the oxygen-minimum zone of the ocean (*14*).

The mechanisms of release of DOM from bacteria have been examined in bioassay experiments using labile substrates as sole carbon sources. The direct release of dissolved D/L-enantiomers of hydrolysable amino acids and amino sugars from bacteria was observed during exponential growth of bacterial cells (*15*). The bioavailability of the DOM released during cell growth was highly variable and included labile, semilabile, and refractory components. The release of dissolved amino acids from bacteria during viral lysis was observed using a model system comprising a bacterial strain and a strain-specific virus (*16*). Combined forms of amino acids were abundant in the lysate, and the nonprotein amino acid diaminopimelic acid, a unique component of the peptide bridge in peptidoglycan, was observed. A model system using glucose as the sole carbon source and a specific bacterium and its ciliate grazer was used to investigate the release of DOM from bacteria during grazing (*17*). The presence of the ciliate enhanced the production of bacterially derived DOM, but the grazing process did not appear to alter the chemical composition of the resulting DOM. The vast majority of molecular masses identified as refractory DOM at the end of the experiments were produced during the first two days of the incubation before the ciliate was added to the culture.

Taken together, these studies indicate that bacterially derived DOM is rapidly produced through direct release from growing cells, viral lysis, and protozoan grazing. Bacterially derived DOM ranges in bioavailability from labile to refractory. The rapid accumulation of DOM that is highly resistant to microbial degradation is both surprising and baffling. The bacterial transformation of labile to semilabile and refractory DOC occurs within hours to days at room temperature and in the dark (*8*). How does this happen? The exact mechanism is unclear, but the process is biologically mediated. Nonspecific enzyme activities could play

[1]Department of Biological Sciences and Marine Science Program, University of South Carolina, Columbia, SC 29208, USA
[2]Department of Marine Biology, University of Vienna, 1090 Vienna, Austria
*To whom correspondence should be addressed. E-mail: benner@mailbox.sc.edu

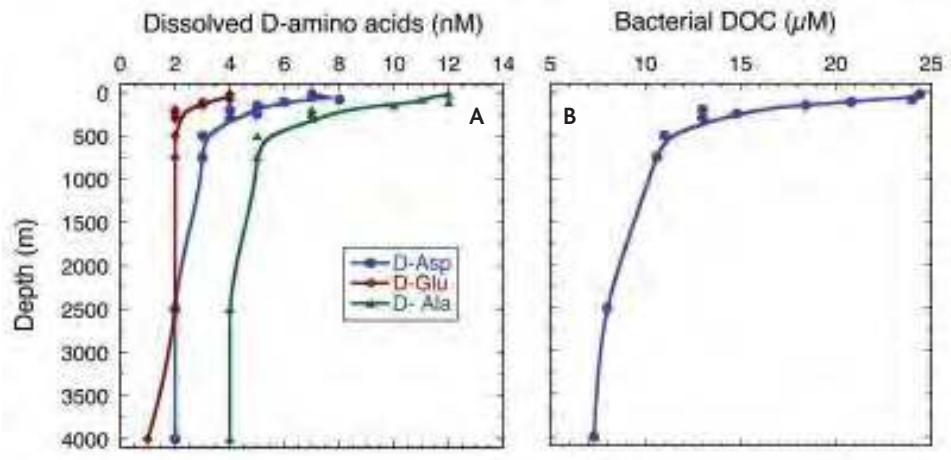

Fig. 1. (**A**) Concentrations of total dissolved D-Aspartic acid (D-Asp), D-Glutamic acid (D-Glu), and D-Alanine (D-Ala) in the water column at the Hawaii Ocean Time Series Station Aloha *(20)*. (**B**) Average concentrations of DOC derived from bacteria as calculated from the yields of total dissolved D-Asp, D-Glu, and D-Ala in the water column and the yields of these D-amino acids in bioassay experiments (*20*).

an important role in producing chemically complex and biologically refractory DOM (*8*). The existence of such a mechanism would suggest that semilabile and refractory DOM are produced largely in the upper ocean where most biological production and decomposition occur.

It is critical to link observations from laboratory experiments to the ocean carbon cycle, and the bioassay experiments provide this connection by demonstrating that semilabile and refractory DOM produced in the MCP include bacterial biomarkers such as the D-enantiomers of alanine (Ala), glutamic acid (Glu), and aspartic acid (Asp). These bacterial biomarkers can be used to trace the production, reactivity, abundance, and distribution of semilabile and refractory DOM in the ocean.

Tracing Bacterially Derived DOC and the MCP in the Ocean

The contributions of bacteria to marine DOM has gained attention over the last decade following the observation that bacteria contribute to marine dissolved organic nitrogen based on the abundance of D-enantiomers of specific amino acids (D-Ala, D-Glu, D-Asp) in marine DOM (*18*). The L-enantiomers of amino acids are common to all organisms and are the building blocks of proteins, whereas specific D-enantiomers are synthesized by bacteria and incorporated into a variety of unusual cell wall and membrane molecules (*19–21*). The D-amino acids are ubiquitous in marine DOM and particulate organic matter and are most useful for tracing bacterial contributions because they can be measured directly in seawater without preconcentration, they are found in all marine bacteria and bacterially derived DOM, they occur in a variety of biochemical components of bacterial cells, and they are not known to occur in combined form in any marine organisms besides bacteria (*15, 20, 22–25*). Other bacterial biomarkers have been observed in DOM, including muramic acid (*26*), diaminopimelic acid (*27*), and short-chain 3-hydroxy fatty acids (*28*), further indicating the diversity of bacterially derived compounds in seawater DOM.

The concentrations and depth distribution of total dissolved D-Ala, D-Glu, and D-Asp in the water column at the Hawaii Ocean Time Series Station Aloha are shown in Fig. 1A. Concentrations of individual D-amino acids range from 4 to 12 nM in surface waters and decline by approximately 70% at a depth of 750 m. The D-amino acids removed in the upper 750 m are considered to be components of semilabile DOM based on ventilation ages (years to decades) for these water masses (*10*). The concentrations of individual D-amino acids in deep waters (2500 and 4000 m) are low (1 to 4 nM) and relatively constant, indicating the refractory nature of bacterially derived DOM in the deep ocean (*20*). The yields of D-amino acids (D-Asp, D-Ala, D-Glu) can be used to estimate the bacterial contributions to DOC in the ocean (*20*). Based on these three D-amino acid biomarkers, the average concentrations of bacterially derived DOC in the water column at Station Aloha are shown in Fig. 1B. Concentrations of bacterially derived DOC range from ~7 to 25 μM, indicating the MCP is a major source of semilabile and refractory DOC in the ocean.

The Ocean Reservoir of Semilabile and Refractory DOC Derived from the MCP

The ocean reservoir of DOC is chemically complex and has multiple origins (*29–32*). The MCP contributes to the semilabile and refractory DOC reservoirs, and bacterial biomarkers provide an approach for tracing and quantifying the contributions of the MCP to marine DOC. The D-amino acid biomarkers have been used to estimate that about 25% of the DOC throughout the ocean water column is of bacterial origin (*20*). The global ocean reservoir of DOC is estimated to be approximately 660 Pg, with about 40 Pg in the form of semilabile DOC and the remaining 620 Pg in the form of refractory DOC (*33*). Based on these totals and the fraction of bacterially derived DOC in each reservoir, approximately 10 Pg of semilabile DOC and approximately 155 Pg of refractory DOC of bacterial origin reside in the global ocean (Fig. 2).

The rates of production of semilabile and refractory DOM in the MCP can be estimated from the annual rate of heterotrophic bacterial production in the upper ocean and the efficiency of DOC release from bacteria. This approach assumes that bacteria use, alter, and transform the fixed carbon derived from primary production that is not respired and remineralized to CO_2 in the euphotic zone. Furthermore, it assumes that bacterial production, a measurable quantity, is representative of these activities. Bacterial production in the upper ocean is estimated to be approximately 15% of net primary production (*34*), or about 7.5 PgC y^{-1}. If it is assumed that 10 to 30% of bacterial production is released as DOC in the MCP (*35*), this means that 0.75 to 2.25 Pg of DOC is produced annually in the upper ocean MCP. Bioassay

experiments indicate that only 1 to 5% of this DOC is refractory on time scales of several months to a year, and for the purpose of this calculation we have assumed that 1%, or 0.008 to 0.023 Pg, is transformed into refractory DOC annually. Based on these estimates, the remaining component of the DOC produced annually in the upper ocean MCP, 0.74 to 2.23 Pg, is presumed to be semilabile DOC (Fig. 2). These calculations also indicate that refractory DOC production from heterotrophic bacteria in the upper ocean MCP could account for 0.015 to 0.023% of annual primary production. Semilabile DOC production in the MCP accounts for 1.5 to 4.5% of annual primary production. For comparison, approximately 0.1% of annual primary production is buried in marine sediments via sinking particles in the biological pump (*36*). Bacteria are present throughout the ocean water column and in marine sediments, but the productivity of these bacteria is not well known. Likewise, the role of Archaea in the MCP also has not been considered in this analysis. Therefore, these estimates of the production of semilabile and refractory DOC in the MCP are likely to be conservative.

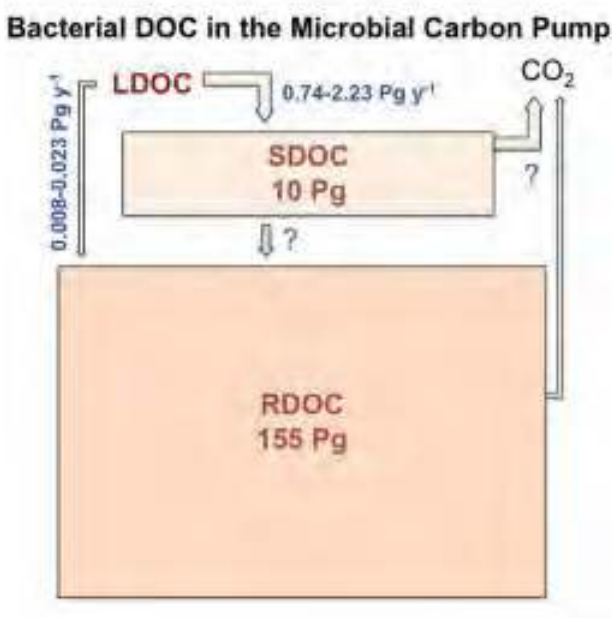

Fig. 2. Global ocean reservoirs of semilabile DOC (SDOC) and refractory DOC (RDOC) derived from bacteria in the microbial carbon pump. Estimated annual fluxes of the bacterial transformation of labile DOC (LDOC) into SDOC and RDOC in the upper ocean microbial carbon pump.

References and Notes

1. D. A. Hansell, C. A. Carlson, Eds., *Biogeochemistry of Marine Dissolved Organic Matter* (Academic Press, London, 2002).
2. H. Ogawa, E. Tanoue, *J. Oceanogr*. **59**, 129 (2003).
3. N. Jiao, *et al.*, *Nat. Rev. Microbiol.* **8**, 593 (2010).
4. J. E. Brophy, D. J. Carlson, *Deep Sea Res.* **36**, 497 (1989).
5. A. Heissenberger, G. J. Herndl, *Mar. Ecol. Prog. Ser.* **111**, 129 (1994).
6. L. J. Tranvik, *FEMS Microbiol. Ecol*. **12**, 177 (1993).
7. K. Stoderegger, G. J. Herndl, *Limnol. Oceanogr.* **43**, 877 (1998).
8. H. Ogawa, Y. Amagi, I. Koike, K. Kaiser, R. Benner, *Science* **292**, 917 (2001).
9. R. Benner, J. D. Pakulski, M. McCarthy, J. I. Hedges, P. G. Hatcher, *Science* **255**, 1561 (1992).
10. K. Kaiser, R. Benner. *Mar. Chem.* **113**, 63 (2009).
11. H. Ogawa, N. Ogura, *Nature* **356**, 696 (1992).
12. G. D. Kramer, G. J. Herndl, *Aquat. Microb. Ecol.* **36**, 239 (2004).
13. K. Shimotori, Y. Omori, T. Hama. *Aquat. Microb. Ecol.* **58**, 55 (2009).
14. Y. Yamashita, E. Tanoue, *Nat. Geosci.* doi:10.1038/ngeo279 (2008).
15. N. Kawasaki, R. Benner, *Limnol. Oceanogr.* **51**, 2170 (2006).
16. Middelboe, M., N. O. G. Jørgensen, *J. Mar. Biol. Ass. U.K.* **86**, 605 (2006).
17. D. F. Gruber, J. P. Simjouw, S. P. Seitzinger, G. L. Taghon, *Appl. Environm. Microbiol*. **72**, 4184 (2006).
18. M. D. McCarthy, J. I. Hedges, R. Benner, *Science* **281**, 231 (1998).
19. Y. Asano, T. L. Lübbehüsen, *J. Biosci. Bioeng.* **89**, 295 (2000).
20. K. Kaiser, R. Benner, *Limnol. Oceanogr*. **53**, 99 (2008).
21. K. H. Schleifer, O. Kandler, *Bact. Rev.* **36**, 407 (1972).
22. Dittmar, T., Fitznar, H. P., G. Kattner, *Geochim. Cosmochim. Acta* **65**, 4103 (2001).
23. B. A. Lomstein, B. B. Jorgensen, C. J. Schubert, J. Niggemann, *Geochim. Cosmochim. Acta*, **70**, 2970 (2006).
24. N. Kawasaki, R. Sohrin, H. Ogawa, T. Nagata, R. Benner, *Aquat. Micro. Ecol.* **62**, 165 (2011).
25. M. T. Pérez, C. Pausz, G. J. Herndl, *Limnol. Oceanogr.* **48**, 755 (2003).
26. R. Benner, K. Kaiser, *Limnol. Oceanogr.* **48**, 118 (2003).
27. N. O. G. Jørgensen, R. Stepanaukas, A. G. U. Pedrson, M. Hansen, O. Nybroe, *FEMS Microbiol. Ecol*. **46**, 269 (2003).
28. S. G. Wakeham, T. K. Pease, R. Benner, *Org. Geochem.* **34**, 857 (2003).
29. R. Benner, "Chemical composition and reactivity" in *Biogeochemistry of marine dissolved organic matter*, D. A. Hansell and C. A. Carlson Eds. (Academic press, New York, 2002), pp. 59–90.
30. T. Dittmar, J. Paeng, *Nat. Geosci.* **2**, 175 (2009).
31. N. Hertkorn, *et al., Geochim. Cosmochim. Acta,* **70**, 2990 (2006).
32. L. A. Ziolkowski, E. R. M. Druffel, *Geophys. Res. Lett.* **37**, doi: 1029/2010GL043963 (2010).
33. D. Hansell, C. A. Carlson, D. J. Repeta, R. Schlitzer, *Oceanogr.* **22**, 52 (2009).
34. H. Ducklow, Bacterial production and biomass in the ocean. In *Microbial Ecology of the Oceans*, D. L. Kirchman Ed. (John Wiley, New York, 2000), pp. 85–120.
35. T. Nagata. Production mechanisms of dissolved organic matter,. In *Microbial ecology of the oceans*, D. L. Kirchman, Ed. (John Wiley, New York, N.Y. 2000), pp. 121–152.
36. J. I. Hedges, *Mar. Chem.* **39**, 67 (1992).

37. This work was supported by the Scientific Committee on Oceanic Research (WG134), the U.S. National Science Foundation (0080782 and 0850653 to RB) and the Austrian Science Foundation (486-B09 and 23234-B11 to GJH).

Role of Photoheterotrophic Bacteria in the Marine Carbon Cycle

Michal Koblížek

Uncovering the ecological role of photoheterotrophic bacteria in the ocean is one of the main accomplishments of marine microbiology of the past decade. Marine photoheterotrophs include two main groups: Aerobic anoxygenic phototrophic (AAP) bacteria and proteorhodopsin (PR)-containing bacteria. These organisms make up large fractions of the microbial communities inhabiting the euphotic zone of world's oceans. In spite of similar metabolisms, AAP and PR-containing bacteria differ in their photochemistry, physiology, and ecology. The ability to use light energy appears to allow more economical utilization of dissolved organic matter, which implies that photoheterotrophic bacteria may play a unique role in the microbial carbon pump.

Discovery of Photoheterotrophic Bacteria in the Ocean

In 2000, two independent studies documented the widespread ability of marine bacteria to utilize light energy. In the first article, which appeared in the September 14 issue of *Nature*, Kolber *et al.* (*1*) reported the observation of distinct signals of bacteriochlorophyll *a*-containing microorganisms in the surface waters of the tropical Pacific. The recorded signals were linked with the presence of aerobic anoxygenic phototrophic (AAP) bacteria. These organisms contain bacteriochlorophyll *a* as the main light-harvesting pigment but, in contrast to purple nonsulfur photosynthetic bacteria, they are obligate aerobes requiring oxygen for their metabolism and growth (*2, 3*). Only one day later, Béjà *et al.* (*4*) announced in *Science* the discovery of a new rhodopsin gene in DNA samples recovered from Monterey Bay in California. Rhodopsins are well-known membrane proteins serving as photoreceptor molecules in Metazoa, including humans, or as proton pumps in halophilic Archaea, but until Béjà's report they were not thought to be present in Proteobacteria. For this reason the newly discovered protein was termed proteorhodopsin (PR) to make a clear distinction from the only distantly related archaeal bacteriorhodopsins and visual rhodopsins (see box on right).

These and follow up studies (*5–7*) have attracted significant scientific attention. The ability to use light energy challenged the classical view of marine bacteria as strictly heterotrophic organisms fully dependent on recycling dissolved organic matter (DOM) produced by photoautotrophic phytoplankton (Fig. 1). An important turning point represented the identification of the PR gene in a SAR11 isolate, *Pelagibacter ubique* (*8*). The SAR11 clade represents the most abundant bacterial group inhabiting the upper ocean (*9*), which suggests that photoheterotrophy could be a common phenomenon.

Light Utilization in Photoheterotrophic Bacteria

The phototrophic competence of AAP and PR-containing bacteria, and the way they use light as an energy source, remains a matter of ongoing research. These organisms contain photochemically active reaction centers, but are not able to grow photoautotrophically, as they require a supply of organic carbon (*3, 5, 10–12*). Experiments with *Erythrobacter* sp. NAP1 and *Dokdonia* sp. MED134 revealed light-enhanced CO_2 incorporation, however the activity was only weak, likely reflecting enhanced anaplerotic carboxylation activity (*5, 11*). In AAP bacteria, light has been shown to inhibit respiration and stimulate synthesis of ATP, which indicates that photophosphorylation replaces oxidative phosphorylation (*12, 13*). Physiological experiments conducted with heterologously expressed PR proteins demonstrated that light exposure led to the formation of proton gradients across the membrane (*4, 14*), which also confirms that PR drives photophosphorylation and provides ATP for cellular metabolism. Thus, AAP and PR-containing bacteria are photoheterotrophic organisms, as they use light energy to supplement their primarily heterotrophic metabolism. The ability to use light energy could allow phototrophs to store more carbon (which would otherwise be respired) in their biomass. Indeed, light-enhanced biomass accumulation has been repeatedly confirmed in AAP bacteria (*5, 15, 16*), but in PR-containing organisms the situation is less clear. The first experiments showed no growth stimulation by light in *Pelagibacter ubique* (*8*). In contrast, later work with *Dokdonia* sp. MED134 and *Vibrio* sp. AND4 demonstrated enhanced growth and better survival under starvation conditions when the bacteria were exposed to light, indicating that PR provided energy for growth (*17, 18*).

Distibution of Photoheterotrophs

In his pioneering paper, Kolber *et al.* (*1*) hypothesized that the ability to utilize light might be beneficial especially in nutrient-poor environments. The first quantification of PR-containing bacteria was attempted from the frequency of PR genes in metagenomic libraries. Using samples from the Mediterranean and Red Sea, it was estimated that PR genes were present in 13% of total bacteria (*19*). A more direct approach was used in the waters of the North Atlantic, applying quantitative polymerase chain reaction technique. It was found that PR-containing bacteria represented between 9 and 53% of total bacteria

MARINE PHOTOHETEROTROPHIC ORGANISMS

Aerobic Anoxygenic Phototrophic (AAP) Bacteria
These organisms harvest light by bacteriochlorophylls and carotenoids. The excitation energy is transferred to pheophytin-quinone-type reaction centers, which drive the electron transport and ATP synthesis. In contrast to their close relatives, purple photosynthetic bacteria, AAP bacteria are strict aerobes. They do not form a compact phylogenetic group, being scattered among a number of clades of Alpha-, Beta-, and Gammaproteobacteria.

Proteorhodopsin-containing Bacteria
Proteorhodopsin is a pigment protein composed of the protein moiety, opsin, and a pigment cofactor, retinal. Proteorhodopsins are analogous to visual rhodopsins and bacteriorhodopsins found in Archaea. The absorption of light by retinal causes the translocation of protons across the membrane driving ATP synthesis (Photophosphorylation). PR genes were found in a number of species including Alpha- and Gammaproteobacteria, Flavobacteria, Actinobacteria, and Archaea.

Institute of Microbiology CAS, Opatovický mlýn, 379 81 Třeboň, Czech Republic
E-mail: koblizek@alga.cz

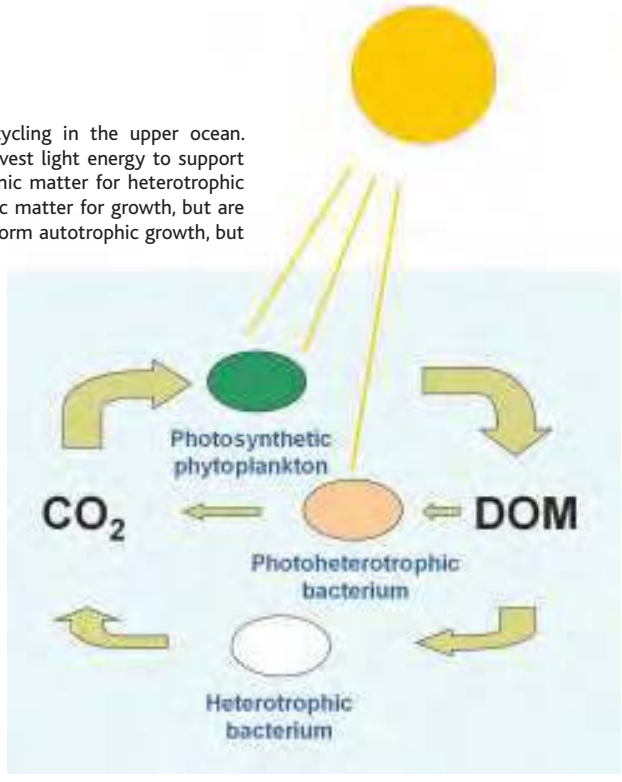

Fig. 1. Schematic representation of dissolved organic matter (DOM) cycling in the upper ocean. Photosynthetic phytoplankton are photoautotrophic organisms, which harvest light energy to support inorganic carbon fixation. These so-called primary producers provide organic matter for heterotrophic and photoheterotrophic species. Photoheterotrophic bacteria utilize organic matter for growth, but are capable of using light energy for their metabolism. They are unable to perform autotrophic growth, but can grow heterotrophically in the dark. Heterotrophic bacteria (Organotrophs) depend on organic matter produced by autotrophic species both as a source of energy and as a substrate for growth.

in the Sargasso Sea, and in the more productive waters of the North Atlantic they still represented 4 to 15% of total bacteria (*20*). AAP bacteria can be conveniently counted by infrared epifluorescence microscopy. Despite some initial controversies, it has been found that AAP bacteria on average constitute 1 to 7% of total prokaryotes in oligotrophic areas (*21–24*). In more productive environments such as coastal waters, shelf seas, and river estuaries, they represent up to 30% of total prokaryotes (*25–27*). The latter data contradicts the assumption that photoheterotrophy would be more advantageous in nutrient poor areas, as AAP bacteria appear to prefer more eutrophic environments. However, Kolber's hypothesis seems to hold for PR-containing bacteria, which have indeed been shown to be abundant in oligotrophic regions (Fig. 2).

Role of Photoheterotrophs in the Marine Carbon Cycle

The role of photoheterotrophs in the microbial carbon pump (MCP) is complex (*28*). Their ability to use light energy can reduce their carbon requirement, which means that less organic matter would be respired and converted into CO_2. This might be especially important in the oligotrophic regions of the ocean (*29*), which are generally considered to be carbon sinks (*30*). The additional energy from light may also help to fuel various energy-demanding processes such as active transport of substrates and nutrients across membranes, production of ectoenzymes, breakdown of complex organic molecules, and cell motility. In spite of the fact that PR genes are present in very diverse organisms (*31*), most of them are likely to be oligotrophic species inhabiting nutrient-scarce ocean areas, potentially giving them a unique place and role in the MCP. In contrast, AAP bacteria seem to be highly active organisms with larger cell sizes (*21*) and high growth rates (*23*). This suggests that despite their smaller numbers, AAP bacteria can process a large part of the available DOM, most likely the more readily accessible labile DOM.

Our knowledge of photoheterotrophic organisms has expanded significantly in the past decade. The need for appropriate tools led to the development of many new experimental techniques. Yet, our understanding of the role photoheterotrophs play in the marine environment and organic matter cycling is still only fragmentary. The increasing number of organ-

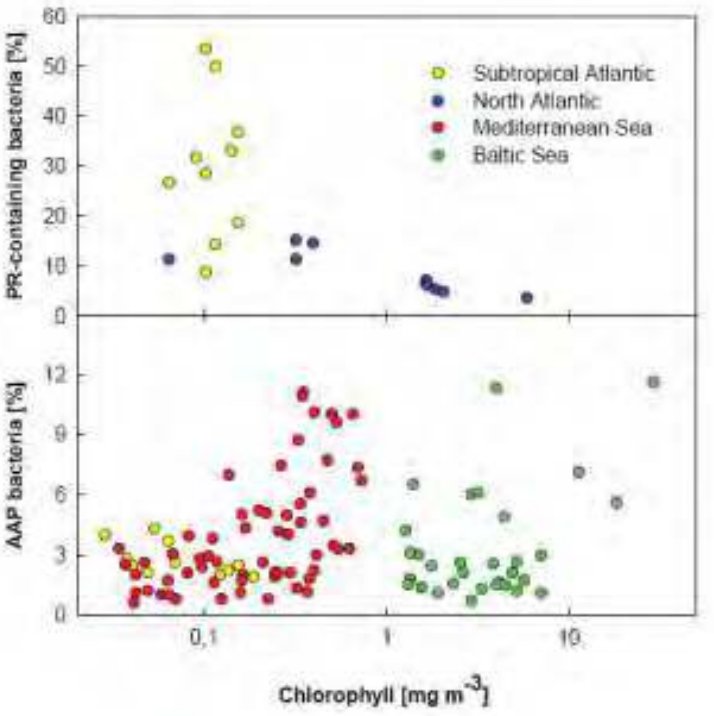

Fig. 2. Contribution of photoheterotrophic bacteria to the microbial community (expressed as a percentage of total prokaryotes) in various marine environments with different trophic status. Proteorhodopsin-containing bacteria abundance data were taken from (*20*). AAP data for the subtropical Atlantic were taken from (*23*), for the Baltic Sea from (*25*), and for the Mediterranean Sea from (*32*).

FIG. 2 KOBLIZEK

isms available in laboratory cultures makes it possible to design better experiments, which, in combination with genomic data, can provide important insights into cell metabolism and photobiology. Field studies should focus on environmental factors driving the distribution and activity of photoheterotrophic species. Manipulation and enrichment experiments can be especially beneficial in elucidating the main bottom-up and top-down factors shaping the natural microbial populations and establishing the role these organisms play in the marine carbon cycle.

References and Notes

1. Z.S. Kolber, C.L. Van Dover, R.A. Niederman, P.G. Falkowski, *Nature* **407**, 177 (2000).
2. T. Shiba, U. Simidu, N. Taga, *Appl. Environ. Microbiol.* **38**, 43 (1979).
3. V.V. Yurkov, J.T. Csotonyi, in *The Purple Phototrophic Bacteria*, *Advances in Photosynthesis and Respiration* volume 28, Hunter, C.N., Daldal, F., Thurnauer, M.C. and Beatty, J.T. Eds. (Springer Verlag, Dordrecht, The Netherlands, 2009), pp. 31–55.
4. O. Béjà *et al*., *Science* **289**, 1902 (2000).
5. Z.S. Kolber *et al*., *Science* **292**, 2492 (2001).
6. O. Béjà, E.N. Spudich, J.L. Spudich, M. Leclerc, E.F. DeLong, *Nature* **411**, 786 (2001).
7. Béjà, O. *et al*., *Nature* **415**, 630 (2002).
8. S.J. Giovannoni *et al*., *Nature* **438**, 82 (2005).
9. R.M. Morris *et al*., *Nature* **420**, 806 (2002).
10. B.M. Fuchs *et al*., *Proc. Natl. Acad. Sci. USA* **104**, 2891 (2007).
11. J.M. González *et al*., *Proc. Natl. Acad. Sci. USA* **105**, 8724 (2008).
12. M. Koblížek, J. Mlčoušková, Z Kolber, J. Kopecký, *Arch. Microbiol.* **192**, 41 (2010).
13. K. Okamura, F. Mitsumori, O. Ito, K.-I. Takamiya, M. Nishimura, *J. Bacteriol.* **168**, 1142 (1986).
14. A. Martinez, A.S. Bradley, J.R. Waldbauer, R.E. Summons, E.F. DeLong, *Proc. Natl. Acad. Sci. USA* **104**, 5590 (2007).
15. Y. Shioi, *Plant Cell Physiol.* **27**, 567 (1986).
16. V.V. Yurkov, H. van Gemerden, *Arch. Microbiol.* **159**, 84 (1993).
17. L. Gómez-Consarnau *et al*., *Nature* **445**, 210 (2007).
18. L. Gómez-Consarnau *et al*., *PLoS Biol* **8**, e1000358, 10.1371/journal.pbio.1000358 (2010).
19. G. Sabehi *et al*., *PLoS Biol.* **3**, e173, 10.1371/journal.pbio.0030273 (2005).
20. B.J. Campbell, L.A. Waidner, M.T. Cottrell, D.L. Kirchman, *Environ. Microbiol.* **10**, 99 (2008).
21. M.E. Sieracki, I.C. Gilg, E.C. Thier, N.J. Poulton, R. Goericke, *Limnol. Oceanogr.* **51**, 38 (2006).
22. M.T. Cottrell, A. Mannino, D.L. Kirchman. *Appl. Env. Microbiol.* **72,** 557 (2006).
23. M. Koblížek, M. Mašín, J. Ras, A.J. Poulton, O. Prášil, *Environ. Microbiol.* **9**, 2401 (2007).
24. N. Jiao *et al*., *Environ. Microbiol.* **9**, 3091 (2007).
25. M. Mašín *et al*., *Aquat. Microbial. Ecol.* **45**, 247 (2006).
26. Y. Zhang, N. Jiao, *FEMS Microbiol. Ecol.* **61**, 459 (2007).
27. M.T. Cottrell, J. Ras, D.L. Kirchman, *ISME J.* **4**, 945 (2010).
28. N. Jiao *et al*., *Nat. Rev. Microbiol.* **8**, 593 (2010).
29. N. Jiao *et al*., *ISME J*. **4**, 595 (2010).
30. P.A. del Giorgio, C.M. Duarte, *Nature* **420**, 379 (2002).
31. J.C. Venter *et al*., *Science* **304**, 66 (2004).
32. E. Hojerová, personal communication

33. This work was supported by GAČR project P501/10/0221, AV ČR project M200200903, project Algatech (CZ.1.05/2.1.00/03.0110), and the Institutional Research Concept AV0Z50200510. M.K. thanks Prof. Nianzhi Jiao and Dr. Isabel Ferrera for constructive comments, and Dr. Matthew T. Cottrell for kindly providing the PR abundance data.

Microbial Heterotrophic Metabolic Rates Constrain the Microbial Carbon Pump

Carol Robinson[1]* and Nagappa Ramaiah[2]

The respiration of dissolved organic matter by heterotrophic bacteria and Archaea represents the largest sink in the global marine biological carbon cycle, an important constraint on organic carbon supply, and the major driver of global elemental nutrient cycles. Direct measurement of heterotrophic production and respiration is difficult. However, the recent development of methods involving in vivo electron transport system activity, bioassay uptake of specific prokaryotic substrates, and nutrient addition incubations are poised to discern the complex interactions between metabolic rate, community structure, and organic and inorganic nutrient availability. In a changing global environment, it is important to understand how increasing sea surface temperature, melting sea ice, ocean acidification, variable dust deposition, and upwelling intensity will impact the metabolism of Bacteria and Archaea and so the balance between carbon sequestration and carbon dioxide evasion to the atmosphere. Continued and improved measures of prokaryotic production and respiration are vital components of this endeavor.

The downward flux of organic carbon from the surface ocean to depth via passive sinking of particles, active transport by animals, and mixing of dissolved organic matter (DOM) is known as the biological carbon pump (BCP). The microbial carbon pump (MCP) is a conceptual component of the BCP, used to describe the microbial production of refractory DOM (RDOM) which can be stored for millennia in the deep sea, rather than being respired to dissolved inorganic carbon and returned to the atmosphere (*1*). Heterotrophic bacteria and Archaea generate RDOM through degradation and transformation of particulate and dissolved organic matter, exudation, and cell lysis (*2, 3*). In addition to assimilation and transformation of recently produced DOM, prokaryotes also degrade 'older' DOM (*4*) derived from photochemically transformed upwelled DOM (*5, 6*) and potentially from methane seeps (*7*). Hence, understanding the magnitude and variability of the production and respiration of bacteria and Archaea is important not only for quantifying the efficiency of the BCP (*8*) and the role of prokaryotes in regulating carbon fluxes (*9*), but also for constraining the flow of DOM through the MCP.

The composition and lability of DOM affect the prokaryotic carbon demand [PrCD = prokaryotic production (PrP) + prokaryotic respiration (PrR)] and the prokaryotic growth efficiency (PrGE = PrP/PrCD, the proportion of the prokaryotic carbon demand used for prokaryotic production). PrGE is influenced by the availability of organic and inorganic substrates as well as the energetic costs of growth in a particular environment, and so tends to be low at times of nutrient limitation or environmental stress and higher during increased primary productivity and supply of nutrients (*8, 10*).

The direct measurement of PrP and PrR and calculation of PrCD and PrGE is technically and interpretatively challenging. This is due to uncertainties associated with factors such as the pre-incubation separation of the heterotrophic bacterioplankton fraction from the rest of the plankton community, the different incubation times required for PrR and PrP measurements, the effect of light on PrP and PrR, the quantification of prokaryotic excretion of DOM, and the conversion factors used to derive rates of carbon production and respiration from radiolabeled thymidine or leucine incorporation and oxygen consumption (*8,9*). Large uncertainties in PrGE contribute significantly to the mismatch between measurements of mesopelagic microbial metabolic activity and estimates of the influx of organic carbon that could support this microbial activity (*11*).

Recent methodological developments have the potential to reduce uncertainties in PrR and PrP determinations. For example, measurements of in vivo electron transport system activity estimated from the reduction of the tetrazolium salt INT are linearly related to in situ rates of respiration, and avoid problems associated with pre-incubation filtration and relatively long incubation times (24 hours) (*12*). Additionally, single cell assays that measure incorporation of selected organic compounds by specific prokaryotic groups compare and contrast the components of DOM taken up by bacteria and Archaea (*13*). Including these assays in time series studies can elucidate the influence of environmental factors such as light on PrP (*14, 15*).

Climate change will likely affect precipitation, river flow, ice melt, atmospheric deposition, and the timing and strength of alongshore winds that stimulate coastal upwelling, and so may significantly change the supply of inorganic and organic substrates to marine prokaryotes. Concomitant increases in sea surface temperature and decreases in pH and carbonate ion concentration could lead to changes in phytoplankton and zooplankton community structure, subsequently impacting foodweb-derived DOC (*16*). In short-term experiments, prokaryotic turnover of phytoplankton-derived polysaccharides was increased at the lower pH levels projected to occur with a doubling of atmospheric CO_2, with the potential to reduce carbon export and enhance respiratory CO_2 production (*17*). Field studies and inorganic and organic nutrient bioassay experiments show PrR and PrGE in coastal regions to be either mainly controlled by the DOC pool or colimited by organic and inorganic nutrients (*18–20*). Climate-driven increases in DOC supply may also impact the plankton community photosynthesis to respiration (P:R) ratio. When released from organic carbon limitation, heterotrophic prokaryotes can outcompete phytoplankton for inorganic nutrients, thereby decreasing the overall P:R ratio, increasing the proportion of DOC that is respired, and decreasing the amount that is sequestered (*21*).

This review aims to highlight our incomplete understanding for the causes of variability in the PrGE and respiratory potential of heterotrophic bacteria and Archaea. As new research supports the pivotal role of these microbes in the present and future ocean (*22, 23*), the lack of routine measurements of PrP and PrR in relation to phylogenetic composition, as well as to DOM characterization and assimilation potential, becomes increasingly difficult to defend.

[1]School of Environmental Sciences, University of East Anglia, Norwich NR4 7TJ, U.K.
[2]National Institute of Oceanography, Dona Paula 403004, Goa, India
*To whom correspondence should be addressed. E-mail: carol.robinson@uea.ac.uk

References and Notes

1. N. Jiao *et al., Nat. Rev. Microbiol.* **8**, 593 (2010).
2. T. Nagata, in *Microbial Ecology of the Oceans* D.L. Kirchman Ed. (John Wiley & Sons, Inc. New York, ed. 1. 2000), pp. 121–152.
3. D. F. Gruber, J. P. Simjouw, S. P. Seitzinger, and G. L. Taghon, *Appl. Environ. Microbiol.* **72,** 4184 (2006).
4. J. Cherrier, J. E. Bauer, E. R. M. Druffel, R. B. Coffin, J. P. Chanton, *Limnol. Oceanogr.* **44,** 730 (1999).
5. R. Benner, B. Biddanda, *Limnol. Oceanogr.* **43,** 1373 (1998).
6. I. Obernosterer, B. Reitner, G. J. Herndl, *Limnol. Oceanogr.* **44,** 1645 (1999).
7. J. W. Pohlman, J. E. Bauer, W. F. Waite, C. L. Osburn, N. R. Chapman, *Nat. Geosci.* **4,** 37 (2011).
8. C. Robinson, in *Microbial Ecology of the Oceans* D.L. Kirchman Ed. (John Wiley & Sons, Inc. ed. 2. 2008), pp. 299–334.
9. J. M. Gasol *et al.*, *Aquat. Microb. Ecol.* **53,** 21 (2008).
10. P. A. del Giorgio, J. J. Cole, in *Microbial Ecology of the Oceans* D. L. Kirchman Ed. (John Wiley & Sons, Inc. New York ed. 1. 2000), pp. 289–325.
11. A. B. Burd *et al., Deep Sea Res. II* **57,** 1557 (2010).
12. S. Martinez-García, E. Fernández, M. Aranguren-Gassis, E. Teira, *Limnol. Oceanogr. Methods* **7,** 459 (2009).
13. D.L. Kirchman, H. Elifantz, A. I. Dittel, R. R. Malmstrom, M. T. Cottrell, *Limnol. Oceanogr.* **52,** 495 (2007).
14. M. J. Church, H. W. Ducklow, D.A. Karl, *Appl. Environ. Microbiol.* **70,** 4079 (2004).
15. T. R. A. Straza, D. L. Kirchman, *Aquat. Microb. Ecol.* **62,** 267(2011).
16. O. Hoegh-Guldberg, J. F. Bruno, *Science* **328,** 1523 (2010).
17. J. Piontek, M. Lunau, N. Handel, C. Borchard, M. Wurst, A. Engel, *Biogeosciences* **7,** 1615 (2010).
18. J. K. Apple, P.A. del Giorgio, *ISME J.* **1,** 729 (2007).
19. L. Alonso-Sáez *et al., Limnol. Oceanogr.* **52,** 533 (2007).
20. S. Martinez-García *et al., Aquat. Microb. Ecol.* **416,** 17 (2010).
21. T. F. Thingstad *et al., Nature* **455,** 387 (2008).
22. J. Arístegui, J. M. Gasol, C. M. Duarte, G. J. Herndl, *Limnol. Oceanogr.* **54,** 1501 (2009).
23. D. L. Kirchman, X. A. G. Moran, H. W. Ducklow, *Nat. Rev. Microbiol.* **7,** 451 (2009).
24. We thank G. Herndl for constructive comments and suggestions. This work was supported by the Scientific Committee on Oceanic Research (WG134), The Royal Society (to CR), and the National Institute of Oceanography, India (to NR).

Virus-Mediated Redistribution and Partitioning of Carbon in the Global Oceans

Markus G. Weinbauer[1,2]*, Feng Chen[3], Steven W. Wilhelm[4]**

Viruses in marine systems influence biogeochemical cycles by releasing organic matter during the lysis of host cells. This process redistributes this biological carbon across a continuum of organic materials, from dissolved to particulate. Estimates of release rates of viral lysis products, studies manipulating viral effects on natural communities, and efforts using virus-host systems indicate that viral lysis changes the chemical composition, distribution, and character of organic matter. The majority of these lysis products can be assimilated rapidly by prokaryotes. Moreover, viral lysis appears to influence the formation and stability of organic particles ("marine snow"), altering carbon flow through the biological pump from the surface to deep ocean. While well defined, the net outcomes of these virus-mediated activities remain uncertain. The consistent experimental observation that viral lysis decreases the growth efficiency of residual prokaryotic communities further suggests that the activity of viruses generates, in part, organic matter that is biologically recalcitrant. While this clearly indicates an influence on the mineralization and transformation of organic matter, new observations across spatial and temporal gradients are needed to develop our understanding of the potential role of viruses in marine carbon cycles.

Viruses are the most abundant "life" forms in the ocean (*1*) and some studies suggest that they significantly impact the mortality rates of marine prokaryotes and eukaryotic algae (*2, 3*), releasing cellular material from infected hosts into the environment. This release of lysis products from all trophic levels as dissolved organic matter (DOM) and particulate organic matter (POM) has been termed the "viral shunt" (*4*) (Fig. 1). Viral lysis is now considered a major source of dissolved organic carbon (DOC) in marine systems, one that rivals leaching from phytoplankton, the collapse of bloom events (sometimes by programmed cell death), sloppy feeding by zooplankton, and egestion by protists.

The DOC pool in the ocean contains approximately the same amount of carbon as is stored as CO_2 in the atmosphere. This DOC, which would otherwise be lost from the rest of the foodweb, is primarily consumed by heterotrophic prokaryotes (Bacteria and Archaea). These prokaryotes are subsequently consumed by small grazers (protists), connecting the DOM to the foodweb via the "microbial loop" (*5*). Thus, quantifying the source(s) of DOM and the fate of prokaryotic carbon production is an important step in understanding the marine carbon cycle. Microorganisms are also involved in the formation and dissolution of particles ("marine snow"). The transfer of carbon into the deep sea via sinking of biogenic particles is a major pathway of the "biological pump" (*6*). Within this framework, microbial activity converts a fraction of organic matter into refractory DOM (RDOM), marine carbon that in the oceans appears to be biologically unavailable to microorganisms; as such, DOC is relatively old (~5,000 years of age). The process driving this conversion has recently been termed the microbial carbon pump (MCP) (*7*). In the following, we summarize the state of knowledge concerning the potential role of viruses and their activity as a source of carbon, RDOM, and precursors for aggregate formation, as well as the implications of this activity for the biological and microbial carbon pumps (*7*).

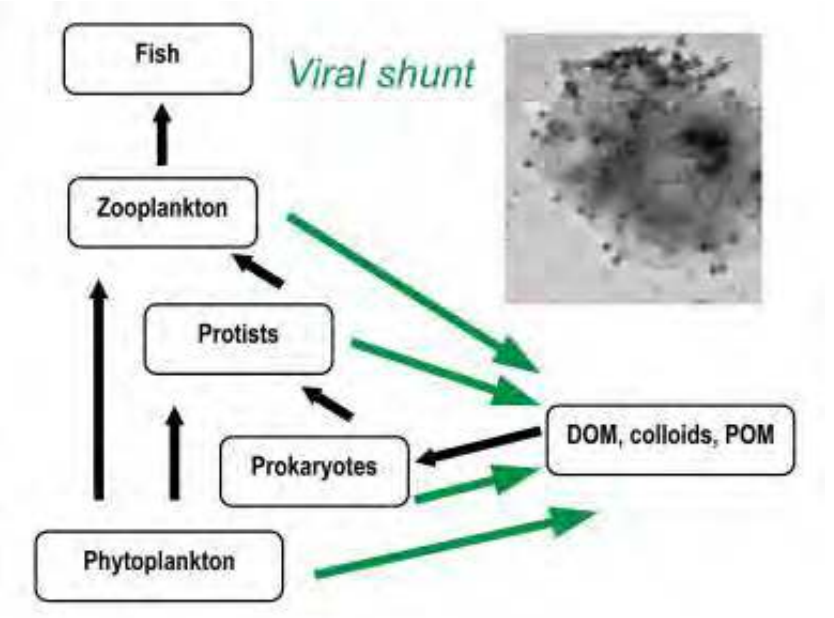

Fig. 1. The viral shunt in marine foodwebs. Viruses divert the flow of carbon and nutrients from secondary consumers (black arrows) by destroying host cells and releasing the contents of these cells into the pool of dissolved organic matter (DOM) in the ocean (green arrows). The electron micrograph insert shows a cyanobacterial cell in the process of lysis.

FIG. 1: WEINBAUER, CHEN AND WILHELM

Viral Lysis Products and Virus-mediated Aggregation of Organic Matter

The composition of virus-generated lysis products is poorly studied. Nevertheless, studies with laboratory virus-host systems (VHSs), as well as microbial communities, have shown that lysis changes the composition of DOM (*8, 9*). In VHSs, material from the bacterial cell wall, including various D-isomers of amino acids, glucosamine, and diaminopimelic acid have been found in the dissolved fraction (*8*). An

[1]Microbial Ecology & Biogeochemistry Group, Université Pierre et Marie Curie-Paris6, Laboratoire d'Océanographie de Villefranche, 06230 Villefranche-sur-Mer, France
[2]CNRS, Laboratoire d'Océanographie de Villefranche, 06230 Villefranche-sur-Mer, France
[3]Institute of Marine Environmental Technology, University of Maryland Center for Environmental Science, Baltimore, MD 21202, USA
[4]Department of Microbiology, University of Tennessee, Knoxville, TN 37996, USA
To whom correspondence should be addressed. *E-mail: wein@obs-vlfr.fr
**E-mail: wilhelm@utk.edu

accumulation of polymeric and total DOM (such as amino acids and carbohydrates) due to viral lysis has also been demonstrated (*8, 9*). VHS studies have also shown a promotion of the formation of submicron colloids (*10*). Overall, viral lysis predictably increases the DOM pool, particularly the polymeric and colloidal components.

Reports of direct release rates of lysis products remain rare due to methodological challenges (for example, *11*). However, research using estimations of cellular carbon:nitrogen:phosphorus quota and mortality rates has shown that viral lysis transforms significant quantities of microbial biomass into DOM and colloidal pools (*12, 13*). Experimental studies with VHSs (*12, 14–16*), model communities (*17*) and natural communities (*11, 18*) indicate that the majority of these lysis products are rapidly (within days) degraded and belong to the labile DOM (LDOM) fraction. This should result in a reduced transfer of carbon to higher trophic levels and fuel the microbial part of the foodweb (*19*).

In an elegant study, the effect of lysis products on bacterial activity was studied using a bacterial VHS and the lysis products from this VHS (*15*). Bacterial carbon production and enzymatic activity increased, while bacterial growth efficiency decreased in the presence of the either added viruses or lysis products. These observations can be explained by an increase in prokaryotic energy demand associated with the degradation of polymeric organic nitrogen and phosphorus from the lysate products. Subsequent research on microbial communities, manipulating the presence and absence of viruses using various experimental approaches, demonstrates a consistent pattern: Lysis increases prokaryotic respiration and decreases growth efficiency (*20, 21*). This means that more organic matter has been processed and turned into CO_2 and that a greater percentage of the nutrients within the DOM are mineralized (16). Within this context it is also conceivable that enhanced prokaryotic respiration and reduced growth efficiency should prime the MCP to produce more RDOM, or at least increase the ratio of RDOM to LDOM and semilabile DOM (SDOM). This is one area that remains ripe for experimental exploration.

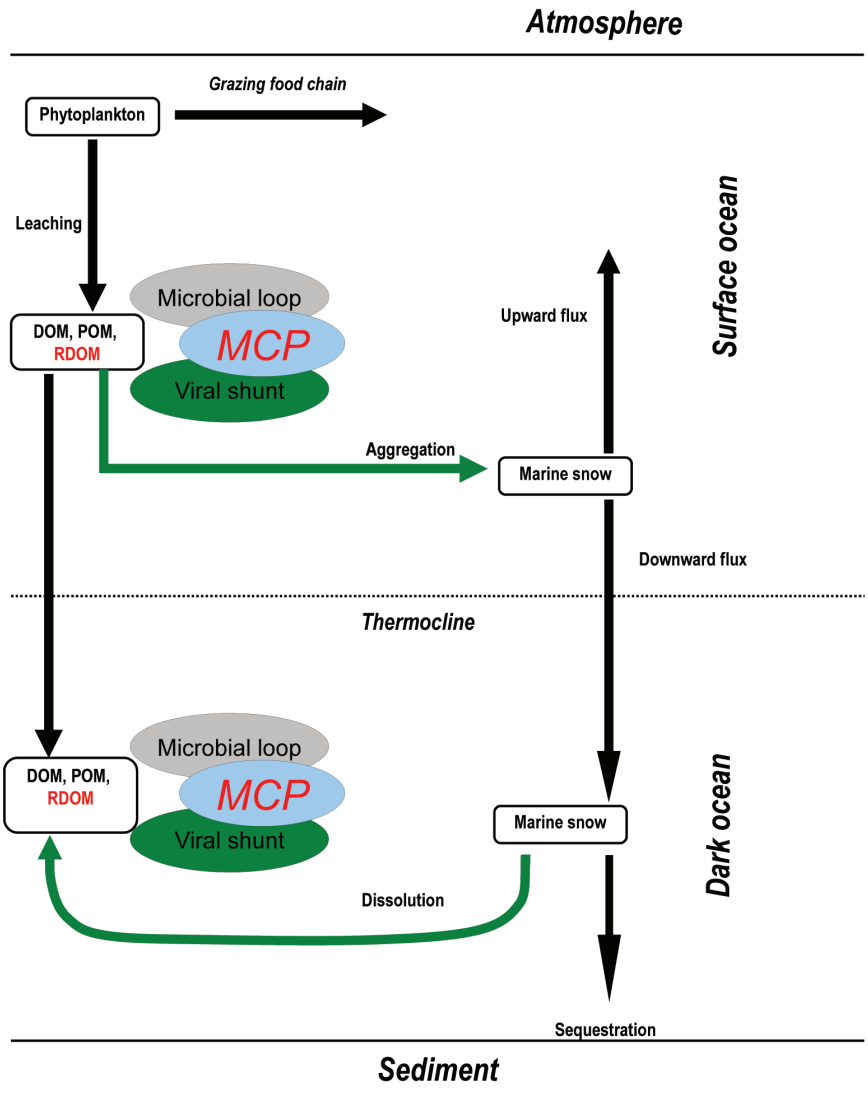

Fig. 2. The viral shunt in the context of oceanic carbon cycling. Potential major influences of virus are shown in green. Note that the grazing food chain, the microbial loop, and the viral shunt are only shown schematically (for more details, see Fig. 1). The role of the microbial carbon pump (MCP) is shown as well. This scheme assumes that aggregation of marine snow dominates in surface water, whereas dissolution dominates in the dark ocean. DOM, dissolved organic matter; POM, particulate organic matter; RDOM, refractory DOM.

Another consequence of virus activity is the potential to influence the aggregation of organic matter (Fig. 2). There is experimental evidence that viruses delay the formation of phytoplankton blooms (*3, 22*) and thus the formation of biotic (organic) particles (*23*). Similar trends have been found for prokaryotic aggregation and particle colonization (*24, 25*). Viruses can, however, increase the size and stability of algal-derived aggregates (*23*), for instance through the formation of colloidal material and the release of "sticky" intracellular contents (*10*). In one mesocosm study, the termination of a phytoplankton bloom by viral lysis was associated with a large production of biological aggregates (*26, 27*).

Viruses and infected cells can also be found on, as well as in, aggregates (*28*). This may increase the dissolution of sinking particles through the direct destruction of particle nucleating bacteria or the release of intracellular enzymes that facilitate aggregate dissolution. The true role of viruses in particle dissolution and aggregation is likely a delicate balance of these two processes (*29*).

Viruses and the Biological Carbon Pump

The export of carbon out of the euphotic zone by the biological pump is a central component of marine carbon cycles (*6*). The location of viral activity within the water column, in respect to the depth and strength of the pycnocline, is thus crucial as it influences whether the lysed material is recycled in the euphotic zone or exported into the deep sea. To describe this, a conceptual model was developed with three scenarios

FIG. 2: WEINBAUER, CHEN AND WILHELM

for infected cells of the bloom-forming alga *Heterosigma akashiwo* and viruses that infect them (*30*). In scenario 1, when stratification is strong or the pycnocline is deep, cells lyse above the pycnocline and lysis products remain in the mixed layer. In scenario 2, when stratification is weak and waters are shallow, infected cells will reach the benthos before lysis and lysis products remain at the sediment-water interface. In scenario 3, cells are also not retained by the pycnocline and lysis products are subject to processes in the deeper water column. The exact fate and quantity of primary production shunted into the DOM and colloidal pool will depend on the actual scenario in play.

In addition to the location of viral infection in the water column, the following mechanisms may influence the biological pump: (i) The conversion of cellular material into the dissolved and colloidal forms should increase the retention time of carbon and nutrients in surface water and thus reduce export; (ii) Aggregation driven by lysis products will increase carbon export unless this aggregation also increases the buoyancy of particles (for example, by retaining gases from metabolism) and thus the retention time in the euphotic zone; (iii) Nutrient (nitrogen, phosphorus, and iron) release within lysis products may act as a feedback mechanism and stimulate primary production with unpredictable consequences for the biological pump; and (iv) If viral lysis stimulates the microbial loop and reduces carbon transfer to higher trophic levels, less carbon is available for zooplankton-mediated particle formation (for example, fecal pellets or larvacean houses); this would shift aggregation to one based on phytoplankton-derived materials.

Since these mechanisms are difficult to disentangle (and others yet might not be recognized), it is still not possible to assess whether the net effect of viral activity is to prime or short-circuit the biological pump (*31*). Indeed, research during the last two decades has revealed that virus activity depends strongly on spatial and temporal scales (even in the deep sea) (*32, 33*). Thus, the role of viruses within the MCP and the biological pump is potentially environment and condition specific.

Viruses and the Microbial Carbon Pump

Functionally there now also appears to be a "horizontal" component (the pumping of biomass into the RDOM pool) within microbial carbon cycles, which, at some level, is undoubtedly influenced by the viral shunt (*7*). In the euphotic zone, viral lysis of picocyanobacteria and autotrophic eukaryotic plankton will contribute, in addition to bacterial cell lysates, to the DOM and subsequently RDOM pools (and finally export). Since representative cyanobacterial VHSs are available for the euphotic zone, they may serve as good models for understanding the dispersal of virus-mediated lysis products in the natural environment.

In the deep ocean (where most of the recalcitrant carbon is found), significant viral activity has been reported for benthic and pelagic systems (*33, 34*). Viral lysis of Bacteria and Archaea (which become more abundant in the dark ocean) should produce mainly LDOM. Since this material will be consumed rapidly (and potentially help sustain high prokaryotic production in the deep sea), lysis may increase the ratio of RDOM to LDOM and SDOM. In a similar manner to the conversion of some LDOM and SDOM into RDOM by prokaryotic activity (*35*), viral lysis in the deep sea should also promote RDOM production directly in the environment where long term storage occurs. Since RDOM is resistant to microbial utilization, is stored in the ocean for millennia, and accounts for more than 95% of the total DOC pool (*7*), alterations of RDOM dynamics within the microbial carbon pump by viral activity will undoubtedly influence the global carbon cycle.

References and Notes

1. Ø. Bergh, K. Y. Børsheim, G. Bratbak, M. Heldal, *Nature* **340**, 467 (1989).
2. L. M. Proctor, J. A. Fuhrman, *Nature* **343**, 60 (1990).
3. C. A. Suttle, A. M. Chan, M. T. Cottrell, *Nature* **347**, 467 (1990).
4. S. W. Wilhelm, C. A. Suttle, *Bioscience* **49**, 781 (1999).
5. F. Azam *et al.*, *Mar. Ecol. Prog. Ser.* **10**, 257 (1983).
6. R. W. Eppley, B. J. Peterson, *Nature* **282**, 677 (1979).
7. N. Jiao *et al.*, *Nat. Rev. Microbiol.* **8**, 593 (2010).
8. M. Middelboe, N. O. G. Jorgensen, *J. Mar. Biol. Ass. UK* **86**, 605 (2006).
9. M. G. Weinbauer, P. Peduzzi, *Mar. Ecol. Prog. Ser.* **127**, 245 (1995).
10. A. Shibata, K. Kogure, I. Koike, K. Ohwada, *Mar. Ecol. Prog. Ser.* **155**, 303 (1997).
11. L. Poorvin, J. M. Rinta-Kanto, D. A. Hutchins, S. W. Wilhelm, *Limnol. Oceanogr.* **49**, 1734 (2004).
12. C. J. Gobler, D. A. Hutchins, N. S. Fisher, E. M. Cosper, S. Sañudo-Wilhelm, *Limnol. Oceanogr.* **42**, 1492 (1997).
13. S. W. Wilhelm, M. G. Weinbauer, C. A. Suttle, W. H. Jeffrey, *Limnol. Oceanogr.* **43**, 586 (1998).
14. G. Bratbak, A. Jacobson, M. Heldal, *Aquat. Microb. Ecol.* **16**, 11 (1998).
15. M. Middelboe, N. O. G. Jørgensen, N. Kroer, *Appl. Environ. Microbiol.* **62**, 1991 (1996).
16. M. Middelboe, L. Riemann, C. F. Steward, W. Hannsen, O. Nybroe, *Aquat. Microb. Ecol.* **33**, 1 (2003).
17. J. Haaber, M. Middelboe, *ISME J.* **3**, 430 (2009).
18. R. T. Noble, J. A. Fuhrman, *Aquat. Microb. Ecol.* **20**, 1 (1999).
19. J. A. Fuhrman, *Nature* **399**, 541 (1999).
20. M. Middelboe, P. G. Lyck, *Aquat. Microb. Ecol.* **27**, 187 (2002).
21. C. Motegi *et al.*, *Limnol. Oceanogr.* **54**, 1901 (2009).
22. C. A. Suttle, *Mar. Ecol. Prog. Ser.* **87**, 105 (1992).
23. P. Peduzzi, M. G. Weinbauer, *Limnol. Oceanogr.* **38**, 1562 (1993).
24. A. Malits, M. G. Weinbauer, *Aquat. Microb. Ecol.* **54**, 243 (2009).
25. L. Riemann, H.-P. Grossart, *Microb. Ecol.* **56**, 505 (2008).
26. C. Brussaard, B. Kuipers, M. Veldhuis, *Harmful Algae* **4**, 894 (2005).
27. C. Brussaard, X. Mari, J. D. L. van Bleijswijk, M. Veldhuis, *Harmful Algae* **4**, 875 (2005).
28. L. M. Proctor, J. A. Fuhrman, *Mar. Ecol. Prog. Ser.* **69**, 133 (1991).
29. M. G. Weinbauer *et al.*, *Aquat. Microb. Ecol.* **57**, 321 (2009).
30. J. E. Lawrence, C. A. Suttle, *Aquat. Microb. Ecol.* **37**, 1 (2004).
31. C. P. Brussaard *et al.*, *ISME J.* **2**, 575 (2008).
32. J. M. Rowe *et al.*, *Aquat. Microb. Ecol.* **52**, 233 (2008).
33. M. G. Weinbauer, I. Brettar, M. G. Höfle, *Limnol. Oceanogr.* **48**, 1457 (2003).
34. R. Danovaro *et al.*, *Nature* **454**, 1084 (2008).
35. H. Ogawa, Y. Amagai, I. Koike, K. Kaiser, R. Benner, *Science* **292**, 917 (2001).

36. The authors thank C.A. Suttle for his mentorship. They also appreciate the thorough comments of G. Bratbak. They also acknowledge the French Science Ministry (ANR-AQUAPHAGE, N°ANR 07 BDIV 015-06; ANR-MAORY; N° ANR 07 BLAN 016) for support to MGW, NSF(OCE) 0825405 and 1061352 for support to SWW and the SCOR Working Group 134.

DOC Persistence and Its Fate After Export Within the Ocean Interior

Craig A. Carlson[1]*, Dennis A. Hansell[2], and Christian Tamburini[3,4]

Biotic and abiotic processing of organic matter originally created through photosynthesis can lead to its accumulation as dissolved organic matter (DOM) in surface waters of the ocean. Components of this dissolved material are resistant to microbial remineralization, persisting long enough to be entrained during ventilation of the ocean interior, and resulting in carbon export to great ocean depths. Upon downward mixing to mesopelagic waters (from >150 to ~1000 m), the exported DOM is susceptible to removal on both short (weeks) and long (years) time scales, with remineralization by deep microbial populations playing an important role. Recent work indicates that specific lineages of subsurface bacterioplankton respond to these export events, remineralizing the same DOM that had been largely resistant to microbial degradation at the sea surface. Free-living (unattached) microbial populations are structured vertically, with that structure defined by unique metabolic capabilities that are important when considering the fate of exported DOM and its lability.

Dissolved organic carbon (DOC) represents the largest pool of reduced carbon in the ocean with a global inventory of approximately 662 petagrams of carbon (PgC) (*1*). The pool contains a myriad of organic molecules, comprising broad fractions of variable lability that turn over on time scales from minutes to millennia (*2, 3*). Of the approximately 50 PgC y^{-1} of global net primary production, greater than 50% is partitioned as DOC to be processed through the microbial foodweb (*3, 4*). The majority of the newly produced DOC is rapidly remineralized by heterotrophic bacterioplankton within ocean's surface layer (*5*). However, about 20% of the annual global ocean net community production (~1.8 PgC y^{-1}) escapes degradation long enough to be exported from the euphotic zone through overturning circulation of the water column. Once exported, the dissolved organic matter (DOM) and its remineralization byproducts travel by isopycnal pathways into the ocean's interior (*1, 6–9*). Figure 1 provides evidence of export with deep water formation in the North Atlantic, where mid-latitude, warm, DOC-enriched surface waters are transported with surface currents to high latitude (Fig. 1A), at which point deep water formation transports the DOC deep into the interior (Fig. 1, B and C) where it slowly declines during southward flow. Additional processes such as the solubilization of sinking particles (*10*) and DOC release from vertically migrating zooplankton (*11*) result in further DOC introduction into the subsurface layers. Factors that regulate persistence of exported DOC include inorganic nutrients required by heterotrophic microbes (*12, 13*), the quality of the exported DOM (*14, 15*), the microbial community structure (*16, 17*), and the expression of proteins involved in cell growth optimization (*18*).

The mechanisms of production that result in DOC compounds that persist from months to millennia are not well described, but both abiotic and biotic processes have been shown to transform DOM to molecular forms that resist rapid microbial degradation. Abiotic processes include adsorption of labile DOC to colloidal material (*19, 20*), modification of chemical bond structure by ultraviolet light exposure (*19–21*), and the formation of compounds like melanoidins via condensation reactions (*22*). Biotic sources of resistant DOM may include direct exudation from phytoplankton [for example, as acylheteropolysaccharides (*14*),

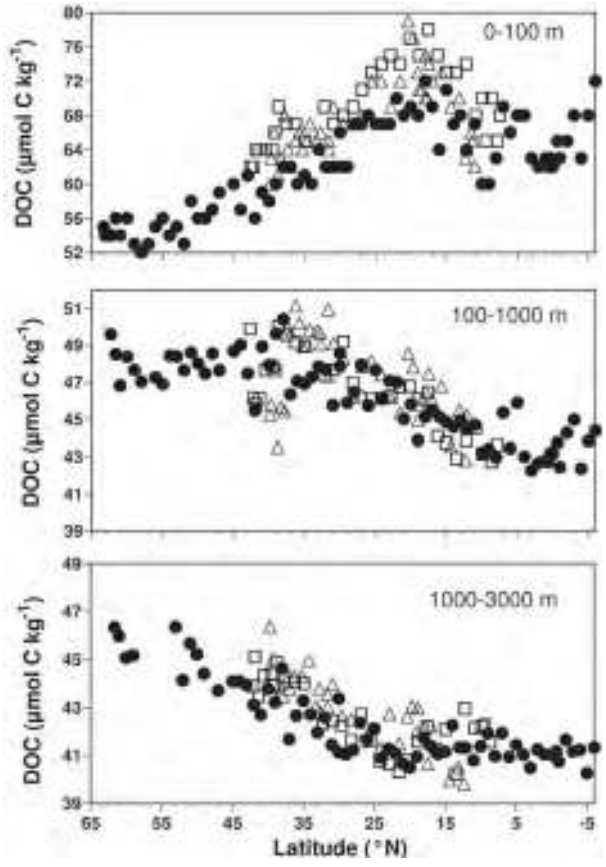

Fig. 1. Meridional distributions of mean dissolved organic carbon (DOC) concentrations for (**A**) the euphotic zone (0 to 100 m), (**B**) the mesopelagic zone (100 to 1000 m), and (**C**) the bathypelagic zone (1000 to 3000 m) within the North Atlantic Basin. Surface waters elevated in DOC at low latitudes are transported to the north with surface circulation. The surface concentrations decrease with overturning circulation, thereby increasing concentrations at depth in the north. Over time, with flow of those deep waters to the south, the exported DOC concentrations decline. Mean DOC concentrations were determined by integrating DOC stocks within each depth horizon for each hydrostation and normalizing to the depth of each depth horizon. Filled circles, open triangles, and open squares are DOC values from the Climate Variability and Predictability (CLIVAR) program's transect lines A16, A22, and A20, respectively. Note scales of the y-axes change between panels. Adapted from (*37*).

[1]Dept. Ecology, Evolution, and Marine Biology, University of California, Santa Barbara, CA 93106-9610, USA
[2]Rosenstiel School of Marine and Atmospheric Science, University of Miami, Miami, FL 33149, USA
[3]Université de la Méditerranée, LMGEM, Centre d'Océanologie de Marseille, Case 901, 13288 Marseille Cedex 9, France
[4]CNRS/INSU, UMR 6117, LMGEM, Case 901, 13288 Marseille Cedex 9, France
*To whom correspondence should be addressed. E-mail: carlson@lifesci.ucsb.edu

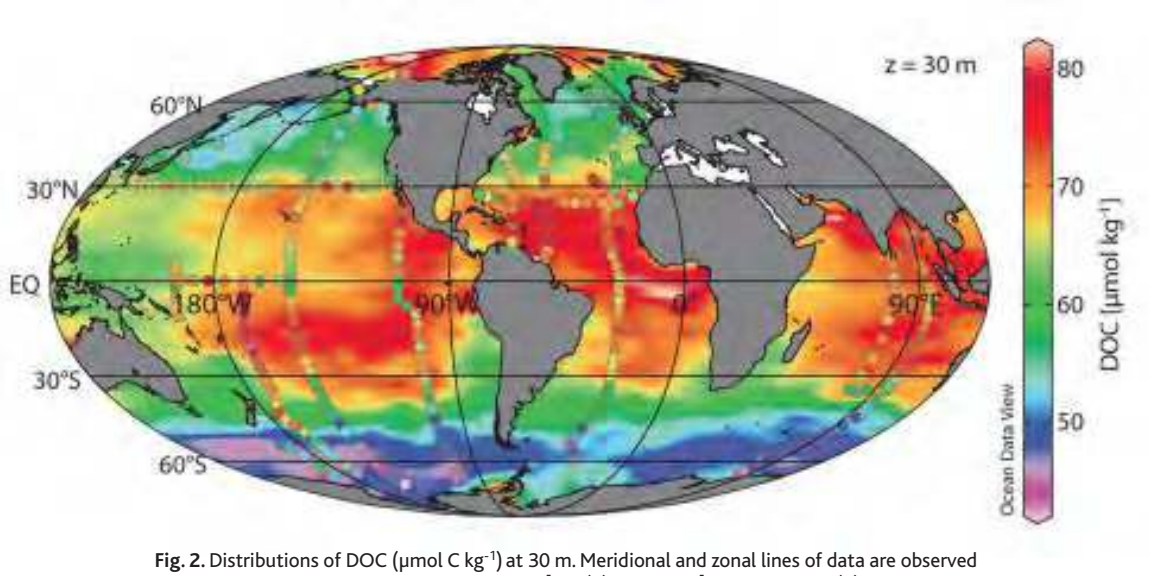

Fig. 2. Distributions of DOC (µmol C kg^{-1}) at 30 m. Meridional and zonal lines of data are observed values, while the background field is modeled [see (*1*) for details]. Adapted from (*1*).

bacterially derived cell wall material (*23–26*), liposome-like colloids produced via microzooplankton grazing (*27*), and the release of metabolites (*28*)]. The preferential removal of specific sugars and amino acids can also transform DOM to recalcitrance (*29–32*).

The production of refractory DOM compounds via heterotrophic microbial processes has been termed the microbial carbon pump (MCP) (*33*). In this conceptual model, a fraction of the bioavailable organic compounds processed by heterotrophic microbes is shunted to a biologically refractory form of organic matter. Experiments with marine microbes have shown that a portion of model biolabile organic compounds are transformed to products that persist for periods of months to years (*34, 35*). Other studies have identified bacterial biomarkers (D-enantiomer amino acids) in the high molecular weight fraction of oceanic DOM, lending support to the hypothesis that some portion of the refractory DOM pool is of heterotrophic prokaryotic origin (*24, 25*). It is estimated that approximately 23% of the bulk oceanic DOC pool (~155 PgC) (*36*) is derived via the MCP.

The accumulation of DOC is most pronounced in surface waters of the well-stratified subtropical gyres, reaching concentrations >80 µmol C kg^{-1} (*1, 37*) (Fig. 2). This accumulation is unambiguous evidence for its resistance to decay. However, DOM that is persistent at one geographical location or depth horizon can be bioavailable at another. For example, of the 1.8 PgC of DOM exported from the euphotic zone, only ~0.2 PgC survives to depths greater than 500 m (*1*). Some mesopelagic bacterial lineages undergo productivity pulses during or shortly following water column overturn events, presumably due to the delivery of surface-derived DOM (*17, 38, 39*) (Fig. 3). The remineralization of exported DOC accounts for up to half the oxygen utilized in the

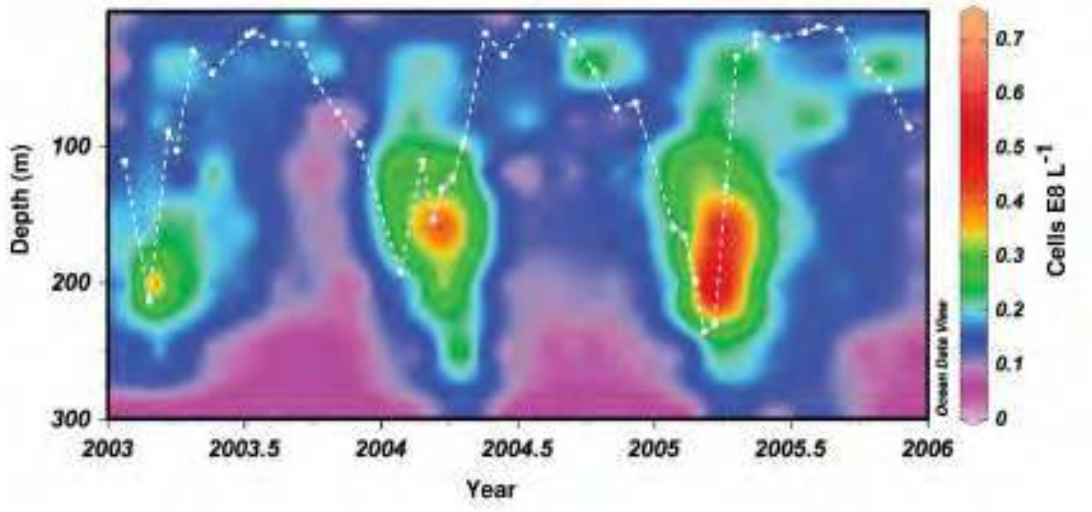

Fig. 3. Contours of plot of SAR11 subclade II cell densities (E8 L^{-1}) in the surface 300 m from 2003 through 2005 at the Bermuda Atlantic Time-series Study site. The white dashed line represents, mixed layer depth and is used to examine distribution patterns in the context of mixing and stratification. The data reported in this figure demonstrate a response of mesopelagic subclade of the bacterioplankton SAR11 during or shortly following deep convective overturn. This response is presumed in part to result from the delivery of surface derived organic matter (i.e., DOC flux) into the mesopelagic during mixing. A portion of the DOC that persisted in the surface waters appears to become available to the organisms in the mespelagic zone triggering biomass production. Adapted from (*39*).

mesopelagic zone (*7, 40, 41*). At >1000 m, DOC removal occurs at much slower rates, accounting for < 20% of oxygen consumption (*37, 42*).

The response of deep microbial lineages to exported DOC indicates that microbial processes in the ocean's interior are capable of metabolizing some of these persistent polymeric compounds. Microbial diversity in oceanic systems is high, although there remains uncertainty with regard to how much of this diversity is functionally significant (*16, 43, 44*). Vertical partitioning of major prokaryotic groups, particularly between the euphotic and aphotic regions of the oceanic water column, is well documented (*16, 17, 38, 39, 45, 46*) and presumably linked to gradients in the character and quantity of DOM as well as to the availability of inorganic nutrients. Genomic and transcriptomic data demonstrate the potential for marine bacterioplankton to utilize a range of DOM targets (*28, 47–49*). DeLong *et al.* (2006) identified a greater number of genes, putatively involved in polysaccharide degradation, in deep microbial populations compared to those found in the surface populations (*16*). The genes associated with the deep microbial assemblages are better suggestive of a surface-attached lifestyle capable of degrading recalcitrant pools of organic matter (*16, 28).*

Specific groups of heterotrophic prokaryotes have been shown to respond differently to the quality and quantity of organic substrates (*38, 49–54*). Thus, organic compounds resistant to microbial degradation at one depth horizon may serve as substrates for deeper population of heterotrophic microbes. For example, D-enantiomeric amino acids derived from the peptidoglycan of bacterioplankton cell walls have been observed to persist within the DOM pool (*24, 25*). However, there is a significant increase in the uptake ratio of D-aspartic acid by microbes in the meso- and bathypelagic realms of the North Atlantic (*55, 56*), indicating that deep microbes more readily utilize D-amino acids. These deep-sea piezophilic microorganisms display metabolic capabilities that allow them to thrive under cold and high-pressure conditions (*57*). Some piezophiles are capable of degrading complex organic matter (*58*) by modifying their gene structure and protein regulation (*59*). For example, in *Photobacterium profundum* SS9 the metabolic pathways used to degrade polymers such as chitin, pullulan, and cellulose are controlled by pressure: upregulation of proteins occurs above 28 MPa and downregulation below 0.1 MPa. Cell-specific ectoenzymatic activities are greater in deep waters compared to the surface (*60–64*), providing additional evidence that deep-sea microorganisms are adapted to degrade more refractory pools of organic matter (*65*), under in situ pressure and temperature (*61, 63*).

The production of refractory DOM can be important in ocean carbon sequestration. First, DOM that persists in the surface ocean long enough for its eventual mixing to greater ocean depths represents a carbon-rich export term, contributing to 20% of the biological carbon pump (*1, 6, 7, 66*). Second, a fraction of this exported DOM can persist for centuries to millennia, thus the carbon remains stored in an organic form and unavailable for exchange with the atmosphere as CO_2. The degree to which the MCP shunts carbon to long-term storage as organic matter, versus brief storage associated with export and rapid, deep remineralization, is unknown. Resolving these fates and identifying causative mechanisms and controls of the MCP remain important challenges.

References and Notes

1. D. A. Hansell, C. A. Carlson, D. J. Repeta, R. Shlitzer, *Oceanogr.* **22**, 202 (2009).
2. D. Kirchman, *Limnol. Oceanogr.* **28**, 858 (1983).
3. C. A. Carlson, in *Biogeochemistry of Marine Dissolved Organic Matter,* D. A. Hansell, C. A. Carlson, Eds. (Academic Press, San Diego, 2002), pp. 911–151.
4. T. Nagata, in *Microbial Ecology of the Oceans,* D. L. Kirchman, Ed. (Wiley-Liss, New York, 2000), pp. 121–152.
5. F. Azam, D. C. Smith, Å. Hagström, *Microb. Ecol.* **28**, 167 (1993).
6. G. Copin-Montégut, B. Avril, *Deep Sea Res.* **40**, 1963 (1993).
7. C. A. Carlson, H. W. Ducklow, A. F. Michaels, *Nature* **371**, 405 (1994).
8. M. Canals *et al*., *Nature* **444**, 354 (2006).
9. J. Martín, J. C. Miguel, A. Khripounoff, *Geophys. Res. Lett.* **37**, 13604 (2010).
10. D. Smith, M. Simon, A. L. Alldredge, F. Azam, *Nature* **359**, 139 (1992).
11. D.K. Steinberg *et al.*, *Deep Sea Res. I* **47**, 137 (2000).
12. J. B. Cotner, J. W. Ammerman, E. R. Peele, E. Bentzen, *Aquat. Microb. Ecol.* **13**, 141 (1997).
13. T. F. Thingstad, A. Hagstrom, F. Rassoulzadegan, *Limnol. Oceanogr.* **42**, 398 (1997).
14. L. I. Aluwihare, D. J. Repeta, R. F. Chen, *Nature* **387**, 166 (1997).
15. R. H. Benner, in *Biogeochemistry of Marine Dissolved Organic Matter,* D. A. Hansell, C. A. Carlson, Eds. (Academic Press, San Diego, 2002), pp. 59–90.
16. E. F. DeLong *et al.*, *Science* **311**, 496 (2006).
17. A. H. Treusch *et al*., *ISME J.* **3**, 1148 (2009).
18. S. M. Sowell *et al., ISME J.* **3**, 931–105 (2008).
19. R. G. Keil, D. L. Kirchman, *Mar. Chem.* **45**, 187 (1994).
20. T. Naganuma *et al., Mar. Ecol. Prog. Ser.* **135**, 309 (1996).
21. R. Benner, B. Biddanda, *Limnol. Oceanogr.* **43**, 1373 (1998).
22. L. C. Maillard, *Compt. Rend.* **154**, 66 (1912).
23. E. Tanoue, S. Nishiyama, M. Kamo, A. Tsugita, *Geochim. Cosmochim. Acta* **59**, 2643 (1995).
24. M. D. McCarthy, J. I. Hedges, R. Benner, *Science* **281**, 231 (1998).
25. R. Benner, K. Kaiser, *Limnol. Oceanogr.* **48**, 118 (2003).
26. K. Kaiser, R. Benner, *Limnol. Oceanogr.* **53**, 1192 (2008).
27. T. Nagata, D. L. Kirchman, *Arch. Hydrobiol.* **35**, 99 (1992).
28. E. B. Kujawinski, *Annu. Rev. Mar. Sci.* **3**, 567 (2011).
29. G. L. Cowie, J. I. Hedges, *Nature* **369**, 304 (1994).
30. R. M. W. Amon, R. Benner, *Limnol. Oceanogr.* **41**, 41 (1996).
31. A. Skoog, R. Benner, *Limnol. Oceanogr.* **42**, 1803 (1997).
32. S. J. Goldberg, C. A. Carlson, D. A. Hansell, N. B. Nelson, D. A. Siegel, *Deep Sea Res. I* **56**, 672 (2009).
33. N. Jiao, *et al*., *Nat. Rev. Microbiol.* **8**, 593 (2010).
34. H. Ogawa, Y. Amagai, I. Koike, K. Kaiser, R. Benner, *Science* **292**, 917 (2001).
35. C. Lønborg, X. A. Álvarez-Salgado, K. Davidson, A. Miller, *Est. Coast. Shelf Sci.* **82**, 682 (2009).
36. R. Benner, G. Herndl, *Molecular Carbon Pump in the Ocean,* N. Jiao, F. Azam, S. Sanders, Eds. *(Science*/AAAS, Washington DC, 2011*),* pp. 46–48.
37. C. A. Carlson *et al*., *Deep Sea Res. II* **57**, 1433 (2010).
38. R. M. Morris *et al*., *Limnol. Oceanogr.* **50**, 1687 (2005).
39. C. A. Carlson *et al*., *ISME J.* **3**, 283 (2009).
40. M. D. Doval, D. A. Hansell, *Mar. Chem.* **68**, 249 (2000).
41. D. A. Hansell, in *Biogeochemistry of Marine Dissolved Organic Matter,* D. A. Hansell, C. A. Carlson, Eds. (Academic Press, San Diego, 2002), pp. 685–716.
42. J. Arístequi, S. Agusti, J. J. Middelburg, C. M. Duarte, in *Respiration in Aquatic Systems,* P. del Giorgio, P. J. L. Williams, Eds. (Oxford Press, Oxford, 2005), pp. 181–205.
43. M. S. Rappé, S. J. Giovannoni, *Annu. Rev. Microbiol.* **57**, 369 (2003).
44. J. C. Venter, *et al.*, *Science* **304**, 66 (2004).
45. S. J. Giovannoni, M. S. Rappé, K. Vergin, N. Adair, *Proc. Natl. Acad. Sci. U.S.A.* **93**, 7979 (1996).
46. K. G. Field *et al., Appl. Environ. Microbiol.* **63**, 63 (1997).
47. S. J. Giovannoni *et al., Science* **309**, 1242 (2005).
48. R. S. Poretsky, S. Sun, X. Mou, M. A. Moran, *Environ. Microbiol.* **12**, 616 (2010).
49. J. McCarren *et al*., *Proc. Natl. Acad. Sci. U.S.A.* **107**, 16420 (2010).
50. M. T. Cottrell, D. L. Kirchman, *Appl. Environ. Microbiol.* **66**, 1692 (2000).
51. C. A. Carlson *et al*., *Limnol. Oceanogr.* **49**, 1073 (2004).
52. C. Arnosti, S. Durkin, W. H. Jeffrey, *Aquat. Microb. Ecol.* **38**, 135 (2005).
53. R. R. Malmstrom, M. T. Cottrell, H. Elifantz, D. L. Kirchman, *Appl. Environ. Microbiol.* **71**, 2979 (2005).
54. A. D. Steen, K. Ziervogel, C. Arnosti, *Org. Geochem.* **41**, 1019 (2010).
55. M. T. Pérez, C. Pausz, G. J. Herndl, *Limnol. Oceanogr.* **48**, 755 (2003).
56. E. Teira, H. van Aken, C. Veth, G. J. Herndl, *Limnol. Oceanogr.* **51**, 60 (2006).
57. C. Tamburini, J. Garcin, A. Bianchi, *Aquat. Microb. Ecol.* **32**, 209 (2003).
58. A. Vezzi S. *et al*., *Science* **307**, 1459 (2005).
59. F. Lauro, D. Bartlett, *Extremophiles* **12**, 15 (2007).
60. H. G. Hoppe, S. Ullrich, *Aquat. Microb. Ecol.* **19**, 139 (1999).
61. C. Tamburini, J. Garcin, M. Ragot, A. Bianchi, *Deep Sea Res. II* **49**, 2109 (2002).
62. R. Zaccone *et al*., *J. Geophys. Res.* **108**, 8117 (2003).
63. C. Tamburini *et al., Deep Sea Res. II* **56**, 700 (2009).
64. F. Baltar, J. Arístegui, J. M. Gasol, G. J. Herndl, *Aquat. Microb. Ecol.* **60**, 227 (2010).
65. H. G. Hoppe, C. Arnosti, G. J. Herndl, in *Enzymes in the Environment: Activity, Ecology and Applications,* R. G. Burns, R. P. Dick, Eds. (Marcel Dekker, New York, 2002), pp. 73–108.
66. C. S. Hopkinson, J. J. Vallino, *Nature* **433**, 142 (2005).

67. This work was supported by Scientific Committee on Oceanic Research (WG134) and NSF (OCE) 0801991, 0850857 to CAC; 0752972 to DAH and CAC; and ANR-POTES, ANR-05-BLAN-0161-01 to CT.

Molecular Characterization of Dissolved Organic Matter and Constraints for Prokaryotic Utilization

Gerhard Kattner[1*], Meinhard Simon[2], Boris P. Koch[1,3]

The chemical structures of marine dissolved organic matter (DOM) are largely unknown. However, ultrahigh resolution mass spectrometry recently allowed the identification of thousands of different molecular formulas and revealed that DOM is composed of a huge number of relatively small molecules (200 to 800 Da). Despite this success in dissecting marine DOM molecules, it remains unclear how biomolecules are transformed into refractory DOM and how the microbial carbon pump (MCP) contributes to this process. Besides a potential general resistance of DOM to prokaryotic attack, the low concentration of individual DOM constituents in the deep ocean may prevent energy-efficient microbial DOM consumption, even though bacteria have the genetic repertoire to exploit a high variety of molecular DOM structures. Further improvements in analytical and genomic technologies that will aid in the elucidation of DOM molecule structure, source, and degradation pathways should reveal the role refractory DOM and the MCP play in the global carbon cycle.

Most of the dissolved organic matter (DOM) produced in surface waters, such as labile proteins, carbohydrates, and lipids, is mineralized by microbial activity, and the remaining material is transformed into semilabile DOM and finally refractory DOM (*1*), a process in which the microbial carbon pump (MCP) plays an important role (*2*). The molecular composition of labile DOM is modified rapidly during decay, creating a material for which chemical structures are largely unknown and currently indeterminable. The decay process results in a large variety of compounds with completely new chemical structures, which exist in predominantly dissolved, but also particulate, forms. These transformations are mediated by microbial, viral, and photochemical activity, and proceed continuously over periods from days to months and beyond to decades and hundreds of years. Dissolved organic carbon (DOC) in the deep ocean therefore has an average age of 4,000 to 6,000 years (*3*).

A puzzling and still unanswered question is why this DOM resists biotic and abiotic decomposition and why it is unavailable to heterotrophic prokaryotes. Without knowing the molecular structures it is impossible to successfully tackle this question. However, it is also important to examine whether the prokaryotes in the ocean, and in particular in the dark ocean where the refractory DOM accumulates, have the genetic repertoire and appropriate conditions to express the suitable genes encoding enzymes that can cleave and decompose the DOM molecular structures. Appropriate metagenomic and metatranscriptomic methods are now available to do this (*4, 5, 6*). In contrast, tools for the structural characterization of DOM in the ocean are limited by a number of factors: (i) Analyses thus far have essentially been restricted to carbohydrates, amino acids, aminosugars, and lipids (*7*), compounds that represent only 10 to 20% of DOM in the near-surface and even less in the deep ocean; (ii) Because only a minor portion of these molecules exist as monomers, they are usually analyzed only after considerable chemical treatment (for example, hydrolysis) and thus the chemical structures in which they were originally embedded remain unknown; (iii) Data are often obtained following isolation and fractionation of DOM using, for example, solid-phase extraction and ultrafiltration, but resulting fractions represent only a small portion of total DOM (~25% for ultrafiltration and ~40% for solid-phase extraction).

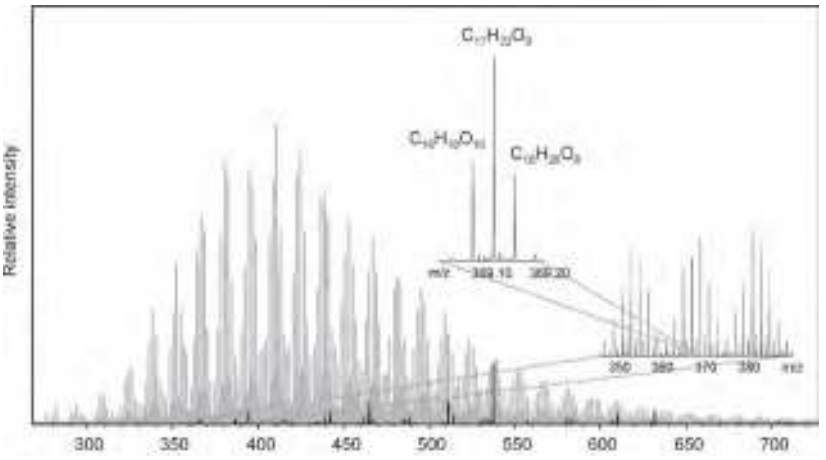

Fig. 1. Different mass arrays of an ultrahigh resolution FT-ICR mass spectrum (electrospray ionization, negative mode) of a marine dissolved organic matter (DOM) sample that was extracted using a solid-phase process [sorbent PPL (*17*)]. From the exact masses, molecular formulas can be calculated for thousands of peaks in each sample.

Successful molecular characterization of DOM using ultrahigh resolution mass spectrometry (Fourier transform ion cyclotron resonance mass spectrometry; FT-ICR MS) represents a significant advance in the field, and progress has also been made applying collision induced dissociation FT-ICR MS (*8*). To date several thousand molecular formulas have been identified (Fig. 1) and a number of these may act as potential markers of DOM sources and modification processes. The occurrence of pseudohomologous series (addition/removal of CH_2, H_2, O_2, or H_2O to/from a given molecular formula) shows that there are regular patterns within the strong complexity of the molecular formulas of DOM (Fig. 2). Approximately one third of the detectable formulas are present in all marine samples and most likely represent a common refractory background in DOM (*9*).

The Problem: Why Microbes Cannot Decompose Refractory Deep-sea DOM

It has been previously argued that concentrations of individual DOM

[1]Alfred Wegener Institute for Polar and Marine Research, Ecological Chemistry, Am Handelshafen 12, D-27570 Bremerhaven, Germany
[2]Institute for Chemistry and Biology of the Marine Environment, University of Oldenburg, Carl-von-Ossietzky-Str. 9-11, D-26111 Oldenburg, Germany
[3]University of Applied Sciences, An der Karlstadt 8, D-27568 Bremerhaven, Germany
*To whom correspondence should be addressed. E-mail: gerhard.kattner@awi.de

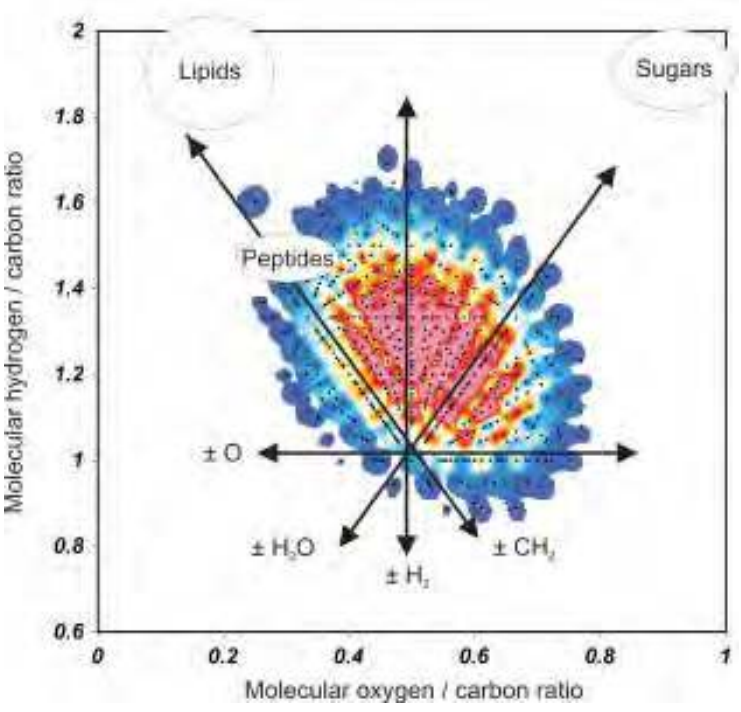

Fig. 2. FT-ICR mass spectrum (electrospray ionization, negative mode) of a solid-phase extracted [sorbent PPL (*17*)] marine deep-sea dissolved organic matter (DOM) sample. Common molecular formulas in marine DOM contain carbon, hydrogen, and oxygen. Each formula in the plot is represented by its molecular element ratio (hydrogen/carbon versus oxygen/carbon) and its relative peak magnitude [color scale, from higher (violet, center) to lower (blue, edge) intensities]. Pseudohomologous series of sequential addition or loss of molecular fragments (along the arrows) point to regularities in the molecular composition of DOM. Average element ratios of lipids, carbohydrates, and peptides (similar ratios for proteins) do not overlap with the element ratios of DOM molecules.

compounds might be far below the chemoreceptive threshold for prokaryotes thus preventing the energy-efficient uptake of DOM (*10*). This notion could explain the slow DOM degradation and its seemingly recalcitrant behavior. Prokaryotes can exploit substrates only above a certain concentration, and their uptake systems have been shown to drive concentrations below this threshold (*11*). High-affinity uptake systems have a substrate affinity constant (K_s) value in the nanomolar range (*12, 13*) but considerations based on FT-ICR MS analyses of DOM imply that concentrations of individual DOM compounds in the deep sea are likely far below this range. An early attempt to induce prokaryotic decomposition of deep-sea DOM by raising the ambient DOM concentration fivefold did not yield any microbial DOM decomposition (*14*) presumably because concentrations of individual compounds were still below this threshold concentration.

The intrinsic stability of chemical structures of deep-sea DOM compounds may further explain their recalcitrance to microbial degradation. The low proportion of hydrogen (average hydrogen to carbon ratio is ~1.25; Fig. 2) reflects a substantial proportion of stable aromatic backbones, structures known to be difficult for prokaryotes to degrade. However, there is very little mechanistic evidence for a principal molecular resistance to bacterial enzymatic attack. Most molecules are highly oxygenated (oxygen to carbon ratio of ~0.45; Fig. 2), which implies that they are not stable, per se, and should be susceptible to utilization by prokaryotes. This high oxygen content, which primarily exists in carboxylic functions [refractory carboxyl-rich alicyclic molecules (*15*)], reflects a high degree of polarity and may therefore require a highly specific and energy-efficient uptake system. Recent studies of the genetic potential of deep-sea prokaryotes revealed that bacteria are capable of taking up and degrading a great variety of DOM compounds including 2,4-dichlorobenzoate, which requires the cleavage of the aromatic ring (*4*). These observations are in line with the assumption that the various DOM compounds are biodegradable by prokaryotes. However, the energetic yield of degrading these highly oxygenated compounds might not be profitable enough to gain metabolic energy for growth and may require complementary consumption of other compounds with a higher energetic yield.

To obtain more detailed information on the composition of DOM, it is necessary to fractionate it into smaller units with similar characteristics. Attempts to do so have already been made using polarity or size criteria, revealing several different mass formulas found exclusively in individual fractions (*16*). Further improvements in fractionating individual molecules using FT-ICR MS will likely be available in the near future and improvements in NMR techniques, for which increasingly little material is necessary to obtain structural information, also seem probable.

It may be some time before unequivocal chemical structures of DOM are identified. This knowledge is crucial to enable the further investigation of the microbial- and photochemical-based degradation and transformation of DOM and to better understand the cycling of DOM in the global ocean.

References and Notes

1. H. Ogawa, Y. Amagai, I. Koike, K. Kaiser, R. Benner, *Science* **292**, 917 (2001).
2. N. Jiao, *et al., Nat. Rev. Microbiol.* **8**, 593 (2010).
3. P. M. Williams, E. R. M. Druffel, *Nature* **330**, 246 (1987).
4. E. F. DeLong, *et al., Science* **311**, 496 (2006).
5. X. Mou, S. Sun, R. A. Edwards, R. E. Hodson, M. A. Moran, *Nature* **451**, 708 (2008).
6. J. McCarren, *et al., Proc. Natl. Acad. Sci. U.S.A.* **107**, 16420 (2010).
7. R. Benner, in *Biogeochemistry of Marine Dissolved Organic Matter,* D. A. Hansell, C. A. Carlson, Eds. (Academic Press, San Diego, 2002), pp. 59–90.
8. M. Witt, J. Fuchser, B. P. Koch, *Anal. Chem.* **81**, 2688 (2009).
9. B. P. Koch, M. Witt, R. Engbrodt, T. Dittmar, G. Kattner, *Geochim. Cosmochim. Acta* **69**, 3299 (2005).
10. H. W. Jannasch, in *Direct Ocean Disposal of Carbon Dioxide*, N. Handa, T. Ohsumi, Eds. (Terra Scientific Publishing Company, Tokyo, 1995), pp. 1–11.
11. K. Komarova-Komar, T. Egli, *Micobiol. Molecul. Biol. Rev.* **62**, 646 (1998).
12. J. W. Ammerman, F. Azam, *Science* **227**, 1338 (1985).
13. W. Martens-Habbena, P. M. Berube, H. Urakawa, J. R. de la Torre, D. A. Stahl, *Nature* **461**, 976 (2009).
14. R. T. Barber, *Nature* **220**, 274 (1968).
15. N. Hertkorn, *et al., Geochim. Cosmochim. Acta* **70**, 2990 (2006).
16. B. P. Koch, K.-U. Ludwichowski, G. Kattner, T. Dittmar, M. Witt, *Mar. Chem.* **111**, 233 (2008).
17. T. Dittmar, B. Koch, N. Hertkorn, G. Kattner, *Limnol. Oceanogr.: Methods* **6**, 230 (2008).

18. We are grateful to R. Benner, C. Stedmon and S. Sanders for constructive comments and suggestions. This work was supported by the Scientific Committee on Oceanic Research (WG134) and Deutsche Forschungsgemeinschaft (TRR 51, to MS).

Shedding Light on a Black Box: UV-Visible Spectroscopic Characterization of Marine Dissolved Organic Matter

Colin A. Stedmon[1]* and Xosé Antón Álvarez-Salgado[2]

The processes that drive the microbial carbon pump (MCP) in the ocean have yet to be fully characterized. Among the topics that are central to addressing this deficit are tracing the microbial production of refractory dissolved organic matter (DOM) by the MCP, and resolving how the chemical composition and structure of DOM changes as a result. A fraction of DOM absorbs ultraviolet (UV) and visible light, while a specific subset of this subsequently exhibits a natural fluorescence. These spectroscopic properties can be used as markers for the turnover of different DOM fractions in the ocean. Recent research has linked the UV-visible characteristics of DOM to its chemical structure, carbon content, and photochemical and microbial reactivity. In addition, widespread measurements of DOM optical properties in the ocean indicate that they can be used to trace the humification processes that lead to the production of part of the refractory DOM pool. These measurements are suited to being carried out using in situ or remote platforms in the ocean and can provide high-resolution temporal and spatial DOM data. In conjunction with other techniques, this will pave the way for new insights into the possible role of the MCP in the global carbon cycle.

The light absorbing and fluorescent fractions of dissolved organic matter (DOM) are referred to as colored or chromophoric DOM (CDOM) and fluorescent DOM (FDOM) (Fig. 1A). For several decades, absorption and fluorescence properties of DOM have been used to follow the spatial and temporal distribution of the bulk DOM, tracing specific humic- and protein-like fluorophores (*1*) and characterizing the aromaticity and relative molecular weight of DOM through optical indices derived from their spectra (*2–4*). Current research in the field is a convergence of four main interests: (i) tracing water mass mixing in estuarine, coastal and continental shelf waters; (ii) quantifying underwater ultraviolet and visible light penetration; (iii) resolving remote sensing of ocean color; and (iv) studying the impact of microbial and photochemical processes on the chemical structure of DOM. The major advantage of using the UV and visible spectroscopic properties of DOM is that it requires very small sample volumes and minimal preparation before analysis. Moreover, the high sensitivity of the current spectrofluorometers allows estimation of the turnover of specific DOM subfractions during both short- and long-term incubation experiments designed to test the susceptibility of DOM to photochemical and/or microbial degradation (*3, 5, 6*). The major pitfall of this approach is that the actual compounds and processes responsible for the measured absorption and fluorescence remain poorly characterized. Resolving this presents a considerable analytical and experimental research challenge, which can in part be addressed by coupling of absorption and fluorescence measurements to molecular level characterization using mass spectrometry. In spite of this limitation, CDOM and FDOM measurements are currently being used as markers of different DOM fractions and to shed light on DOM production, turnover, and fate in the ocean and how this might impact the role of the microbial carbon pump (MCP) in the ocean carbon cycle (*7*) (Fig. 1B).

In surface waters, autotrophic and heterotrophic activity and photochemical degradation largely control the molecular characteristics and distribution of DOM (for now putting aside the effects of the mixing of waters of different origins). This is reflected in FDOM and CDOM profiles (Fig. 2) that show sharp changes in concentration and character depending on the balance of dominating processes (biological production, and combined photochemical and microbial transformation and removal). At the ocean surface, ultraviolet light penetrates and acts to either directly decompose to colorless the organic compounds, CO, and CO_2, or to alter the remaining DOM, influencing its chemical composition and availability to microbes (*8–10*). This is evident from ocean profiles of CDOM and FDOM (*11, 12*), but is often not as clear when using other bulk DOM measurements such as dissolved organic carbon (DOC). The effects of photodegradation diminish rapidly with increasing depth as the high-energy wavelengths are attenuated. Away from the immediate surface, photic and aphotic microbial processing dominate, with subsurface maxima in absorption and protein-like fluorescence of CDOM often found in association with the productive plankton biomass (Fig. 2).

In the dark ocean, DOM is continually modified by microbes and the effect of the MCP on DOM optical characteristics becomes more apparent. Entrainment of DOM produced in the photic zone through seasonal vertical mixing (*13*) and the constant supply of organic matter from sinking particles (*14*) drives much of this activity, although the latter most likely dominates. The net result is an increase in the humic character of CDOM and FDOM, measured as a relative increase in longer wavelength absorption and humic-like fluorescence signals (Fig. 2). Although not entirely the same, this parallels the humification process that occurs in soils (Fig. 1B), but with alternate precursor material. The increases observed in CDOM and FDOM in the meso- and bathypelagic ocean are correlated to apparent oxygen utilization (AOU) and nutrient remineralization (*11, 12, 15–18*). These trends reveal the MCP in action, representing the gradual accumulation of a persistent DOM fraction that is directly linked to heterotrophic activity, with the humic CDOM/FDOM essentially representing biologically refractory metabolites. Data supporting this trend have recently been collected in all the major oceans (*12, 16, 18*). High-resolution measurements using in situ instruments are revealing that the techniques are sensitive enough to indicate differences in the ratio of humic fluorescence production to AOU for individual intermediate and bottom water masses. Additionally, detailed spectral characterization has shown that this humic fluorescence signal is actually composed of two independent fractions, which accumulate at different rates in the deep ocean.

Armed with expanding global datasets and with the dark ocean as an incubator, the research community is gradually resolving the UV-visible spectroscopic signature of refractory DOM produced by the MCP. The combination of long ocean-mixing time scales, the absence of photochemistry, and the limited input of labile DOM makes the dark ocean an ideal environment for further studies in this area.

[1]Department of Marine Ecology, National Environmental Research Institute, Aarhus University, Roskilde, Denmark
[2]IIM-CSIC, Instituto de Investigaciones Marinas, Consejo Superior de Investigaciones Científicas, Vigo, Spain
*To whom correspondence should be addressed. E-mail: cst@dmu.dk

Additional widespread sampling, experimentation, and methodological refinements linking UV-visible spectroscopic character of DOM to molecular level characterization (*19*) and carbon content (*20*) stand to pave the way for enhancing the utility of these optical measurements. In conjunction with the technological advances in optical instrumentation, this will lead to the development of improved in situ instruments measuring fluorescence or absorption at specific wavelengths or spectral bands with high spatial and temporal resolution, and designed to be routinely deployed on moorings, gliders, and profiling instrumentation.

Fig 1. (**A**) Colored and fluorescent DOM (CDOM and FDOM, respectively) together represent a subfraction of the total DOM pool. Part of DOM does not absorb UV and visible light and is largely characterized as monomeric and polymeric aliphatic compounds such as carbohydrates, lipids, and aliphatic amino acids. The presence of conjugated double bonds (polyenes) results in absorption of UV and visible light. The presence of aromatic rings often also results in fluorescence. The large arrow indicates increasing aromaticity, conjugation, and carbon to hydrogen (C/H) ratio. Examples of CDOM absorption spectra and excitation-emission matrices are shown over the CDOM and FDOM domains, respectively. Structure of tryptophan, a natural amino acid, and vanillin, a constituent of lignin, are shown as examples of fluorescent CDOM. The grey lines indicate the position of their respective fluorescence excitation-emission peaks. (**B**) Soils of the sea: The processing of organic matter (particulate and dissolved, colored and colorless) by the microbial carbon pump (MCP) (*7*) not only results in formation of refractory DOM (RDOM) but also an alteration of the remaining organic matter, often referred to as humification and in principle similar to what occurs in soils. During processing by the MCP, colorless or weakly colored bioavailable DOM (BDOM) and particulate organic material (POM) is transformed into colored refractory CDOM. The large arrow indicates that during this process both the carbon-specific absorption and apparent fluorescence quantum yield increase.

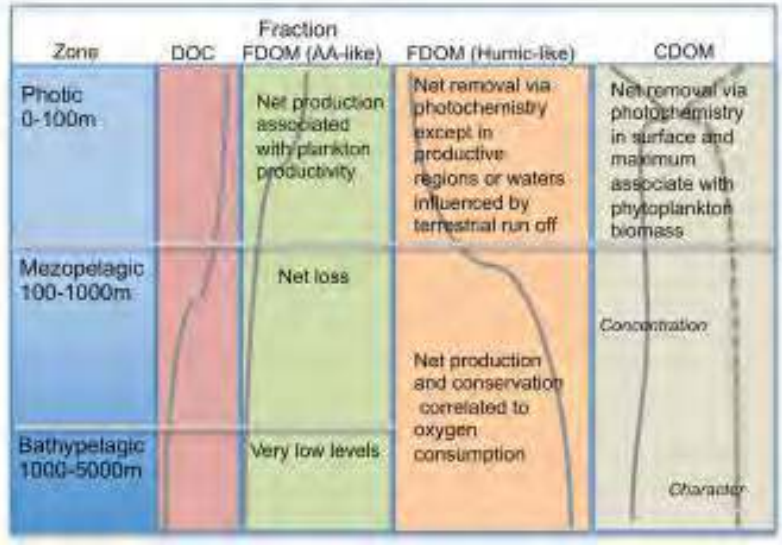

Fig 2. Generalized vertical distribution of the quantity and quality of DOM in the ocean. Idealized vertical profiles of dissolved organic carbon (DOC) concentration, fluorescence intensity of amino acids (FDOM AA-like), and humic organic matter (Humic-like), and the concentration (solid line) and character (dotted line) of colored dissolved organic matter (CDOM). CDOM character is depicted as the slope of the absorption spectrum in the UV-visible wave-length range.

References and Notes

1. P. G. Coble, *Chem. Rev.* **107**, 402 (2007).
2. J. L. Weishaar, *et al.*, *Environ. Sci. Technol.*, **37**, 4702 (2003).
3. J. Helms, *et al*., *Limnol. Oceanogr.* **53**, 955 (2008).
4. S. A. Green, N. V. Blough, *Limnol. Oceanogr.* **39**, 1903 (1994).
5. C. A. Stedmon, S.S. Markager, *Limnol. Oceanogr.* **50**, 1415 (2005).
6. M. Nieto-Cid, X. A. Álvarez-Salgado, F. F. Perez, *Limnol. Oceanogr.* **51**, 1391 (2006).
7. N. Jiao, *et al.*, *Nat. Rev. Microbiol.* **8**, 593 (2010).
8. R. J. Kieber, L. H. Hydro, P. J. Seaton, *Limnol. Oceanogr.* **42**, 1454 (1997).
9. M. A. Moran, R. G. Zepp, *Limnol. Oceanogr.* **42**, 1307 (1997).
10. R. Benner, B. Biddanda, *Limnol. Oceanogr.* **43**, 1373 (1998).
11. K. Hayase, N. Shinozuka, *Mar. Chem.* **48**, 283 (1995).
12. N. B. Nelson, D. A. Siegel, C. A. Carlson, C. M. Swan, *Geophy. Res. Lett.* **37,** L03610 (2010).
13. D. A. Hansell, C. A. Carlson, D. J. Repeta, R. Schlitzer, *Oceanography* **22**, 52 (2009).
14. J. Arístegui, J. M. Gasol, C. M. Duarte, G. J. Herndl, *Limnol. Oceanogr.* **54,** 1501 (2009).
15. R. F. Chen, J. L. Bada, *Mar. Chem.* **37**, 191 (1992).
16. Y. Yamashita, E. Tanoue, *Nat. Geo.* doi:10.1038/ngeo279 (2008).
17. Y. Yamashita, A. Tsukasaki, T. Nishida, E. Tanoue, *Mar. Chem.* **106**, 498 (2007).
18. L. W. Cooper, *et al., J. Geophys. Res.* **110**, G02013 (2005).
19. G. Kattner, M. Simon, B. P. Koch, *Molecular Carbon Pump in the Ocean (2011),* pp. 60–61.
20. C. G. Fischot, R. Benner, *Geophys. Res. Lett.* **38**, L03610 (2011).

21. This work was supported by the Scientific Committee on Oceanic Research (WG134), the Danish Council for Strategic Research (10-093903), the Galician General Direction for R+D+i (07MMA002402PR), and the Spanish Ministry of Science and Innovation (MALASPINA, grant number CSD2008–00077). M. J. Pazó helped with illustrations. Discussions with G. Kattner and R. Benner have contributed to improve the manuscript.

Application of Functional Gene Arrays (GeoChips) in Monitoring Carbon Cycling

Joy D. Van Nostrand and Jizhong Zhou*

Functional gene arrays (FGAs) provide a way, through in-depth genomic analysis, to link environmental processes with microbial communities. They comprise probes for a wide range of genes involved in functional processes of interest (e.g., carbon degradation, C- and N-fixation, metal resistance) from many different microorganisms, both cultured and uncultured. The most comprehensive FGA reported to date is the GeoChip 3.0, which includes approximately 28,000 probes covering approximately 57,000 gene variants from 292 functional gene families involved in carbon, nitrogen, phosphorus and sulfur cycling, energy metabolism, antibiotic resistance, metal resistance, and organic contaminant degradation. This technology has been used successfully to examine the effects of environmental change on microbial communities. This article provides an overview of GeoChip development and utilization with an emphasis on studies examining various aspects of carbon cycling.

DNA microarrays can overcome many of the limitations of other molecular techniques such as the need for polymerase chain reaction (PCR) amplification steps, which restricts the number of genes that can be detected due to limitations in primer availability and coverage. Microarrays provide information on the functional abilities of microbial communities and can also provide phylogenetic information at a higher resolution than other 16S rRNA-based methods and with fewer sampling errors. GeoChip provides a species-strain level of resolution (*1*) while 16S rRNA gene-based sequencing only provides a genus-species level of resolution (Zhili He, personal communication). They are less time-consuming and often cheaper to use than other methods, and have the ability to provide more accurate comparisons since they can interrogate multiple samples using the same set of probes (*2*). One disadvantage, however, is the inability of arrays to interrogate novel sequences.

GeoChip Functional Gene Arrays

Functional gene arrays (FGAs) are composed of probes for microbial genes involved in functional processes, such as nitrification or carbon degradation (*3–5*). The most comprehensive FGAs are the GeoChip arrays, which contains probes for thousands of functional genes (*4, 5*). The first reported FGA used PCR amplicon probes and demonstrated that such arrays are an effective tool for genomic studies of microbial communities (*3*). Later versions use oligonucleotide probes (*1*, *6*), which, although less sensitive, provide higher specificity since they are easily customized to afford a more targeted probe design (*7*).

The GeoChip has gone through several development iterations, from the first proof-of-concept array to the current version 4.0, with the ultimate goal of providing a comprehensive probe set with high specificity and able to distinguish between highly homologous genes (*4, 5*). GeoChip 4.0 uses the Nimblegen array format, covering 410 functional gene families including probes for carbon, nitrogen, phosphorus, and sulfur cycling, metal resistance and reduction, virulence genes, stress response, and bacterial phage genes.

GeoChip Development

Probe design. Gene regions selected for targeting on an array should encode the catalytic or active sites of proteins key to the functions of interest. To find these, public DNA databases are searched for suitable genes using broad search terms. Seed sequences from only those genes that have had protein identity and function experimentally determined are used to confirm sequence identity for all downloaded sequences using HMMER alignment (*8*). Probes (50-mer) are then designed using CommOligo software (*9*) based on experimentally determined criteria (sequence homology, continuous stretch length, and free energy) (*10*), and screened against the GenBank database to ensure specificity.

Target preparation and hybridization. The use of high quality nucleic acid starting material to query microarrays is extremely important. Purified DNA should have absorbance ratios of A_{260}:A_{280} > 1.8 and A_{260}:A_{230} > 1.7. The A_{260}:A_{230} ratio has the most influence on hybridization success (*11*). Whole community genome amplification (WCGA) can increase the amount of DNA available using a small quantity of initial DNA (1 to 100 ng) and provide a sensitive (10 fg detection limit) and representative amplification (*12*). To examine activity, RNA can be used. Stable isotope probing is another means to evaluate activity, by hybridizing ^{13}C-DNA after incubation with a ^{13}C-labeled carbon source, such as biphenyl (*13*). Nucleic acids are then labeled with cyanine dye, purified, dried, and resuspended in a hybridization buffer. GeoChips are hybridized at 42 to 50°C and 40 to 50% formamide (*4, 14, 15*).

Issues in Microarray Application

Sensitivity. The current sensitivity for oligonucleotide arrays using environmental samples is approximately 50 to 100 ng (10^7 cells) (*1, 6, 16*) or ~5% of the microbial community (*16*), providing coverage of only the most dominant community members. Several strategies can be used to increase sensitivity, including (i) amplifying target DNA or RNA (*12, 17*), (ii) increasing probe length (*7, 18*) [although this also decreases specificity (*19*)], (iii) increasing probe concentration per spot (*19*), (iv) decreasing hybridization buffer volume (*20*), (v) mixing during hybridization (*21*), (vi) alternate labeling (*7*), and (vii) reducing ozone concentrations (*22*).

Specificity. Specificity is especially important since so many environmental microorganisms remain uncharacterized. Strategies to increase specificity include (i) modifying probe design criteria (*4, 18*) or (ii) increasing hybridization stringency by elevating temperature or formamide concentration.

Quantitation. There is a correlation between signal intensity and DNA concentration, indicating that microarrays can provide quantitative information. Oligonucleotide probes (50-mer) have been shown to maintain a linear relationship (r=0.98–0.99) over a concentration range of 8 to 1000 ng (*1*), while RNA has a linear response over the range of 50 to 100 ng (*17*).

Application of the GeoChip

GeoChips have been used to examine a variety of microbial communities at contaminated sites (*1, 4, 6, 12, 15, 23, 24*), in marine environments (*25*), and in soils (*2*).

Institute for Environmental Genomics and Dept. of Botany and Microbiology, University of Oklahoma, Norman, OK USA

*To whom correspondence should be addressed. E-mail: jzhou@ou.edu

Insights into carbon cycling. The latest GeoChips (versions 3.0 and 4.0) include coverage of many genes that are useful for studying the microbial carbon pump (*26*). GeoChip version 3.0 contains probes for 41 genes involved in carbon cycling, including four CO_2 fixation genes and 25 genes involved in carbon degradation (labile to refractory), methanogenesis, two for methane oxidation, acetogenesis, and another eight miscellaneous enzymes. GeoChip 4.0 has expanded gene coverage to include those for bacterial lysis by viruses, which may be involved in the release of dissolved organic carbon in the oceans (*26*). Genes for carbon fixation and degradation in algae and other microbial eukaryotes will be included in future versions.

While not directly examining carbon pumps, several GeoChip studies have provided insights into carbon cycling in the marine environment. GeoChip analysis has indicated that carbon fixation, methane oxidation, and methanogenesis may be occurring in deep-sea basalts, activities that had not previously been associated with this environment (*14*). In a study examining deep sea hydrothermal vent microbial communities, GeoChips detected RuBisCO genes that perform an important initial step in carbon fixation from photosynthetic microorganisms, supporting the assertion that organisms able to grow by acquiring geothermal radiation may live in environments lacking light, such as this one (*27*). In addition, detection of a large number of genes involved in the Calvin Benson Bassham cycle suggested that autotrophic microorganisms within the hydrothermal vent communities may principally use this cycle rather than the Krebs cycle, providing a greater insight into carbon cycling occurring in the deep ocean (*27*).

Previous research focusing on the effects of elevated CO_2 levels in soil communities may lend some insight into how climate change can affect the global carbon cycle, including carbon pumps in the ocean. In one study, results of GeoChip 3.0 analysis following a ten-year exposure of grassland to elevated CO_2 indicated that there were both overall changes in the soil microbial community's functional structure and composition (as evidenced by distinct clustering of ambient and elevated CO_2 samples in detrended correspondence analysis) as well as a significant increase in carbon fixation (*28*).

Summary

GeoChip arrays have garnered a great deal of attention and have been demonstrated to be useful for studying microbial ecology, linking microbial communities with geochemical cycling, and addressing high-level ecological questions pertaining to global climate change and ecological theory. The GeoChip provides sensitive, specific, and potentially quantitative information regarding microbial communities. However, many technical, experimental, and data analysis challenges remain, including a need to improve the sensitivity and quantitative accuracy of the arrays and to develop bioinformatic tools and techniques to analyze, evaluate, and interpret the vast amounts of data being generated.

References and Notes

1. S. M. Tiquia, *et al.*, *Biotechniques.* **36**, 1 (2004).
2. J. Zhou, S. Kang, C. W. Schadt, and C. T. Garten, Jr., *Proc. Natl. Acad. Sci. U.S.A.* **105**, 7768 (2008).
3. L. Wu, *et al.*, *Appl. Environ. Microbiol.* **67**, 5780 (2001).
4. Z. He, *et al.*, *ISME J.* **1**, 67 (2007).
5. Z. He, *et al.*, *ISME J.* **4**, 1167 (2010).
6. S. K. Rhee, *et al.*, *Appl. Environ. Microbiol.* **70**, 4303 (2004).
7. V. J. Denef, *et al.*, *Environ. Micrbiol.* **5**, 933 (2003).
8. S. R. Eddy, *Bioinformatics.* **14**, 755 (1998).
9. X. Li, Z. He, J. Zhou, *Nucleic Acids Res.* **33**, 6114 (2005).
10. Z. He, L.-Y. Wu, X.-Y. Li, M. W. Fields, J.-Z. Zhou, *Appl. Environ. Microbiol.* **71**, 3753 (2005).
11. J. Ning, *et al.*, *Appl. Microbiol. Biotechnol.* **82**, 983 (2009).
12. L.Wu, X. Liu, C. W. Schadt, J. Zhou, *Appl. Environ. Microbiol.* **72**, 4931 (2006).
13. M. B. Leigh, *et al.*, *ISME J.* **1**, 134 (2007).
14. O. U. Mason, *et al.*, *ISME J.* **3**, 231 (2009).
15. P. J. Waldron, *et al.*, *Environ. Sci. Technol.* **43**, 3529 (2009).
16. L. Bodrossy, *et al.*, *Environ. Microbiol.* **5**, 566 (2003).
17. H. Gao, *et al.*, *Appl. Environ. Microbiol.* **73**, 563 (2007).
18. Z. He, L. Wu, M. W. Fields, J. Zhou, *Appl. Environ. Microbiol.* **71**, 5154 (2005).
19. A. Relógio, C. Schwager, A. Richter, W. Ansorge, J. Valcárcel, *Nucleic Acids Res.* **30**, e51 (2002).
20. L. Wu, *et al.*, *Environ. Sci. Technol.* **38**, 6775 (2004).
21. C. J. Schaupp, G. Jiang, T. G. Myers, M. A. Wilson, *BioTechniques.* **38**, 117 (2005).
22. W. Branham, *et al.*, *BMC Biotechnol.* **7**, 8 (2007).
23. J. Xiong, *et al.*, *Appl. Environ. Microbiol.* (2010), doi:10.1128/AEM.00500-10.
24. T. C. Hazen, *et al.*, *Science.* **330**, 204 (2010).
25. N. E. Kimes, J. D. Van Nostrand, E. Weil, J. Zhou, P. J. Morris, *Environ. Microbiol.* **12**, 541 (2010).
26. N. Jiao, *et al.*, *Nat. Rev. Microbiol.* **8**, 593 (2010).
27. F. Wang, *et al.*, *Proc. Natl. Acad. Sci. U.S.A.* **106**, 4840 (2009).
28. Z. He, *et al.*, *Ecol. Lett.* **13**, 564 (2010).

29. This work was supported by ENIGMA (DE-AC02-05CH11231), Environmental Remediation Science Program, Oklahoma Applied Research Support, Oklahoma Center for the Advancement of Science and Technology, Oklahoma Bioenergy Center, the State of Oklahoma (AR062-034).

Toward a Mechanistic Approach to Modeling Bacterial DOC Pathways: A Review

Marie Eichinger[1, 2*], Jean-Christophe Poggiale[1, 2], and Richard Sempéré[1, 2]

Dissolved organic carbon (DOC) can be mineralized into CO_2 through bacterial respiration, reenter the trophic chain if bacterial biomass is grazed, or be partly stored in a recalcitrant form for millennia in the deep ocean by bacterial production during DOC degradation. This review compares mathematical models used to represent these pathways in the context of the current knowledge of bacterial metabolism, and examines how they may be related to the biological carbon pump and the microbial carbon pump. In view of the ever-changing environments in which bacteria exist, the authors propose that models of DOC degradation should be based on data from experiments in which bacteria are subjected to external constraints, such as DOC availability, temperature, and ocean depth. Further, the need for combining experimental and mechanistic modeling approaches to advance our understanding of the factors that affect oceanic DOC cycling and organic carbon storage is discussed.

Modeling dissolved organic carbon (DOC) degradation remains challenging due to factors including the complex nature of DOC, the variety of microorganisms using different metabolic pathways necessary for DOC breakdown, and the various oceanic physicochemical conditions that regulate bacterial metabolism. In this review, we identify those variables (for example, DOC concentration and bacterial biomass) relevant to accurately model bacterial-driven DOC pathways and forcing factors (forces external to the system, acting upon it, for example, temperature and depth).

The Multi-G model represents DOC degradation using DOC concentration as a single variable. DOC concentration decay is assumed to be at a constant rate and is therefore represented by first order kinetics (Eq. 1, Table 1) (*1, 2*). Multi-G-based models do not include specific biological activity (Fig. 1A), even though bacteria are recognized as the main agents of DOC degradation (*3*). A more accurate representation of DOC dynamics requires the inclusion of more detailed information about bacterial metabolism (*4*). The Monod model is an example of the next generation of model, which includes bacterial biomass as a variable (Eq. 2, Table 1). This model is the most widely used in ecosystem studies, taking into account bacterial population growth as a result of DOC consumption (*5–7*). It assumes that assimilated DOC is instantaneously converted to bacterial biomass with constant bacterial growth efficiency (BGE), and that the complementary proportion (1-BGE) is used for bacterial respiration (Fig. 1B). Although the predicted results obtained when applying the Monod model agree well with experimental observations (*8*), certain parameters such as BGE vary widely as a function of DOC chemical characteristics (*9*) and environmental conditions [temperature (*10*), and depth (*8*)]. This model fails, however, when DOC availability changes suddenly, making it inappropriate for modeling natural ecosystems that are subject to frequent environmental variations (*11*).

Variability in DOC and nutrient quality and availability may have some effects on the physiological status of bacterial communities (*12*). These effects on bacterial stoichiometry have been modeled using the Droop equations, where, for example, carbon and phosphorus (*13*), or carbon, nitrogen, and phosphorus (*14*), are limiting. According to this model, population growth depends on a pool of internal nutrients inside the bacterial cells (Fig. 1C; Eq. 3, Table 1), such as an internal reserve of organic carbon that allows cells to survive periods of starvation. This can also be taken into account using the dynamic energy budget (DEB) model (*15*), where population growth resulting from DOC consumption is modeled using at least two bacterial variables, the reserve and the structure of the cell (Fig. 1D; Eq. 4, Table 1). The DEB model is also appropriate for handling variable resource environments and variable bacterial stoichiometry because it can be extended to deal with systems using several substrates (*15*) (Fig. 1E). Furthermore, DEB considers the concept of maintenance that reflects the fact that bacteria use intracellular DOC not only for growth but also for physiological activities that do not produce new biomass (osmotic regulation, maintenance of intracellular pH, macromolecule turnover) (*16, 17*). The importance of such considerations in changing environments has been demonstrated in experiments in which bacteria are exposed to episodic inputs of labile DOC (LDOC), where DOC utilization for maintenance is detectable during starvation (*11*). Maintenance cannot be neglected, since bacterial survival under starvation conditions is a fundamental aspect of bacterial existence and something bacteria experience often (*17*). In some studies of marine DOC cycling, maintenance modeling is restricted to the respiration process (R_B in Eq. 3, Table 1) (*13, 16, 18*). These models may prove useful for estimating the contribution from bacteria to the biological carbon pump, but not to the microbial carbon pump (MCP), since the latter assesses the role of microbial processes in refractory DOC (RDOC) generation and in carbon storage in the ocean (*19*). By contrast, in the DEB model, maintenance activity incorporates not only respiration, but also a set of processes which can include RDOC production (Fig. 1D). This RDOC contributes to the total RDOC in the ocean. Since the DEB model accounts for this RDOC production explicitly, its use is relevant for connecting the biological carbon pump and the MCP.

Although RDOC production by marine bacteria has been studied both under controlled experimental conditions (*20–22*) and in situ (*23*), mechanisms of this production are still unresolved. Only a few models include bacterially derived DOC at either a microbial level (*11, 20, 24*) or at an ecosystem level (*25*). A study based on pure cultures indicated that bacterial RDOC production may occur as a stress response when LDOC availability is low; this can be represented using the DEB model where, in the case of starvation, maintenance costs are mainly paid not by bacterial reserve, but rather by bacterial structure, leading to the production of RDOC (*20*).

In order to extrapolate how long-term changes (e.g. warming) influence DOC dynamics and organic carbon storage in marine waters,

[1]Université de la Méditerranée, LMGEM, Centre d'Océanologie de Marseille, Case 901, 13288 Marseille Cedex 9, France
[2]CNRS/INSU, UMR 6117, LMGEM, Case 901, 13288 Marseille Cedex 9, France
*To whom correspondence should be addressed. E-mail: marie.eichinger@univmed.fr

Fig. 1. Schematic representation of fluxes in Multi-G model (**A**), Monod model (**B**), Droop model with LDOC and dissolved phosphorus (DP) as limiting nutrients (**C**), DEB model with LDOC as the single limiting nutrient (**D**), and DEB model for two limiting nutrients, here LDOC and DP (**E**). Only the DEB model considers bacterial RDOC production, which can contribute to the total RDOC pool in the ocean. If these models are included in larger models accounting for primary production and export of organic carbon, then all models except the Multi-G can be indirectly linked to the biological carbon pump.

BB, bacterial biomass; BGE, bacterial growth efficiency; RES, reserve; STR, structure; LDOC, labile DOC; RDOC, refractory DOC; DP, dissolved phosphorus; Q_C, cellular carbon content; Q_P, cellular phosphorus content; RES_C, carbon reserve; RES_P, phosphorus reserve; A, assimilation; G, growth; R, respiration; M, maintenance.

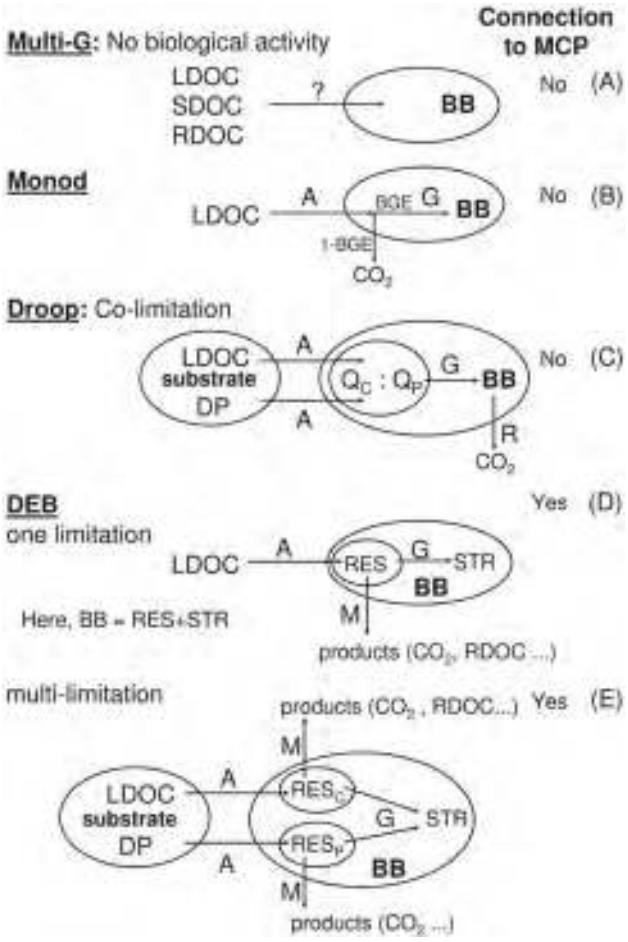

mathematical models describing DOC concentration should account for the effects of these changes on the rates of DOC production and consumption. Few modeling studies consider the temperature effect on bacterial metabolic rates; some authors have used an exponential function to predict the effects of temperature changes on the rate of population growth (*7*), whereas others have applied the Q10 model to DOC assimilation and maintenance respiration (*24*) or to the population growth rate (*6*). The Q10 function represents one of the easiest ways to incorporate temperature dependence into a mathematical model. It estimates the change in a particular variable that would result from a temperature increase of 10°C. The Arrhenius function provides a more sophisticated way to consider temperature variations in a model, incorporating a high and low tolerance range (*15*). This representation might be useful in view of the wide range of temperatures in which bacteria can survive. However, to the best of our knowledge, it has never been used to model DOC generation and degradation by bacteria.

Although properties of bacterial metabolism like BGE (*8*) and bacterial production (*26*) are known to vary as a function of depth, the direct effects of continuously increasing pressure are poorly understood (*27*). Recent data suggest that bacterial production and extracellular hydrolytic enzyme activities are generally higher under in situ pressures than at atmospheric pressures, but the reasons for this remain unclear

Table 1. Equations of each model described in the review. t, time; LDOC, labile DOC; SDOC, semilabile DOC; RDOC, refractory DOC; BB, bacterial biomass, B_C, bacterial biomass in carbon, V_{max} maximum LDOC uptake rate; K, half-saturation constant.

Eq. No.	Model	Equations	State variables/parameter description
(1)	Multi-G	$[DOC] = [LDOC]e^{-k_1 t} + [SDOC]e^{-k_2 t} + [RDOC]$	k_1 = LDOC degradation rate k_2 = SDOC degradation rate
(2)	Monod	$\frac{dLDOC}{dt} = -V_{max}\frac{LDOC}{K + LDOC}BB$ $\frac{dBB}{dt} = -BGE\frac{dLDOC}{dt}$	BGE = bacterial growth efficiency (*8*)
(3)	Droop Co-limitation between LDOC and dissolved P	$\frac{dLDOC}{dt} = -V_C B$ $\frac{dB_C}{dt} = V_C B - R_B B$ $\frac{dB}{dt} = \mu_B B$ $V_C = V_{max}\frac{Q_C^{max} - Q_C}{Q_C^{max} - Q_C^{min}}\frac{LDOC}{K + LDOC}$ $R_B = \rho_{gro} Q_C \mu_B + \rho_{resp}(Q_C - Q_{min})$ $\mu_B = \mu_B^{max}\left(1 - \frac{Q_P^{min}}{Q_P}\right)\left(1 - \frac{Q_C^{min}}{Q_C}\right)$	B = bacterial number R_B = respiration rate μ_B = specific growth rate ρ_{gro} and ρ_{resp} = portions of respiration allocated to growth and maintenance Q_C^{min}, Q_C^{max} and Q_C = minimum, maximum and actual cellular carbon content, respectively Q_P^{min} and Q_P = minimum and actual cellular phosphorus content, respectively (*13*)
(4)	DEB	$\frac{dLDOC}{dt} = -V_{max}\frac{LDOC}{K + LDOC}LDOC \cdot STR$ $\frac{dRES}{dt} = -eff_{RL}\frac{dLDOC}{dt} - maint_{RES}STR - eff_{RS}\frac{dSTR}{dt}$ $\frac{dSTR}{dt} = \frac{k_{RES}RES - maint_{RES}STR}{RES + eff_{RS}STR}STR$	RES = energy reserve STR = structural biomass (with RES + STR = BB) LDOC is assimilated into RES with efficiency eff_{RL}, maintenance ($maint_{RES}$) is supported by RES energy, eff_{RS} is the efficiency of RES transfer to STR, and k_{RES} is the reserve turnover rate (*20*)

(*28*). In view of the number of bacteria present at depth, this issue needs to be more thoroughly investigated. Similarly, insufficient information on the effects of pH on bacteria-driven DOC degradation precludes its inclusion in current models. There is some evidence that lower pH increases bacterial production and degradation, but bacterial respiration and BGE have not yet been studied with respect to ocean acidification (*3*). Changes in seawater chemistry due to ocean warming and acidification are expected to enhance microbial activity and channel a greater fraction of the fixed carbon into DOC (*29, 30*), thus potentially increasing the importance of the MCP in the oceanic carbon flow. The relevance of the MCP in carbon cycling and storage, and how these changes might affect it should also be investigated using appropriate models.

References and Notes

1. C. S. J. Hopkinson, J. J. Vallino, A. Nolin, *Deep Sea Res. II* **49**, 4461 (2002).
2. Y. Yamanaka, E. Tajika, *Global Biogeochem. Cycles* **11**, 599 (1997).
3. J. Liu, M. G. Weinbauer, C. Maier, M. Dai, J. P. Gattuso, *Aquat. Microb. Ecol.* **61**, 291 (2010).
4. F. Talin, C. Tolla, C. Rabouille, J. C. Poggiale, *Acta Biotheor.* **51**, 295 (2003).
5. T. R. Anderson, P. J. l. B. Williams, *Global Biogeochem. Cycles* **13**, 337 (1999).
6. J. Bendtsen, C. Lundsgaard, M. Middelboe, D. Archer, *Global Biogeoch. Cycles* **16**, Art. No. 1127 (2002).
7. R. C. Tian, A. F. Vézina, D. Deibel, R. Rivkin, *Global Biogeochem. Cycles* **17** (2003).
8. M. Eichinger, J. C. Poggiale, F. Van Wambeke, D. Lefèvre, R. Sempéré, *Aquat. Microb. Ecol.* **43**, 139 (2006).
9. R. M. W. Amon, R. Benner, *Limnol. Oceanogr.* **41**, 41 (1996).
10. R. B. Rivkin, L. Legendre, *Science* **291**, 2398 (2001).
11. M. Eichinger *et al.*, *Biogeosciences* **7**, 1861 (2010).
12. C. A. Carlson *et al.*, *Aquat. Microb. Ecol.* **30**, 19 (2002).
13. E. K. Hall, C. Neuhauser, J. B. Cotner, *ISME J.* **2**, 471 (2008).
14. T. F. Thingstad, *Mar. Ecol. Prog. Ser.* **35**, 99 (1987).
15. S. A. L. M. Kooijman, *Dynamic energy budget theory for metabolic organisation* (Cambridge University Press, Cambridge, ed. 3, 2010).
16. R. Cajal-Medrano, H. Maske, *Aquat. Microb. Ecol.* **38**, 125 (2005).
17. R. Y. Morita, *Bacteria in oligotrophic environment: starvation - survival lifestyle* (Chapman & Hall, New York, 1997)
18. J. G. Baretta-Bekker, B. Riemann, J. W. Baretta, E. Koch Rasmussen, *Mar. Ecol. Prog. Ser.* **106**, 187 (1994).
19. N. Jiao *et al.*, *Nat. Rev. Microbiol.* **8**, 593 (2010).
20. M. Eichinger *et al.*, *Aquat. Microb. Ecol.* **56**, 41 (2009).
21. D. F. Gruber, J. P. Simjouw, S. P. Seitzinger, G. L. Taghon, *Appl. Environ. Microb.* **72**, 4184 (2006).
22. H. Ogawa, Y. Amagai, I. Koike, K. Kaiser, R. Benner, *Science* **292**, 917 (2001).
23. K. Kaiser, R. Benner, *Limnol. Oceanogr.* **53**, 99 (2008).
24. L. Polimene, J. I. Allen, M. Zavatarelli, *Aquat. Microb. Ecol.* **43**, 127 (2006).
25. L. Polimene *et al.*, *J. Geophys. Res. Oceans* **112**, doi:10.1029/2006JC003529 (2007).
26. T. Reinthaler *et al.*, *Limnol. Oceanogr.* **51**, 1262 (2006).
27. C. Tamburini *et al.*, *Deep Sea Res. II* **56**, 1533 (2009).
28. T. Nagata *et al.*, *Deep Sea Res. II* **57** 1519 (2010).
29. J. Raven *et al.*, *Ocean acidification due to increasing atmospheric carbon dioxide*. (The Royal Society, London, 12, 2005).
30. U. Riebesell *et al.*, *Nature* **450**, 545 (2007).

31. Acknowledgements: The authors are grateful to members of the SCOR Working Group on the "Microbial Carbon Pump in the Ocean" for helpful discussions. Special thanks to N. Jiao, F. Azam, R. Benner, and G. Herndl for fruitful comments on the manuscript. This work was supported by the French CNRS/INSU and Université de la Méditerranée.

Get a Career Plan that Works.

An exceptional career requires insightful planning and management. That's where *Science* Careers comes in. From job search to career enhancement, *Science* Careers has the tools and resources to help you achieve your goals. Get yourself on the right track today and get a real career plan that works. Visit **ScienceCareers.org**.

Science Careers

From the journal *Science* AAAS

ScienceCareers.org

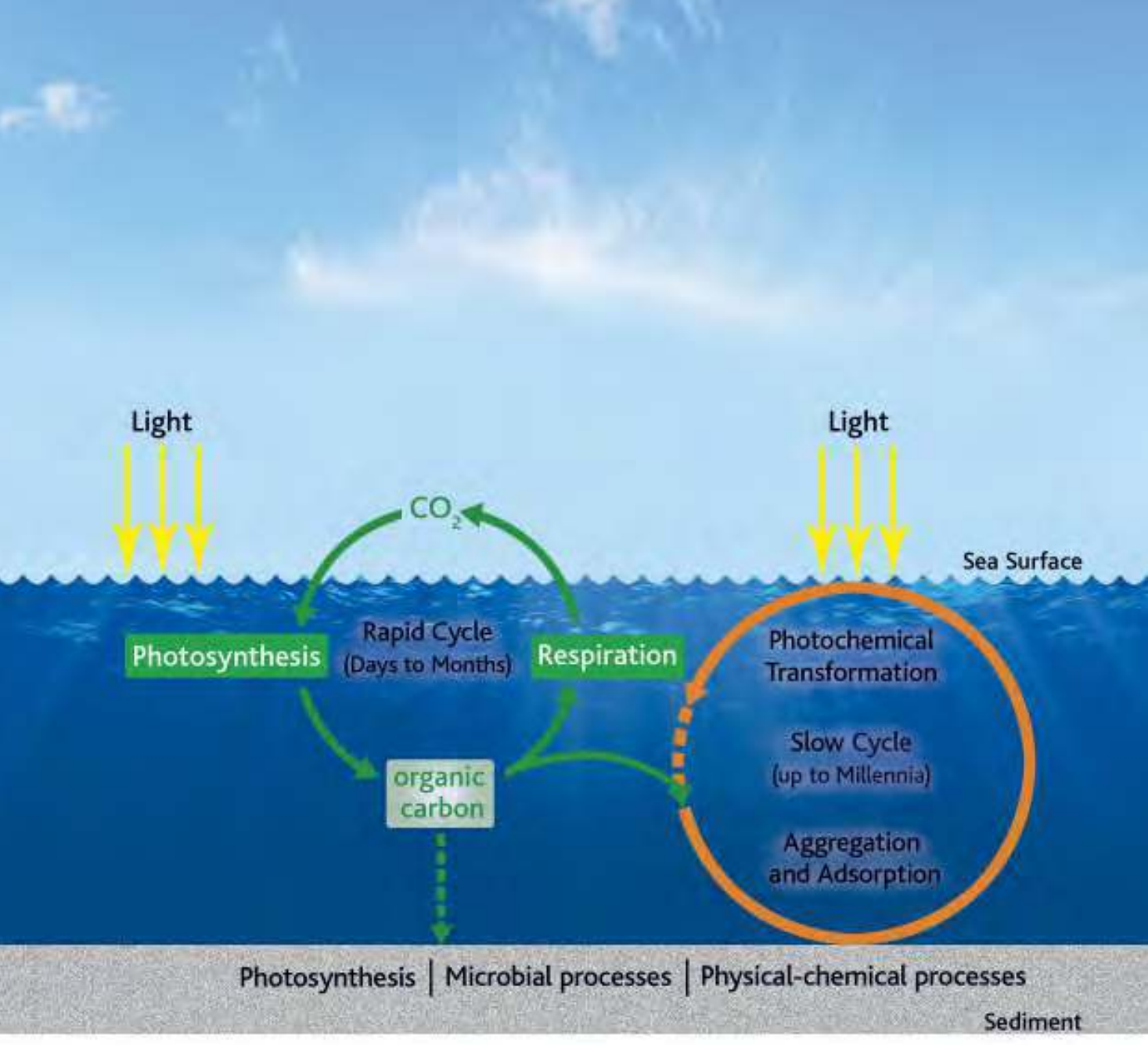
Light
Light
CO_2
Sea Surface
Photosynthesis
Rapid Cycle
(Days to Months)
Respiration
Photochemical
Transformation
Slow Cycle
(up to Millennia)
organic
carbon
Aggregation
and Adsorption
Photosynthesis | Microbial processes | Physical-chemical processes
Sediment